

MORECAMBE OFFSHORE WINDFARM GENERATION ASSETS

Document status

Version	Purpose of document	Authored by	Reviewed by	Approved by	Review date
<u>V1.0F01</u>	Application	Manchester Advanced Radar Services Ltd	Morecambe Offshore Windfarm Ltd	Morecambe Offshore Windfarm Ltd	April 2024
<u>F02</u>	<u>Examination Update</u>	<u>Manchester Advanced Radar Services Ltd</u>	<u>Morecambe Offshore Windfarm Ltd</u>	<u>Morecambe Offshore Windfarm Ltd</u>	<u>January 2025</u>

Prepared by:

Prepared for:

Manchester Advanced Radar Services Ltd Morecambe Offshore Windfarm Ltd.

Document Number: REWS-FE01B

Contents

1	INTRODUCTION	2
1.1	Overview	2
1.2	Background	3
2	SCOPE OF ASSESSMENT	5
2.1	Target masking	5
2.2	Shadowing effects	5
2.3	Rerouted traffic	6
2.4	Adaptive detection threshold modelling	6
2.5	Tracker modelling	7
2.6	Ultra-High Frequency communication links	7
2.7	Other effects	8
3	MODELLING PARAMETERS	9
3.1	Wind turbine parameters	9
3.2	Windfarm parameters	13
3.3	Morecambe Generation Assets indicative wind turbine and offshore substations/platform layouts	13
3.4	Assessment region and study area	14
3.5	REWS modelling	16
3.6	Detection threshold (CFAR)	17
3.7	Target modelling	18
3.8	Wind turbine shadow modelling	18
3.9	Measurements and modelling of RCS of wind turbines	19
4	REWS RETURNS AND VESSEL DETECTION MODELLING RESULTS	22
4.1	Overview	22
4.2	Assessment of the base case scenario	22
4.3	Assessment of the Morecambe Generation Assets	38
4.4	Cumulative assessment	52
4.4.2	Cumulative REWS assessment of Morecambe Generation Assets with Mona Offshore Wind Project and Morgan Offshore Wind Project: Generation Assets	54
4.4.3	Conclusions and comments on the cumulative REWS assessment of Morecambe Generation Assets with other proposed windfarms in the study area	67
5	ASSESSMENT OF THE REROUTED TRAFFIC ON REWS ALARM RATES	69
5.1	Overview	69
5.2	Routes and alarms modelling	69
5.3	Modelling the base case traffic (pre-development of the Morecambe Generation Assets)	70
5.4	Modelling the predicted shipping reroutes around the Morecambe Generation Assets in isolation and cumulatively with other windfarms in the study area	76
5.5	Modelling results and comparison of the base case and the predicted shipping reroutes around the Morecambe Generation Assets in isolation and around Morecambe Generation Assets with Mona Offshore Wind Project and Morgan Generation Assets cumulatively	79
5.6	Remarks on the TCPA/CPA alarm modelling results	81
5.7	Conclusions of the TCPA/CPA alarm modelling	82
6	MICROWAVE COMMUNICATION LINKS ASSESSMENT	84
6.1	Overview	84
6.2	Modelling parameters	85
6.2.2	Communication link parameters	86
6.2.3	Wind turbine parameters	86
6.2.4	Exclusion zones modelling	88
6.2.5	Nearfield calculations	88
6.2.6	Diffraction region calculations	88
6.2.7	Reflection region calculations	89
6.3	Exclusion zone modelling results	91

6.4	Remarks on the microwave communication links modelling.....	92
7	SUMMARY AND FINAL REMARKS.....	93
7.1	General REWS returns modelling summary	93
7.2	General TCPA/CPA modelling summary.....	94
7.3	Assumptions and further considerations	95
	REFERENCES.....	96
1	INTRODUCTION	2
1.1	Overview.....	2
1.2	Background.....	3
2	SCOPE OF ASSESSMENT.....	5
2.1	Target masking.....	5
2.2	Shadowing effects	5
2.3	Rerouted traffic	6
2.4	Adaptive detection threshold modelling.....	6
2.5	Tracker modelling	7
2.6	Ultra-High Frequency communication links.....	7
2.7	Other effects	8
2.8	Spirit Energy comments and report updates	8
	2.8.2 11	
3	MODELLING PARAMETERS	12
3.1	Wind turbine parameters	12
3.2	Windfarm parameters	16
3.3	Morecambe Generation Assets indicative wind turbine and offshore substations/platform layouts.....	16
3.4	Assessment region and study area	17
3.5	REWS modelling.....	19
3.6	Detection threshold (CFAR)	20
3.7	Target modelling	21
3.8	Wind turbine shadow modelling.....	21
3.9	Measurements and modelling of RCS of wind turbines	22
4	REWS RETURNS AND VESSEL DETECTION MODELLING RESULTS	25
4.1	Overview.....	25
4.2	Assessment of the base case scenario	25
4.3	Assessment of the Morecambe Generation Assets	60
	4.3.1 Masking and Detection Assessment.....	60
	4.3.2 Assessment of turbine shadowing on Spirit Energy assets	88
4.4	Cumulative assessment	96
	4.4.2 Cumulative REWS assessment of Morecambe Generation Assets with Mona Offshore Wind Project and Morgan Offshore Wind Project: Generation Assets	98
	4.4.3 Conclusions and comments on the cumulative REWS assessment of Morecambe Generation Assets with other proposed windfarms in the study area.....	124
5	ASSESSMENT OF THE REROUTED TRAFFIC ON REWS ALARM RATES	126
5.1	Overview.....	126
5.2	Routes and alarms modelling	126
5.3	Modelling the base case traffic (pre-development of the Morecambe Generation Assets)	127
5.4	Modelling the predicted shipping reroutes around the Morecambe Generation Assets in isolation and cumulatively with other windfarms in the study area.....	134
5.5	Modelling results and comparison of the base case and the predicted shipping reroutes around the Morecambe Generation Assets in isolation and around Morecambe Generation Assets with Mona Offshore Wind Project and Morgan Generation Assets cumulatively	139
5.6	Remarks on the TCPA/CPA alarm modelling results	142
5.7	Conclusions of the TCPA/CPA alarm modelling	143
6	MICROWAVE COMMUNICATION LINKS ASSESSMENT.....	145

MORECAMBE OFFSHORE WINDFARM GENERATION ASSETS

6.1	Overview	145
6.2	Modelling parameters	146
6.2.2	Communication link parameters	147
6.2.3	Wind turbine parameters	147
6.2.4	Exclusion zones modelling	149
6.2.5	Nearfield calculations	149
6.2.6	Diffraction region calculations	149
6.2.7	Reflection region calculations	150
6.3	Exclusion zone modelling results	152
6.4	Remarks on the microwave communication links modelling	153
7	SUMMARY AND FINAL REMARKS	154
7.1	General REWS returns modelling summary	154
7.2	General TCPA/CPA modelling summary	155
7.3	Assumptions and further considerations	156
	REFERENCES	157

Tables

Table 3.1: MDS parameters for the REWS modelling 13

Table 3.2: Radar modelling parameters 16

Table 5.1: Commercial shipping routes in the region and the number of vessels travelling on each route per day 70

Table 5.2: Ferry shipping routes in the region and the number of vessels travelling on each route per day 71

Table 5.3: The estimated change in yearly alarm rates against the base case (green = reduced alarms / no change, white = small alarm increase/decrease, orange = elevated alarm increase) 81

Table 6.1: Exclusion zones around the Spirit Energy microwave communication links 91

Table 6.2: Exclusion zones around the ENI Energy microwave communication links 92

Table 2.1: Relevant representation by Spirit Energy and report updates 8

Table 3.1: MDS parameters for the REWS modelling 16

Table 3.2: Radar modelling parameters 19

Table 5.1: Commercial shipping routes in the region and the number of vessels travelling on each route per day 127

Table 5.2: Ferry shipping routes in the region and the number of vessels travelling on each route per day 128

Table 5.3: The estimated change in yearly alarm rates against the base case (green = reduced alarms / no change, white = small alarm increase/decrease, orange = elevated alarm increase) 142

Table 6.1: Exclusion zones around the Spirit Energy microwave communication links 152

Table 6.2: Exclusion zones around the ENI Energy microwave communication links 153

Figures

Figure 2.1: Illustration of radar shadowing with diffraction effects (Butler and Johnson, 2003) 5

Figure 2.2: 2D CFAR cells around a given cell with wind turbine present 7

Figure 3.1: Modelled turbine geometry (referenced to HAT) 10

Figure 3.2: Indicative Morecambe Generation Assets MDS layout with Mona Offshore Wind Project and Morgan Generation Assets and nearby oil and gas platforms with REWS 12

Figure 3.3: Morecambe Generation Assets REWS study area 15

Figure 3.4: The radar antenna elevation and azimuth patterns 17

Figure 3.5: Optical blockage and partial shadowing 19

Figure 3.6: Wind turbine layout at Hornsea Project One array area and the location of the radar system used in the study. The red area denotes the region shown in Figure 3.7 (Terma, 2021) 20

Figure 3.7: Compressed radar image in range-azimuth coordinates showing a zoomed area of the Hornsea Project One array area around a substation platform (Z13). A vessel is visible between Z13 and WTG G05. The signal level (in dB) is colour coded (Terma, 2021) 20

Figure 3.8: Power received by the REWS on ENI's Douglas platform 21

Figure 4.1: Modelled layout of the base case scenario showing the location of the existing windfarms and the coverage of the REWS in the region 23

Figure 4.2: ENI Energy's Douglas platform REWS clutter map showing returns from the wind turbines and sea clutter 24

Figure 4.3: ENI Energy's Douglas platform REWS detection threshold 25

Figure 4.4: Modelled power received from 1000 m² target (coverage) 26

Figure 4.5: ENI Energy's Douglas platform REWS detection plot showing loss regions for a 1000 m² target 27

Figure 4.6: Enlarged portion of the detection plot showing the effect of wind turbine shadowing 28

Figure 4.7: Harbour Energy's Millom West platform REWS clutter map showing returns from the wind turbines and sea clutter 29

Figure 4.8: Harbour Energy's Millom West platform REWS detection threshold 30

Figure 4.9: Harbour Energy's Millom West platform REWS detection plot showing loss regions for a 1000 m² target 31

Figure 4.10: ENI Energy's OSI REWS clutter map showing returns from the wind turbines and sea clutter 32

Figure 4.11: ENI Energy's OSI REWS detection threshold 33

Figure 4.12: ENI Energy's OSI REWS detection plot showing loss regions for a 1000 m² target 34

Figure 4.13: Spirit Energy's South Morecambe AP1 platform REWS clutter map showing returns from the wind turbines and sea clutter 35

Figure 4.14: Spirit Energy’s South Morecambe AP1 platform REWS detection threshold..... 36

Figure 4.15: Spirit Energy’s South Morecambe AP1 platform REWS detection plot showing loss regions for a 1000 m² target. 37

Figure 4.16: Modelled layout of the Morecambe Generation Assets showing the indicative location of the wind turbines and the location of oil and gas platforms in the region. 39

Figure 4.17: ENI Energy’s Douglas platform REWS clutter map showing returns from the Morecambe Generation Assets wind turbines and sea clutter. 40

Figure 4.18: ENI Energy’s Douglas platform REWS detection threshold over the Morecambe Array Area.... 41

Figure 4.19: ENI Energy’s Douglas platform REWS detection plot showing loss regions for a 1000 m² target. 42

Figure 4.20: Harbour Energy’s Millom West platform REWS clutter map showing returns from the Morecambe Generation Assets wind turbines and sea clutter. 43

Figure 4.21: Harbour Energy’s Millom West platform REWS detection threshold over the Morecambe Generation Assets Array Area. 44

Figure 4.22: Harbour Energy’s Millom West platform REWS detection plot showing loss regions for a 1000 m² target. 45

Figure 4.23: ENI Energy’s OSI REWS detection clutter map showing returns from the Morecambe Generation Assets wind turbines and sea clutter. 46

Figure 4.24: ENI Energy’s OSI REWS detection threshold over the Morecambe Generation Assets Array Area. 47

Figure 4.25: ENI Energy’s OSI REWS detection plot showing loss regions for a 1000 m² target. 48

Figure 4.26: Spirit Energy’s South Morecambe AP1 platform REWS clutter map showing returns from the Morecambe Generation Assets wind turbines and sea clutter. 49

Figure 4.27: Spirit Energy’s South Morecambe AP1 platform REWS detection threshold over the Morecambe Generation Assets Array Area. 50

Figure 4.28: Spirit Energy’s South Morecambe AP1 platform REWS detection plot showing loss regions for a 1000 m² target. 51

Figure 4.29: REWS study area for the cumulative assessment. 53

Figure 4.30: Modelled cumulative layout of the Morecambe Generation Assets with Mona Offshore Wind Project and Morgan Generation Assets showing the indicative location of the wind turbines and the location of oil and gas platforms in the region. 55

Figure 4.31: ENI Energy’s Douglas platform REWS clutter map showing returns from the wind turbines and sea clutter. 56

Figure 4.32: ENI Energy’s Douglas platform REWS detection threshold. 57

Figure 4.33: ENI Energy’s Douglas platform REWS detection plot showing loss regions for a 1000 m² target. 58

Figure 4.34: Harbour Energy’s Millom West platform REWS clutter map showing returns from the wind turbines and sea clutter. 59

Figure 4.35: Harbour Energy’s Millom West platform REWS detection threshold. 60

Figure 4.36: Harbour Energy’s Millom West platform REWS detection plot showing loss regions for a 1000 m² target. 61

Figure 4.37: ENI Energy’s OSI REWS detection clutter map showing returns from the wind turbines and sea clutter. 62

Figure 4.38: ENI Energy’s OSI REWS detection threshold. 63

Figure 4.39: ENI Energy’s OSI REWS detection plot showing loss regions for a 1000 m² target. 64

Figure 4.40: Spirit Energy’s South Morecambe AP1 platform REWS clutter map showing returns from the wind turbines and sea clutter. 65

Figure 4.41: Spirit Energy’s South Morecambe AP1 platform REWS detection threshold. 66

Figure 4.42: Spirit Energy’s South Morecambe AP1 platform REWS detection plot showing loss regions for a 1000 m² target. 67

Figure 5.1: Existing commercial routes within and around the Morecambe Generation Assets Array Area... 73

Figure 5.2: Existing ferry routes within and around the Morecambe Generation Assets Array Area. 74

Figure 5.3: Modelled existing shipping routes (1,000 variations each route). 75

Figure 5.4: Modelled shipping routes post construction of the Morecambe Generation Assets. 77

Figure 5.5: Modelled shipping routes post construction of the Morecambe Generation Assets with Mona Offshore Wind Project and Morgan Generation Assets cumulatively. 78

Figure 5.6: Modelled yearly alarm rates for the Conwy platform. 79

Figure 5.7: Modelled yearly alarm rates for the Douglas Complex. 79

Figure 5.8: Modelled yearly alarm rates for the Hamilton platform..... 79

Figure 5.9: Modelled yearly alarm rates for the Hamilton North platform..... 79

Figure 5.10: Modelled yearly alarm rates for the Lennox platform..... 80

Figure 5.11: Modelled yearly alarm rates for the OSI..... 80

Figure 5.12: Modelled yearly alarm rates for the Calder platform..... 80

Figure 5.13: Modelled yearly alarm rates for the Millom West platform..... 80

Figure 5.14: Modelled yearly alarm rates for the North Morecambe platform..... 80

Figure 5.15: Modelled yearly alarm rates for the South Morecambe AP1 platform..... 80

Figure 5.16: Modelled yearly alarm rates for the South Morecambe DP6 platform..... 81

Figure 5.17: Modelled yearly alarm rates for the South Morecambe DP8 platform..... 81

Figure 6.1: Layout of the modelled platforms and the communication links considered..... 85

Figure 6.2: Geometry and parameters used in the wind turbine bistatic RCS modelling..... 87

Figure 6.3: Bistatic RCS modelling results of the proposed MDS wind turbine..... 87

Figure 6.4: Illustration of the nearfield and diffraction exclusion zones..... 89

Figure 6.5: The signal to noise ratio around the Douglas — Hamilton link..... 90

Figure 6.6: Illustration of the refraction exclusion zone resulting in C/I less than 33 dB..... 90

Figure 6.7: Simplified illustration of all exclusion zones around the Douglas — Hamilton link..... 91

Figure 2.1: Illustration of radar shadowing with diffraction effects (Butler and Johnson, 2003)..... 5

Figure 2.2: 2D CFAR cells around a given cell with wind turbine present..... 7

Figure 3.1: Modelled turbine geometry (referenced to HAT)..... 13

Figure 3.2: Indicative Morecambe Generation Assets MDS layout with Mona Offshore Wind Project and Morgan Generation Assets and nearby oil and gas platforms with REWS..... 15

Figure 3.3: Morecambe Generation Assets REWS study area..... 18

Figure 3.4: The radar antenna elevation and azimuth patterns..... 20

Figure 3.5: Optical blockage and partial shadowing..... 22

Figure 3.6: Wind turbine layout at Hornsea Project One array area and the location of the radar system used in the study. The red area denotes the region shown in Figure 3.7 (Terma, 2021)..... 23

Figure 3.7: Compressed radar image in range-azimuth coordinates showing a zoomed area of the Hornsea Project One array area around a substation platform (Z13). A vessel is visible between Z13 and WTG G05. The signal level (in dB) is colour coded (Terma, 2021)..... 23

Figure 3.8: Power received by the REWS on ENI's Douglas platform..... 24

Figure 4.1: Modelled layout of the base case scenario showing the location of the existing windfarms and the coverage of the REWS in the region..... 27

Figure 4.2: ENI Energy's Douglas platform REWS clutter map showing returns from the wind turbines and sea clutter..... 29

Figure 4.3: ENI Energy's Douglas platform REWS detection threshold..... 31

Figure 4.4: Modelled power received from 420 m2 target (coverage)..... 34

Figure 4.5: ENI Energy's Douglas platform REWS detection plot showing loss regions for a 420 m2 target..... 37

Figure 4.6: Enlarged portion of the detection plot showing the effect of wind turbine shadowing..... 39

Figure 4.7: Harbour Energy's Millom West platform REWS clutter map showing returns from the wind turbines and sea clutter..... 41

Figure 4.8: Harbour Energy's Millom West platform REWS detection threshold..... 44

Figure 4.9: Harbour Energy's Millom West platform REWS detection plot showing loss regions for a 420 m2 target..... 46

Figure 4.10: ENI Energy's OSI REWS clutter map showing returns from the wind turbines and sea clutter..... 48

Figure 4.11: ENI Energy's OSI REWS detection threshold..... 51

Figure 4.12: ENI Energy's OSI REWS detection plot showing loss regions for a 420 m2 target..... 53

Figure 4.13: Spirit Energy's South Morecambe AP1 platform REWS clutter map showing returns from the wind turbines and sea clutter..... 55

Figure 4.14: Spirit Energy's South Morecambe AP1 platform REWS detection threshold..... 57

Figure 4.15: Spirit Energy's South Morecambe AP1 platform REWS detection plot showing loss regions for a 420 m2 target..... 59

Figure 4.16: Modelled layout of the Morecambe Generation Assets showing the indicative location of the wind turbines and the location of oil and gas platforms in the region..... 62

Figure 4.17: ENI Energy's Douglas platform REWS clutter map showing returns from the Morecambe Generation Assets wind turbines and sea clutter..... 64

[Figure 4.18: ENI Energy’s Douglas platform REWS detection threshold over the Morecambe Array Area.... 66](#)

[Figure 4.19: ENI Energy’s Douglas platform REWS detection plot showing loss regions for a 420 m2 target.69](#)

[Figure 4.20: Harbour Energy’s Millom West platform REWS clutter map showing returns from the Morecambe Generation Assets wind turbines and sea clutter. 71](#)

[Figure 4.21: Harbour Energy’s Millom West platform REWS detection threshold over the Morecambe Generation Assets Array Area..... 73](#)

[Figure 4.22: Harbour Energy’s Millom West platform REWS detection plot showing loss regions for a 420 m2 target..... 75](#)

[Figure 4.23: ENI Energy’s OSI REWS detection clutter map showing returns from the Morecambe Generation Assets wind turbines and sea clutter. 77](#)

[Figure 4.24: ENI Energy’s OSI REWS detection threshold over the Morecambe Generation Assets Array Area..... 79](#)

[Figure 4.25: ENI Energy’s OSI REWS detection plot showing loss regions for a 420 m2 target. 81](#)

[Figure 4.26: Spirit Energy’s South Morecambe AP1 platform REWS clutter map showing returns from the Morecambe Generation Assets wind turbines and sea clutter. 83](#)

[Figure 4.27: Spirit Energy’s South Morecambe AP1 platform REWS detection threshold over the Morecambe Generation Assets Array Area..... 85](#)

[Figure 4.28: Spirit Energy’s South Morecambe AP1 platform REWS detection plot showing loss regions for a 420 m2 target..... 87](#)

[Figure 4.29: Illustration of the dimensions of a typical 100GT vessel used for the shadowing analysis 89](#)

[Figure 4.30: Paths that are considered within the shadowing analysis 90](#)

[Figure 4.31: Results showing loss of detection of a vessel over 9 radar rotations due to turbine shadowing 93](#)

[Figure 4.32: Probability of losing a vessel in optical-shadowing over multiple radar rotations..... 93](#)

[Figure 4.33: Frequency distribution of the distances between targets and the shadow casting turbines 94](#)

[Figure 4.34: Target returns attenuation levels vs range from the shadow-casting tower 95](#)

[Figure 4.35: Power received from target and detection threshold vs range 95](#)

[Figure 4.36: Probability of losing a vessel over multiple radar rotations when considering diffraction and creeping wave effects 96](#)

[Figure 4.37: REWS study area for the cumulative assessment. 97](#)

[Figure 4.38: Modelled cumulative layout of the Morecambe Generation Assets with Mona Offshore Wind Project and Morgan Generation Assets showing the indicative location of the wind turbines and the location of oil and gas platforms in the region. 100](#)

[Figure 4.39: ENI Energy’s Douglas platform REWS clutter map showing returns from the wind turbines and sea clutter. 102](#)

[Figure 4.40: ENI Energy’s Douglas platform REWS detection threshold..... 104](#)

[Figure 4.41: ENI Energy’s Douglas platform REWS detection plot showing loss regions for a 420 m2 target.106](#)

[Figure 4.42: Harbour Energy’s Millom West platform REWS clutter map showing returns from the wind turbines and sea clutter. 108](#)

[Figure 4.43: Harbour Energy’s Millom West platform REWS detection threshold..... 110](#)

[Figure 4.44: Harbour Energy’s Millom West platform REWS detection plot showing loss regions for a 420 m2 target..... 112](#)

[Figure 4.45: ENI Energy’s OSI REWS detection clutter map showing returns from the wind turbines and sea clutter. 114](#)

[Figure 4.46: ENI Energy’s OSI REWS detection threshold. 116](#)

[Figure 4.47: ENI Energy’s OSI REWS detection plot showing loss regions for a 420 m2 target. 118](#)

[Figure 4.48: Spirit Energy’s South Morecambe AP1 platform REWS clutter map showing returns from the wind turbines and sea clutter. 120](#)

[Figure 4.49: Spirit Energy’s South Morecambe AP1 platform REWS detection threshold..... 122](#)

[Figure 4.50: Spirit Energy’s South Morecambe AP1 platform REWS detection plot showing loss regions for a 420 m2 target..... 124](#)

[Figure 5.1: Existing commercial routes within and around the Morecambe Generation Assets Array Area. 130](#)

[Figure 5.2: Existing ferry routes within and around the Morecambe Generation Assets Array Area. 131](#)

[Figure 5.3: Modelled existing shipping routes \(1,000 variations each route\). 133](#)

[Figure 5.4: Modelled shipping routes post-construction of the Morecambe Generation Assets. 136](#)

[Figure 5.5: Modelled shipping routes post-construction of the Morecambe Generation Assets with Mona Offshore Wind Project and Morgan Generation Assets cumulatively. 138](#)

[Figure 5.6: Modelled yearly alarm rates for the Conwy platform. 139](#)

[Figure 5.7: Modelled yearly alarm rates for the Douglas Complex. 139](#)

[Figure 5.8: Modelled yearly alarm rates for the Hamilton platform. 140](#)

[Figure 5.9: Modelled yearly alarm rates for the Hamilton North platform. 140](#)

[Figure 5.10: Modelled yearly alarm rates for the Lennox platform. 140](#)

[Figure 5.11: Modelled yearly alarm rates for the OSI. 140](#)

[Figure 5.12: Modelled yearly alarm rates for the Calder platform. 141](#)

[Figure 5.13: Modelled yearly alarm rates for the Millom West platform. 141](#)

[Figure 5.14: Modelled yearly alarm rates for the North Morecambe platform. 141](#)

[Figure 5.15: Modelled yearly alarm rates for the South Morecambe CPC. 141](#)

[Figure 5.16: Modelled yearly alarm rates for the South Morecambe DP6 platform. 142](#)

[Figure 5.17: Modelled yearly alarm rates for the South Morecambe DP8 platform. 142](#)

[Figure 6.1: Layout of the modelled platforms and the communication links considered. 146](#)

[Figure 6.2: Geometry and parameters used in the wind turbine bistatic RCS modelling. 148](#)

[Figure 6.3: Bistatic RCS modelling results of the proposed MDS wind turbine. 148](#)

[Figure 6.4: Illustration of the nearfield and diffraction exclusion zones. 150](#)

[Figure 6.5: The signal to noise ratio around the Douglas – Hamilton link. 151](#)

[Figure 6.6: Illustration of the refraction exclusion zone resulting in C/I less than 33 dB. 151](#)

[Figure 6.7: Simplified illustration of all exclusion zones around the Douglas – Hamilton link. 152](#)

Glossary

Term	Meaning
Allision	The act of striking or collision of a moving vessel against a stationary object.
Clutter	Clutter is the term used for unwanted echoes in electronic systems, particularly in reference to radars. Such echoes are typically returned from ground, sea, rain, animals/insects, chaff and atmospheric turbulences, and can cause serious performance issues with radar systems.
Doppler signature	Doppler signature is the parameter used by Doppler enabled radars to produce velocity data about objects at a distance. It does this by bouncing a microwave signal off a desired target and analysing how the object's motion has altered the frequency of the returned signal. This variation gives direct and highly accurate measurements of the radial component of a target's velocity relative to the radar.
Hops	In relation to microwave communication links, hops refer to the number of transient stations that a communication signal needs to travel to (to be amplified, redirected and retransmitted) before reaching its final receiver location.
Radar Cross-Section (RCS)	RCS is the measure of a target's ability to reflect radar signals in the direction of the radar receiver. An object reflects a limited amount of radar energy back to the source. A larger RCS indicates that an object is more easily detected.
Radar returns	The electromagnetic signal that has been reflected back to the radar antenna. Such reflections contain information about the location and distance of the reflecting object.
Radar shadow	Radar shadow is the region whereby the radar beam is unable to fully illuminate a region due to blockage from terrain or structures within the area of coverage. Radar shadowing causes objects within the shadow region to produce reduced radar returns which can affect the radar's ability to detect such objects.
Target detection	A radar's ability to distinguish between radar returns from wanted targets and returns from clutter and/or the system's noise level.

Acronyms

Acronym	Description
AD	Air Defence
AIS	Automatic Identification System
AMSL	Above Mean Sea Level
ATC	Air Traffic Control
C/I	Carrier-to-interference ratio
CA	Constant Averaging
CAD	Computer Aided Design
CFAR	Constant False-Alarm Rate
CPA	Closest Point of Approach
ERRV	Emergency Response and Rescue Vessels

MORECAMBE OFFSHORE WINDFARM GENERATION ASSETS

Acronym	Description
IALA	International Association of Marine Aids to Navigation and Lighthouse Authorities
LAT	Lowest Astronomical Tide
LoS	Line of Sight
MDS	Maximum Design Scenario
MTI	Moving Target Indicator
NUI	Normally Unmanned Installation
OSI	Offshore Storage Installation
RCS	Radar Cross Section
REWS	Radar Early Warning System
TCPA	Time to the Closest Point of Approach
UHF	Ultra-High Frequency
VTS	Vessel Traffic Services

Units

Unit	Description
%	Percentage
°	Degrees
dB	Decibel
dBm ²	Decibel square metres
ft	Feet
GHz	Gigahertz
GT	Gross tons
hr	Hours
kHz	Kilohertz
m	Metre
m ²	Square metres
km	Kilometre
kt	Knot
kW	Kilowatt
mm	Millimetres
ms ⁻¹	Metres per second
MW	Megawatt
nm	Nautical miles
ns	Nanoseconds

MORECAMBE OFFSHORE WINDFARM GENERATION ASSETS

Unit	Description
RPM	Rotations per minute

RADAR EARLY WARNING SYSTEMS AND MICROWAVE COMMUNICATION LINKS TECHNICAL REPORT

1 INTRODUCTION

1.1 Overview

- 1.1.1.1 This updated document is an annex to Chapter 17 Infrastructure and Other Users of the Environmental Statement (Document Reference 5.1.17) and considers the potential effect of the Morecambe Offshore Windfarm Generation Assets (hereafter referred to as ‘Morecambe Generation Assets’ or ‘the Project’) on Radar Early Warning Systems (REWS) and Line of Sight (LoS) microwave communication links located on offshore oil and gas platforms during the operations and maintenance phase. The document was updated to take into account comments made by Spirit Energy in their Relevant and Written Representations. Specifically, this annex considers the effects of the Morecambe Generation Assets on the ability of REWS to detect vessels within the vicinity of the windfarm and the effect of rerouted traffic on the REWS alarm rates. There may be effects associated with the construction and decommissioning phase of the Morecambe Generation Assets in regard to increased vessel movement within the Morecambe Array Area (windfarm site). This is not within the scope of this study as it needs detailed data regarding vessel movement during the construction and decommissioning phases, which might be governed by separate agreements between the REWS operators and the Applicant. As such, this assessment considers the Maximum Design Scenario (MDS) for the operations and maintenance phase of the Project.
- 1.1.1.2 REWS uses the radar returns to monitor and track vessels within the detection region and alert the operator when a proximity violation or an allision threat is detected. The modelling work presented within this report considers a REWS configuration, which was based on technical information provided by the REWS operators (see section 3.5). It addresses the effects of the Morecambe Generation Assets (assessed in isolation and cumulatively) on vessel detection due to raised thresholds, clutter returns and radar shadowing effects generated from the wind turbines. (see section 4.3.1). The updated report presents additional modelling results to assess the impact of shadowing in more detail to assess the detection and tracking performance of the REWS within the shadow regions (see Section 4.3.2). The REWS also uses a defined set of rules to identify a breach of the Closest Point of Approach (CPA) and Time to Closest Point of Approach (TCPA) alarms. This report presents modelling work and analysis results that aims to predict the effect of traffic rerouted as a result of the presence of the operational Morecambe Generation Assets on the CPA/TCPA alarm rates.
- 1.1.1.3 The report considers four REWS installations that are in proximity to the Morecambe Array Area. The four identified platforms are operated by Harbour Energy (Millom West platform), ENI UK Ltd. (Douglas platform and the Offshore Storage Installation (OSI)) and Spirit Energy (South Morecambe AP1 platform). These four REWS installations provide radar coverage and protection for a number of other nearby offshore platforms (i.e. Conwy, Douglas DA, Douglas DW, Hamilton, Hamilton North, Lennox, Calder, North Morecambe DPPA, South Morecambe CPP1, South Morecambe DP1, South Morecambe DP6 and South Morecambe DP8).
- 1.1.1.4 This report also provides the technical information and modelling results considering the potential cumulative impact of the Morecambe Generation Assets in combination with other projects currently present in the region and potential future projects; namely Mona Offshore Wind Project and Morgan Offshore Wind Project Generation Assets (hereafter referred to as ‘Morgan Generation Assets’) . The proposed Awel y Môr offshore wind farm is also located in the study area, however, no modelling was

undertaken for this wind farm as it is located sufficiently far from the Project and is not expected to add to the potential impact on the REWS when considering the cumulative assessment.

- 1.1.1.5 Additionally, offshore oil and gas platforms often use microwave communications links to transmit operational data and communicate status and other critical information regarding the operation and maintenance of these platforms. However, offshore windfarms may be located within the same regions of the oil and gas platforms and may interfere with the performance of the link and may reduce the effectiveness and efficiency of communication protocol.
- 1.1.1.6 This assessment considers the potential impact of the proposed Morecambe Generation Assets on the existing microwave communications links onboard the ENI Energy platforms and the Spirit Energy Platforms operating in the Irish Sea.

1.2 Background

- 1.2.1.1 Wind turbines and associated offshore structures (such as Offshore Substation Platforms (OSPs)) located within the LoS of radars, may interfere with the radar performance and degrade its ability to distinguish between the wind turbines and associated offshore structures, and returns from targets of interest.
- 1.2.1.2 REWS are primarily used to detect and track vessels navigating in the vicinity of offshore oil and gas assets and provide collision warning when vessels are in breach of defined CPA and TCPA parameters. The impact of offshore windfarms on REWS may arise from a number of factors such as high radar returns from the wind turbines and associated offshore structures, increased number of detections and false alarm/track generation.
- 1.2.1.3 Offshore wind turbines are large structures with geometries and materials that may cause them to have a high radar cross-section (RCS). Furthermore, the rotation of the wind turbine blades produces a time-variable RCS fluctuation and a Doppler frequency shift that can confuse radars that rely on moving target indicator (MTI) filters to distinguish between static objects and moving targets of interest. The interference to Doppler based Air Traffic Control (ATC) and Air Defence (AD) radars due to the rotating blades and the large reflection of the radar signal has been well reported and explained (Jago and Taylor, 2002; Poupart, 2003; Wind Energy, Defence & Civil Aviation Interests Working Group, 2002). However, this technical report discusses and models the potential impact of the Morecambe Generation Assets on the REWS used on oil and gas platforms which have been identified as potentially being affected by the Morecambe Generation Assets due to their location. Typically, REWS does not employ Doppler processing and MTI filters as it operates in naval environments whereby the returns from the sea surface (and the movement of the waves) may generate radar returns with Doppler signatures similar to that of surface vessels. REWS can be integrated with newer radar transceivers that are capable of Doppler processing if deemed necessary.
- 1.2.1.4 For non-Doppler based radars such as the REWS, the potential impact from offshore windfarms may arise due to the large radar returns. The large RCS of wind turbines may cause target spreading at extended ranges and potential detections through the sidelobes at close ranges. This will cause smearing and cluttering of the radar screen and potentially mask other targets in the area. In addition, depending on the thresholding techniques used within a radar system, the presence of wind turbines and associated offshore structures may increase the threshold over parts of Morecambe Array Area, which potentially may cause smaller targets to be lost.

- 1.2.1.5 Degradation of the radar performance may also be caused by the radar shadow due to the presence of wind turbines within the LoS of the radar, as shown in [Figure 2.1](#)~~Figure 2.1~~. Shadowing may cause smaller targets to temporarily disappear from the radar display as it moves in and out of the shadow regions. The extent of the impact caused by shadowing depends on the size and height of the wind turbine and the target of interest (i.e. different effects may be observed if looking at surface targets or air targets). However, previous studies and trials showed that the effect of shadowing can be considered to be an effect of secondary importance that may have little impact on the REWS performance due to the size of vessels that the REWS is typically interested in detecting (Butler and Johnson, 2003; Greenwell, 2016).
- 1.2.1.6 This report uses modelling techniques developed at the University of Manchester to model and predict the impact of wind turbines and associated offshore structures on radar systems. These models have been verified and were compared against real-life radar and RCS measurements and it is noted that the modelling results showed very good correlation with measurements (Danooon 2014, 2018). The models used within this report allow the radar returns coming both from the wanted target and the Morecambe Generation Assets to be simulated so that the effects on radar detection can be evaluated. The results from the models can then be used to indicate the regions within which vessels can be detected and tracked. Section 3 below describes the different modelling techniques utilised in the assessments.

2 SCOPE OF ASSESSMENT

2.1 Target masking

2.1.1.1 The size, geometry and construction materials of wind turbines cause them to have a very large radar return. This may cause target spreading (smearing) at extended ranges and potential detections through the sidelobes at close ranges. Such effects will add clutter to the radar screen and potentially mask other targets in the area. This may also affect the tracking software performance when vessels are travelling within the Morecambe Array Area causing the radar tracks of vessels to be seduced and merged into the larger returns generated from the wind turbines. This report addresses the impact of target masking and compares the levels of the wind turbine radar returns against that of a typical vessel within the radar detection range. This report does not consider the effects of varying wind turbine returns on the tracker as this requires a detailed knowledge of the employed tracking software, which is proprietary information (discussed further in paragraph 2.5.1.1). Despite this, it remains possible to draw robust conclusions.

2.2 Shadowing effects

2.2.1.1 The extent and length of the shadow region cast by a wind turbine depends on the size of the wind turbine, the distance to the radar antenna, the height of the radar and the height of the target of interest. The severity of the shadow will also depend on the distance of the target from the wind turbine. This is illustrated in [Figure 2.1](#) ~~Figure 2-1~~.

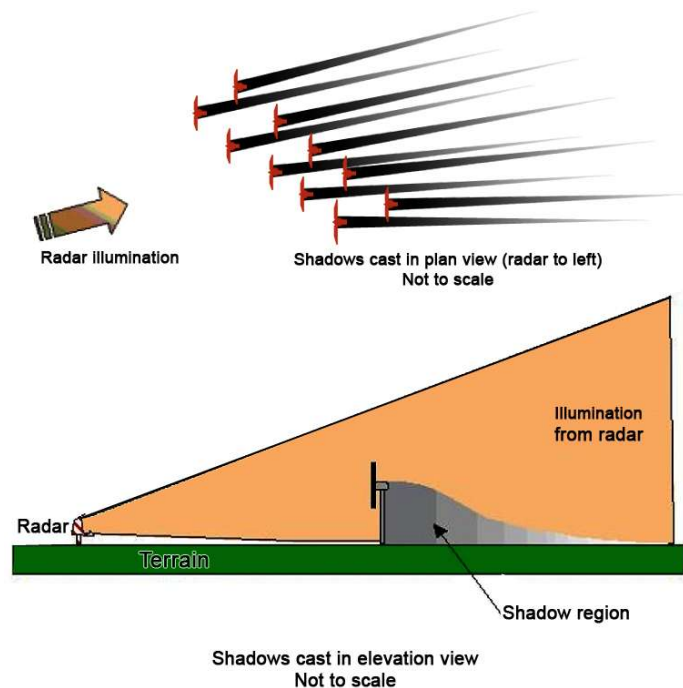


Figure 2.1: Illustration of radar shadowing with diffraction effects (Butler and Johnson, 2003).

2.2.1.2 Due to the diffraction of the radar waves around the wind turbine, increasing the range between the target and the wind turbine will reduce the severity of the attenuation to the target's returns. It has been reported that a target 1km behind the wind turbine will experience a 6dB reduction in the returned power while targets that are significantly

further suffer only 2dB reduction in the received radar echo (Butler and Johnson, 2003). This is an important characteristic of the radar shadow and is illustrated in [Figure 2.1](#)~~Figure 2.1~~. This is in good agreement with the recent measurement campaign carried out by Ultra Electronics to assess the effects of windfarms on the REWS performance located in the east Irish Sea (Greenwell, 2016). The measurement campaign and the work presented in Danoon and Brown (2014) indicate that shadowing may not have a significant effect on the performance of the REWS due to the diffraction effects and the size of the vessel, which might be larger than the shadow region generated from individual wind turbines.

2.2.1.3 For completeness, [and to address some of the comments by Spirit Energy \(Table 2.1\)](#), a shadowing assessment has been undertaken within this assessment and is used in conjunction with the study of the rerouting of traffic around the Morecambe Generation Assets (see section 2.3). Within this assessment the radar shadows were modelled based on [both](#) optical shadowing [and approximations for diffraction effects](#). Optical shadows conservatively assume no diffraction effects and therefore ignore the improvement in the shadow region at extended ranges. Depending on the wind turbine size and radar height, the optical shadows may extend all the way to the radar horizon. ~~The use of optical~~[Optical](#) shadows ~~is was~~ used to assess scenarios which might have an impact on the radar's performance. [while diffraction approximations were used to assess the likelihood of target losses at extended ranges. Details of the modelling parameters and results are presented in Section 4.3.2.](#)

2.3 Rerouted traffic

2.3.1.1 Some of the existing shipping routes will be altered by the physical presence of the Morecambe Generation Assets, and vessels may be rerouted nearer to existing platforms covered by the REWS as they deviate around either project (as shown in [Figure 4.20](#)~~Figure 4.20~~ and described in detail within Appendix 14.1 Navigation Risk Assessment of the Environmental Statement (Document Reference 5.2.14.1). This may cause an increase in the CPA/TCPA alarm rates. The effects of the rerouting of traffic on the alarm rates are discussed in section 6.

2.4 Adaptive detection threshold modelling

2.4.1.1 A REWS deploys a number of techniques for clutter thresholding, target extraction and tracking. The use of adaptive thresholding algorithms such as Constant False Alarm Rate (CFAR) is very common within offshore REWS installations. A variety of CFAR algorithms can be used to adjust the threshold around noisy/cluttered areas to avoid unwanted and false detections depending on the clutter within the local environment. REWS uses CFAR techniques to dynamically adjust the detection threshold over sea and rain clutter. Digital signal processing is applied to calculate a constant false alarm rate for plot-extraction by generating a radar threshold below which all radar samples are ignored as they are considered to be noise or clutter. The threshold is calculated individually for each radar cell using a two-dimensional sliding window area technique whereby surrounding cells in both range and azimuth are considered. Typically, the mean and standard deviation of samples is calculated, and the threshold is set to the mean value plus a factor derived from the standard deviation of the sample.

2.4.1.2 Finally, it is worth noting that as CFAR uses multiple adjacent range and azimuth cells (see [Figure 2.2](#)~~Figure 2.2~~) to derive the detection threshold, the presence of a single turbine will affect the threshold of multiple cells around it as shown in [Figure 2.2](#)~~Figure 2.2~~.

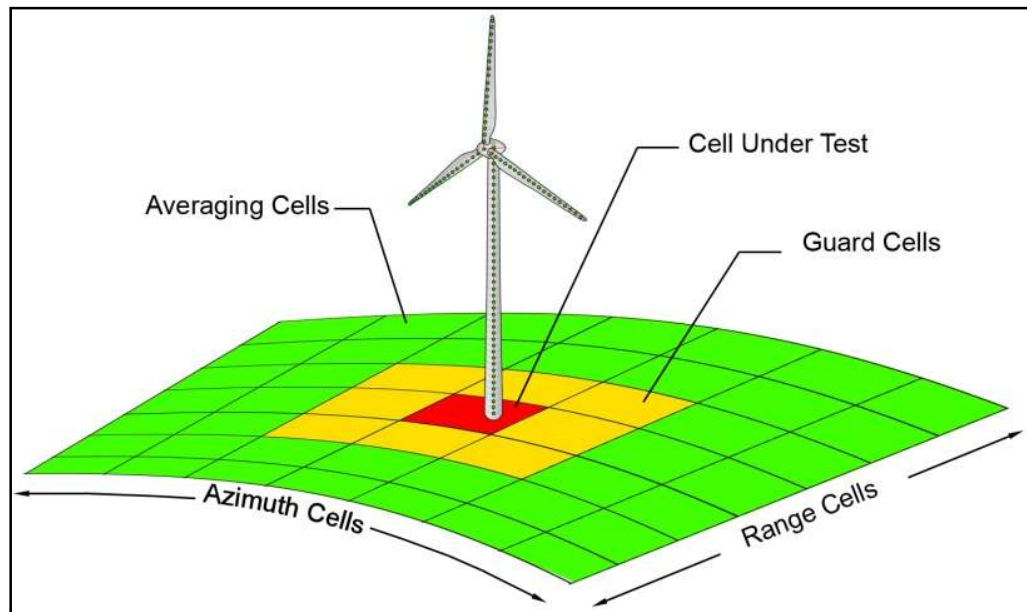


Figure 2.2: 2D CFAR cells around a given cell with wind turbine present.

2.5 Tracker modelling

2.5.1.1 Radar trackers provide the radar operator with a processed and clear image of the location and bearing of moving targets in the area of interest. It is also very common for currently used radar trackers to compensate for momentary loss of detection of a target over multiple radar rotations and maintain an active track. The presence of advanced tracking within REWS can greatly benefit and enhance the operator’s ability to maintain radar visibility of moving targets near or within a windfarm. REWS deploy proprietary tracker algorithms, which may vary depending on the system supplier. The impact of the windfarm on the tracker performance cannot be accurately modelled without detailed knowledge of the tracker and the proprietary tracking algorithms - which are not available for this assessment and so were not included in this assessment. However, it is expected that the tracker software along with integration of Automatic Identification System (AIS) within the REWS data will enhance the detection and tracking of vessels within the Morecambe Generation Assets.

2.6 Ultra-High Frequency communication links

2.6.1.1 Depending on the REWS system and the tracker software, it is possible that returns from the wind turbines will add new target detections to the track-table. The track-tables are shared with Emergency Response and Rescue Vessels (ERRVs) via ultra-high frequency (UHF) radio links. UHF links use a low-bandwidth telemetry system and have a limit on the total number of tracks that can be transmitted. The maximum size of the track-table is a system limitation that depends largely on the hardware used and hence cannot be modelled. A typical number for the maximum track-table size is assumed to be between 400 and 600 tracked targets. Depending on the tracking software, the number of tracks within the track-table can be reduced by applying non-acquire zones over the windfarm area or by applying filters to track moving targets only. UHF communications are different and separate systems than the radar. They operate at different frequencies than the radar frequency and use different modulation techniques to transmit and receive data. Therefore, the potential impact of windfarms

on the performance of UHF communication systems cannot be modelled and assessed using the radar models used within this assessment. As such, the effects of the Morecambe Generation Assets on UHF communication links are considered outside the scope of this work.

2.7 Other effects

- 2.7.1.1 False tracks may be initiated due to the variation of the wind turbines' radar returns over multiple range-cells. However, the radar tracker requires consecutive detections over a number of radar rotations, which will reduce the likelihood of false track initiation. Furthermore, to raise a TCPA alarm, the track vector must continue to breach the TCPA condition for multiple radar rotations. Thus, raising false alarms due to range-cell spreading is considered very unlikely and was not included in this assessment.
- 2.7.1.2 It is also possible to model the effects of multiple reflections of the radar signal within the Morecambe Array Area, and between the wind turbines and nearby large targets, using the radar and WinR (Wind Turbine RCS) models developed at the University of Manchester. However, as the closest modelled turbine in the Morecambe Array Area is approximately 2km away from the nearest REWS, the effects of the multiple reflections were considered to be of second order (not a primary cause or concern) and were not included in the models (QinetiQ, 2005; Baker, 2007).
- 2.7.1.3 Depending on the detailed structure of the REWS host platform, the presence of external fittings near the radar antenna such as masts, wires and other structural elements may cause distortion of the antenna pattern and possibly the appearance of false reflection if a flat surface is near the antenna. The inclusion of such structures will greatly increase the modelling complexity and is not expected to affect the overall findings of the assessment. Therefore, these effects were not modelled.

2.8 Spirit Energy comments and report updates

- 2.8.1.1 The report was updated following the written relevant representation by Spirit Energy (EN010121-000448-Spirit - Morecambe OWL RR - Final 19082024(231931631.1) 1.pdf). Table 2.1 summarises the comments and the updates to the modelling procedures and results within the report.

Table 2.1: Relevant representation by Spirit Energy and report updates.

Observations/corrections	Updates/Comments
<p><u>The Closest Point of Approach (CPA) and Time to Closest Point of Approach (TCPA) for Amber/Red alarms used for modelling the impact for Spirit is different to the actual distances and times used. Spirit has the following alarms set for all manned and unmanned installations (apart from DPPA):</u></p> <ul style="list-style-type: none"> • <u>“AMBER” alarms at a CPA of 0.27nm. (0.27 nm = 500 metres) and a TCPA of 45 minutes</u> • <u>“RED” alarms at a CPA of 0.27 nm. (0.27 nm = 500 metres) and a TCPA of 30 minutes</u> <p><u>Note: DPPA warning times are reduced on an Amber Alarm to 30.4 minutes due to Walney 1 and 2 Windfarms.</u></p> <p><u>The study for REWS modelling sets the following parameters for manned installations; an Amber TCPA alarm is raised if a vessel is 40 minutes away and a Red alarm is raised if the vessel is 30 minutes away. For normally un-manned installations (NUI) an Amber TCPA alarm is raised if a vessel is 25 minutes away and a Red alarm is raised if the vessel is 15 minutes away.</u></p> <p><u>With the reduction of the TCPA time for raising the alarm, the effective REWS coverage distance can be reduced significantly especially for NUI installations, where the coverage can be reduced for a vessel travelling at 12 knots speed from 9nm (45 min TCPA) down to 5nm (25 min). The reduced modelled distances would compromise safety and that further assessment will be required with the correct alarm distances (noted above) that are the performance standard safe distances for management of collision risk.</u></p>	<p><u>Taking into account the parameters provided by Spirit Energy, the modelling parameters were amended to match with the REWS settings by Spirit Energy.</u></p> <p><u>The update of the parameters resulted in less alarm rates due to the reduction of the Amber CPA zone. The updated results of the study are presented in Section 5.5</u></p>
<p><u>The assessment of shadowing effects considers only vessels passing behind the shadowed sector along the edge of the windfarm / wind turbines. Maritime and Coastguard agency guidance MGN 543 (Offshore Renewable Energy Installations (OREIs) - Guidance on UK Navigational Practice, Safety and Emergency Response) indicates that merchant vessels can pass through OREIs (Offshore Renewable Energy Installations). The presence of OREIs will degrade the ability to identify such vessels. The study indicates that each shadow sector could be as wide as 20m which is significantly wider than a 1000 GRT vessel which can pass through the windfarm array without being detected by the REWS system. This will result in significant delay for REWS system to issue TCPA alarms, resulting in inability for Spirit to maintain Safety Case Performance Standard for vessel collision. With close proximity of the windfarm, and assuming that it will be positioned 1.5nm from the Central Processing Complex, a vessel travelling at 12 knots speed might only be detected as late as 7.5 minutes from collision with the Central Processing Complex.</u></p>	<p><u>Shadowing is expected to occur, and it is also expected to have some impact on the REWSs’ ability to detect vessels within the shadow regions. However, moving objects are expected to experience momentary loss of detection due to the shadowing effect. Additionally, the intensity of the radar shadow decreases at extended ranges, which may reenable target detection.</u></p> <p><u>As such, the study looked at the effect of shadowing on the detection of moving vessels. The results of the shadowing analysis are presented in Section 4.3.2</u></p>

<u>Observations/corrections</u>	<u>Updates/Comments</u>
<p><u>A vessel with 1000 GRT travelling within the windfarm will have significantly smaller area than 1000m². Assuming vessel with circa 14m breadth and height of superstructure of 30m, the target size will be 420m².</u></p>	<p><u>The study was updated to consider the detection performance for targets that has an RCS of 420m². The results indicate that no significant change was noted in the detection performance of the REWS. The results are presented in Section 4.3.1 and Section 4.4.</u></p>
<p><u>It is assumed that a vessel travelling within the windfarm should be supported by the tracker software and AIS system which cannot be relied on as an effective mean of the vessel monitoring. To use the tracker software the vessel should be acquired by the REWS system prior to entering the windfarm to allow further monitoring of the vessel movement. To enable such approach all vessels travelling in the direction of the windfarm from South/South-East/South-West should be selected by the REWS system for further monitoring.</u></p>	<p><u>Typical REWS installations would integrate the radar returns with the AIS data. At the time of issue of this report, no further information obtained regarding the details of the REWS system and the availability/integration of AIS data.</u></p>
<p><u>Also, such approach does not negate the scenario in which a vessel “appears” from the windfarm 1.5nm / 7.5min (travelling at 12 knots speed) from collision with the Central Processing Complex platform. Such monitoring potentially requires a new full-time role offshore and modification for the existing REWS to enable such functionality. The Central Processing Complex REWS does not have an AIS system and the tracking system noted in the Applicant’s mitigation measures and therefore currently cannot perform in the way envisaged by the assessment.</u></p>	
<ul style="list-style-type: none"> <u>• It is also worth noting that AIS system has its own limitations like following:</u> <u>• It must consider that positional data contained within the transmissions may be inaccurate.</u> <u>• AIS data is also susceptible to spoofing or jamming.</u> <u>• If an AIS unit is malfunctioning onboard the vessel, there are chances the navigator may receive false data, thus might not be aware of the actual position of the virtual aid to navigation.</u> <u>• There can be GPS errors causing positional inaccuracies.</u> <u>• Equipment installed onboard the offshore platform may not show them at all.</u> <u>• Control Room personnel may not be properly trained/ familiar with AIS</u> 	

<u>Observations/corrections</u>	<u>Updates/Comments</u>
<p><u>The assessment assumptions state that “there will be small gaps in the detection map due to the elevated thresholds and shadowing effects from the wind turbines, however these effects will be largely mitigated”. The assessment does not take into account vessels travelling through the Project, nor that all proposed mitigations – REWS Tracking techniques and AIS data tracking is not available on the Central Processing Complex. In addition, the offshore manning would need to be increased to ensure 24/7 effective vessel tracking and management of collision risks.</u></p>	<p><u>As radar processing and tracking algorithms are proprietary information, the specific tracking algorithm used within the Spirit Energy REWS cannot be assessed directly. However, since the primary function of REWS is to detect and track vessel and issue alarms if a safety criterion is breached, it must be noted that all REWS involves signal processing and tracking to enable the alarm functions.</u></p> <p><u>Hence, this study can only provide qualitative assessment on the detection performance, which is based on typical tracking algorithm performance.</u></p>
<p><u>This paragraph suggests that shadow sectors from turbine nulls varies between 4m and 15m, yet paragraph 3.8.1.3 suggests 20m, which would fully exceed the width of the 1000 GRT vessel heading through the windfarm. This inconsistency should be clarified.</u></p>	<p><u>The updated report looks at the effects of shadowing generated by the proposed project based on the MDS parameters. The updated modelling results now consider the effect of shadowing on the detection of moving vessels. The results of the shadowing analysis are presented in Section 4.3.2</u></p>

2.8.2

3 MODELLING PARAMETERS

3.1 Wind turbine parameters

3.1.1.1 The maximum dimensions of the wind turbines proposed for Morecambe Generation Assets have been defined in the MDS in Chapter 5 Project Description of the Environmental Statement (Document Reference 5.1.5), and are shown in [Table 3.1Table 3.1](#).

3.1.1.2 In order to accurately predict the RCS of wind turbines at different orientations and ranges, the wind turbines need to be modelled as continuous curved surfaces that represent the geometry of the wind turbine. This includes the shape of the tower, the nacelle and the airfoil profile of the blades. However, the MDS only provides the main features and dimensions of the wind turbines, and it does not provide details of the tower, blades, nacelle and hub geometries. Therefore, to undertake this study and to better model the RCS of the wind turbines, a realistic model of pre-existing turbine surfaces was used. This was achieved by using a realistic blade shape and airfoil profile of a 5MW turbine that was scaled up to match the MDS parameters. The shape of the nacelle, hub and tower were also scaled to match the MDS turbines. The resultant scaled turbine matches the MDS parameters and has a realistic geometry that can then be used to model the RCS and radar returns.

3.1.1.3 The scaled Computer Aided Design (CAD) geometries for the modelled turbines (i.e. 35 turbines with a rotor diameter of 260m and a hub height of 155m above Highest Astronomical Tide (HAT) (159.82m above Mean Sea Level (MSL)) used to compute the RCS of the wind turbines are shown in [Figure 3.1Figure 3.1](#) below. Details such as ladders, warning lights, wind measurement/lightning protection equipment etc. were removed from the wind turbine CAD for RCS modelling as these will not have a significant effect on the scattering profile which is dominated by the larger components (i.e. tower, blades and nacelle), and will greatly increase the computational complexity.

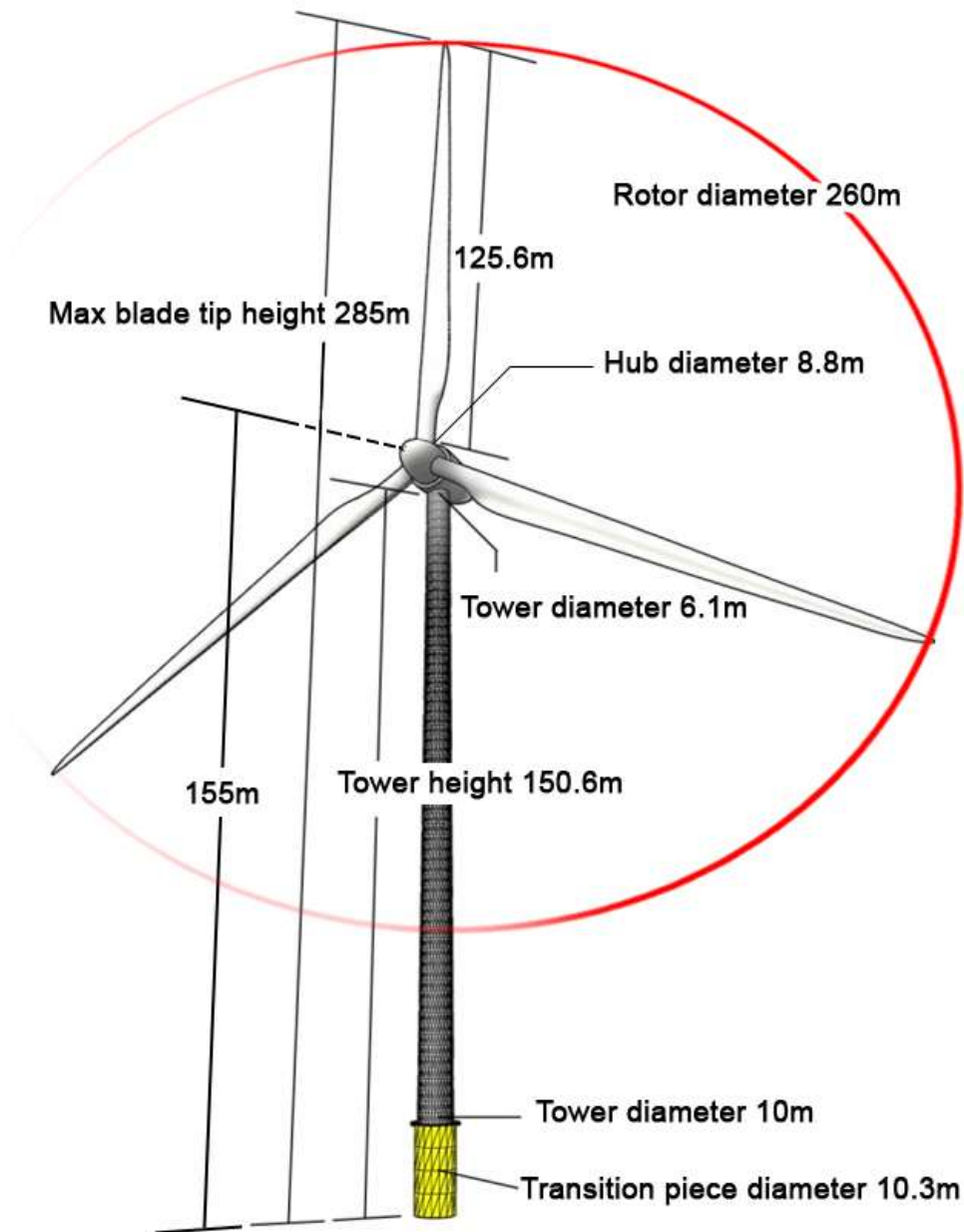


Figure 3.1: Modelled turbine geometry (referenced to HAT).

3.1.1.4

Within this assessment, it has been assumed that the wind turbines are mounted on a monopile foundation with a transition piece leading to the tower. Traditionally, a monopile with the transition piece design gives a very large radar return, which in some cases might dominate the wind turbine RCS. This is due to the shape and construction materials of the transition piece which makes it highly reflective to the radar. The upright cylindrical and parallel, metallic sides of the transition piece will reflect the radar energy directly to the radar which may make up to 80% of the total radar signature generated from the wind turbine. Other supporting structures, such as jacket foundations are expected to have tapered sides and smaller reflective areas which will not be as prominent as a monopile foundation. Monopile foundations therefore have been modelled to provide a worst-case modelling scenario. The MDS layout of the wind turbines is presented in [Figure 3.2](#), which shows an indicative layout of the Morecambe Generation Assets. This indicative layout takes into account

embedded mitigation that no wind turbines or offshore substation platforms would be located within 1.5nm of oil and gas platforms with a helicopter deck, or within 500m of pipelines, umbilicals or cables. This indicative layout was used for the assessment of the proposed project in isolation and cumulatively with Mona Offshore Wind Project and Morgan Generation Assets.

- 3.1.1.5 The exact layout for the turbines within the Mona Offshore Wind Project and Morgan Generation assets were not available for inclusion in the study. However, in order to undertake the cumulative assessment, the layouts were produced inhouse and were based on publicly available data such as the site boundaries, number of turbines, minimum separation and the proposed size of the turbines within the MDS of these projects. This is discussed further in Section 4.4.2.
- 3.1.1.6 When assessing the potential impact of the Morecambe Generation Assets in isolation, and in combination with other projects in the assessment area, the wind is conservatively assumed to be coming from the radar site in the direction of the centre of the Morecambe Array Area. This results in the majority of the wind turbines facing the radar, which will then give the maximum RCS value. As the RCS of each wind turbine is individually computed, the blades' rotation angle on each wind turbine is generated randomly as a value between 0° and 119°. This results in a different RCS for each wind turbine rather than an unrealistic unified rotation angle across all turbines.

MORECAMBE OFFSHORE WINDFARM GENERATION ASSETS

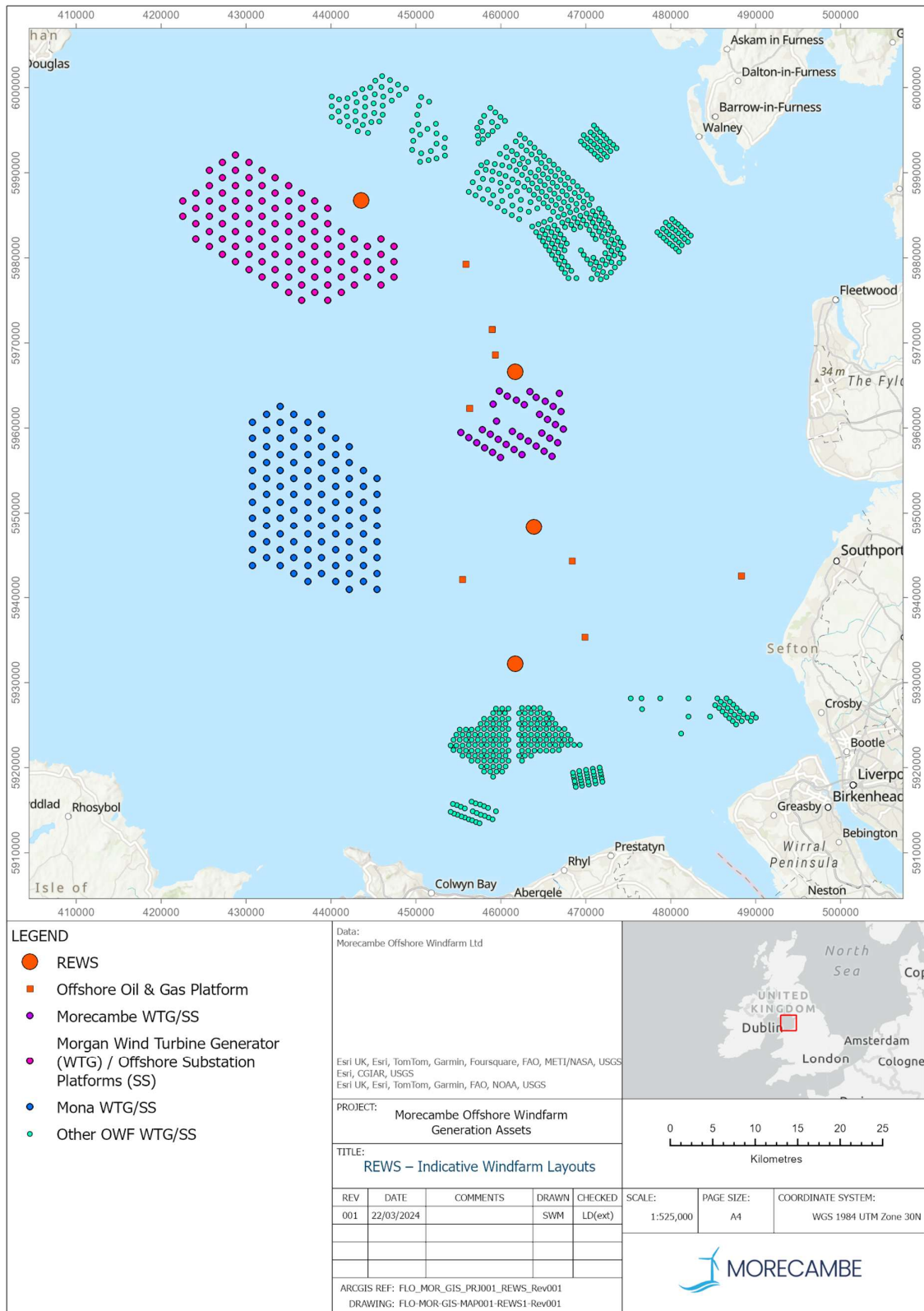


Figure 3.2: Indicative Morecambe Generation Assets MDS layout with Mona Offshore Wind Project and Morgan Generation Assets and nearby oil and gas platforms with REWS.

3.2 Windfarm parameters

3.2.1.1 A summary of the MDS parameters for the REWS modelling for the Morecambe Generation Assets is presented in ~~Table 3.1~~~~Table 3.4~~. A layout option of 35 smaller turbines was selected for this study rather than a layout with 30 larger turbines. This layout was chosen as it is expected to be the worst-case scenario for the radar. The increase in the physical size of the turbine will cause a larger radar echo, however, it is not expected to cause more significant adverse effects on the shadowing or the loss of detection around the turbine. However, having more turbines will increase the shadowing zones and will also introduce more blind zones within the REWS detection region.

3.2.1.2 It is noted that there is a discrepancy of 5m for the maximum blade tip height (290m vs 285m) and maximum hub height (160m vs 155m) in parameters used in the model compared to the maximums secured within the draft DCO, this is a result of the model being produced before the air gap was increased from 20m to 25m. However, it should be noted that the model attempts to use realistic geometries for the turbines. The exact scattering profile will vary depending on many factors such as the details of the geometry, aerofoil of the blade and the blade bending due to wind loading. Therefore, for the purposes of this assessment, the small difference in the maximum heights is not expected to significantly affect the general scattering characteristics/levels and will still provide valid modelling results.

Table 3.1: MDS parameters for the REWS modelling.

Morecambe Generation Assets parameter	Value
Maximum number of wind turbines	35
Rotor diameter	260 m
Hub height (centre point)	155 m above highest astronomical tide (HAT)
Hub height (lowest point)	150.6 m above HAT
Maximum blade tip height	285 m above HAT
Blade length	125.6 m
Turbine tower upper diameter	6.1 m
Turbine tower lower diameter	10 m
Transition piece diameter	10.3 m
Number of offshore substations platforms within the array area	2
Maximum dimensions of offshore substation platforms	50 m (length) x 50 m (width) x 70 m (height)
Total RCS of offshore substations and platforms	3,500 m ²

3.3 Morecambe Generation Assets indicative wind turbine and offshore substations/platform layouts

3.3.1.1 ~~The~~An indicative worst-case layout of the Morecambe Generation Assets was imported into the models using proposed coordinates for each wind turbine and

offshore substation platform. The locations of the offshore substation platforms and the imported turbine locations are shown in [Figure 3.2](#)~~Figure 3.2~~.

3.3.1.2 Two offshore substation platforms are allocated within the envelope proposed windfarms. The exact geometry and location profile of the substations is not defined at this stage and is not considered to be of significant importance to the radar modelling results. However, when considering offshore substations, it is important to include an approximated source of radar echoes and a structure that will cast a radar shadow. Therefore, the modelling results that are shown within this report assume that the offshore substation platforms are large offshore structures. The radar scattering from the substations was estimated by modelling a number of scattering points distributed within a rectangular box. The dimensions of the offshore substation platforms are presented in [Table 3.1](#)~~Table 3.4~~. The total RCS of each substation was set to be 3,500 m². This is an approximate value used to assess the impact of the substation on the shadowing and the radar detection threshold. The exact scattering characteristic will depend on the substation's geometry and construction material as well as its range from the radar antenna.

3.3.1.3 Once the locations of the wind turbines and the offshore substation platforms were defined, a desk-based review of charts was undertaken alongside consultation with oil and gas operators in order to identify the location of nearby offshore oil and gas platforms and any REWS installations that might be affected by the presence of Morecambe Generation Assets. The location of offshore oil and gas platforms and the identified REWS host platforms are also shown in [Figure 3.2](#)~~Figure 3.2~~.

3.4 Assessment region and study area

3.4.1.1 Typically, a 30 km (16 nm) detection range is assumed to be the minimum requirement for REWS to detect and track smaller vessels (less than 4m length with metallic/steek hull -100 m² RCS). This indicates that some of the identified REWS installations will have a direct LoS with the Morecambe Array Area. The four REWS installations are located on Harbour Energy's Millom West platform, ENI Energy's Douglas platform and the OSI, and Spirit Energy's South Morecambe AP1 platform. These REWS installations provide a good overlapping radar coverage in the area to protect other oil and gas assets in the region (see [Figure 4.1](#)~~Figure 4.1~~).

MORECAMBE OFFSHORE WINDFARM GENERATION ASSETS

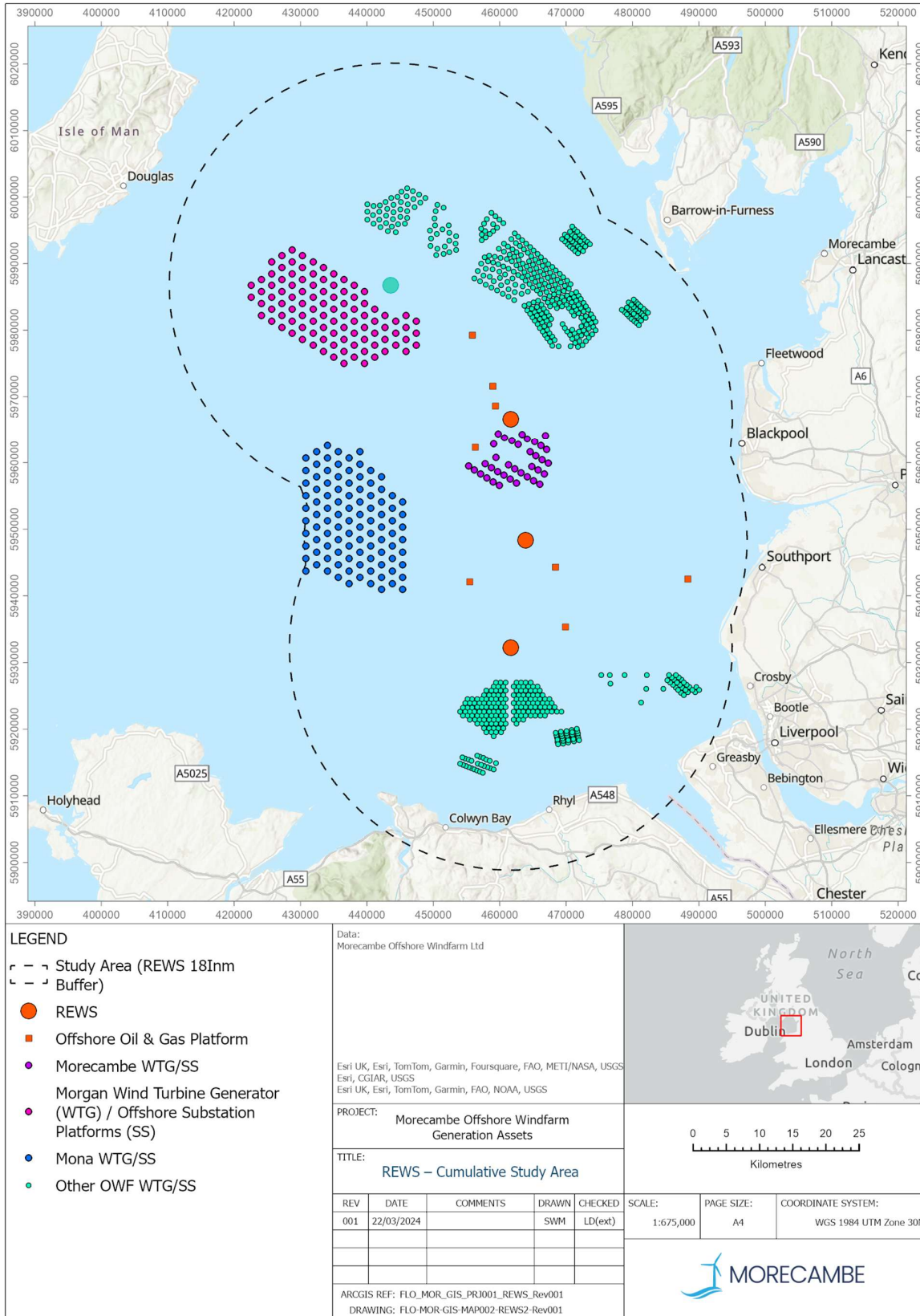


Figure 3.3: Morecambe Generation Assets REWS study area.

3.5 REWS modelling

- 3.5.1.1 REWS provides coverage over offshore oil and gas installations and provides early warning to the operators' when vessels breach the alarm settings. REWS use pre-set allision alarm rules. Typically, for both manned and normally unmanned installations (NUI) an Amber alarm is raised if a vessel is within CPA of 0.627 nm and a Red alarm is also raised if the CPA is 0.27 nm. For both manned and unmanned installations an Amber TCPA alarm is raised if a vessel is 4045 minutes away and a Red alarm is raised if the vessel is 30 minutes away. ~~For normally un-manned installations (NUI) an Amber TCPA~~These alarm ~~is raised if a vessel is 25 minutes away and a Red alarm is raised if~~parameters were updated to correlate with the vessel is 15 minutes away.~~parameters that Spirit Energy provided within their relevant representations (Table 2.1).~~ Should a vessel breach these rules an automatic alarm is raised to alert the operator. It is worth noting that TCPA alarms are only triggered if the vessel's vector remains in breach of the TCPA condition for a set number of radar rotations. For assessed REWS, it was assumed that there is a delay of 90 seconds (or 36 radar rotations) before an alarm is triggered. This setting is included to avoid alarms due to temporary vector breach of the TCPA while vessels are turning.
- 3.5.1.2 In addition to radar data, REWS are often integrated with AIS fitted onboard ships. If a vessel is fitted with an AIS transponder and is detected by the radar, the REWS will include the AIS data into the track data. AIS is a very useful source of vessel information and location data that can complement the radar data when temporary losses are experienced. While explicit confirmation is unavailable, it is assumed that Spirit Energy may incorporate AIS data within their REWS system.
- 3.5.1.3 Within this assessment, the performance of the REWS is based on the specification of Raytheon's Pathfinder/ST MK2 X-band transceiver with Mariners Pathfinder X-band 12 ft antenna system. The details of the modelling parameters used are shown in Table 3.2~~Table 3.2~~ and the antenna pattern used in the modelling is shown in Figure 3.4~~Figure 3.4~~.

Table 3.2: Radar modelling parameters.

Modelling parameter	Value
Gain	30 dB
Transmitter power	25 kW
Frequency	9.411 GHz
Pulse width	250 ns
Rotation rate	25 rotations per minute (RPM)
Pulse repletion frequency	2.0 kHz
Noise figure	5.5 dB
Dissipative losses	1.0 dB
Beam-shape losses	0.6 dB
Azimuth beam width	0.7°
Elevation beam width	23.0°
Antenna height	55 m AMSL

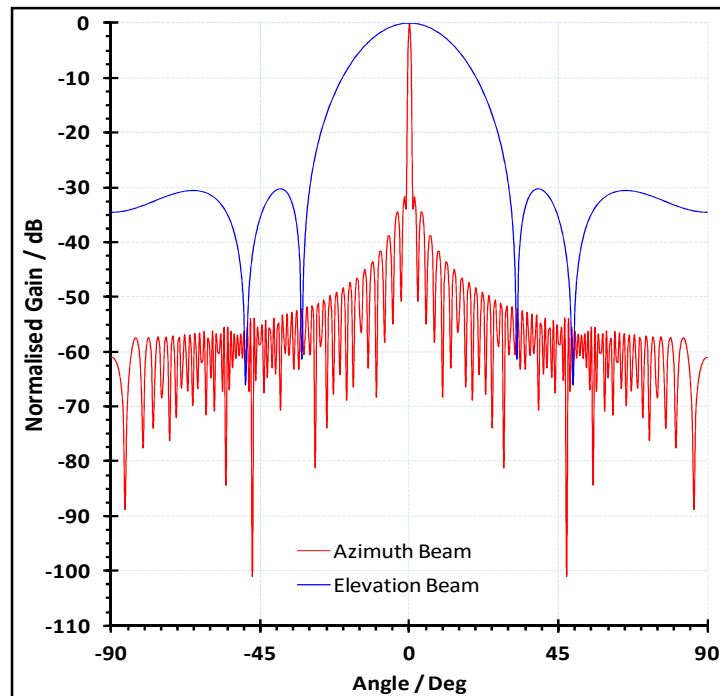


Figure 3.4: The radar antenna elevation and azimuth patterns.

3.5.1.4 In order to establish a baseline for the radar detection under standard conditions used for REWS acceptance testing, the modelling is conducted at a rainfall rate of 0 mm/hr and sea-state 3 (wind speeds 9.6 ms⁻¹ and average wave height of 1.3 m). When computing returns from the sea surface and the rain clutter the models provide the mean levels of returns.

3.5.1.5 REWS processing deploys scan-to-scan correlation, which improves the noise and clutter suppression. However, this is not considered in depth as part of this study as it requires detailed knowledge of the proprietary software used within the system’s signal processing.

3.5.1.6 It is worth noting that only the medium pulse width of 250 ns was used throughout the assessment. This gives an approximated range resolution of 37.5 m which is then equated to the range-cell length. As the wind turbine rotor diameter is much larger than the range cell length (depending on the yaw angle with respect to the radar), parts of the blades will fall into adjacent range-cells as the wind turbine blades rotate. This phenomenon will be referred to as ‘range-cell spreading’ within this document.

3.6 Detection threshold (CFAR)

3.6.1.1 There are multiple variations of CFAR that can be used where different weights can be applied to each cell prior to the final averaging. However, within this document and to examine the effect of the Morecambe Generation Assets on the threshold levels, a Constant Averaging (CA) CFAR is applied over the clutter map. The CA-CFAR modelled within this assessment uses two range cells on both sides of the cell under test as the guard region while the averaging considers six range cells on both sides of the guard region. In Azimuth the modelled CA-CFAR uses one guard cell and two averaging cells on both sides in azimuth. The overall resultant threshold was set to provide a constant 10⁻⁵ probability of false alarm.

3.7 Target modelling

3.7.1.1 REWS are mainly interested in detecting and tracking surface targets such as large fishing boats, maintenance vessels and larger ships and tankers. The role of the REWS is to alert the operator when a vessel is on an allision course with the platform. Although air targets may also appear on the radar display, the management and trafficking of air targets is controlled by other radar systems such as ATC primary and secondary radars or AD radar systems. Thus, the analysis of the potential impact of the Morecambe Generation Assets on REWS is limited to surface targets only.

3.7.1.2 Large vessels in excess of 1,000 gross tons (GT) are the primary concern when it comes to managing the safety of offshore platforms (Love, 2014). However, within this report, the test target was set to represent a large sized maintenance vessel with a steel/metallic hull. The As indicated by the comments from Spirit Energy, the test vessel is assumed to have an RCS of 4000m²420 m² and a height of 6m. These parameters are typically used for REWS performance analysis and system acceptance testing and they comply with the International Association of Marine Aids to Navigation and Lighthouse Authorities (IALA) Vessel Traffic Services (VTS) guidelines for radar modelling of different vessel types. The test vessel was set to have an average speed of 17 knots (31.5 km/hr).

3.8 Wind turbine shadow modelling

3.8.1.1 As discussed in section 2.2, when turbines are placed within the LoS of radar systems, radar shadowing will occur behind the structure. The extent and length of the shadow region depends on the size of the wind turbine, the distance to the radar antenna, the height of the radar and the height of the target of interest. Shadowing produced by turbines may cause targets to be lost as they move in and out of the shadow region. Depending on the size of the shadow region, this may cause existing tracks to be lost or discontinued.

3.8.1.2 As REWS are mainly used to detect and track surface moving targets (ships, boats etc.), only surface or near-surface shadowing is considered. This can be approximated by using the optical shadowing/blockage cast by the wind turbine over the sea surface. The use of optical blockage to estimate the radar shadowing will give pessimistic results but is deemed acceptable for objects that are much larger than the radar wavelength at relatively short ranges (such as offshore wind turbines). Optical blockage does not account for diffraction effects around the structure which would normally reduce the shadow length. Diffraction and partial shadowing of an object has been shown to significantly improve the radar detection. Practical measurements and other studies show that the shadowing effects from the wind turbines may reduce the overall detection range of the radar but may not severely affect the detection of objects within the shadow regions.

3.8.1.3 One thousand gross tons (GT) plus vessels (which are the main safety concern to offshore platforms) vary in size and typical vessel lengths are between 15m and 60m. However, the shadows from the wind turbines are relatively narrow and are typically between 4m and 20m in width. This indicates that a large 1,000GT vessel will be partially shadowed by the wind turbine as it moves through the shadow regions (as shown in Figure 3.5Figure 3.5. Partial shadowing will allow some of the radar energy to be reflected back to the radar and it might be possible for this energy to be detected by the REWS. Hence, smaller vessels can be assumed as point scatterers while larger vessels can be assessed for partial shadowing. The results of vessel detection within the shadow region is presented in Section 4.3.2.

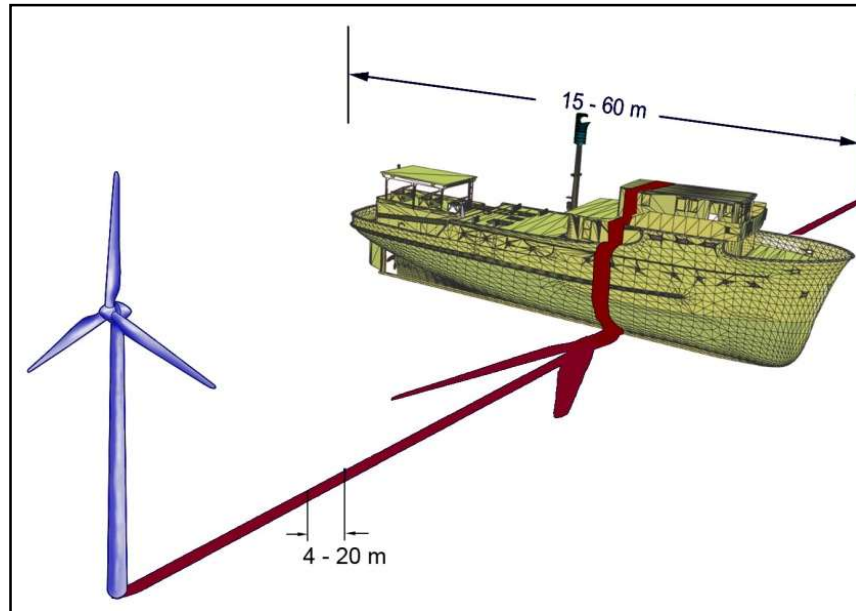


Figure 3.5: Optical blockage and partial shadowing.

3.9 Measurements and modelling of RCS of wind turbines

3.9.1.1

A number of studies have attempted to determine the RCS of wind turbines through measurements of the power received by a radar in the region. A study undertaken by Terma within Hornsea Project One (Terma, 2021) highlights the difference between measured and theoretical RCS values of wind turbines obtained from computational modelling. The wind turbines deployed at Hornsea Project One have a rotor diameter of 154 m and a hub height of 117.9m AMSL. Although these turbines are smaller than the MDS turbines considered for the Morecambe Generation Assets, they are still considered to be very large structures for radars. The results of the field study show that the power received from turbines within Hornsea Project One are within reasonable levels and the radar is able to detect a vessel travelling within the array area. The layout showing the location of the radar within the windfarm is shown in [Figure 3.6](#). The power received by the radar is shown in [Figure 3.7](#) and shows that the radar, which is using pulse compression to improve resolution and power levels, can detect a service vessel travelling within the array area.

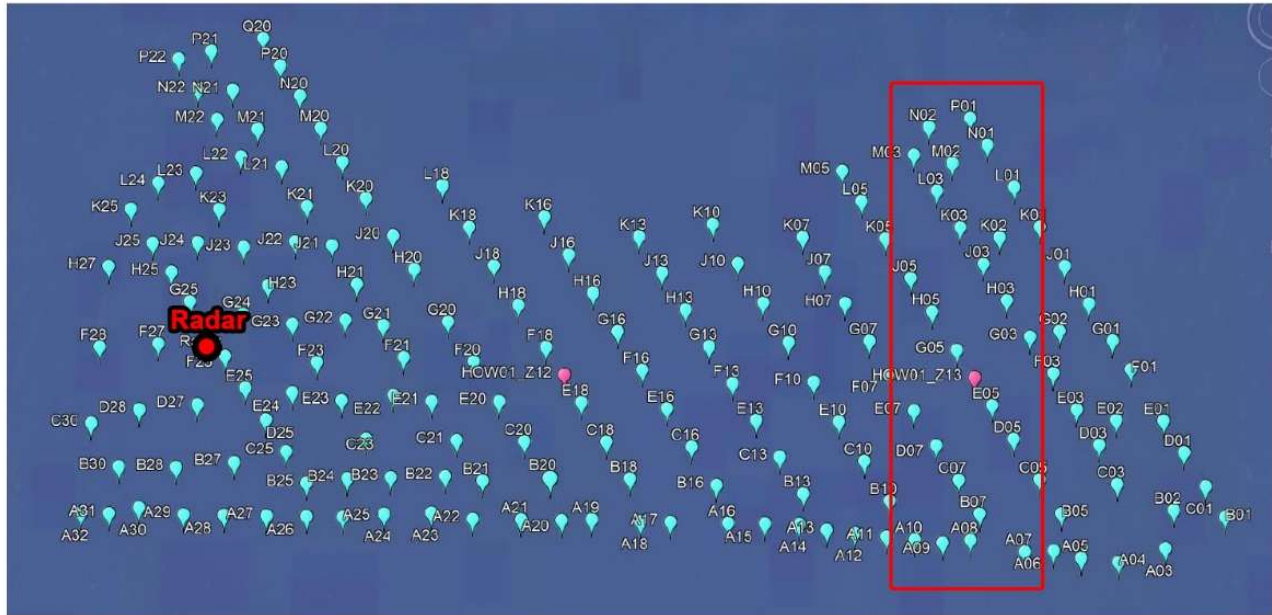


Figure 3.6: Wind turbine layout at Hornsea Project One array area and the location of the radar system used in the study. The red area denotes the region shown in [Figure 3.7](#) (Terma, 2021).

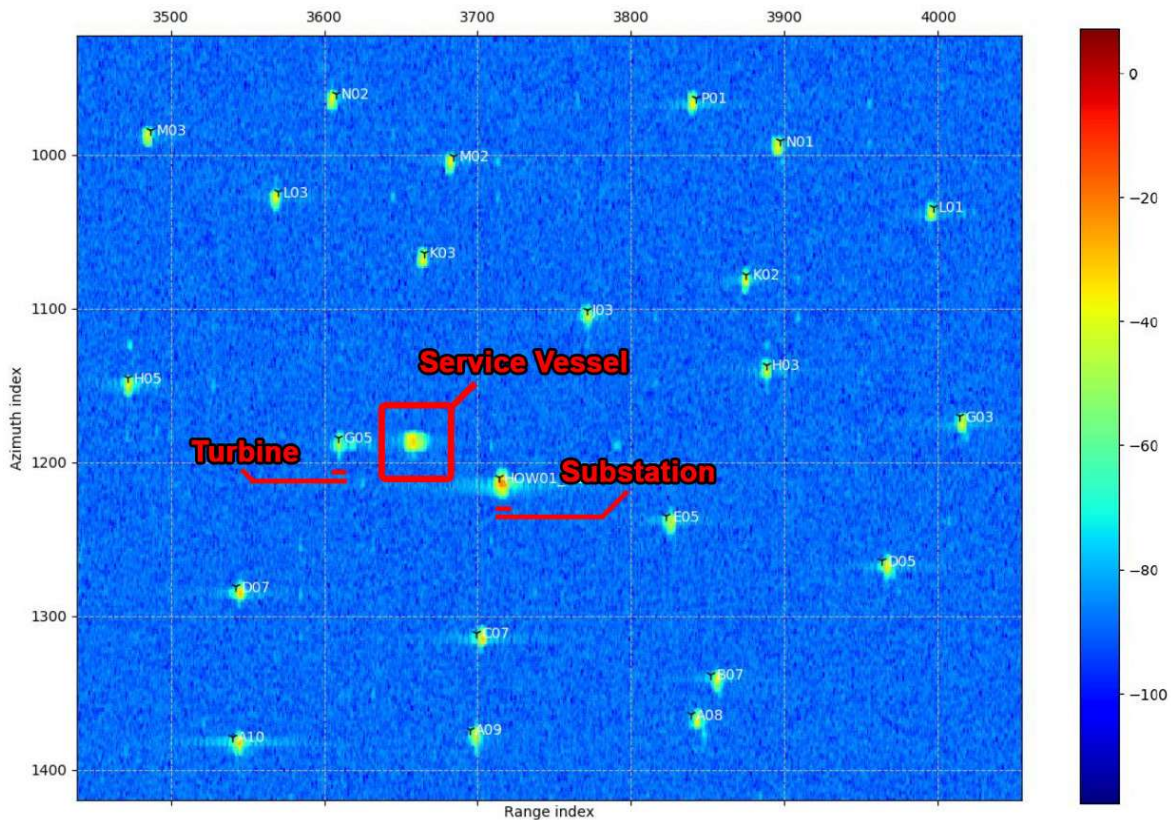


Figure 3.7: Compressed radar image in range-azimuth coordinates showing a zoomed area of the Hornsea Project One array area around a substation platform (Z13). A vessel is visible between Z13 and WTG G05. The signal level (in dB) is colour coded (Terma, 2021).

- 3.9.1.2 A key finding of the Terma study was that turbines located within 10km of the radar had a lower RCS than traditional RCS models would suggest. Traditional RCS modelling methods would often need to utilise a number of assumptions in order to reduce the complexity of the RCS modelling and computational efforts needed. Many of these assumptions are related to the effect of the range (distance from the radar) on the radar signature from these large objects. Objects within close range to the radar (within the near-field) often have a lower RCS value.
- 3.9.1.3 Although the models used within this technical report address many of these assumptions and account for the effect of range on the scattering profile and signal levels from the wind turbines, the utilised models still need to make certain assumptions regarding the exact geometry of the wind turbine, the materials used, and the exact blade profile under wind loading (as blades bend due to wind loading). Some of these assumptions would result in higher-than-expected RCS values but are still considered within acceptable limits and produce similar results to the measurements shown in the Terma study as illustrated in [Figure 3.8](#).

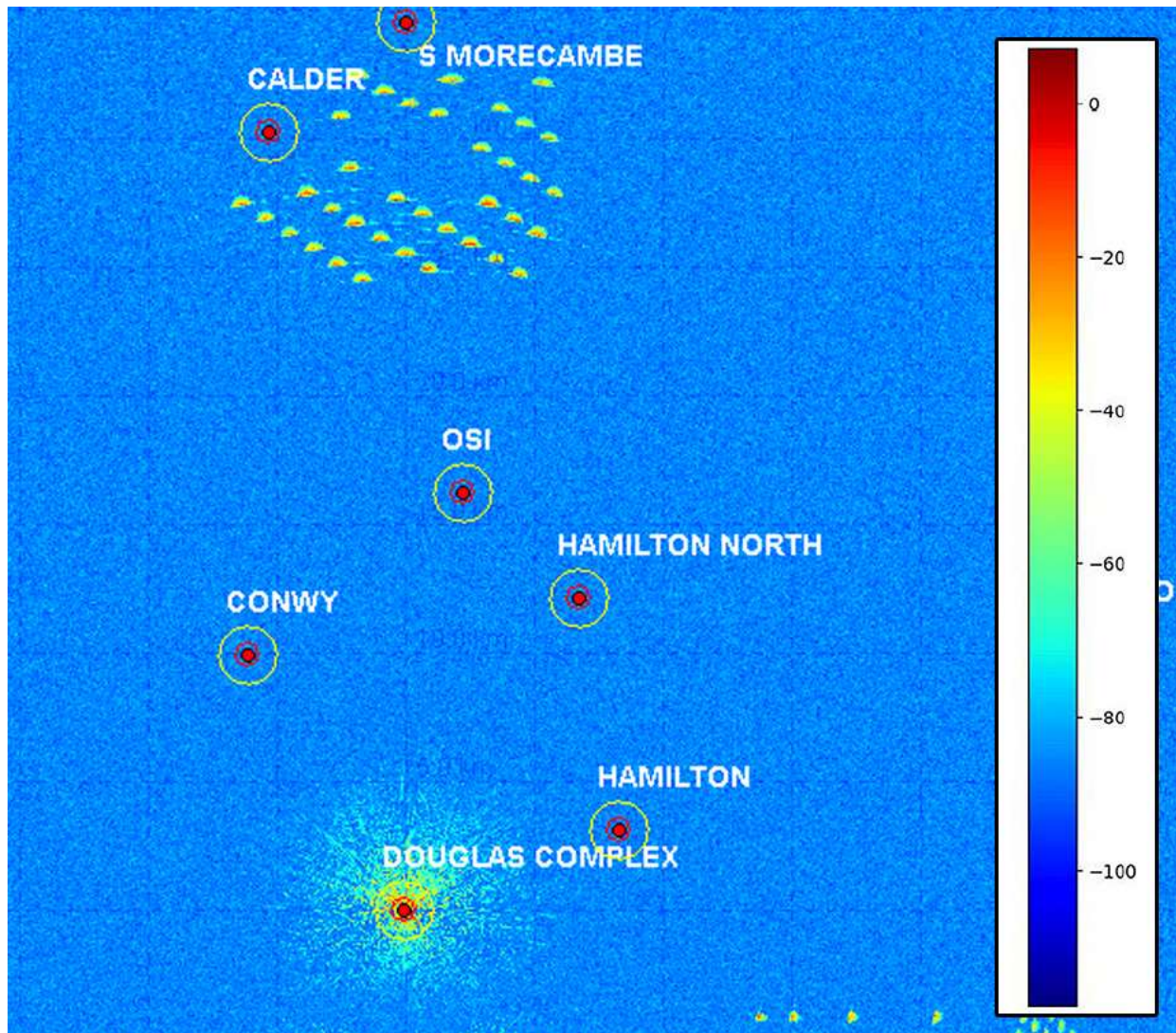


Figure 3.8: Power received by the REWS on ENI's Douglas platform.

4 REWS RETURNS AND VESSEL DETECTION MODELLING RESULTS

4.1 Overview

4.1.1.1 There are a number of REWS installations near the Morecambe Array Area. Currently this region has a number of regular vessels travelling along routes passing through the area. Therefore, ENI Energy, Harbour Energy and Spirit Energy have multiple REWS installations in the region to monitor and protect their assets ([Figure 3.2](#)~~Figure 3.2~~).

4.2 Assessment of the base case scenario

4.2.1.1 To establish the potential effect of the Morecambe Generation Assets on REWS installation in the region, the assessment starts by looking at the base case scenario where only the existing windfarms are modelled. The location of the existing windfarms and the locations of the oil and gas platforms are shown in [Figure 4.1](#)~~Figure 4.1~~. The REWS installations are also shown in [Figure 4.1](#)~~Figure 4.1~~ with their coverage area denoted by the large red circles, which illustrate the 16nm range. The red circle around each platform denotes the 0.27nm Red CPA alarm ~~while (which is also the yellow circle denotessame for the 0.6nm Amber CPA alarm-).~~

4.2.1.2 For platforms with REWS installations the presence of windfarms may have potential effects on the REWS' ability to detect and track vessels travelling through windfarm areas. If the REWS is unable to detect and track the vessel within the windfarm, it may cause the REWS to issue delayed TCPA alarms, resulting in insufficient response times to deal with potential allision threats. The assessment modelled the returns and target detection at the REWS installations on ENI Energy's Douglas platform, Harbour Energy's Millom West platform, ENI Energy's OSI and Spirit Energy's South Morecambe AP1 platform (in that order). The assessment starts by considering the power received at the radar, then it establishes the expected threshold levels, followed by a comparison between the threshold level to the expected vessel returns to determine the detection regions.

4.2.1.3 Starting with ENI Energy's Douglas platform, [Figure 4.2](#)~~Figure 4.2~~ shows the power received (radar returns) from the existing turbines along with the assumed clutter generated from the sea surface. The green regions represent areas where radar returns are being detected. Brighter shades of green indicate higher returns while darker green regions indicate low returns.

4.2.1.4 To further assess the REWS' ability to detect vessels within the windfarm areas, a CFAR threshold over the detection region was modelled using a 2D CA CFAR (as highlighted in section 3.6). The modelling results for ENI Energy's Douglas REWS are shown in [Figure 4.3](#)~~Figure 4.3~~. The figure shows the regions with higher detection threshold as brighter shades of green. The strong returns from the wind turbines will significantly alter the threshold levels. It can be noted that the threshold is raised over multiple cells around each wind turbine since the CFAR threshold averages the returns over a 2D sliding window of multiple cells in azimuth and range.



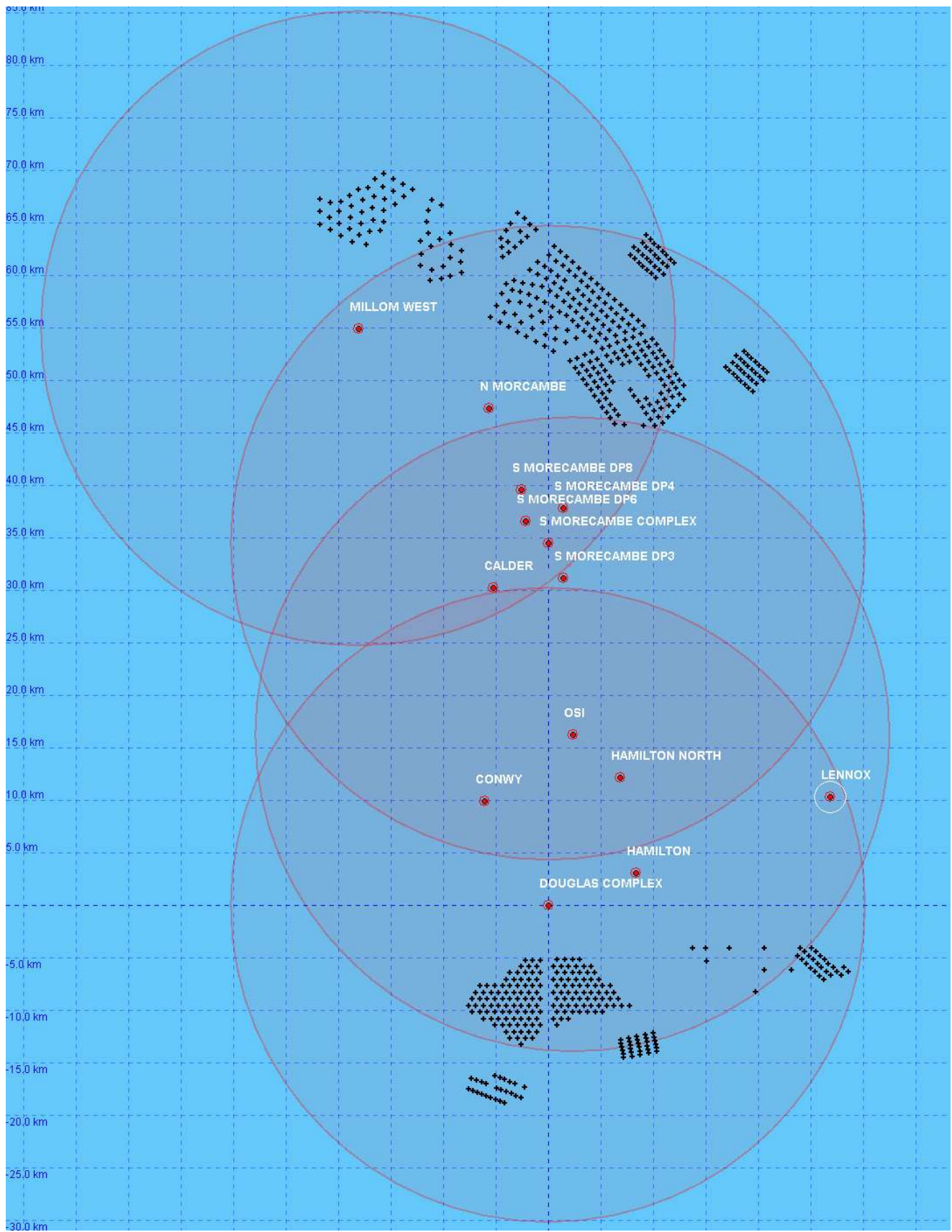
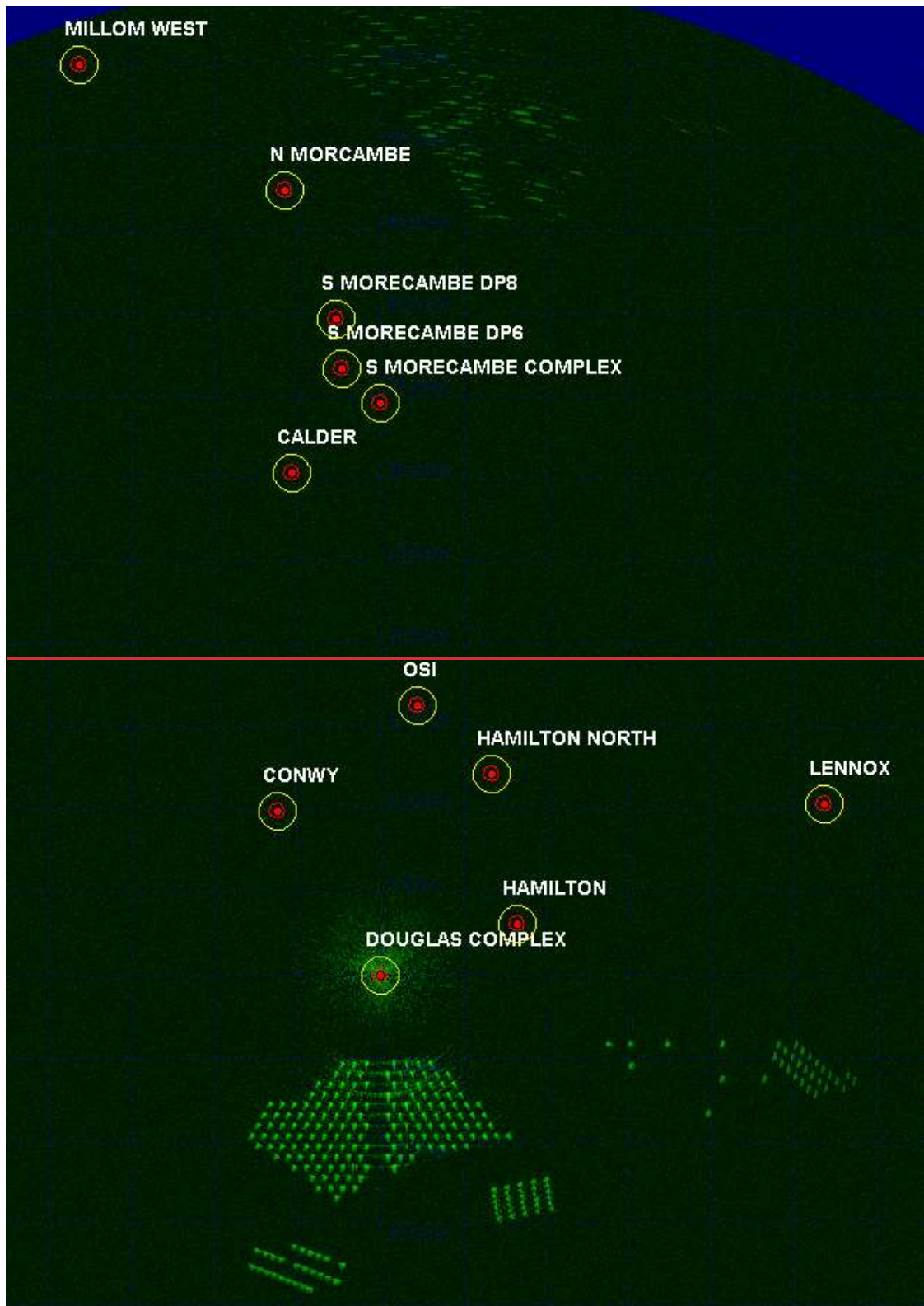


Figure 4.1: Modelled layout of the base case scenario showing the location of the existing windfarms and the coverage of the REWS in the region.



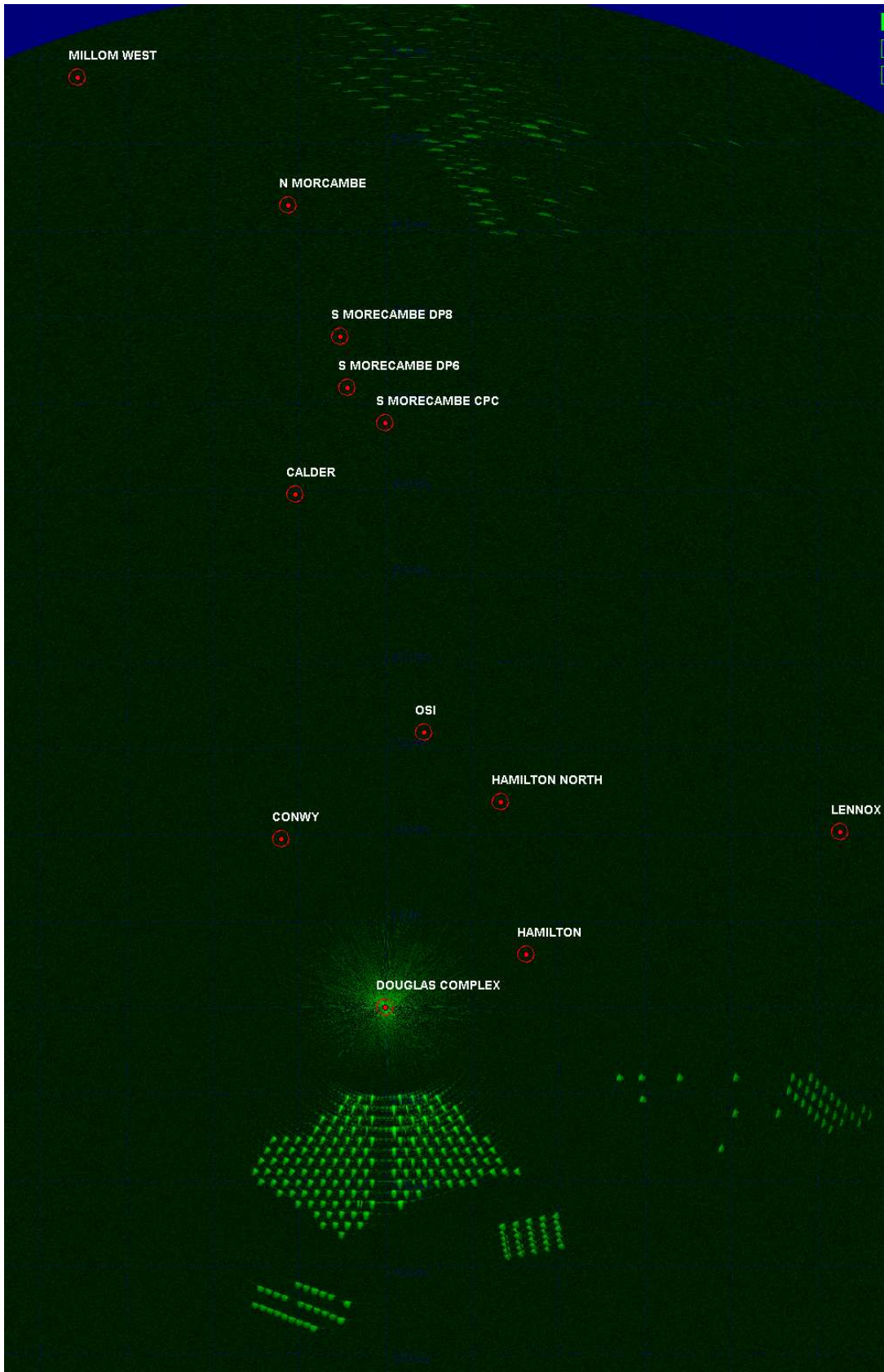
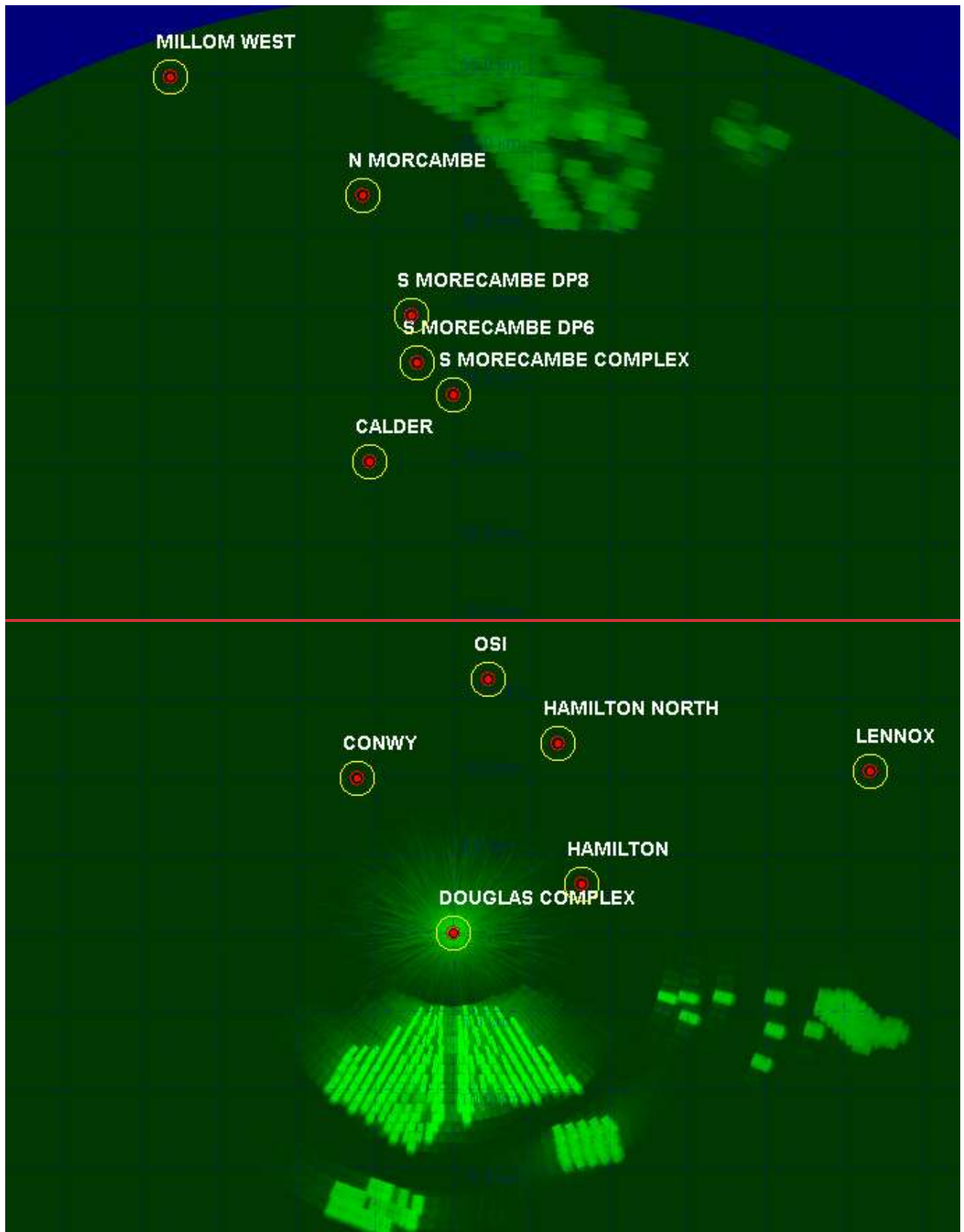


Figure 4.2: ENI Energy’s Douglas platform REWS clutter map showing returns from the wind turbines and sea clutter.



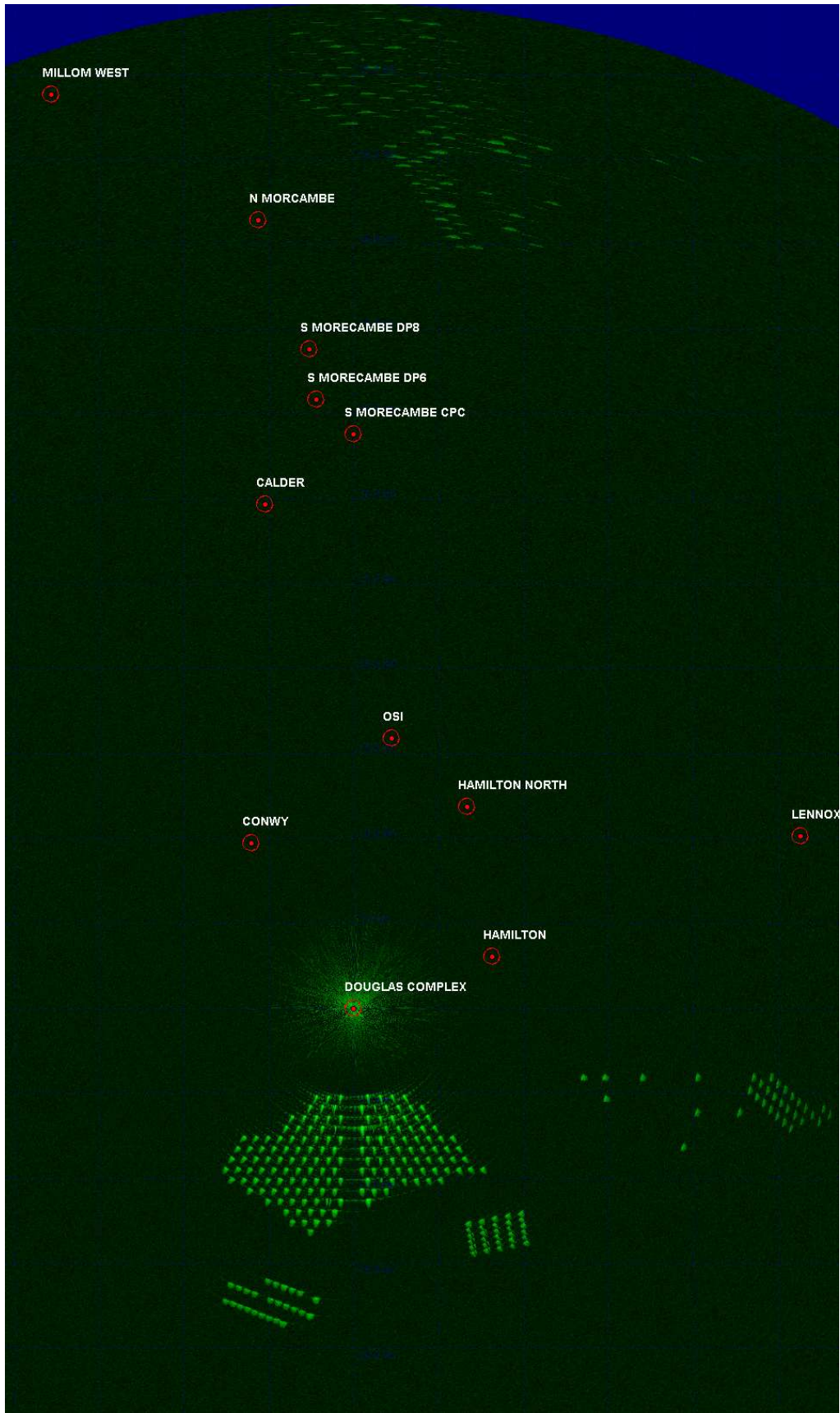
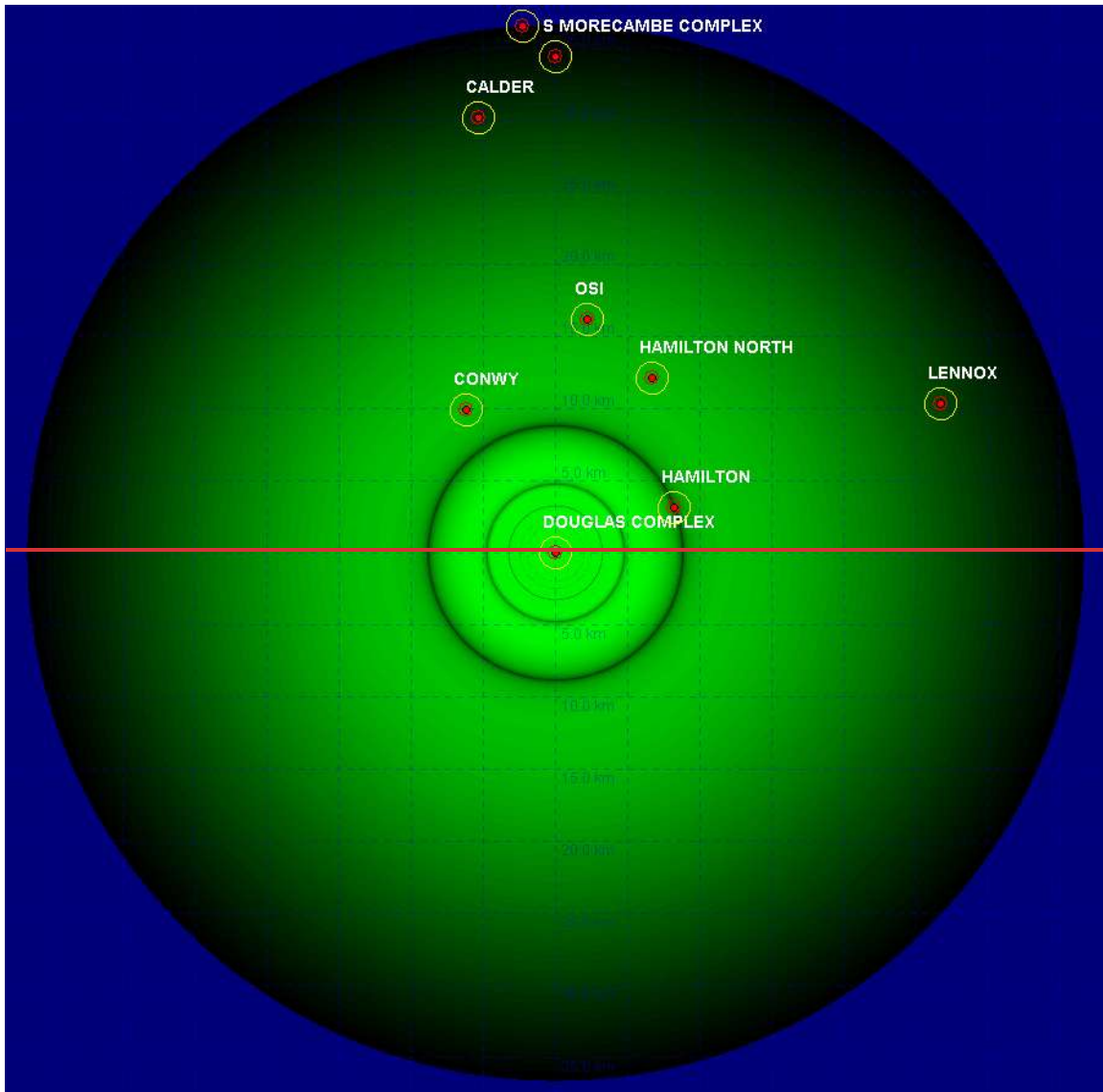


Figure 4.3: ENI Energy's Douglas platform REWS detection threshold.

4.2.1.5 In order to establish the detection regions for a given vessel, the returns from the ~~1000m²~~420 m² RCS test vessel are modelled with respect to range and plotted around the REWS as shown in ~~Figure 4.4~~Figure 4.4. ~~Figure 4.4~~Figure 4.4 shows that the vessel has high returns at close ranges which then reduces as range increases up to approximately ~~21nm~~(39km~~19nm~~ 35km). The blue region in the figure represents the region beyond the radar detection range (~~21nm~~19nm) that has not been modelled. Higher returns are illustrated by brighter shades of green.



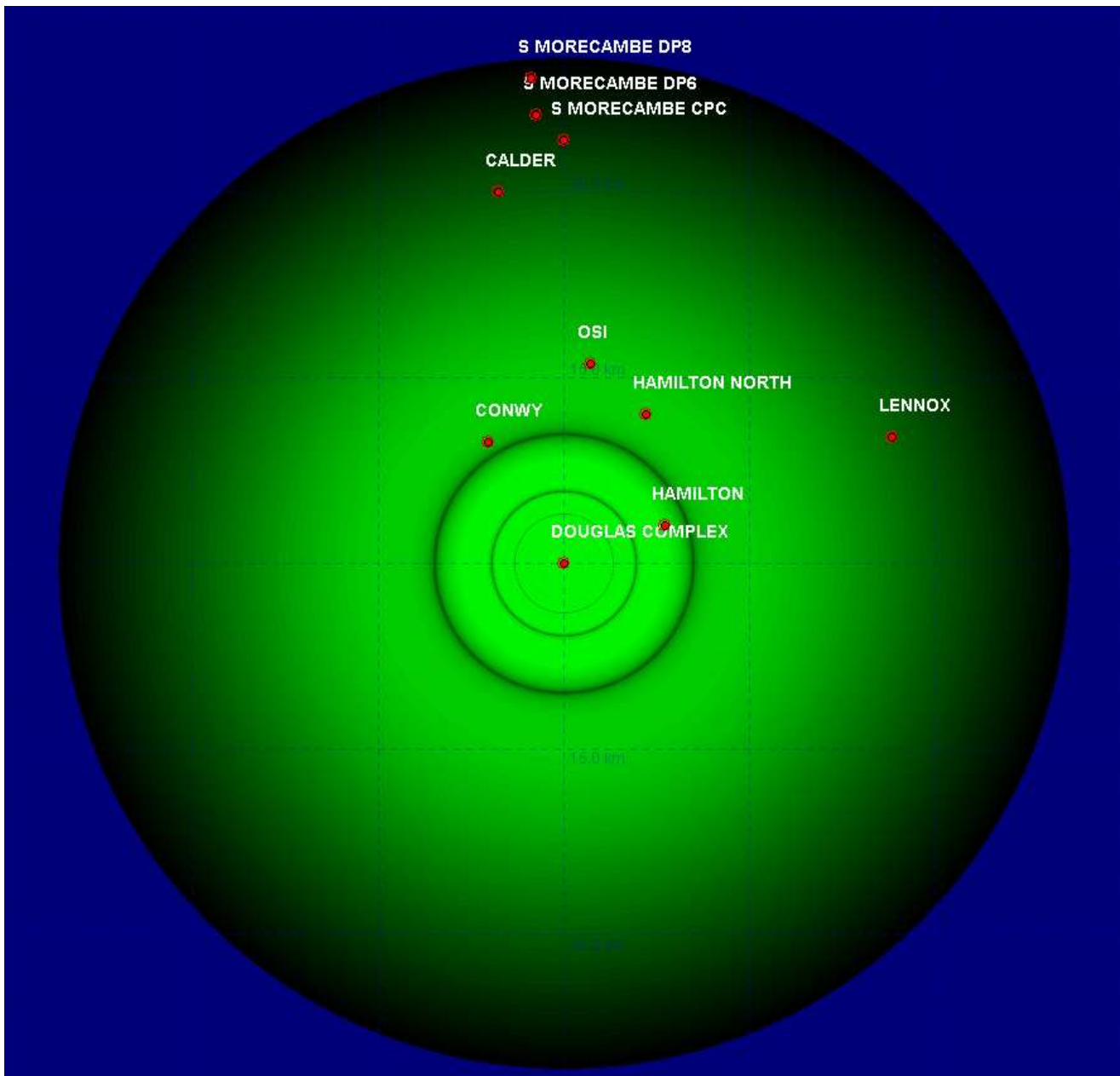


Figure 4.4: Modelled power received from 4000m² target (coverage).

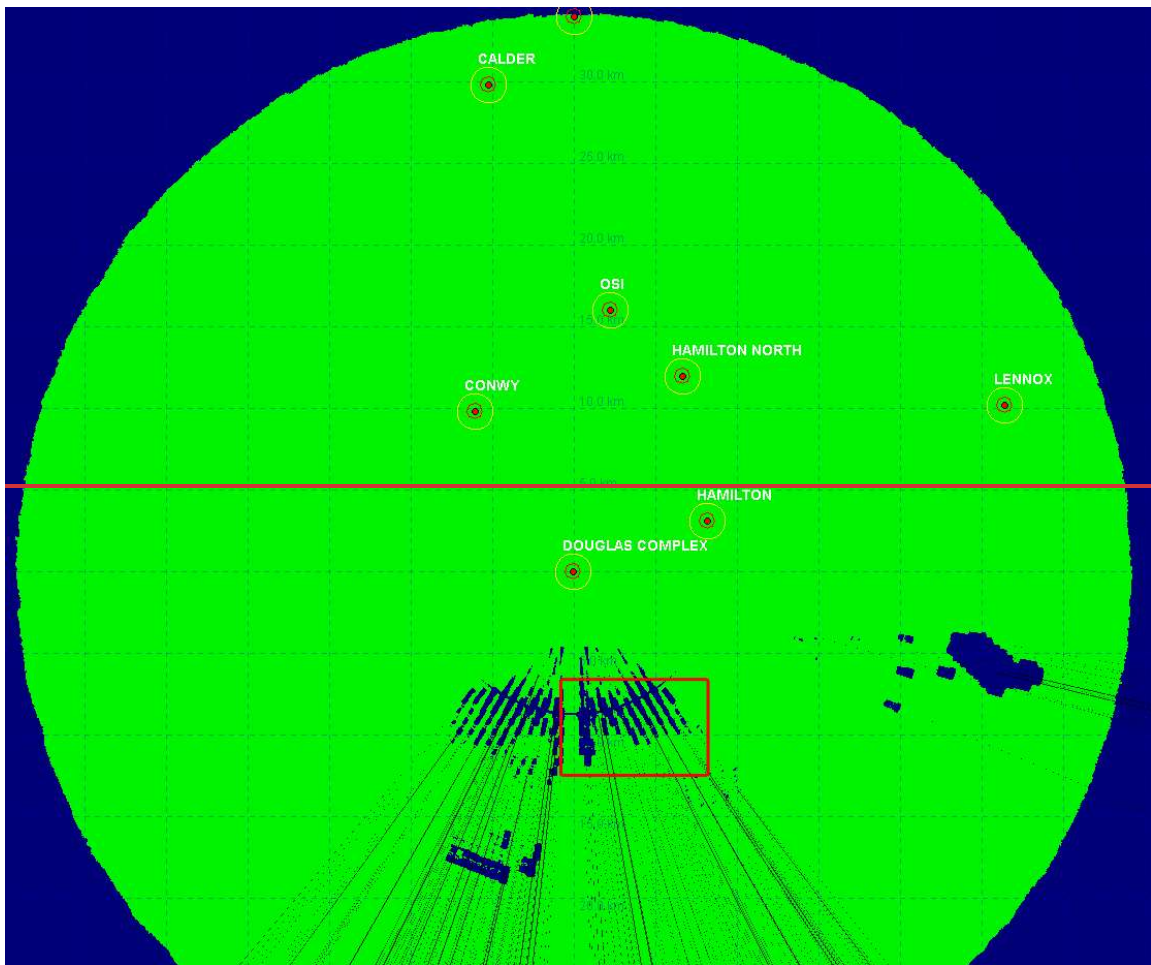
4.2.1.6 The returns from the vessel are then compared against the CFAR detection threshold shown in [Figure 2.2](#) to establish the detection regions. If the vessel returns are above the CFAR threshold, then the vessel is detected, however, if the returns are below the threshold, the target is assumed to be undetected within that region. [Figure 4.5](#) shows the detection plot for the 4000m² test vessel. Dark areas within the plot denote regions where the vessels will not be detected. The shadow regions are very narrow and are not visible within the figures due to the scale. The effects of the shadow regions are illustrated in [Figure 4.6](#), which shows the effect of shadowing on the returns from the vessel. The narrow lines illustrate the shadow generated from each wind turbine.

4.2.1.7 The results show that at close ranges, the REWS easily detects the test vessel as the returns are above the detection threshold. Once the vessel is travelling within the

nearby windfarm, the raised threshold over the cells around each wind turbine can cause loss of detection. This effect, in combination with the shadowing effects, may cause the REWS to lose tracks of the vessels and fail in raising TCPA alarms in a timely manner as stated for the CPA/TCPA alarm requirements.

4.2.1.8

The same modelling process was followed for Harbour Energy's Millom West platform, ENI Energy's OSI, Spirit Energy's South Morecambe AP1 platform. The results for the base case on these REWS installations are shown in [Figure 4.7](#) to [Figure 4.15](#).



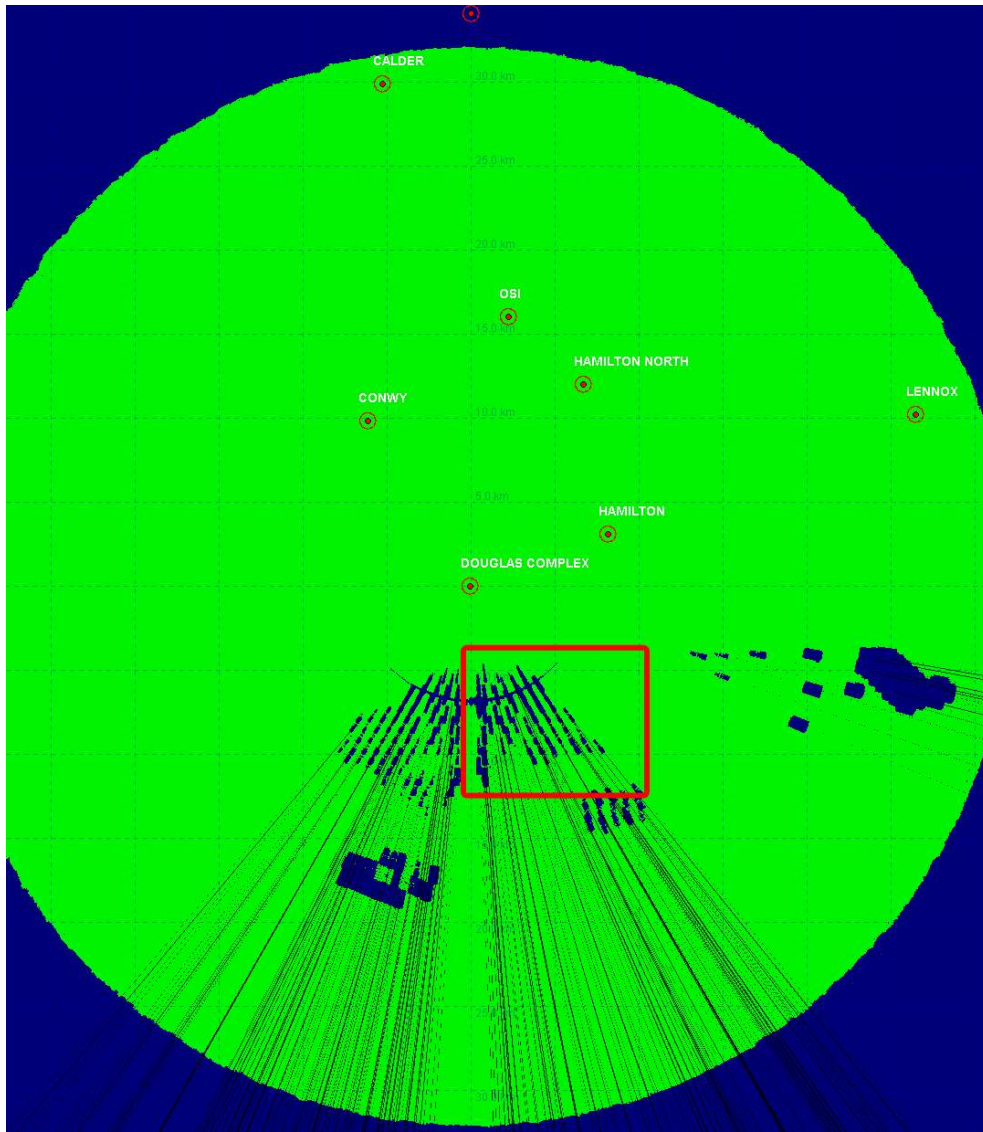
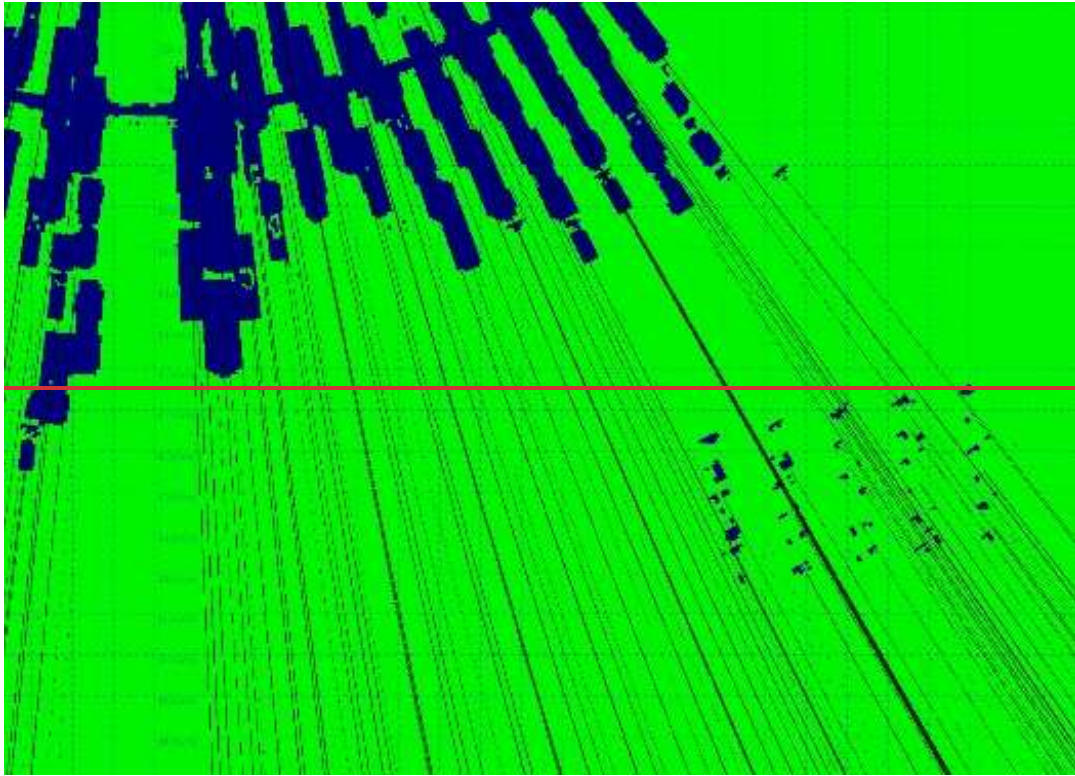


Figure 4.5: ENI Energy's Douglas platform REWS detection plot showing loss regions for a 4000420 m2 target.



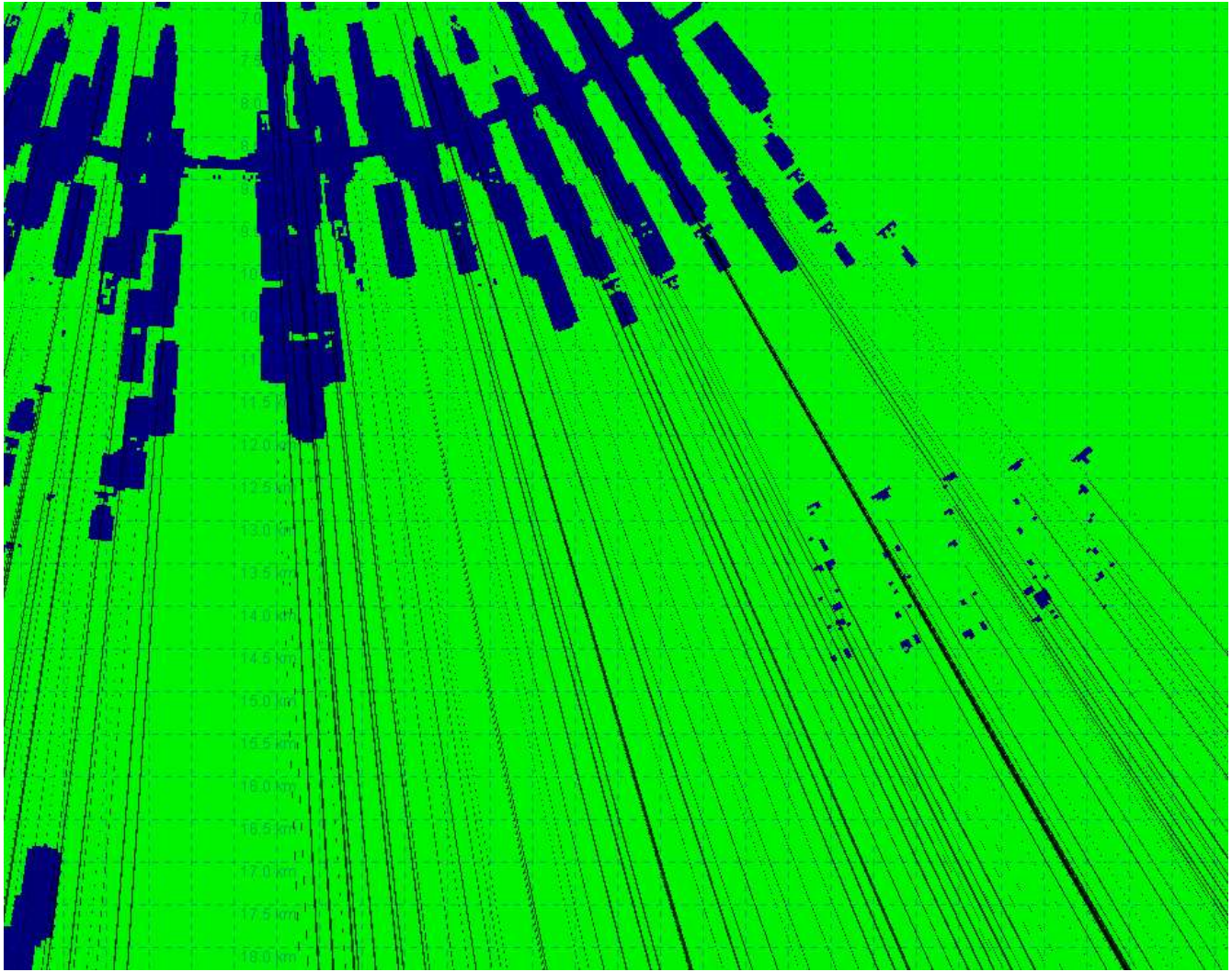
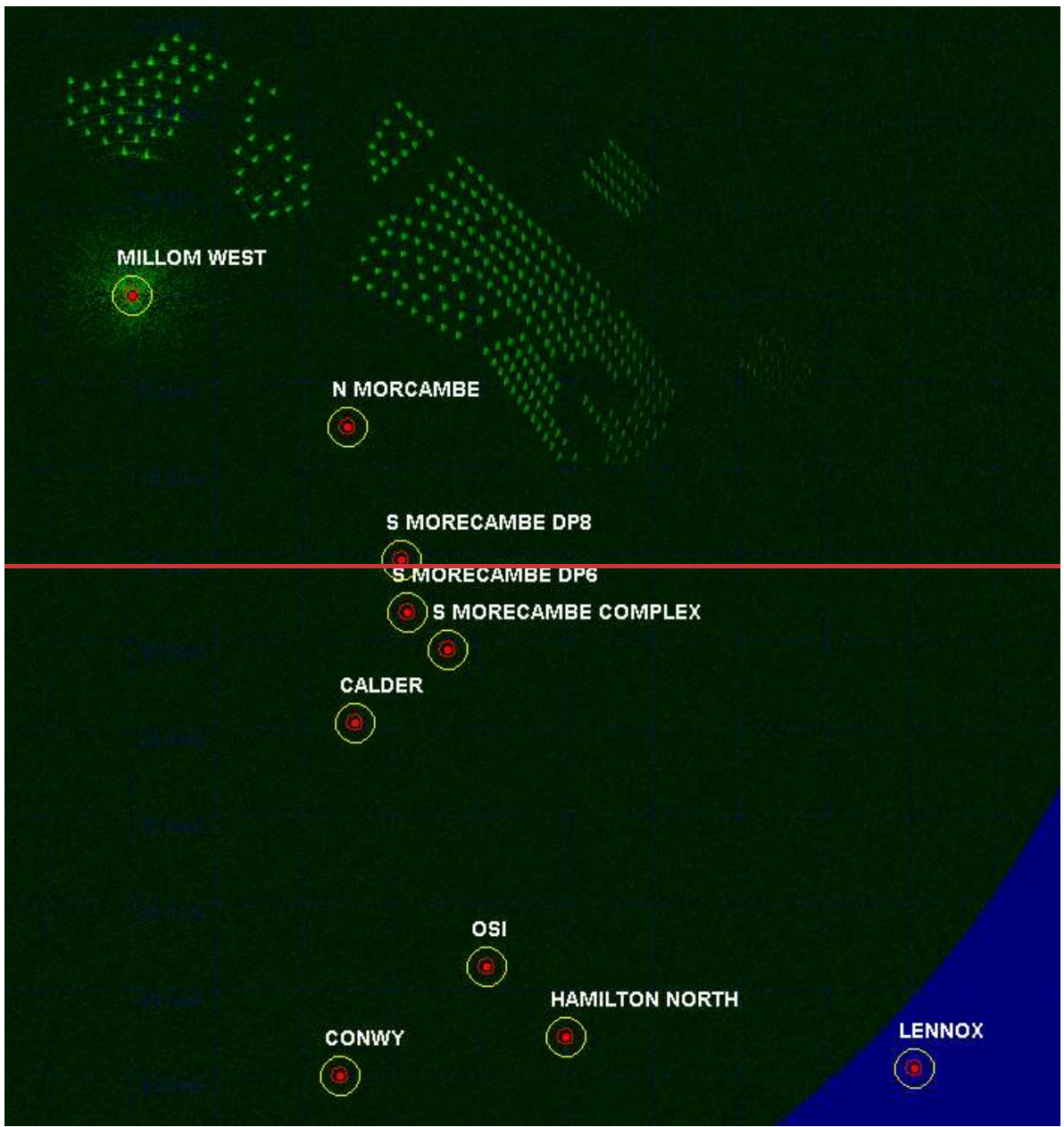


Figure 4.6: Enlarged portion of the detection plot showing the effect of wind turbine shadowing.



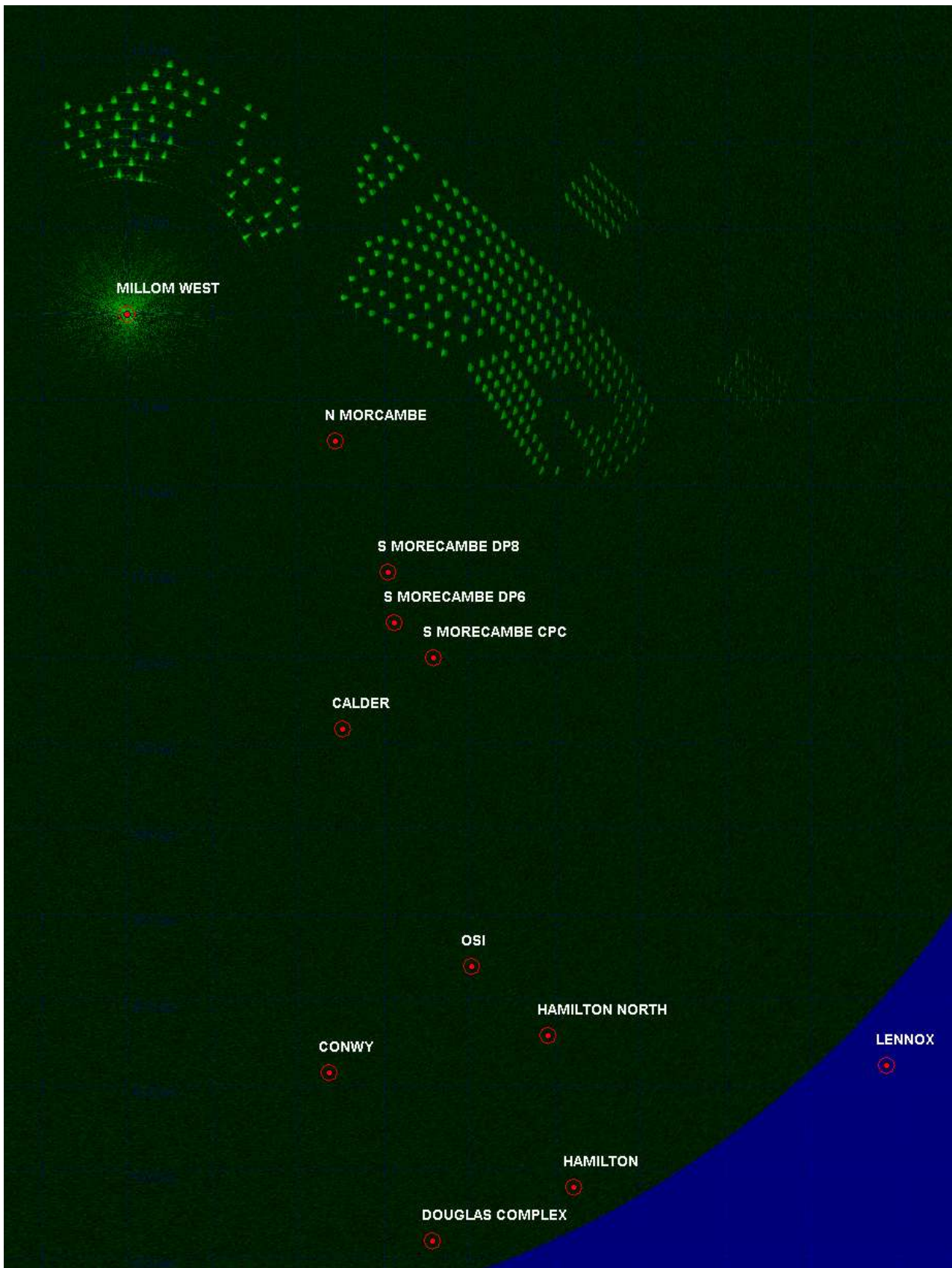


Figure 4.7: Harbour Energy's Millom West platform REWS clutter map showing returns from the wind turbines and sea clutter.

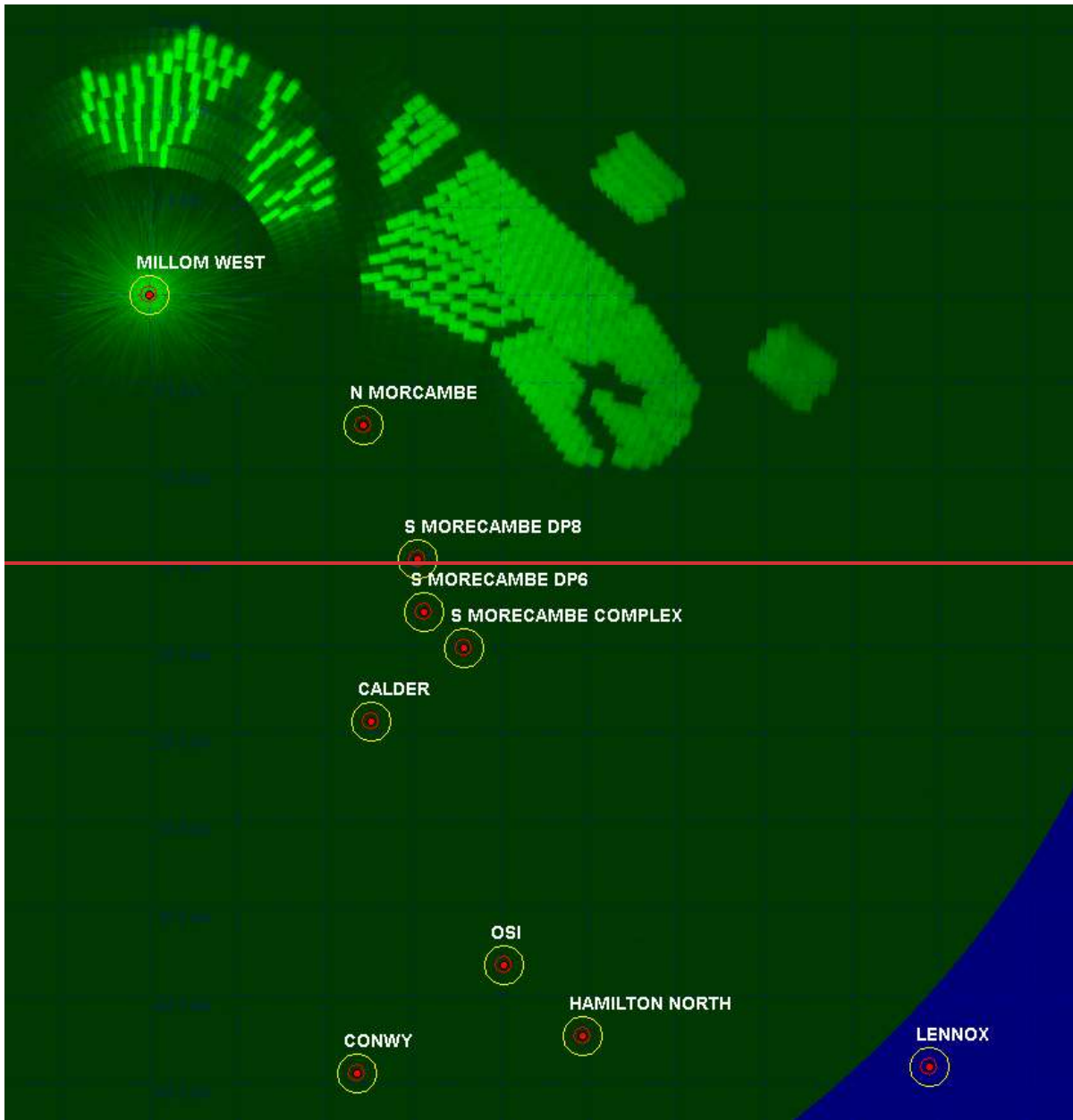
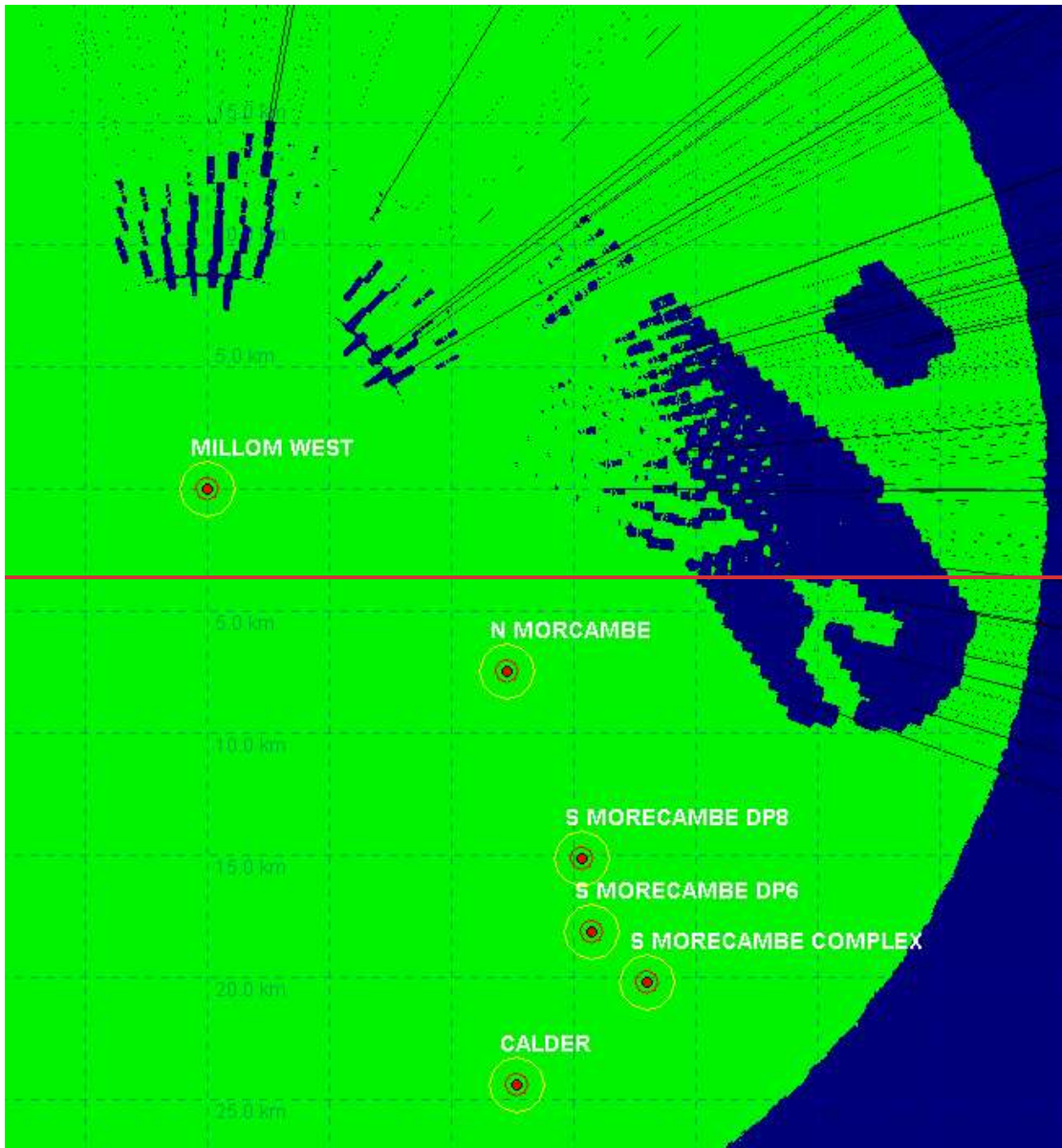




Figure 4.8: Harbour Energy's Millom West platform REWS detection threshold.



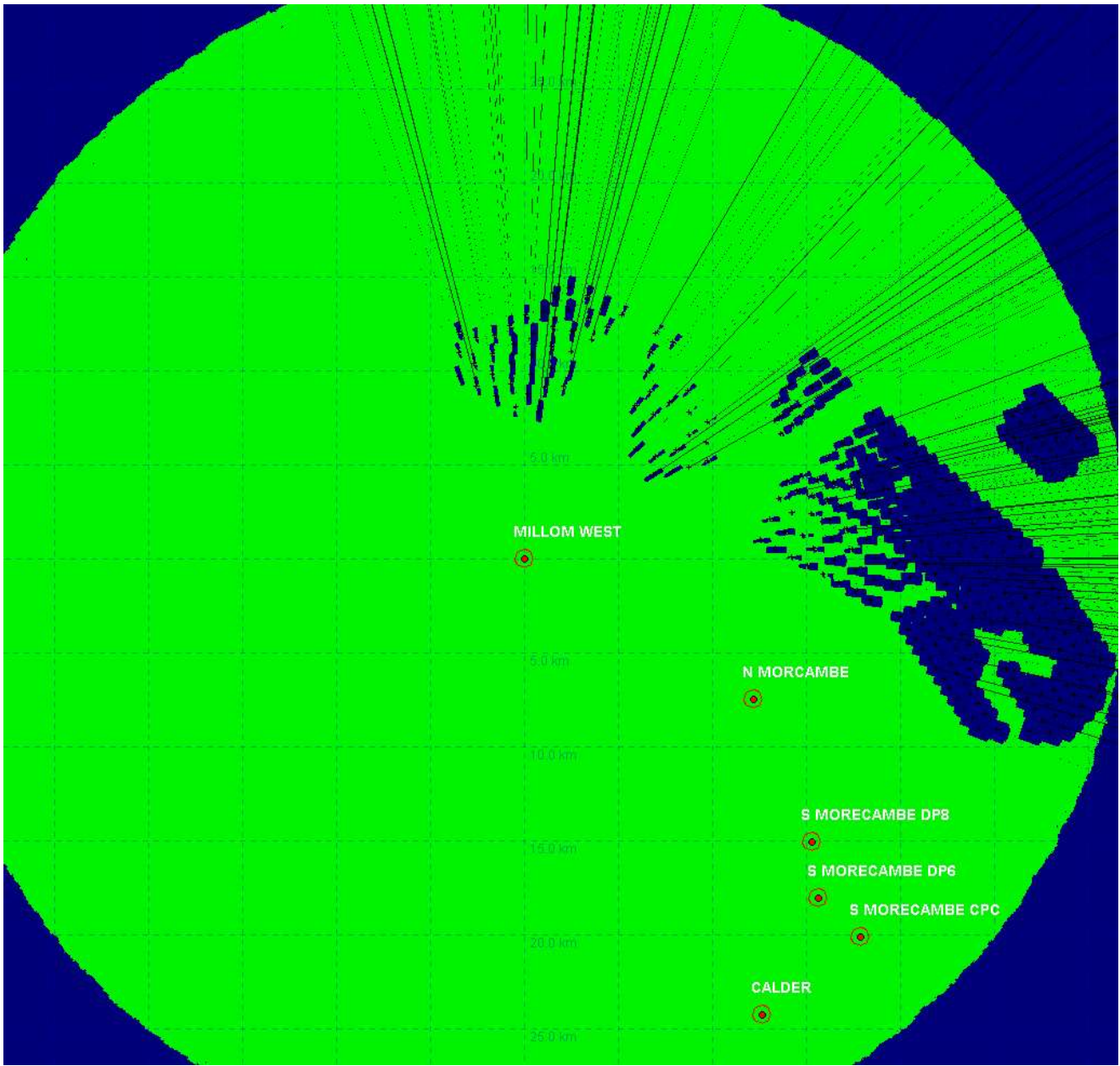


Figure 4.9: Harbour Energy's Millom West platform REWS detection plot showing loss regions for a **1000420** m2 target.



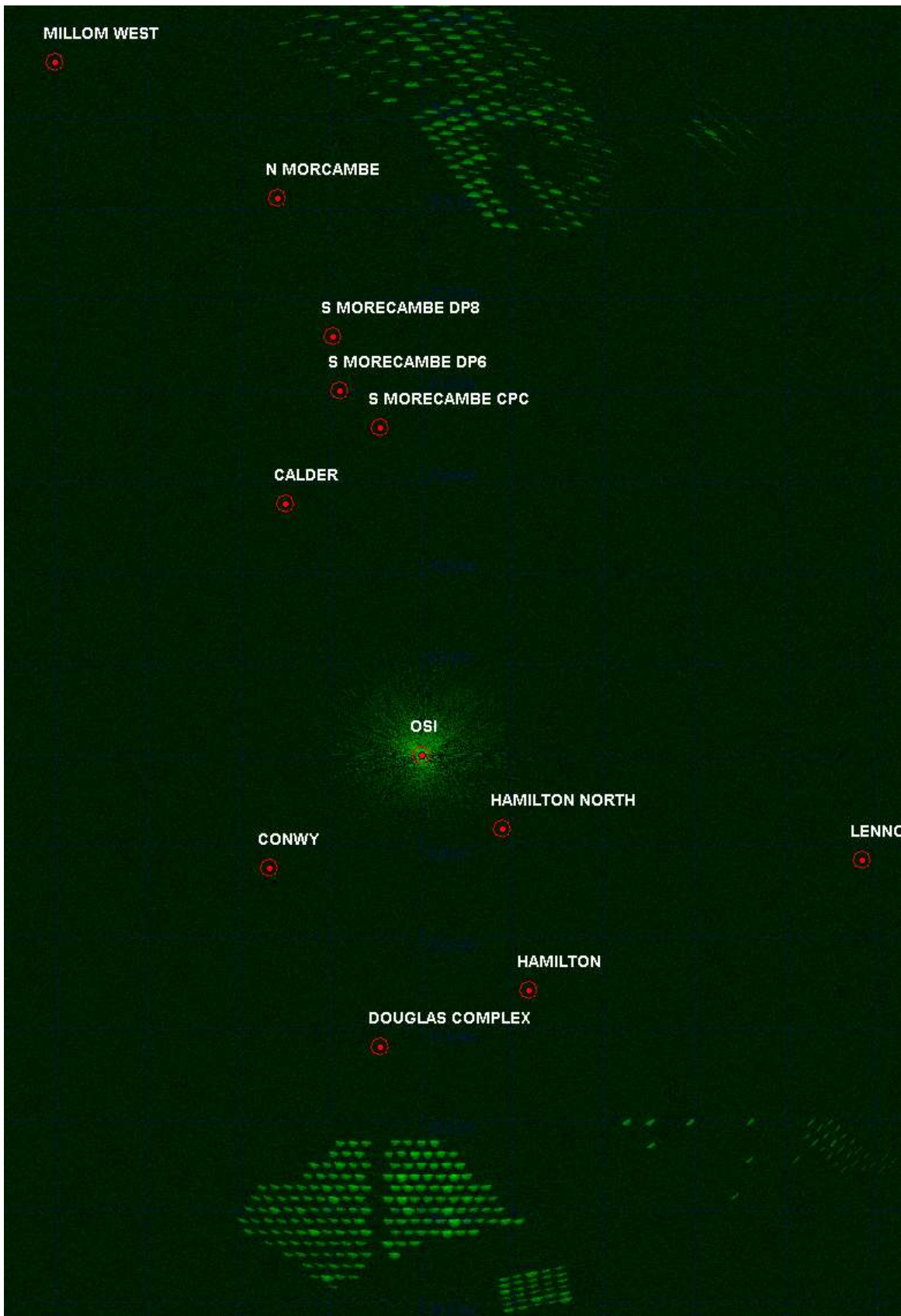


Figure 4.10: ENI Energy's OSI REWS clutter map showing returns from the wind turbines and sea clutter.



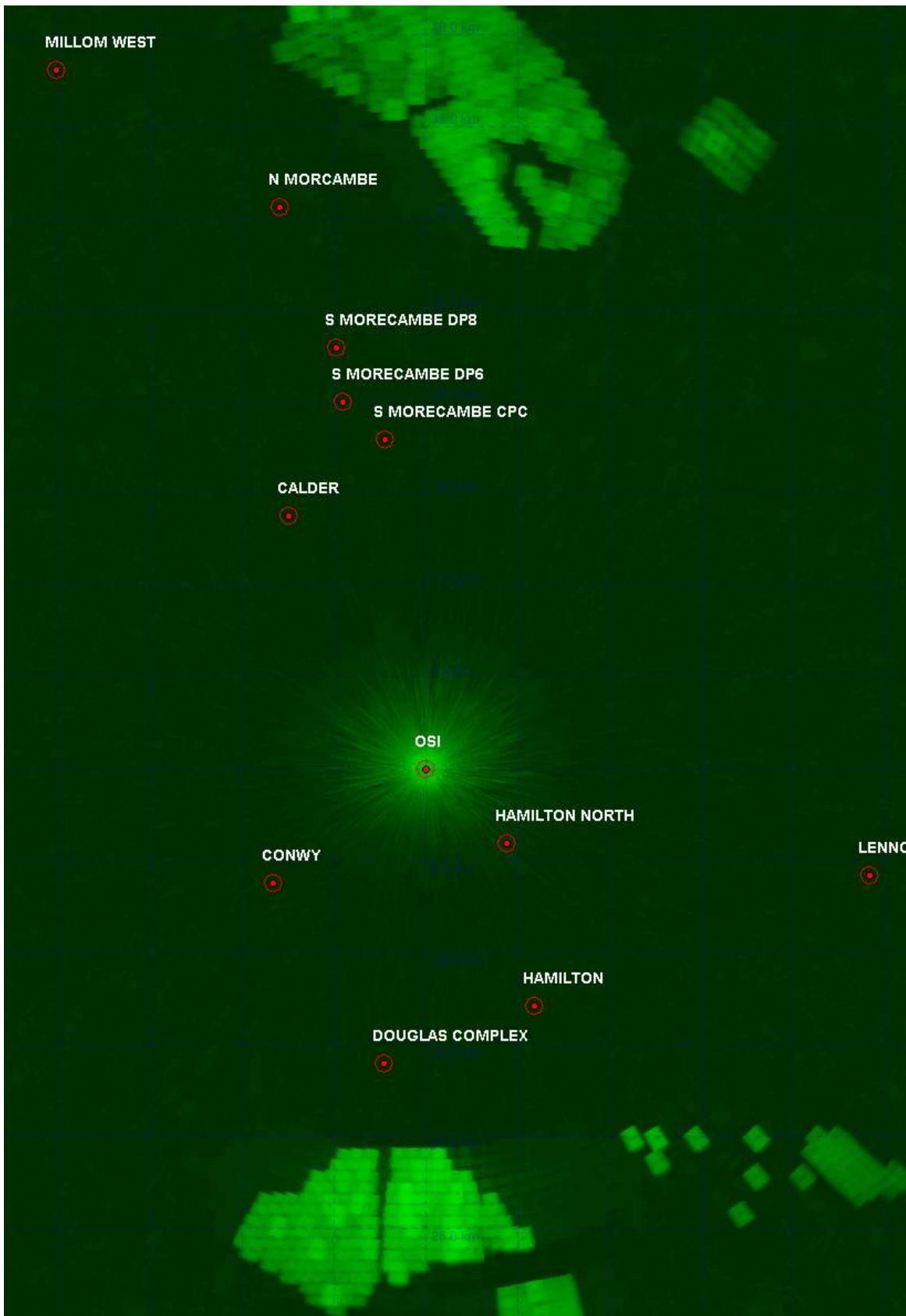
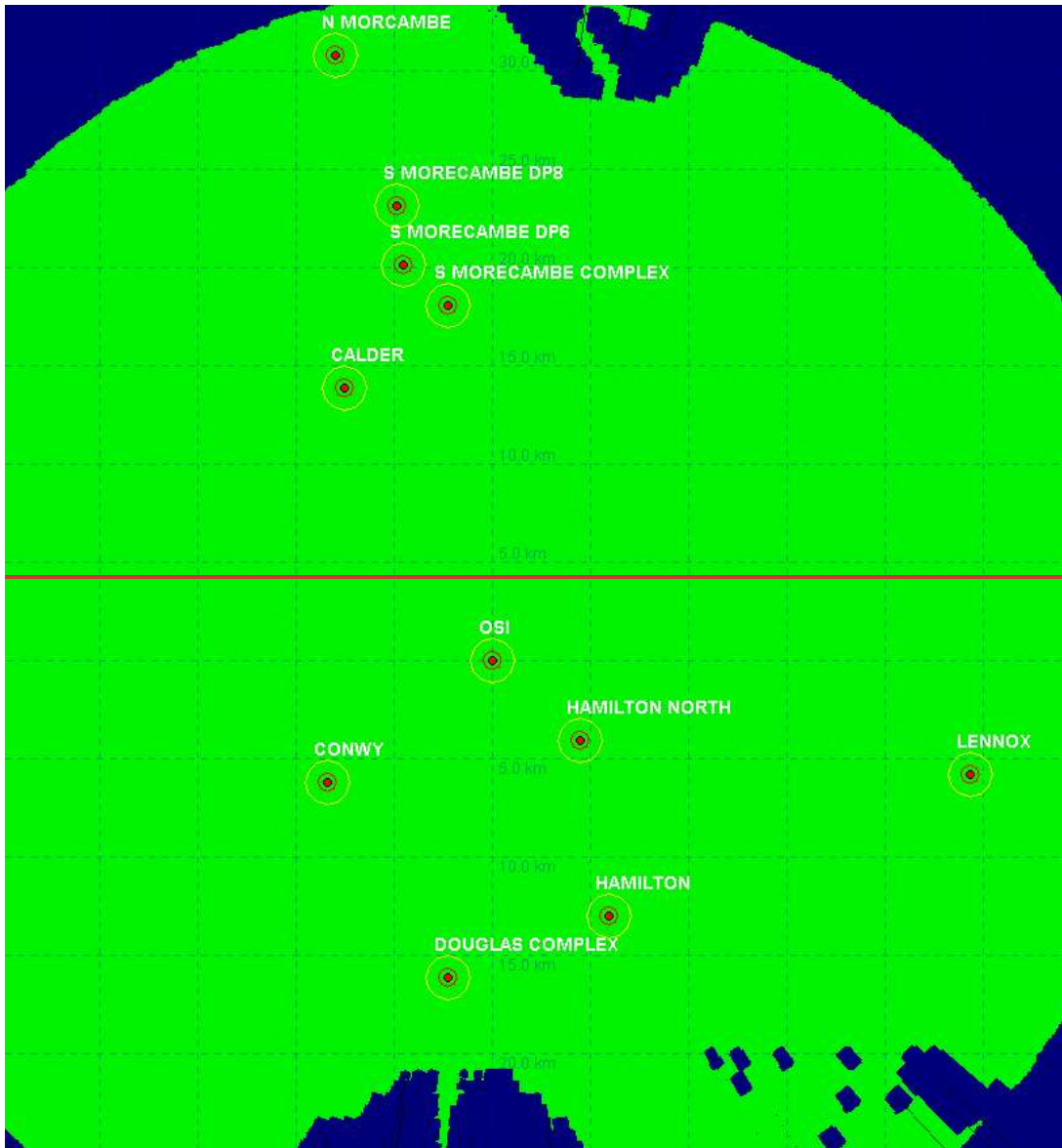


Figure 4.11: ENI Energy’s OSI REWS detection threshold.



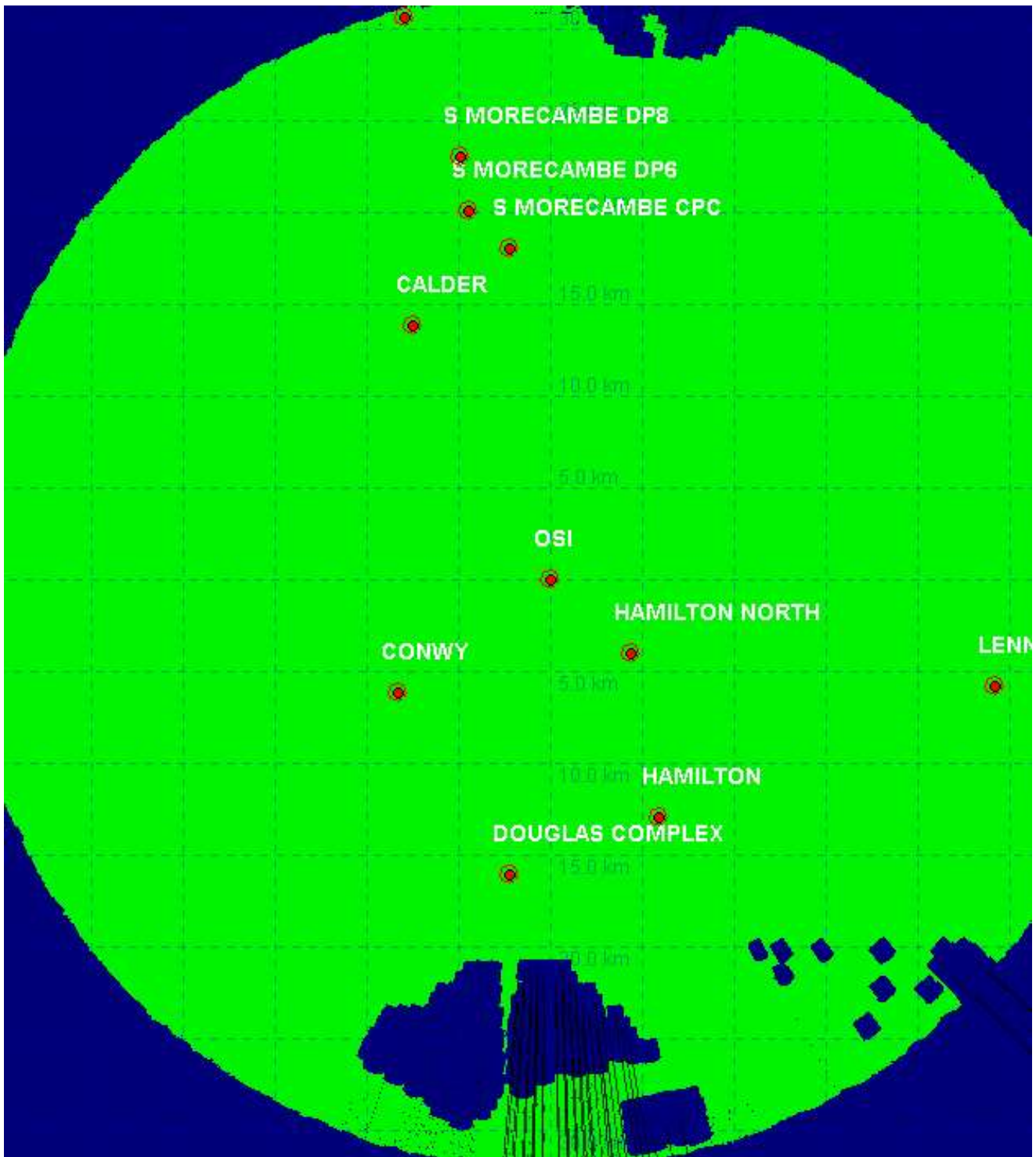
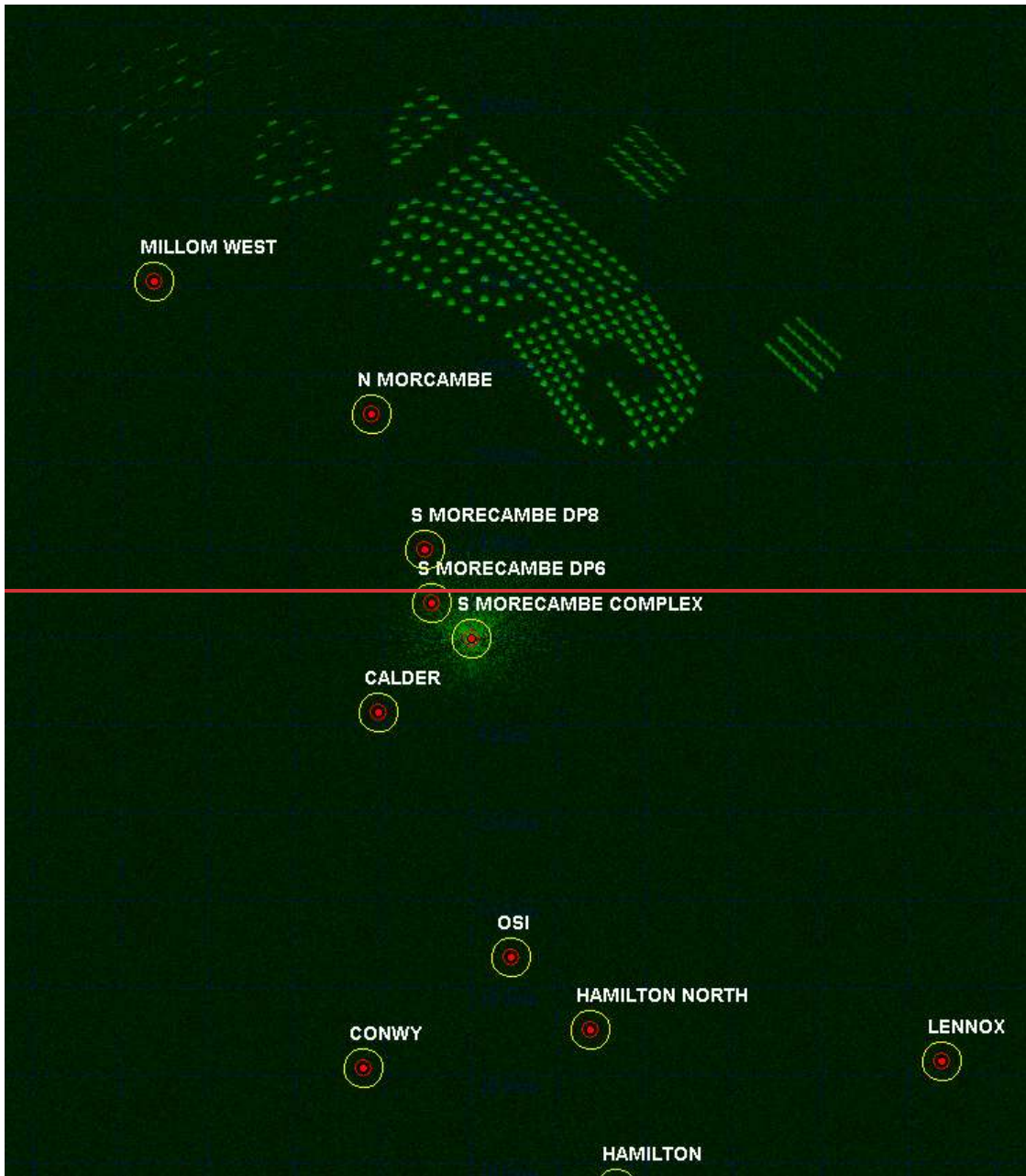


Figure 4.12: ENI Energy's OSI REWS detection plot showing loss regions for a **1000420** m² target.



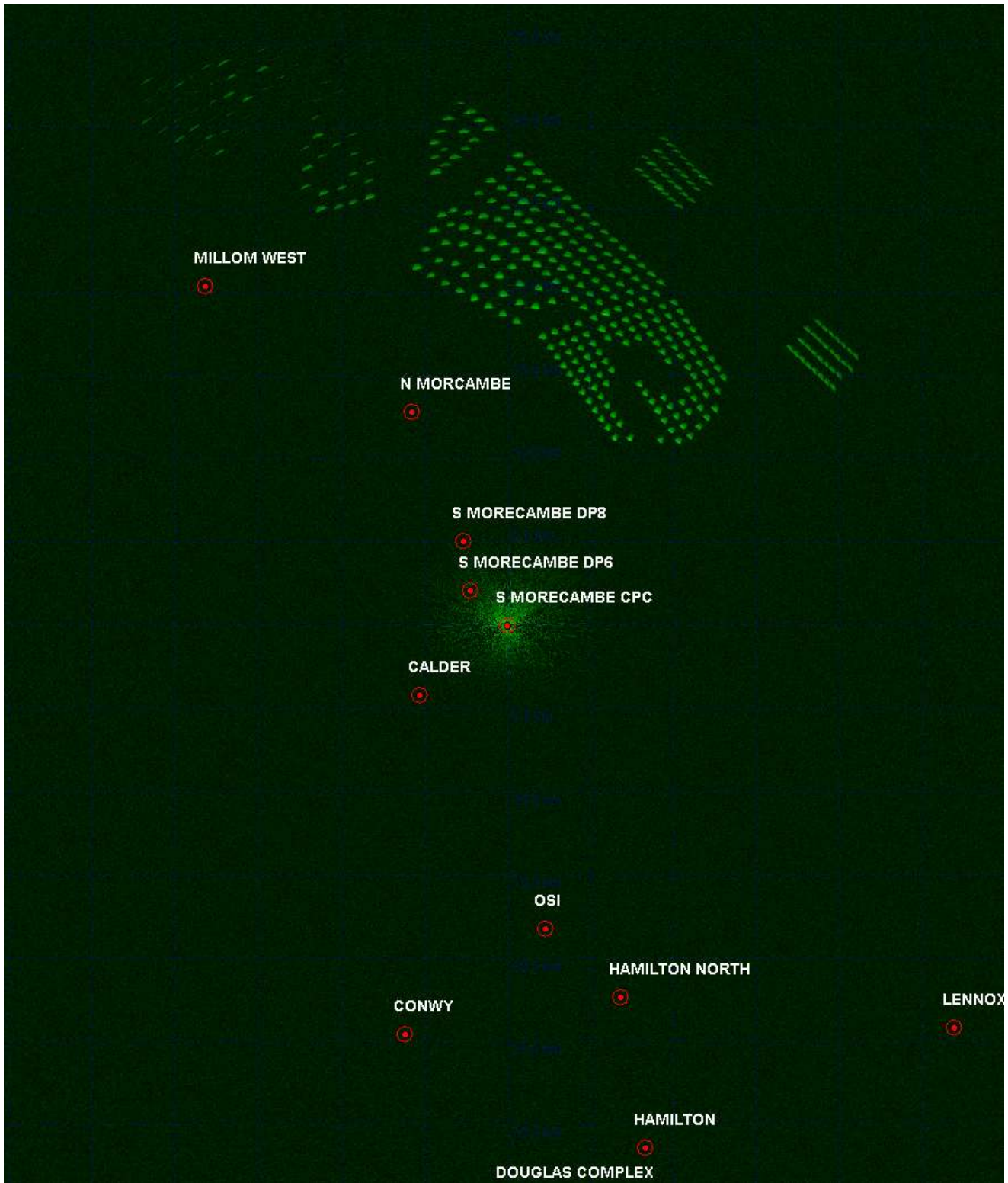
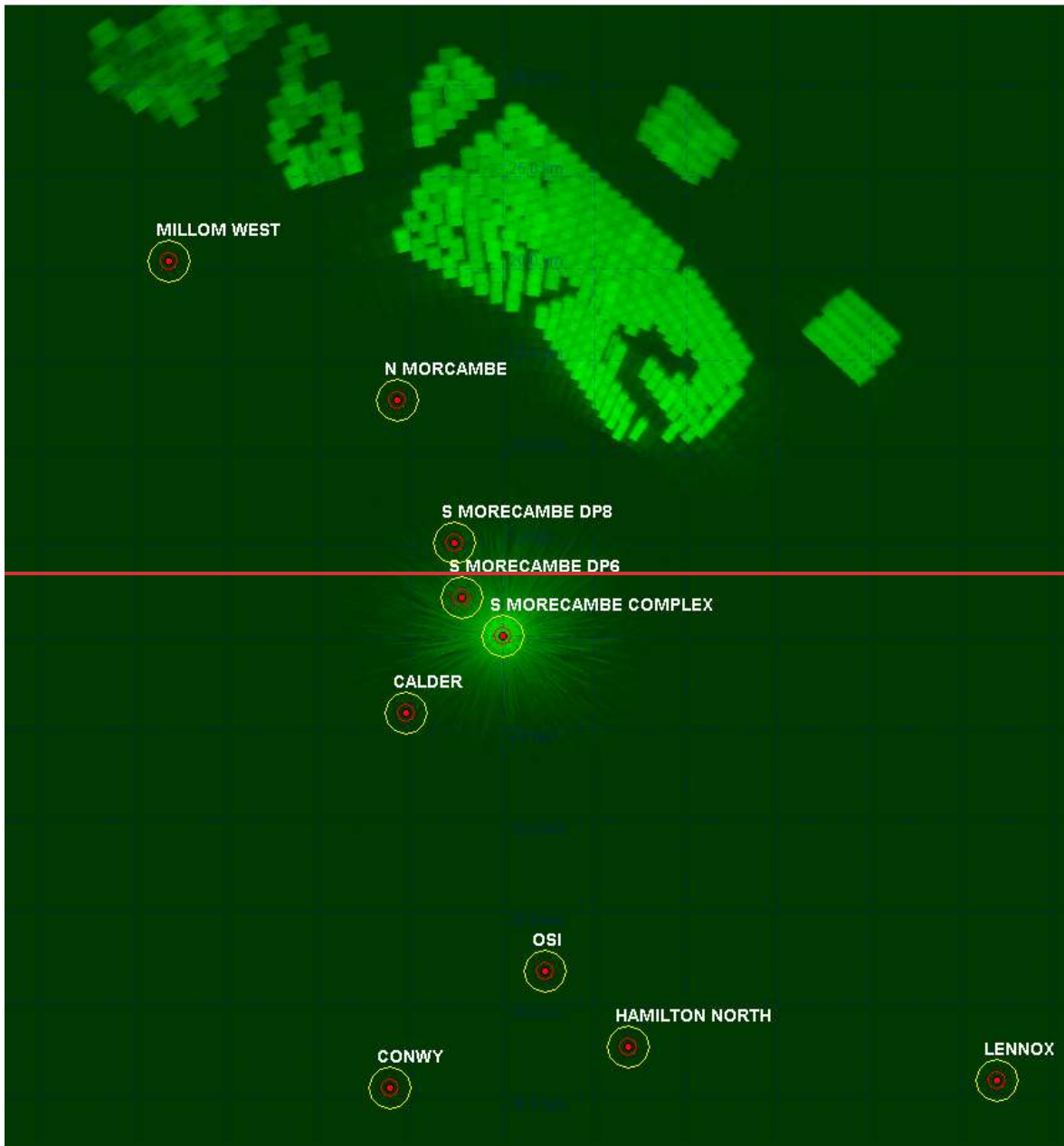


Figure 4.13: Spirit Energy’s South Morecambe AP1 platform REWS clutter map showing returns from the wind turbines and sea clutter.



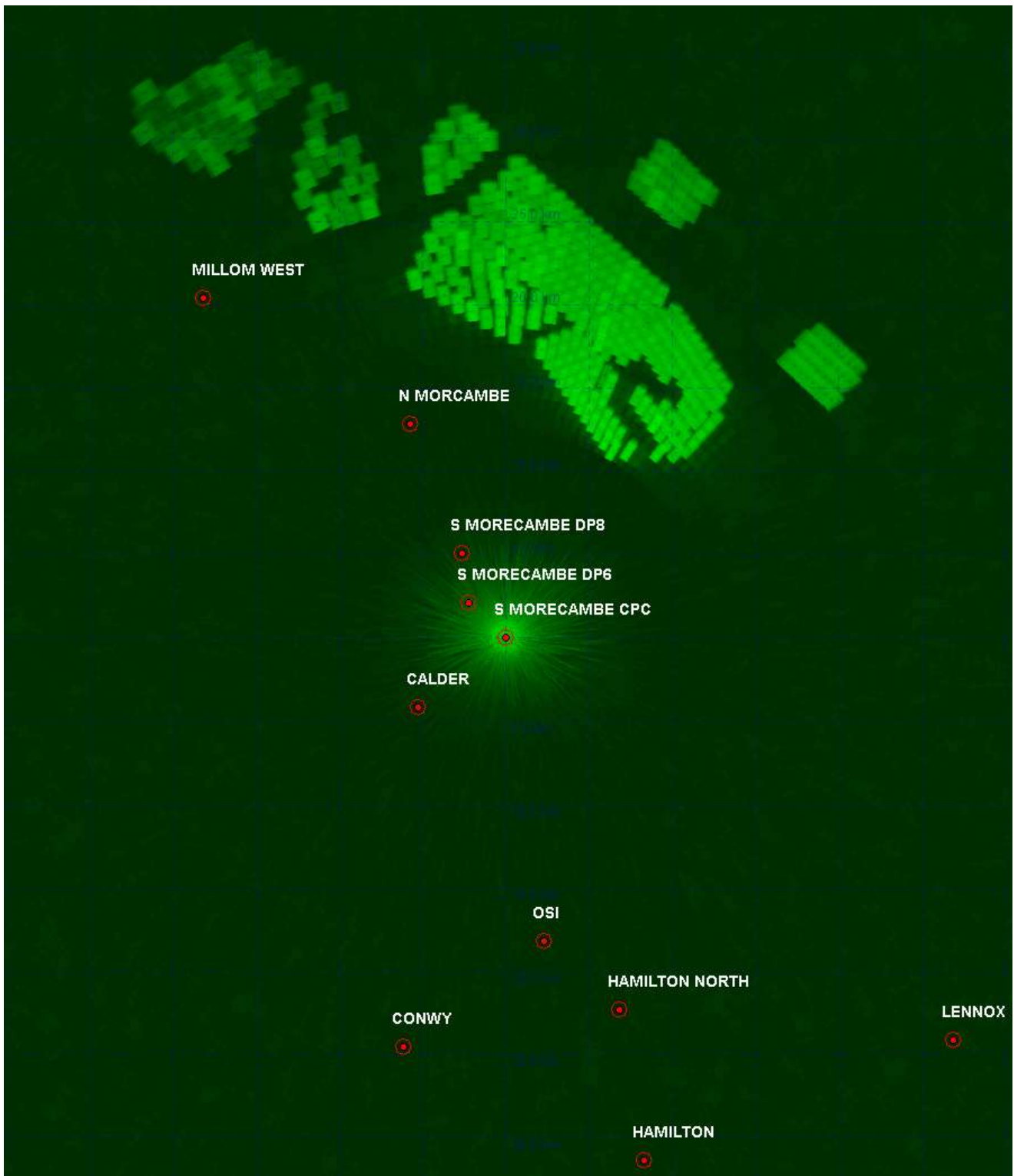
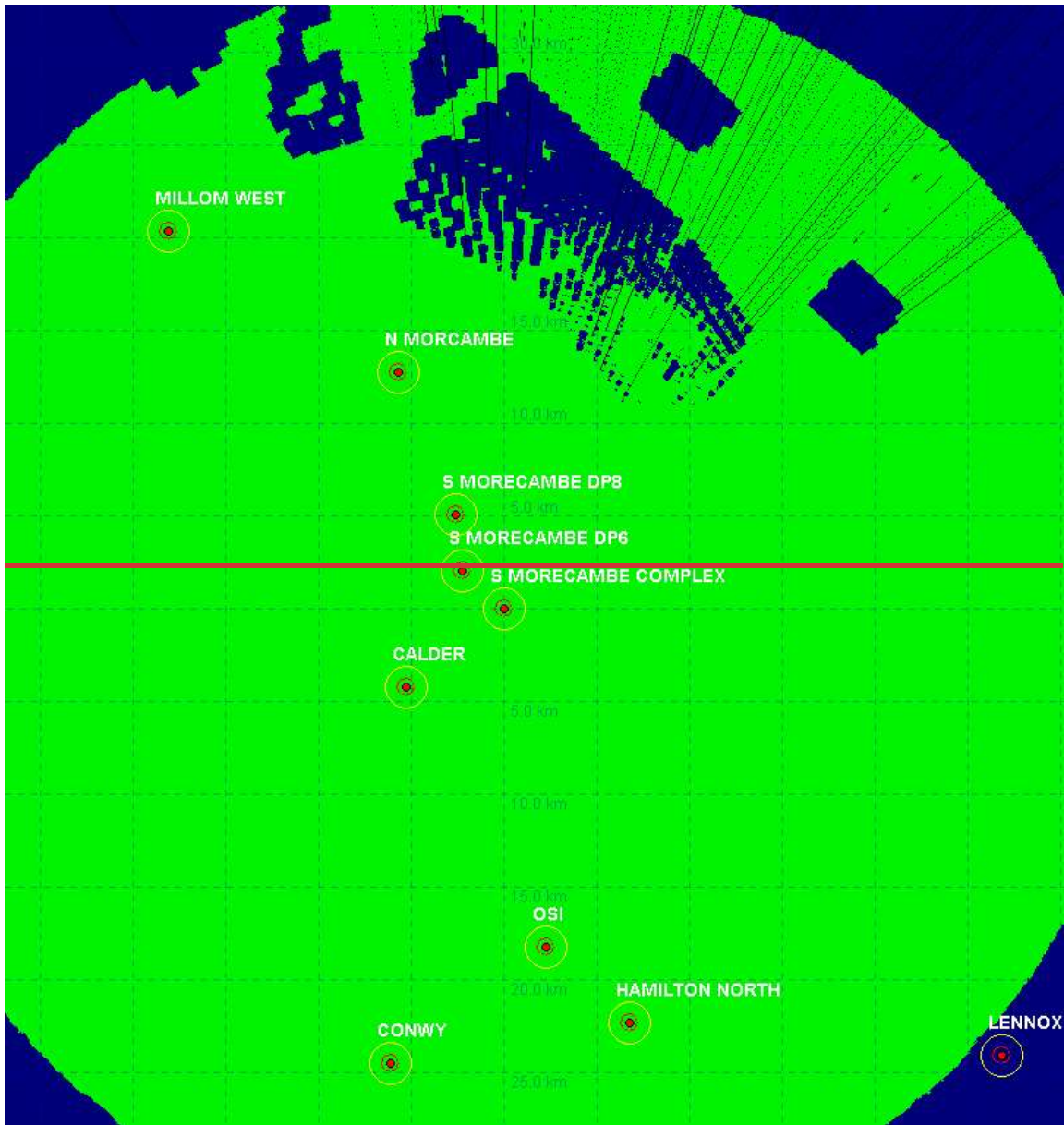


Figure 4.14: Spirit Energy’s South Morecambe AP1 platform REWS detection threshold.



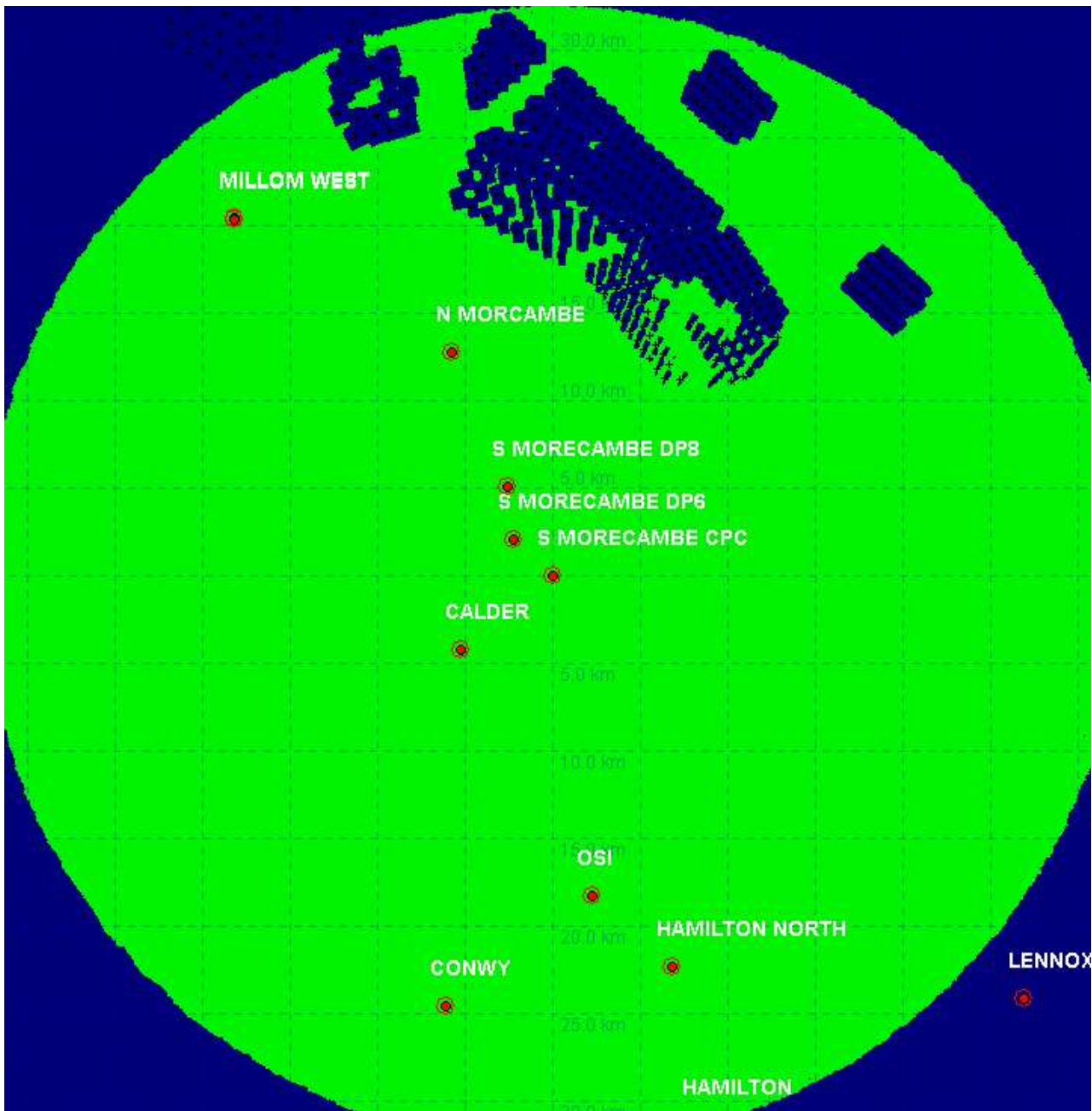


Figure 4.15: Spirit Energy’s South Morecambe AP1 platform REWS detection plot showing loss regions for a **1000420** m2 target.

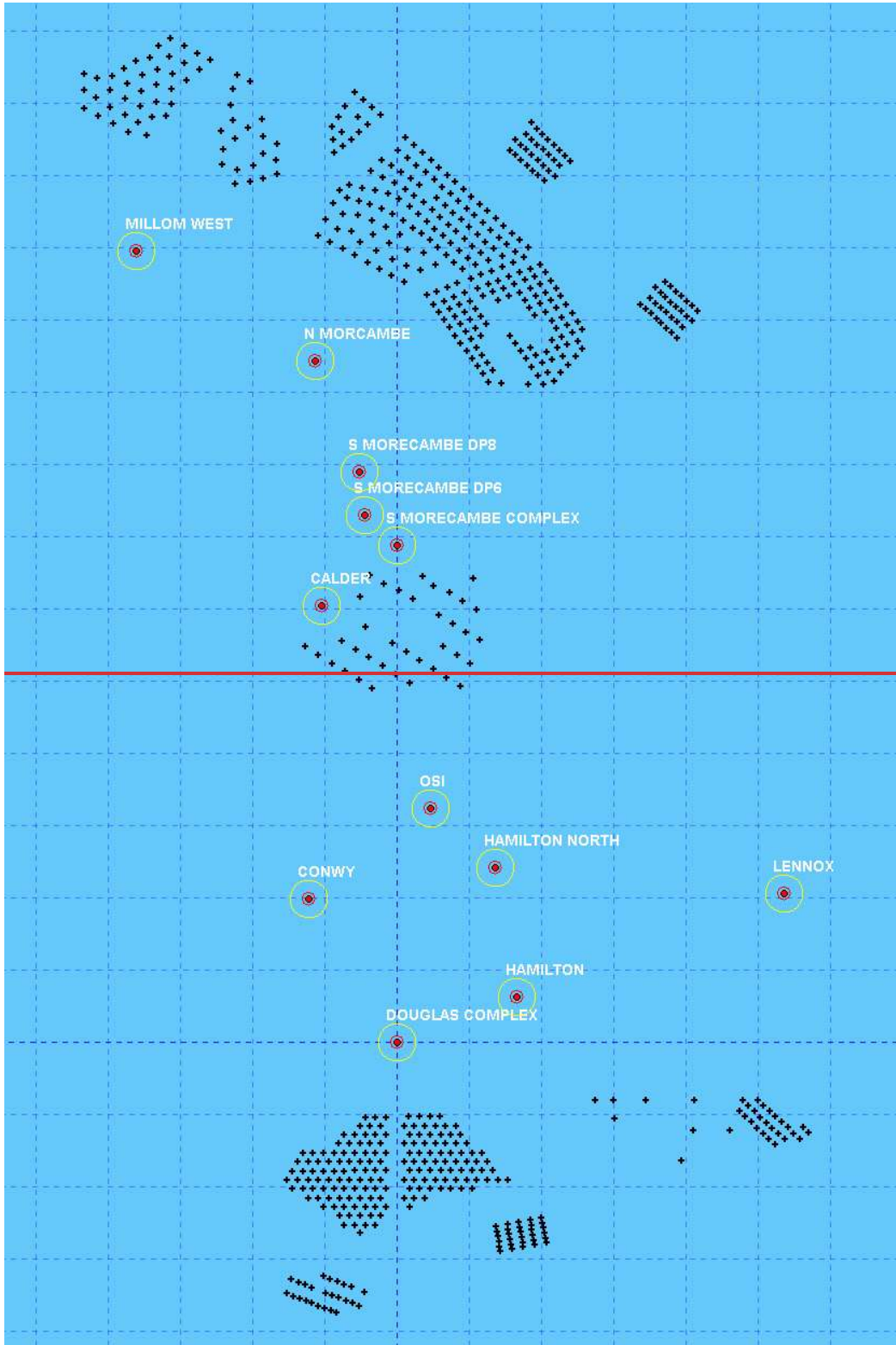
4.2.1.9

The overall results show that the REWS can easily detect the test vessel as the returns are above the detection threshold over majority of the coverage region. However, once a vessel is travelling within a windfarm, the raised threshold over the cells around each wind turbine can cause loss of detection. This can be seen in all the assessed platforms with line-of-sight coverage to nearby windfarms. In some cases, such as Spirit Energy’s South Morecambe AP1 REWS, the effects on the detection region are more pronounced due to its proximity to the Walney Phase 1, Walney Phase 2 and West of Duddon Sands windfarms, which has relatively small separation distances between its turbines.

4.3 Assessment of the Morecambe Generation Assets

4.3.1 Masking and Detection Assessment

- 4.3.1.1 In a similar manner as the base case modelling, the potential impact of the Morecambe Generation Assets on the REWS is assessed. The modelled layout is shown in [Figure 4.16](#) while the REWS returns, expected threshold levels and the detection regions are illustrated in [Figure 4.17](#) to [Figure 4.28](#).



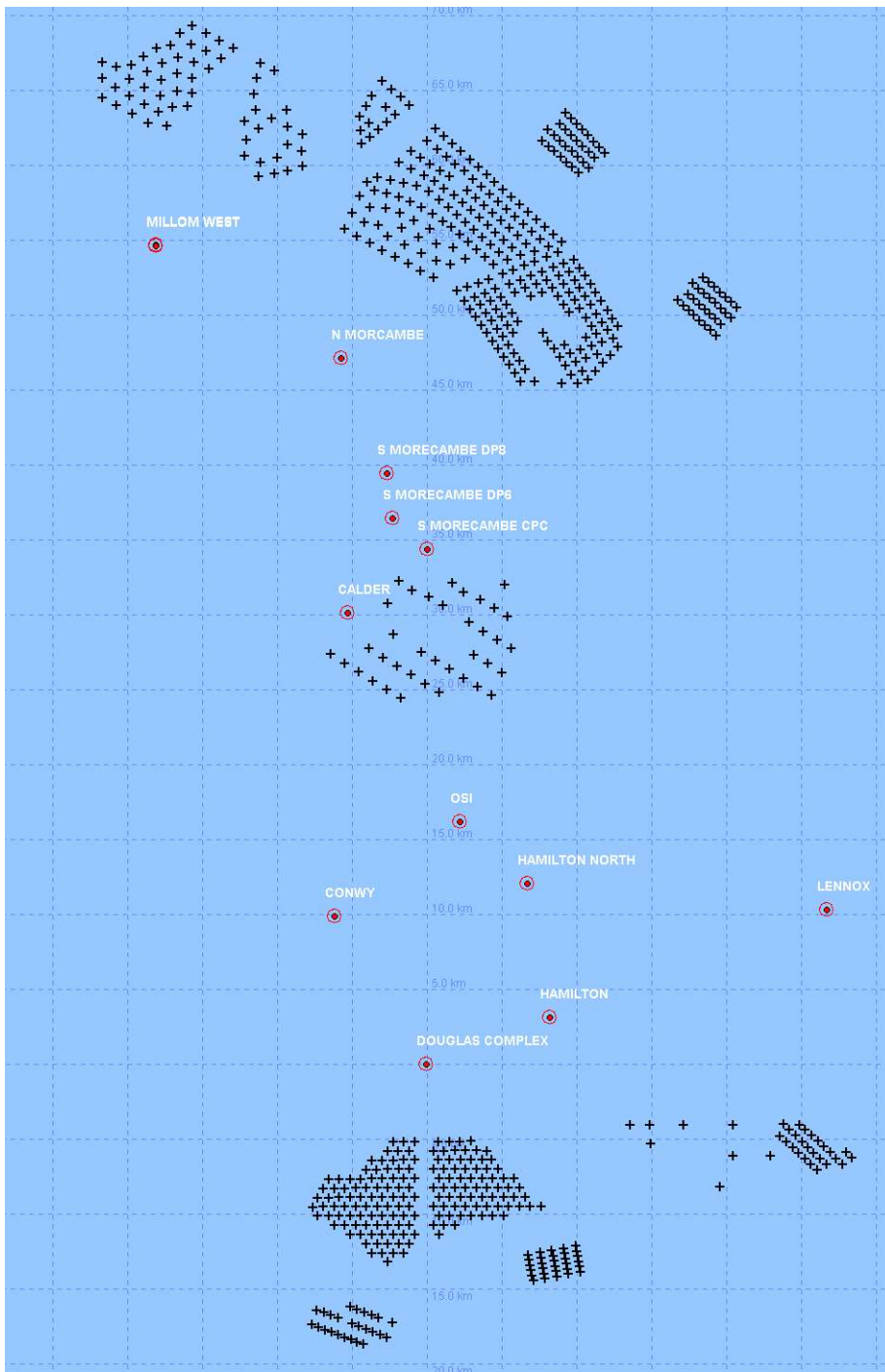
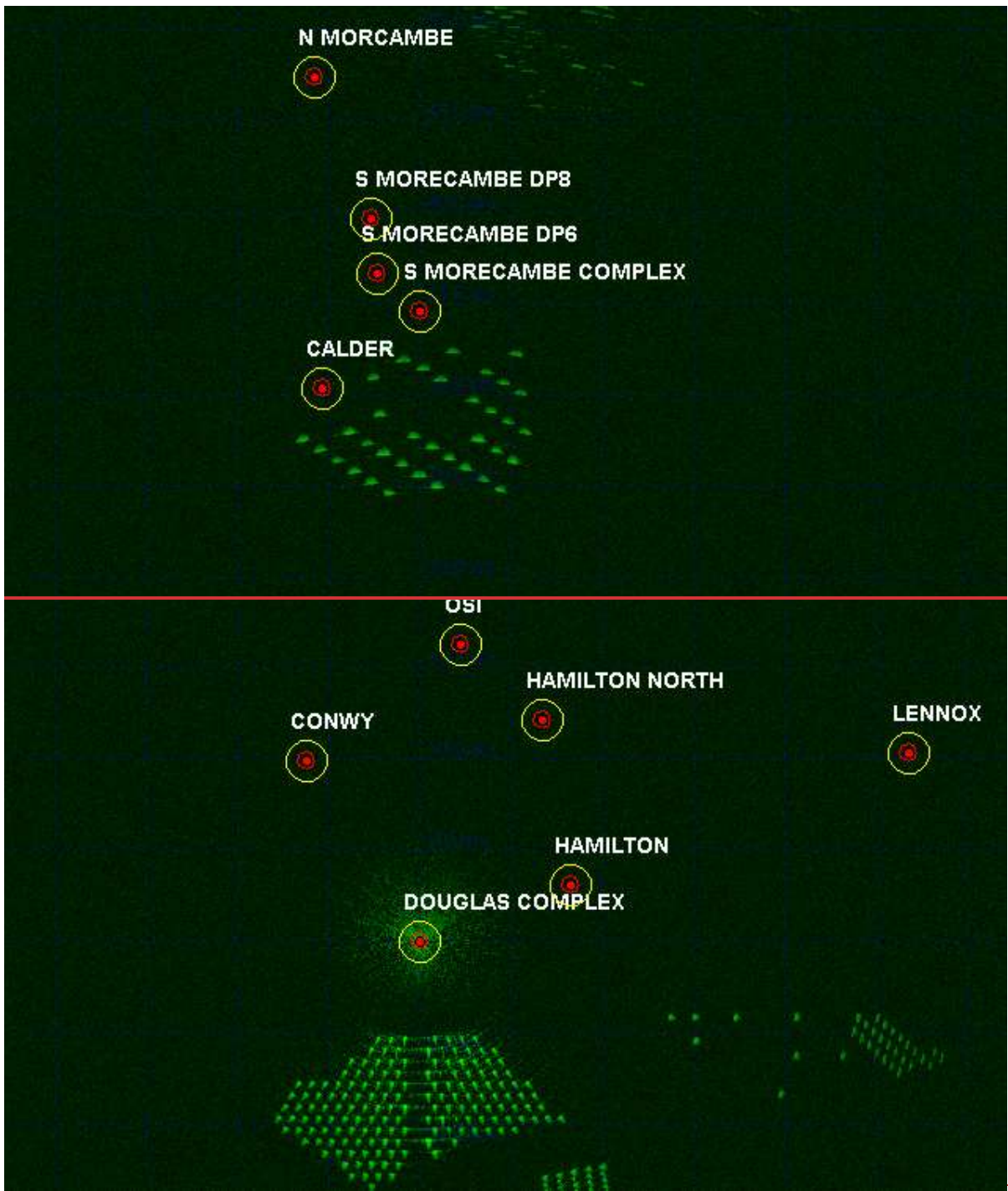


Figure 4.16: Modelled layout of the Morecambe Generation Assets showing the indicative location of the wind turbines and the location of oil and gas platforms in the region.



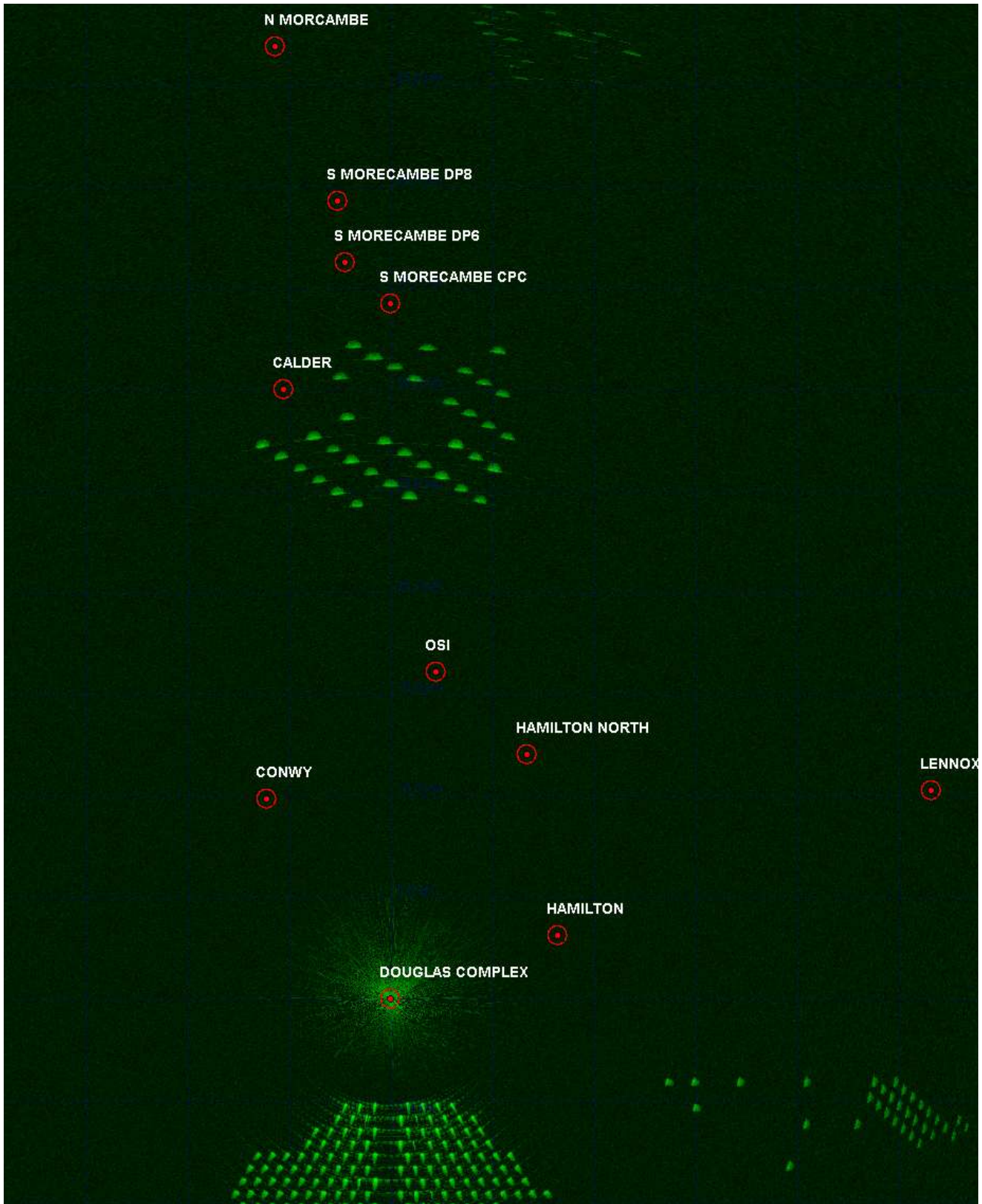
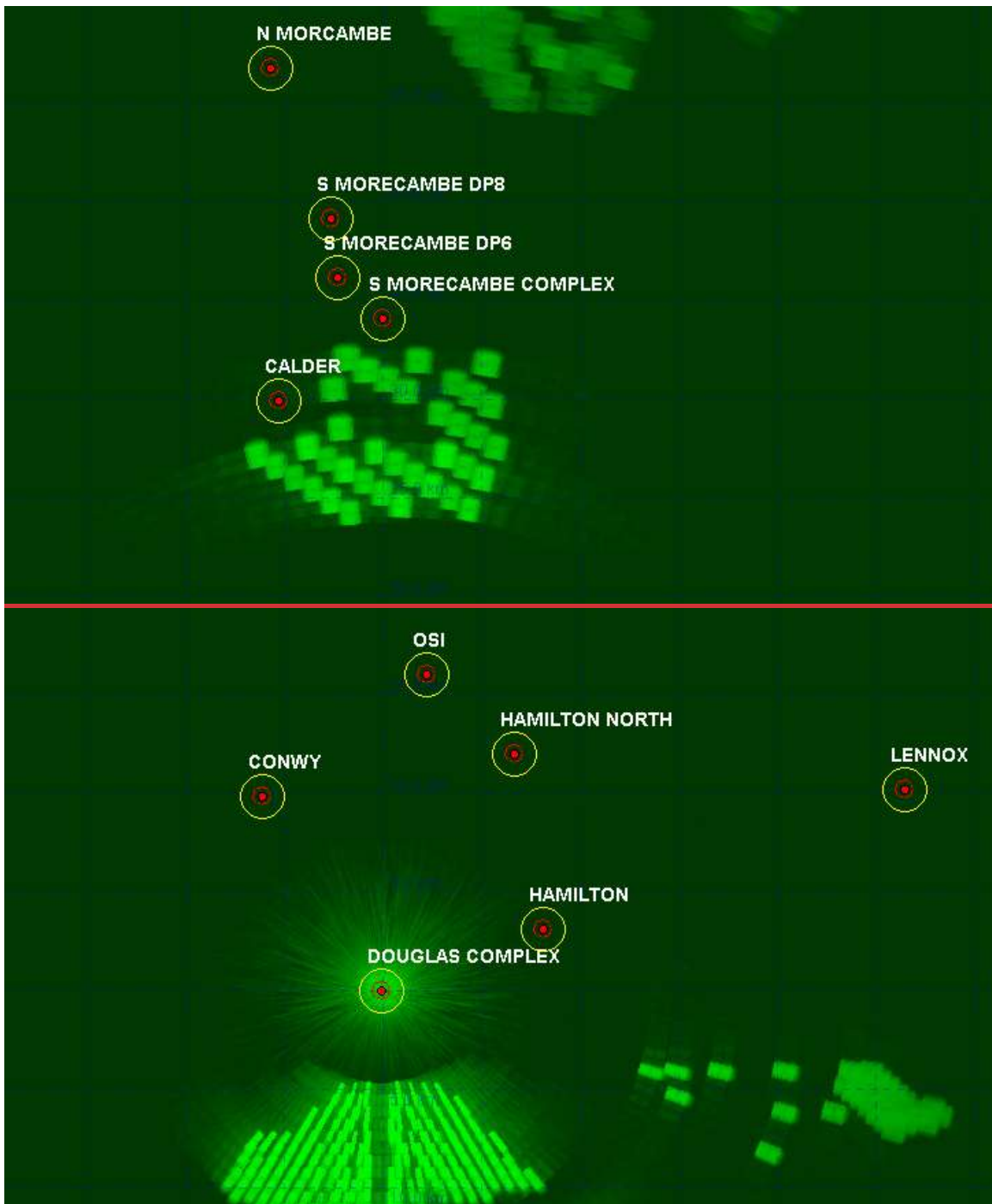


Figure 4.17: ENI Energy’s Douglas platform REWS clutter map showing returns from the Morecambe Generation Assets wind turbines and sea clutter.



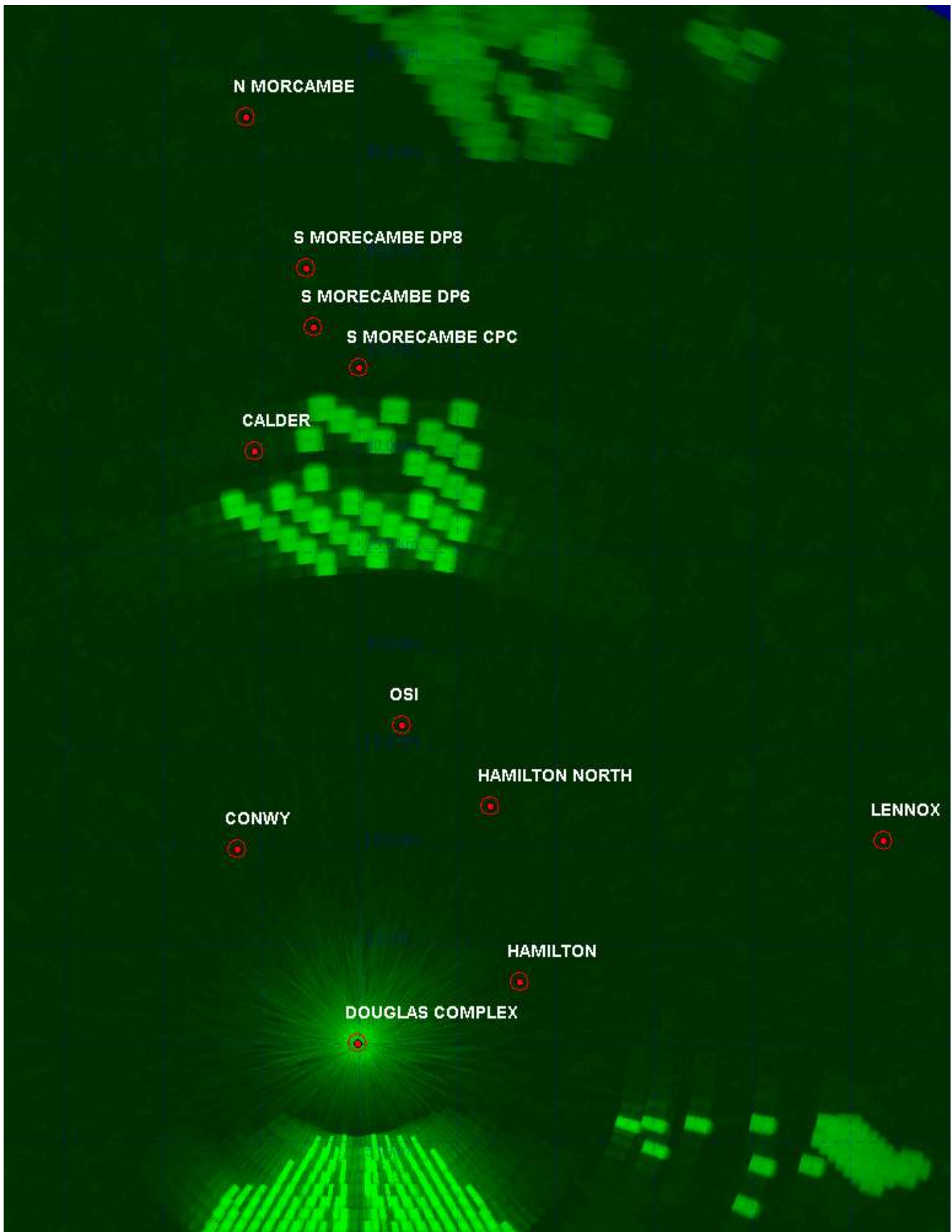
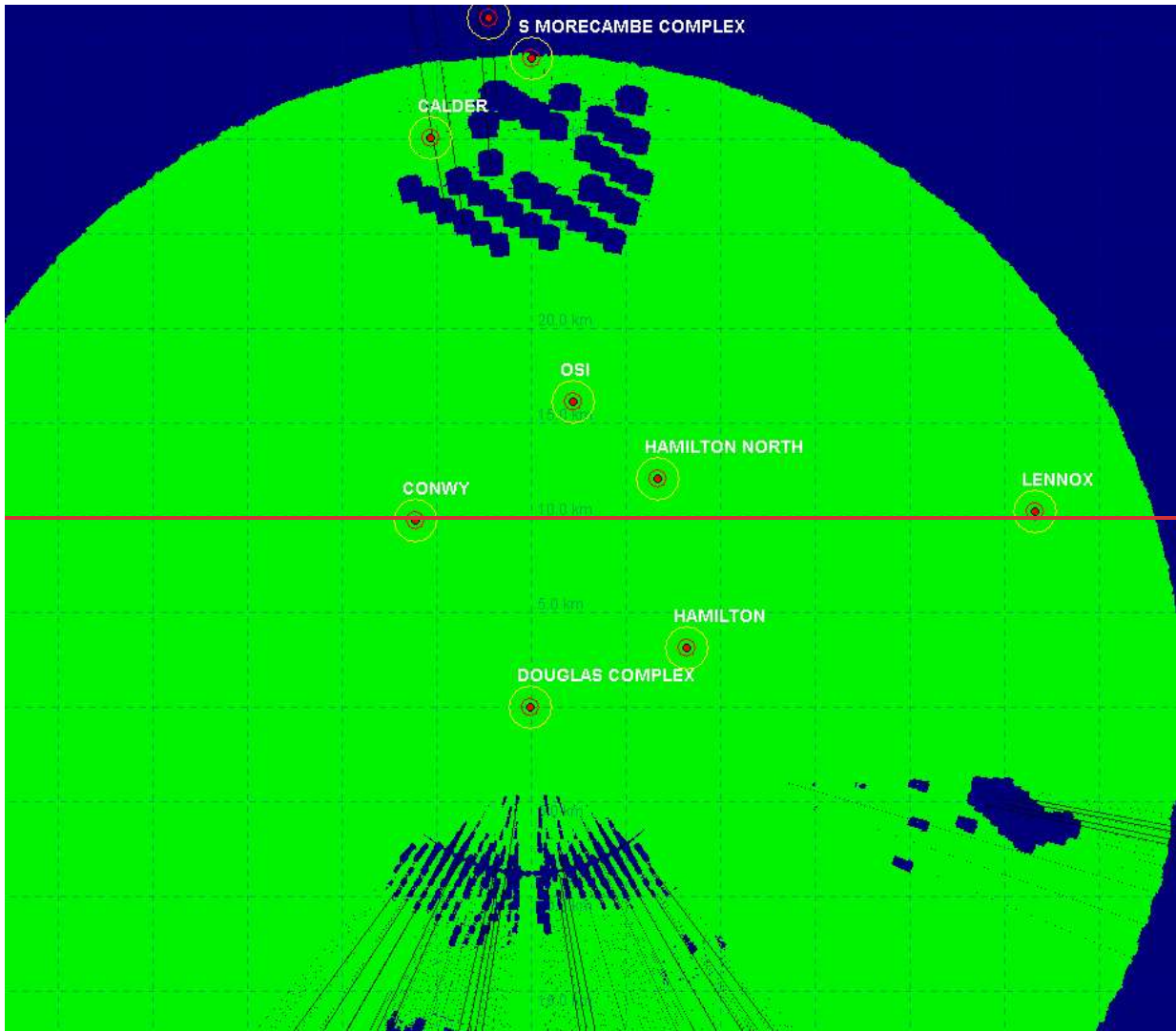


Figure 4.18: ENI Energy's Douglas platform REWS detection threshold over the Morecambe Array Area.



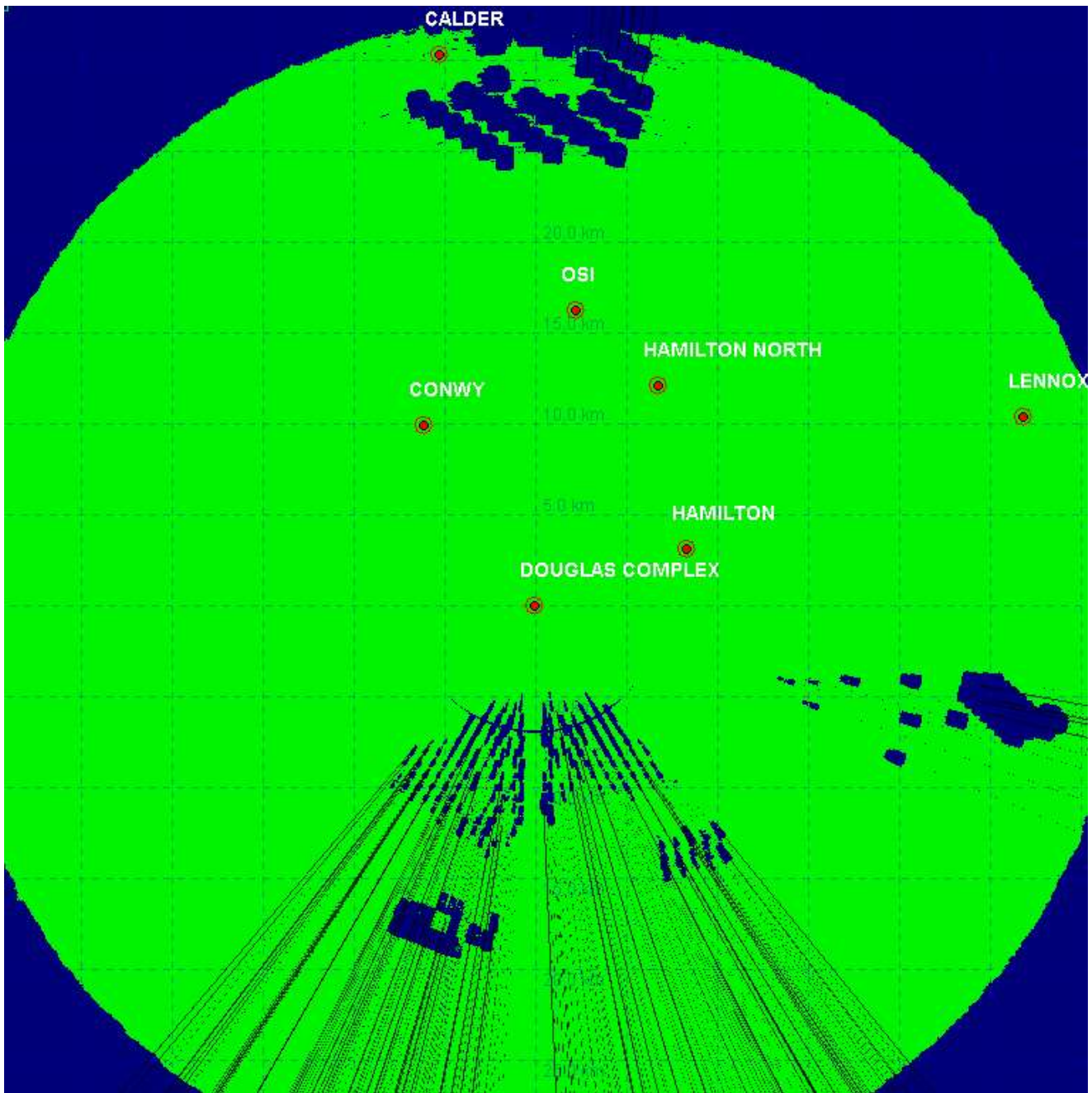


Figure 4.19: ENI Energy's Douglas platform REWS detection plot showing loss regions for a 4000420 m2 target.

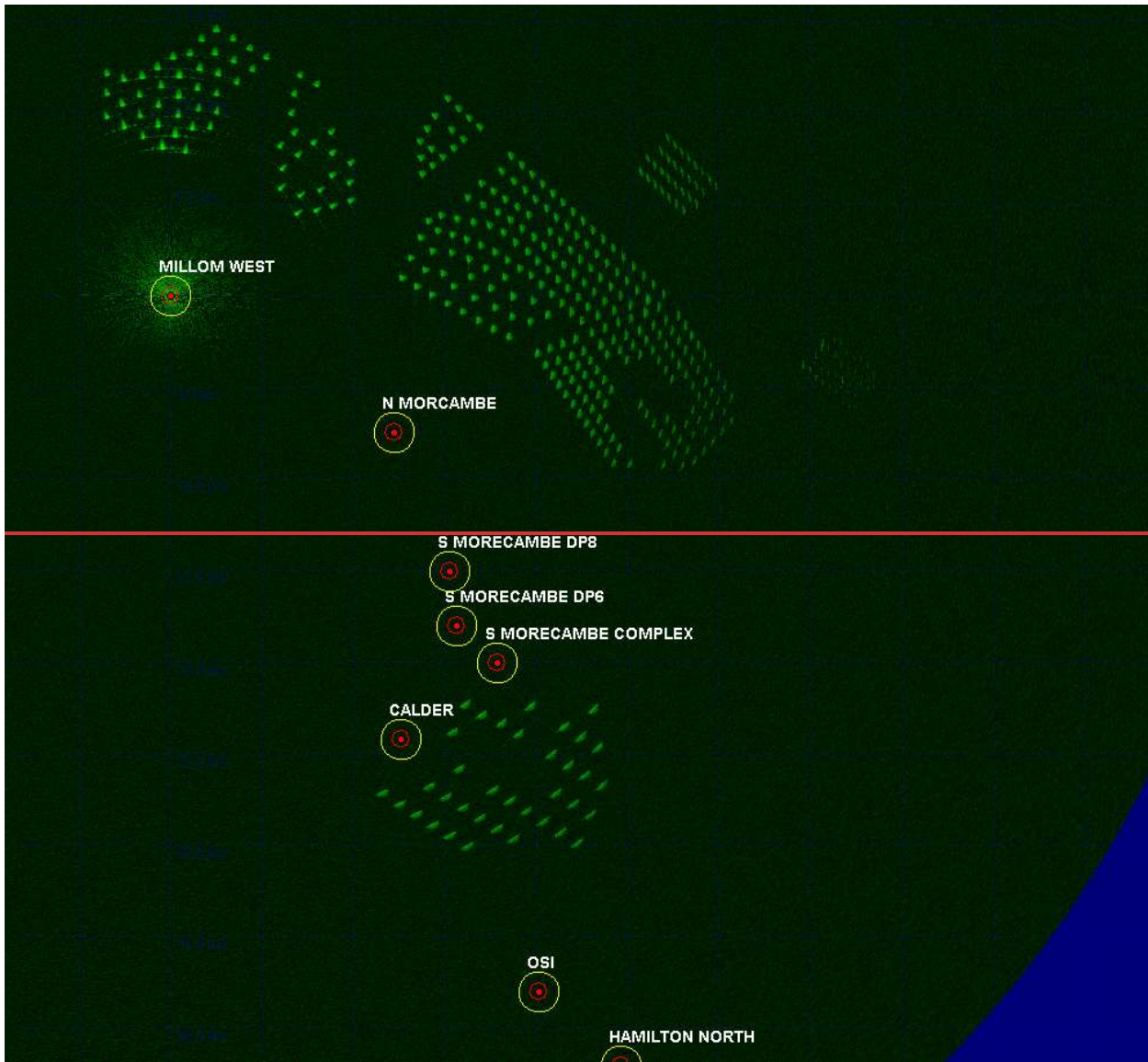
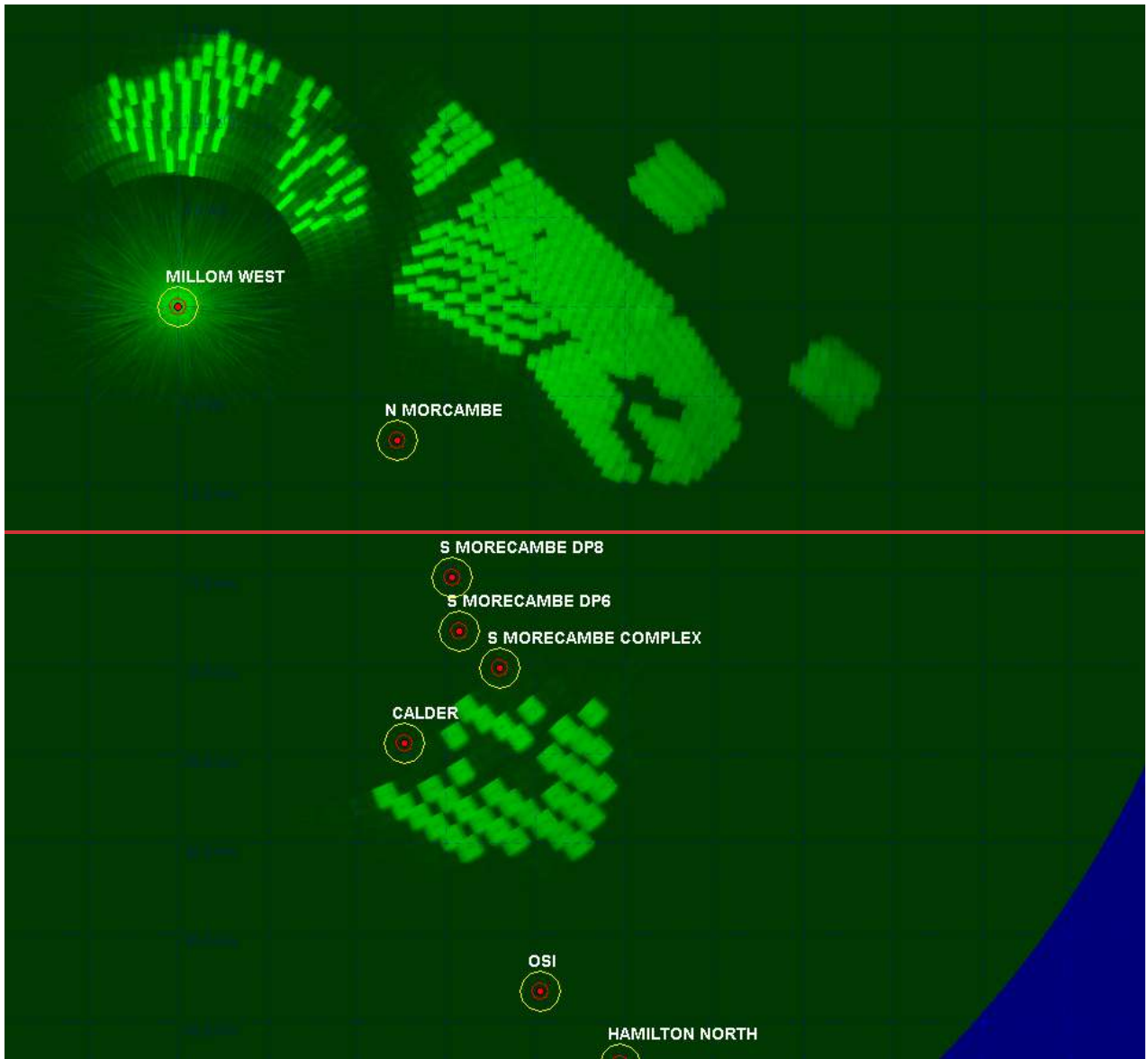




Figure 4.20: Harbour Energy’s Millom West platform REWS clutter map showing returns from the Morecambe Generation Assets wind turbines and sea clutter.



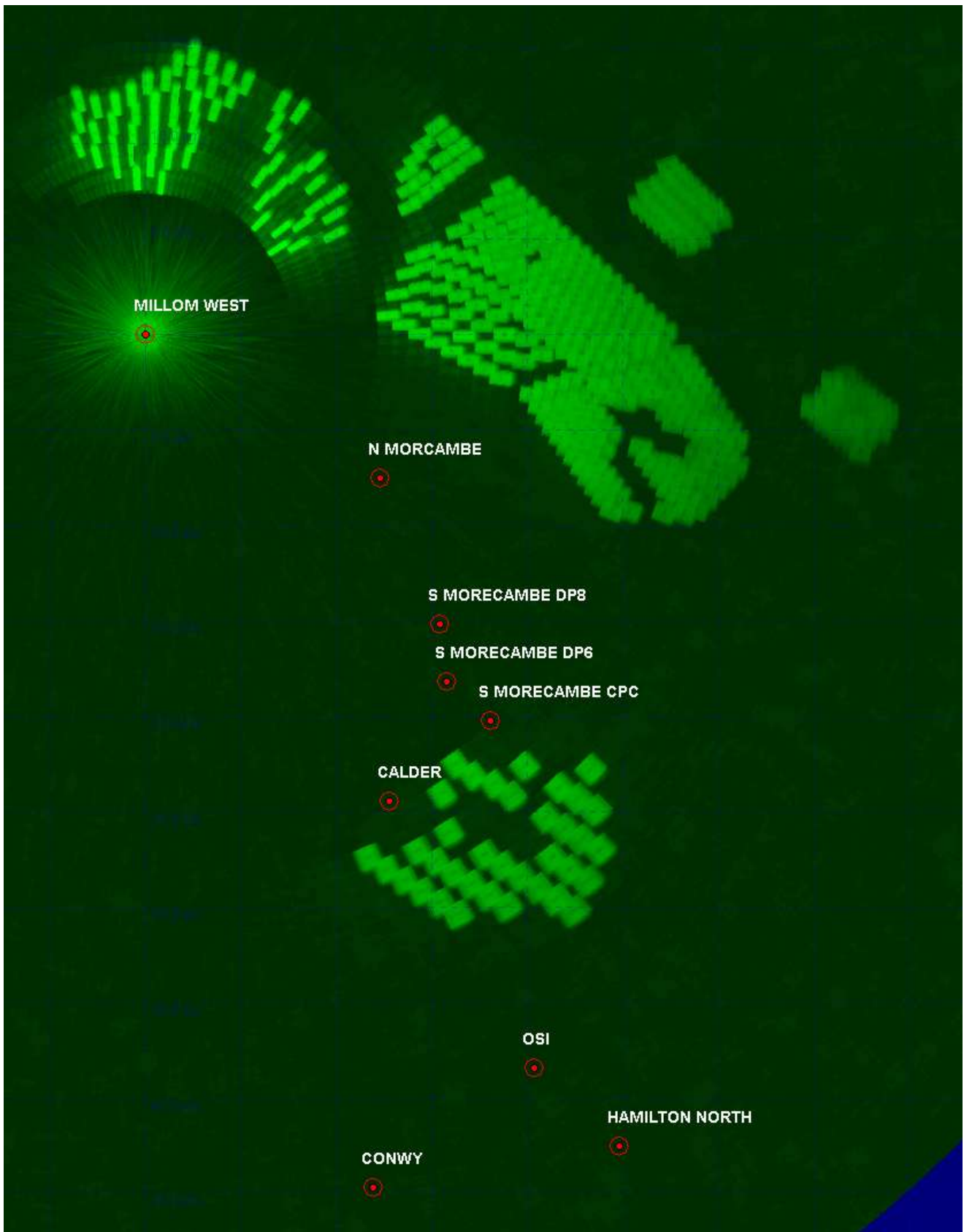
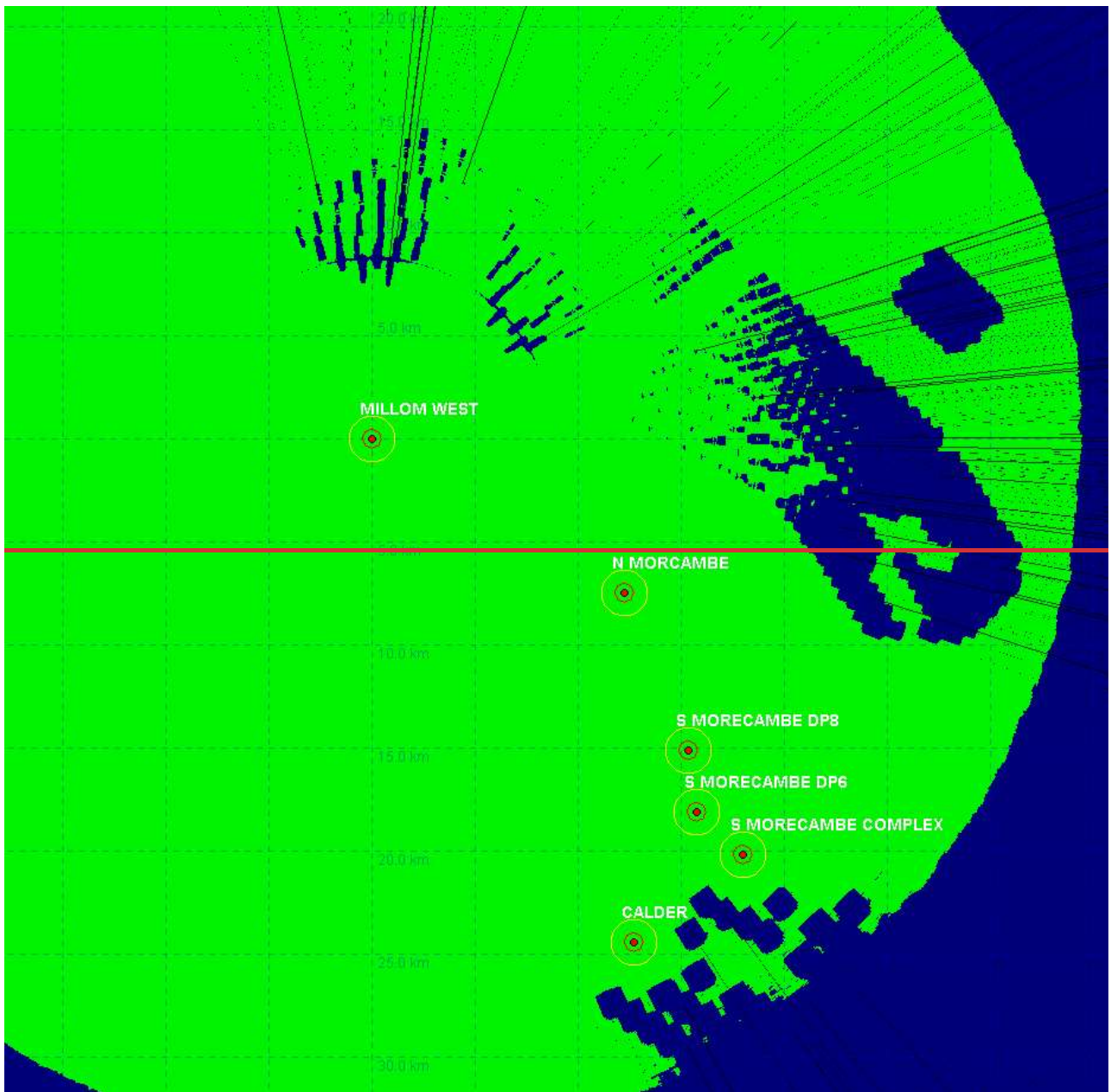


Figure 4.21: Harbour Energy’s Millom West platform REWS detection threshold over the Morecambe Generation Assets Array Area.



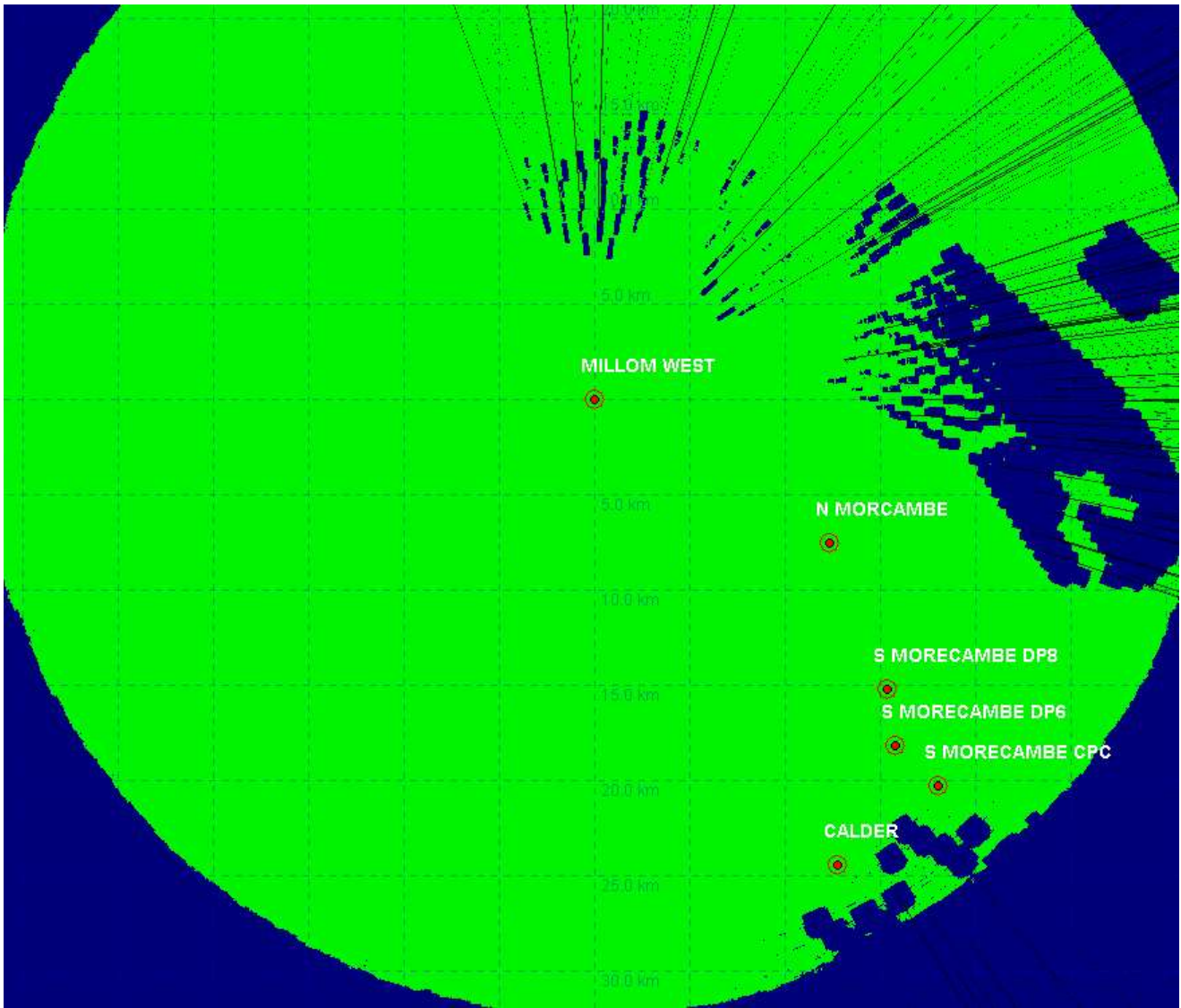
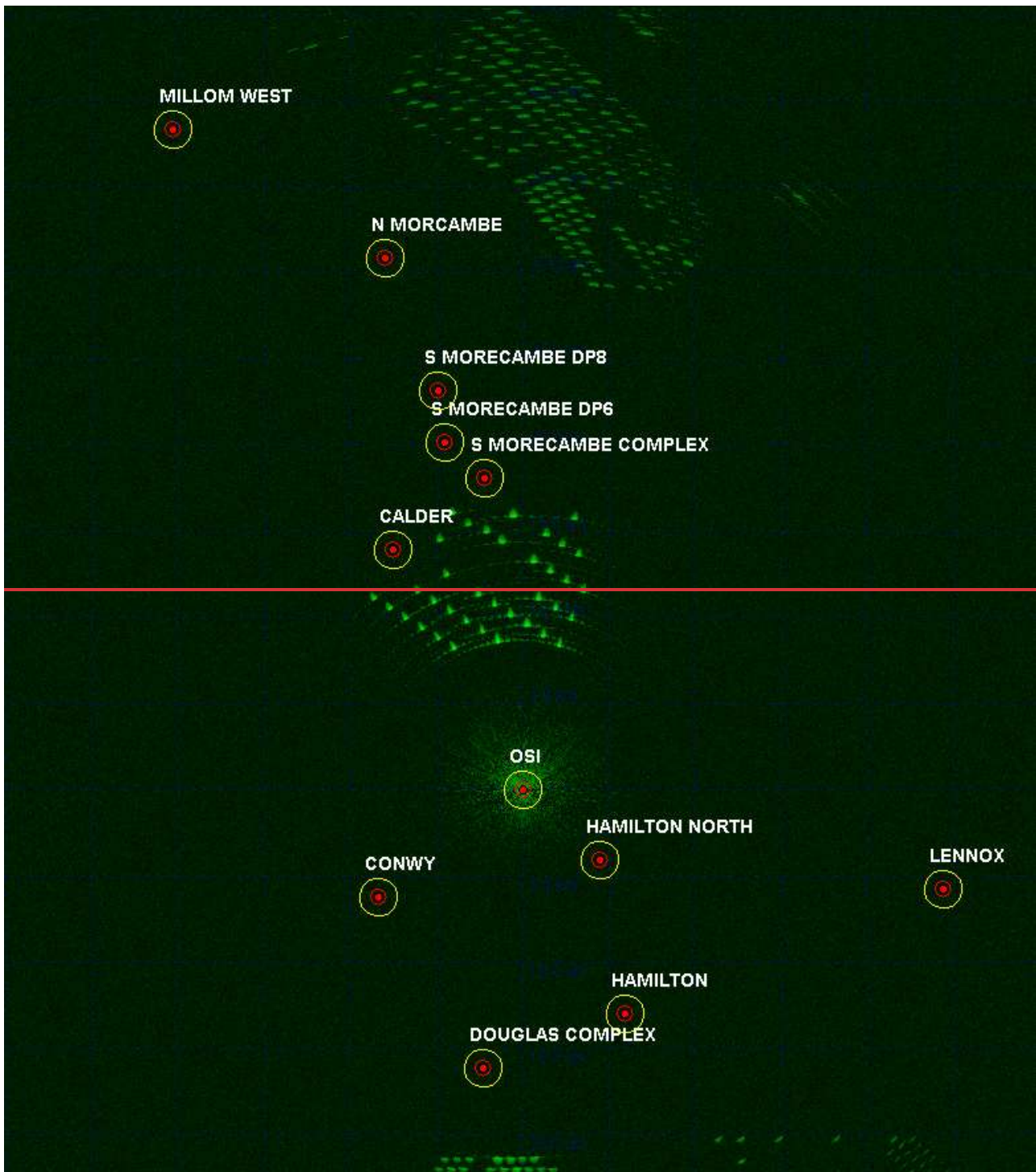


Figure 4.22: Harbour Energy’s Millom West platform REWS detection plot showing loss regions for a **1000420** m2 target.



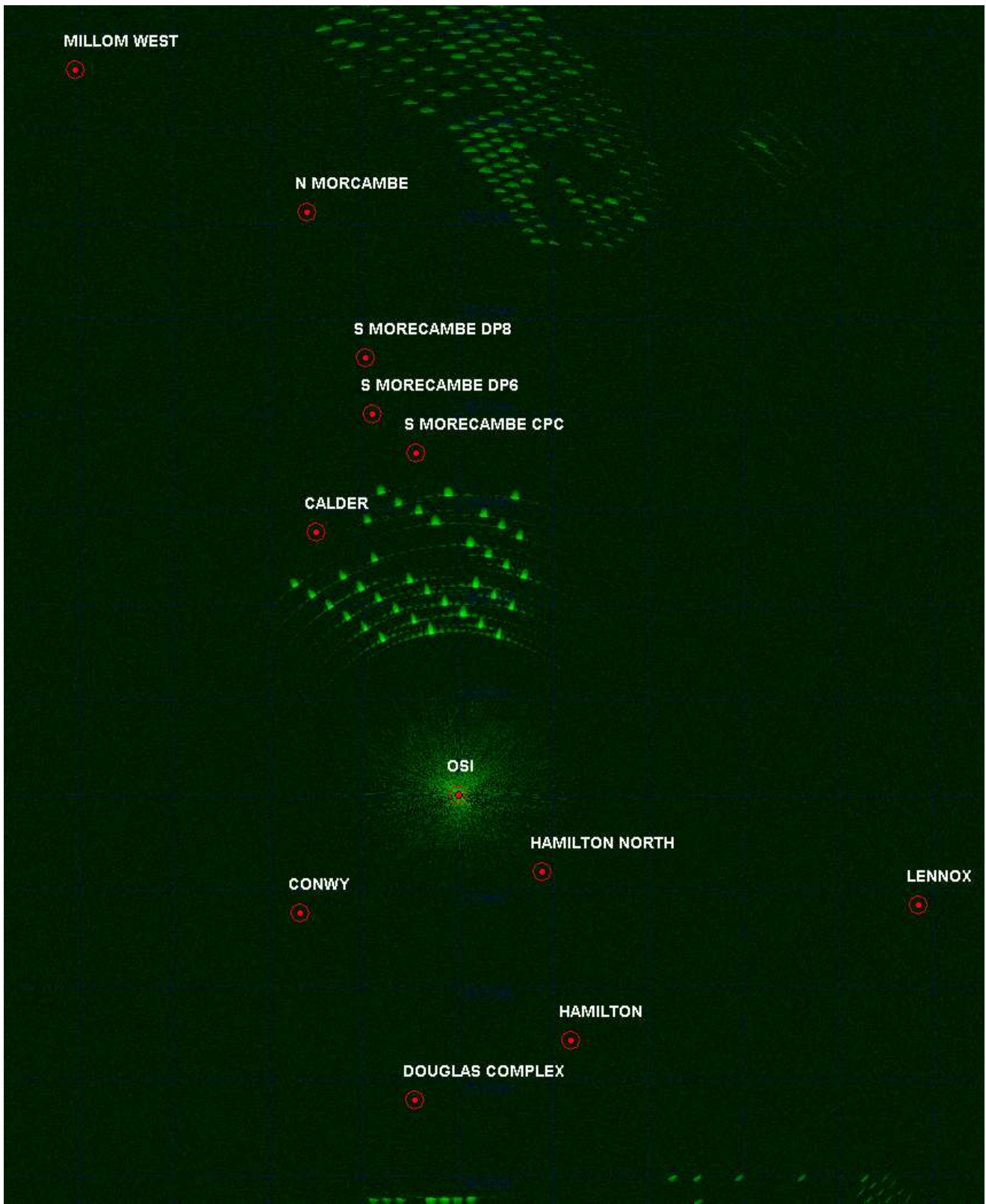
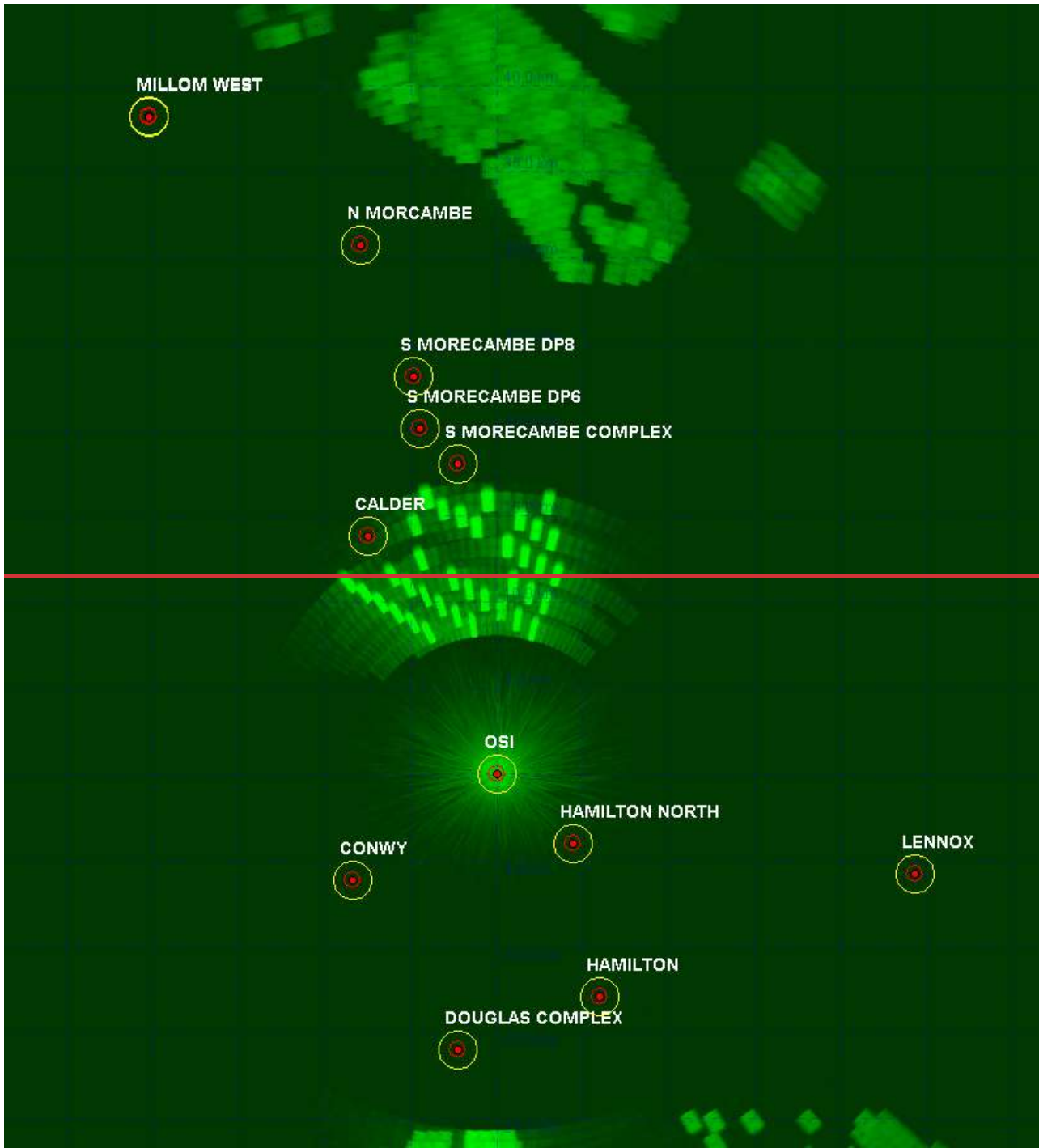


Figure 4.23: ENI Energy's OSI REWS detection clutter map showing returns from the Morecambe Generation Assets wind turbines and sea clutter.



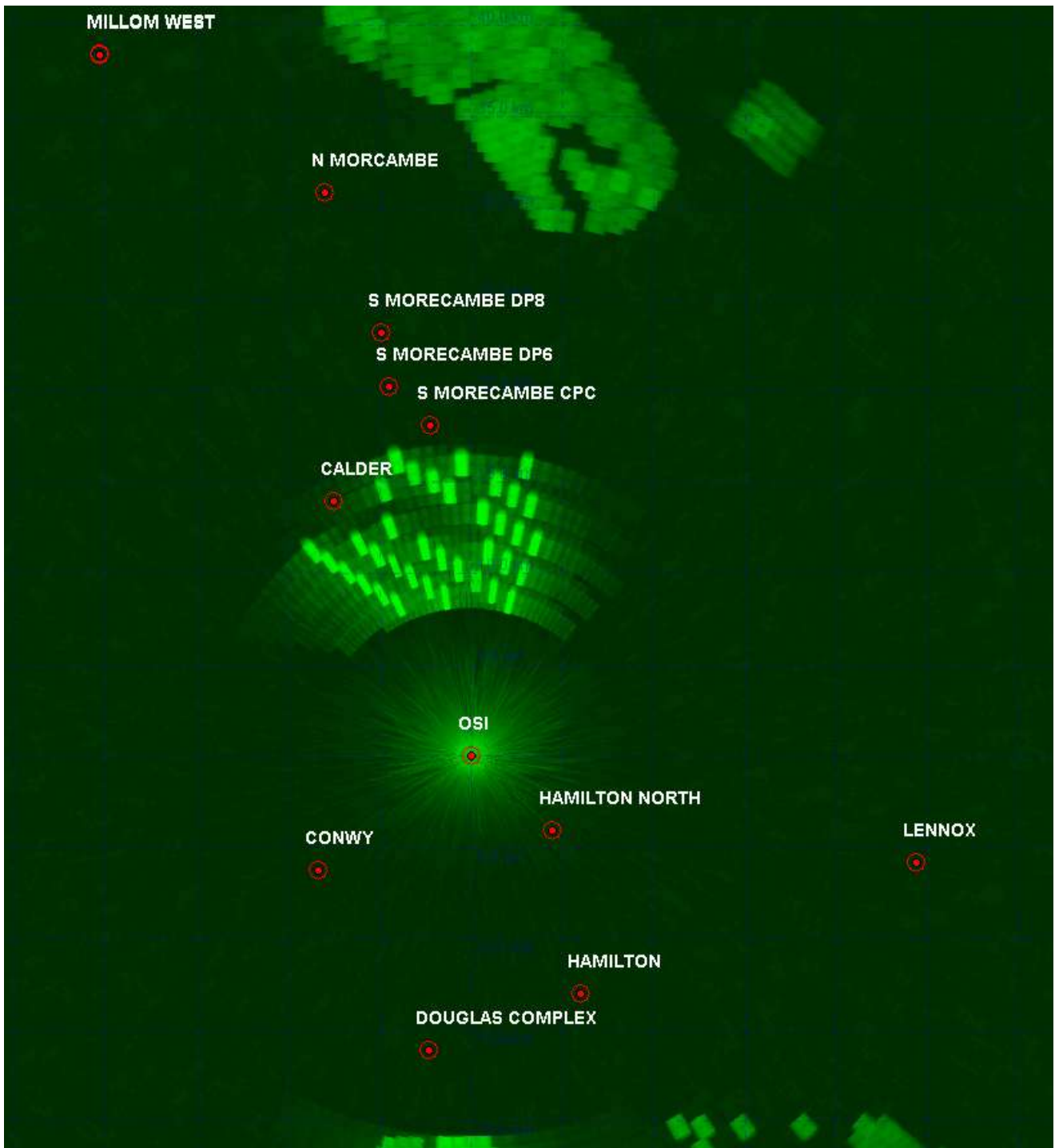
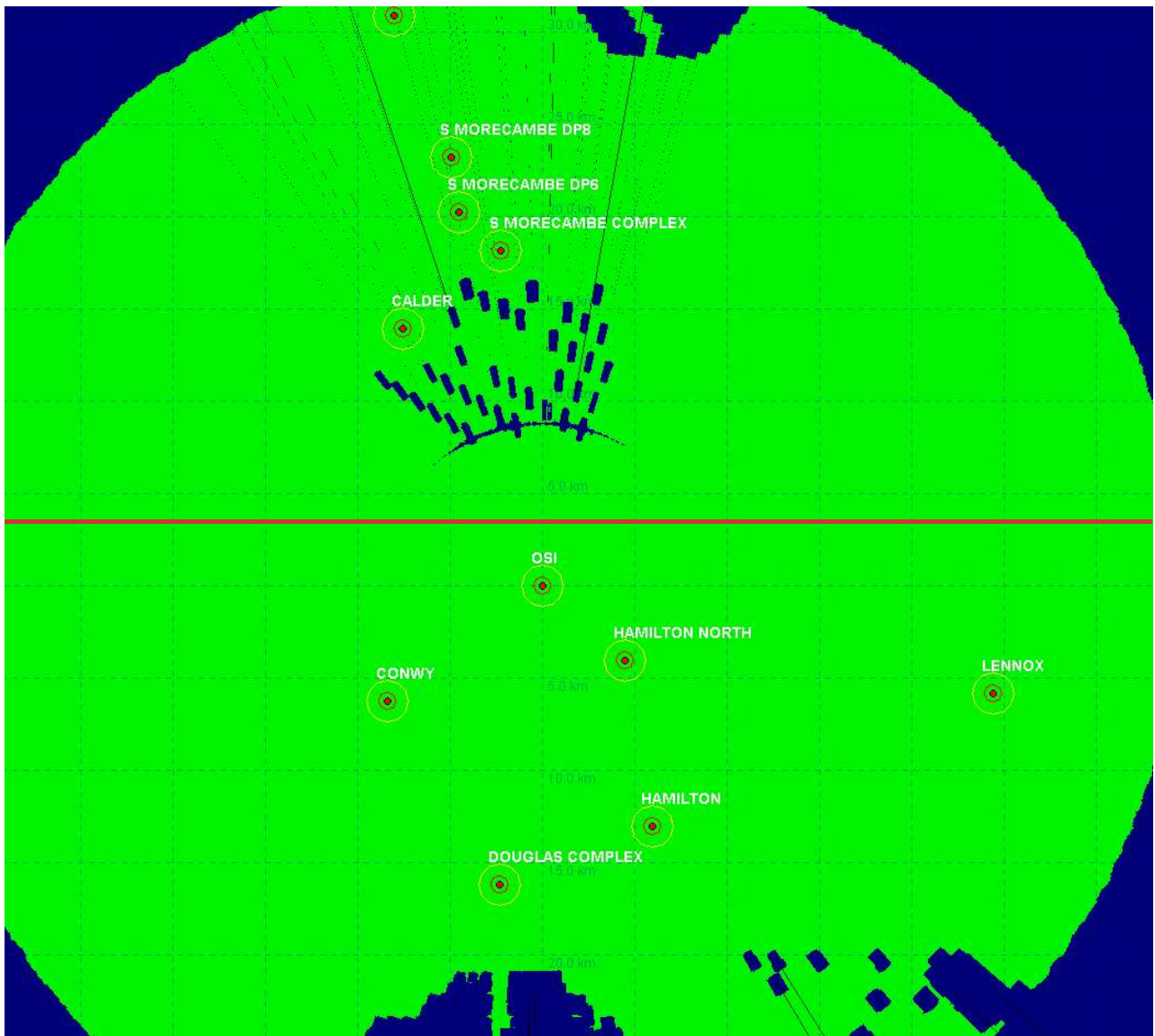


Figure 4.24: ENI Energy's OSI REWS detection threshold over the Morecambe Generation Assets Array Area.



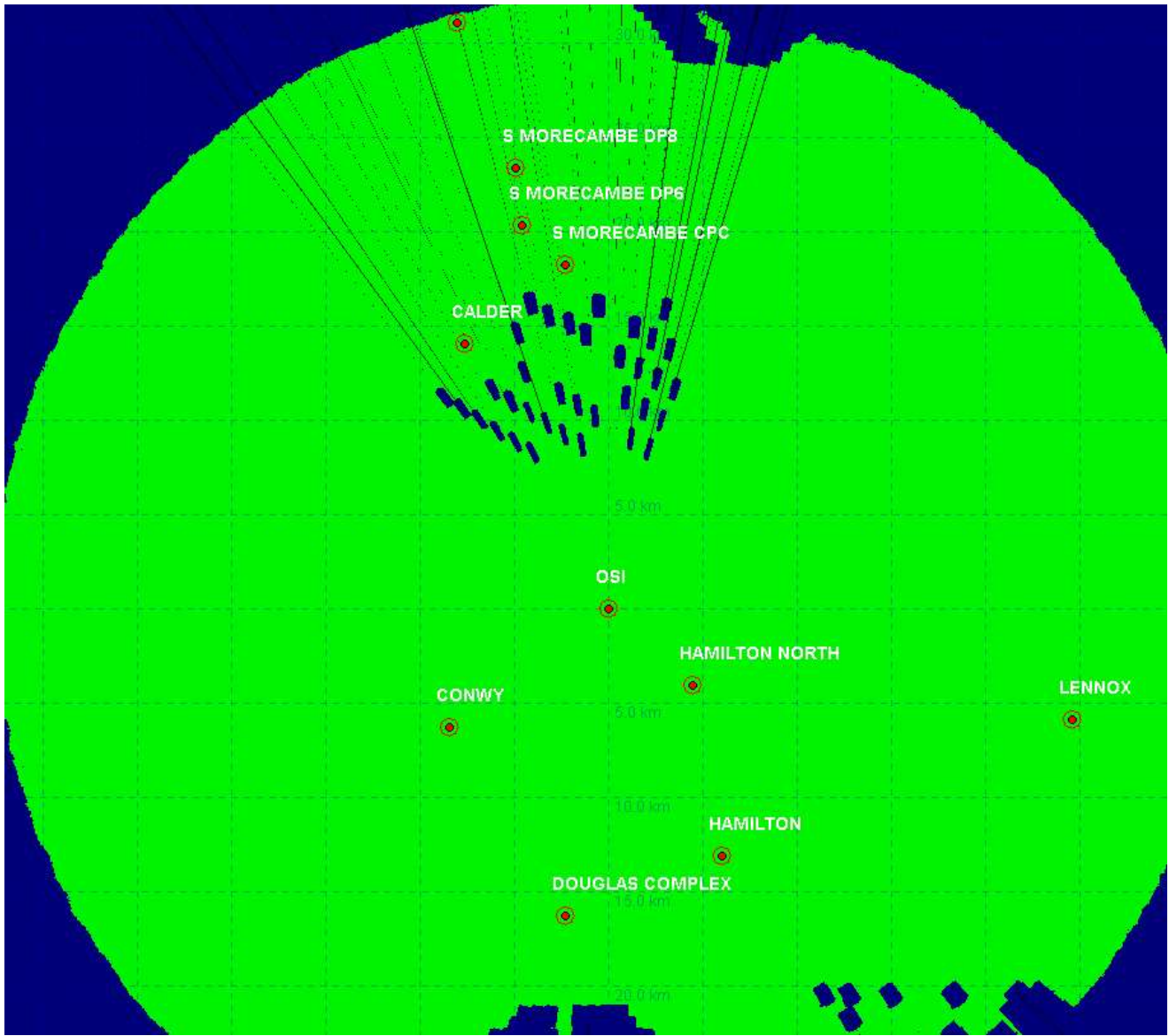
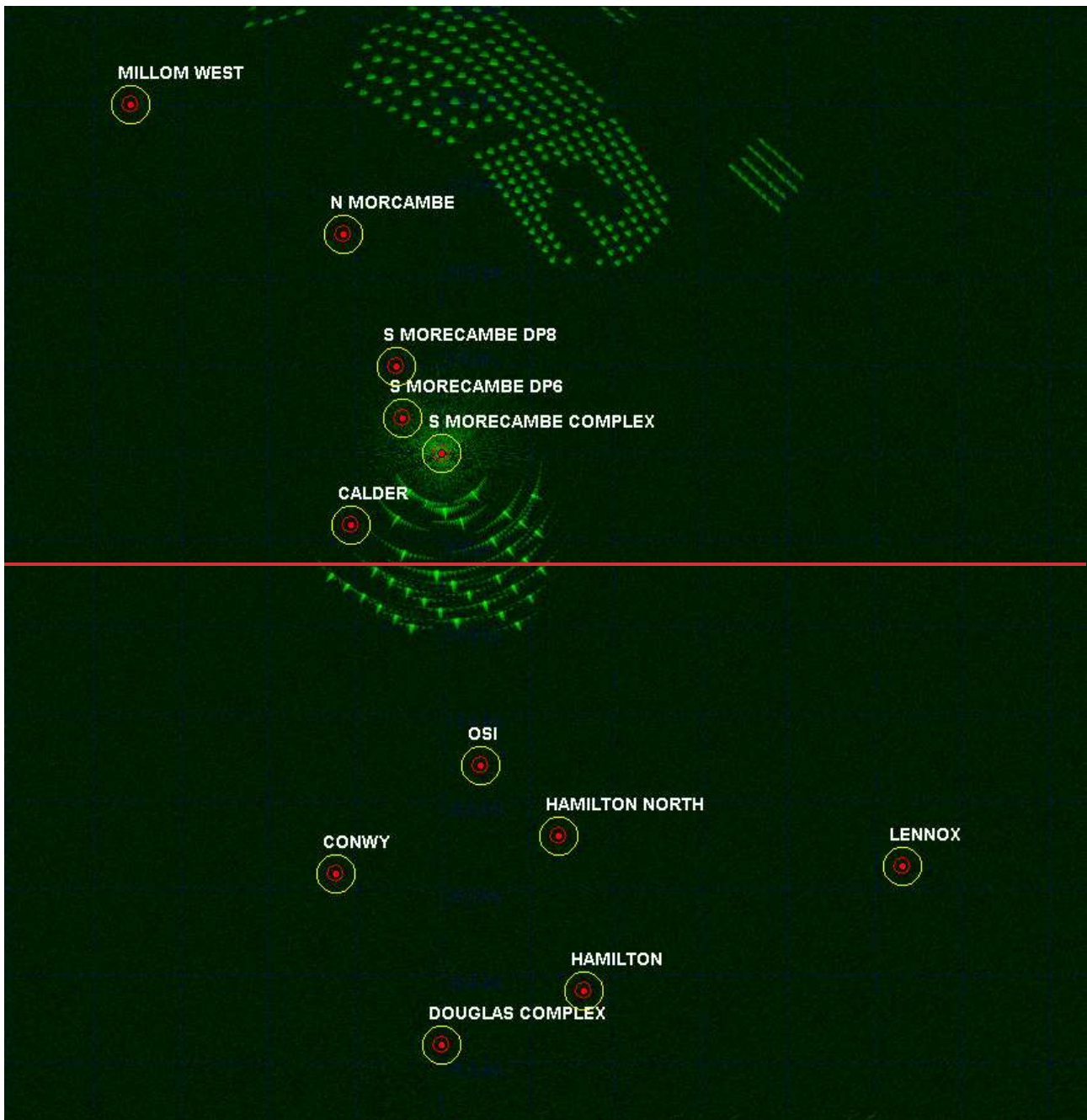


Figure 4.25: ENI Energy's OSI REWS detection plot showing loss regions for a **1000420** m² target.



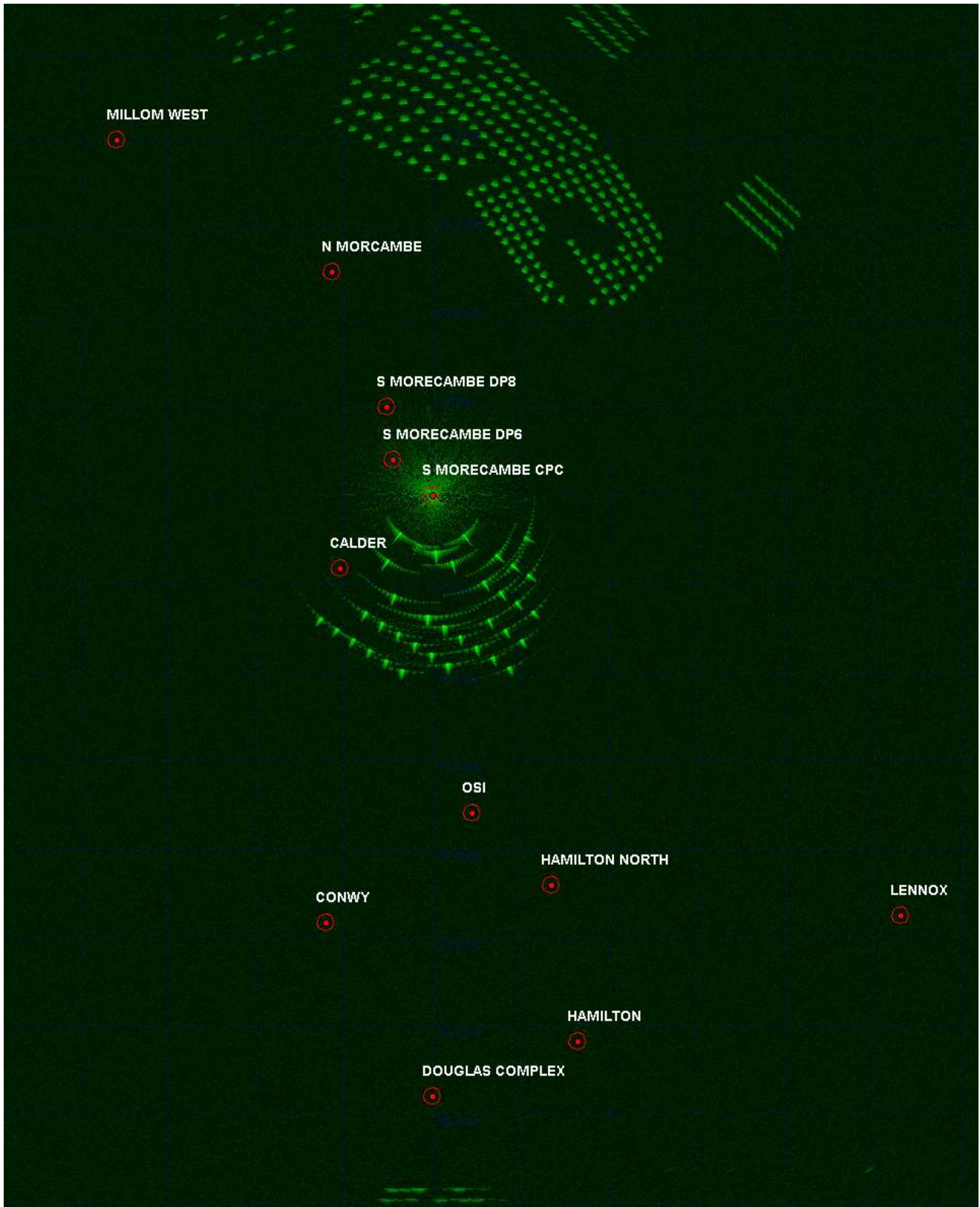
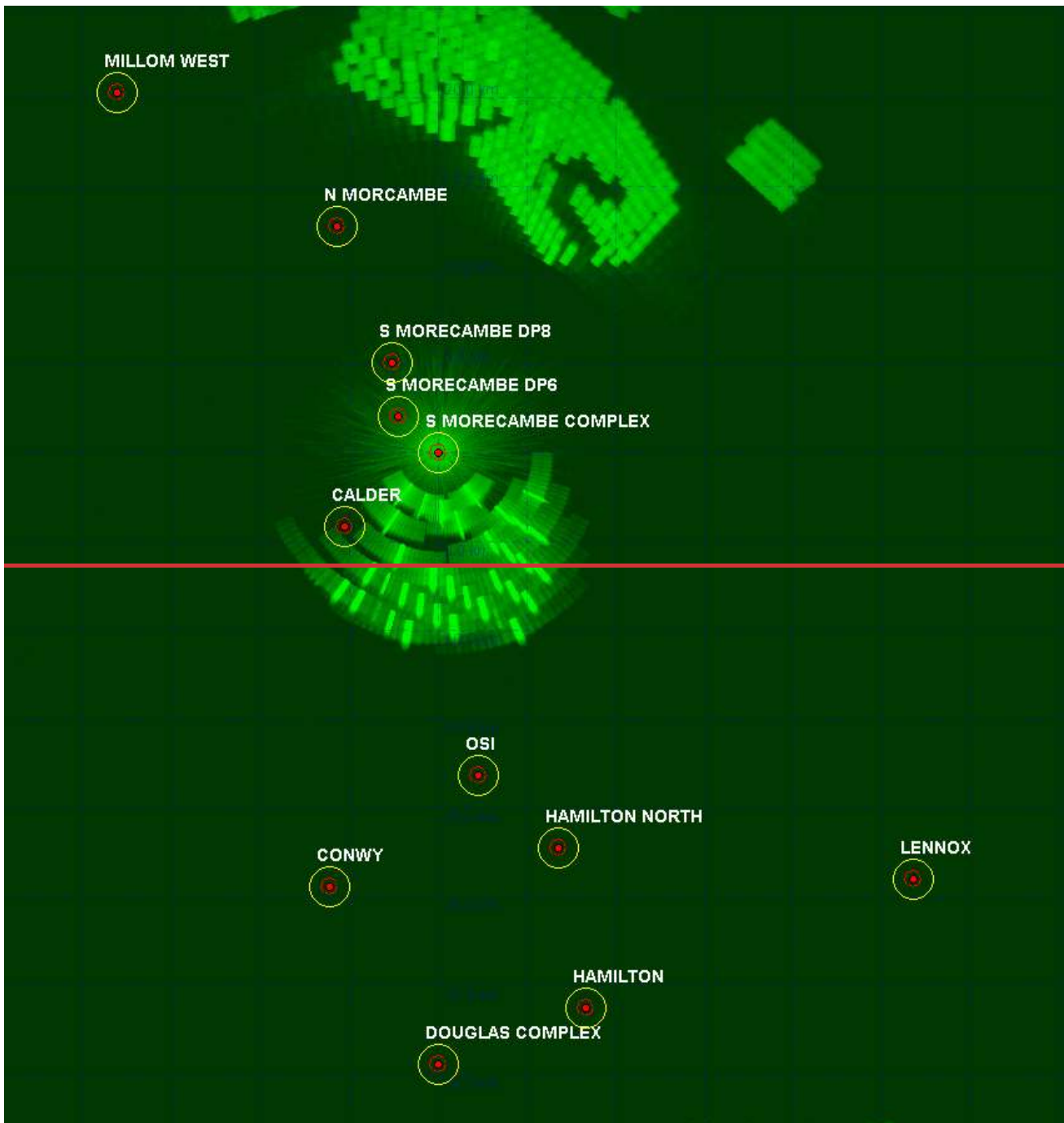


Figure 4.26: Spirit Energy's South Morecambe AP1 platform REWS clutter map showing returns from the Morecambe Generation Assets wind turbines and sea clutter.



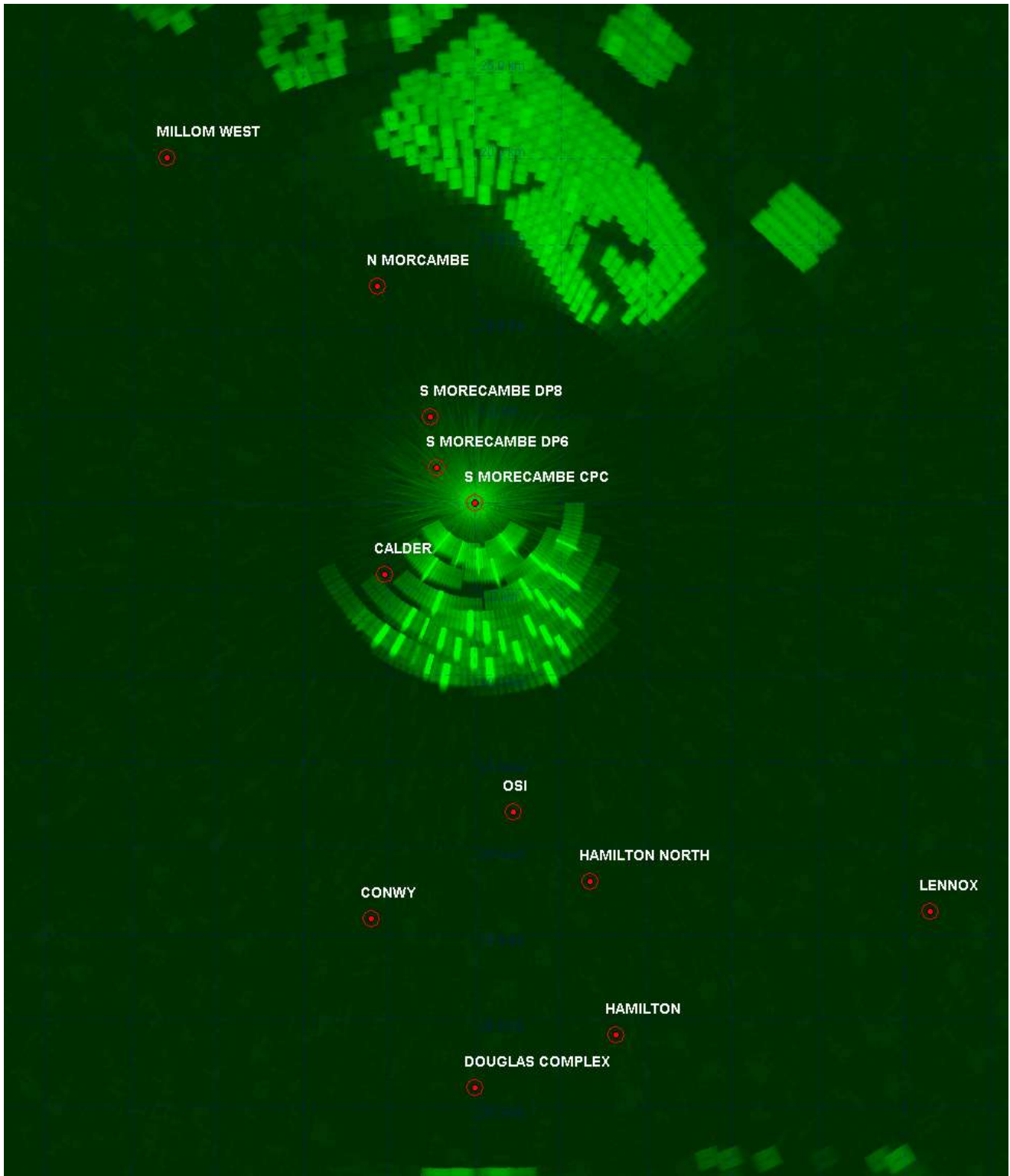
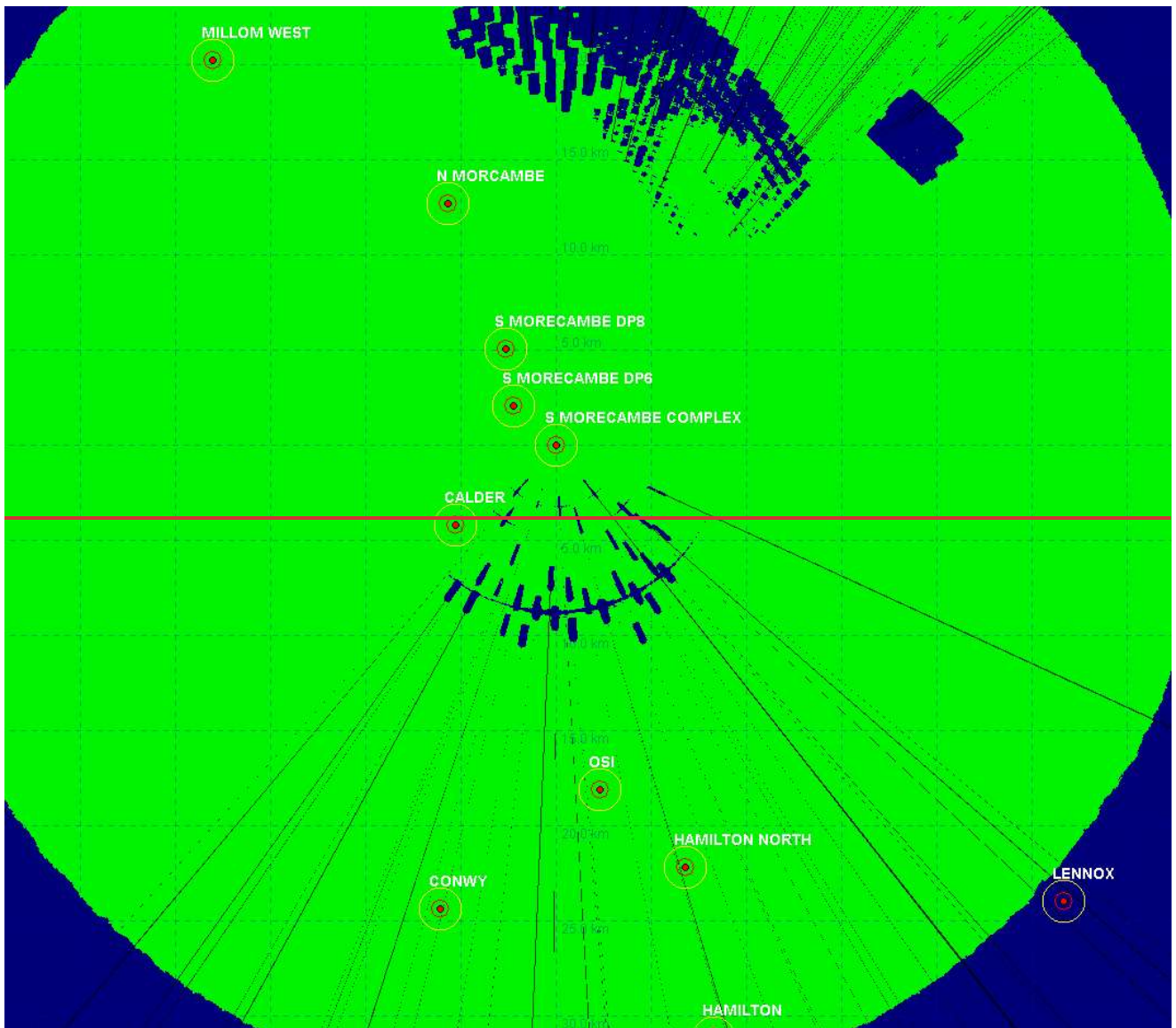


Figure 4.27: Spirit Energy's South Morecambe AP1 platform REWS detection threshold over the Morecambe Generation Assets Array Area.



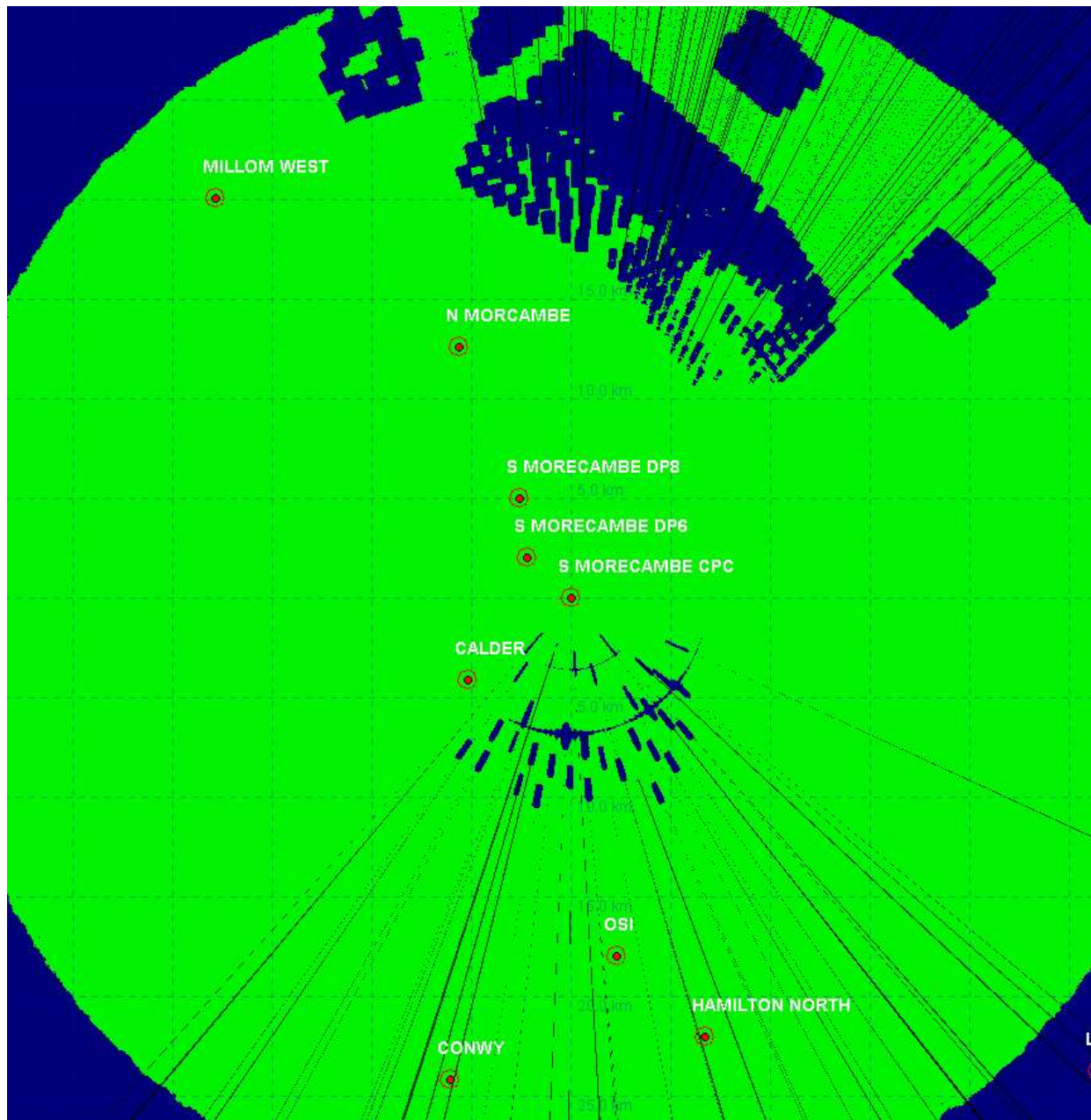


Figure 4.28: Spirit Energy’s South Morecambe AP1 platform REWS detection plot showing loss regions for a **1000420** m2 target.

4.3.1.2 As shown in the base case modelling, the results indicate that the raw, single scan detection performance of the REWS due to the presence of the Morecambe Generation Assets is affected adversely within the windfarm regions. Radar detection of vessels travelling within the Morecambe Generation Assets may be lost temporarily as they move close to the modelled turbines located within the radar range. The loss of detection is mainly caused by the elevated threshold levels due to the presence of the wind turbines while a small number of losses are expected to occur due to shadowing. In response to the comments by Spirit Energy in their written relevant representations (Section 2.8) and to better understand the effects of shadowing on the detection and tracking of vessels in the Project array area, an additional study was conducted to assess the impact of shadowing on REWS detection (see Section 4.3.2 below).

4.3.2 Assessment of turbine shadowing on Spirit Energy assets

4.3.2.1 This updated section was included within the report to address the shadowing concerns raised by Spirit Energy within their written relevant representations (Section 2.8).

4.3.2.2 The Morecambe Generation Assets array area is located close to some of Spirits' offshore assets (namely, the South Morecambe CPC, South Morecambe DP 6, South Morecambe DP 8 and the North Morecambe platform). With the REWS located on the South Morecambe CPC, the nearest turbine could be approximately 2.7 km (1.5 nm) from the REWS installation (depending on the final design/layout). It is also noted that, the Maritime and Coastguard agency guidance MGN 543 (Offshore Renewable Energy Installations (OREIs) - Guidance on UK Navigational Practice, Safety and Emergency Response) indicates that merchant vessels may pass through OREIs. The presence of OREIs may degrade the REWSs' ability to detect and track such vessels due to shadowing effects. This may raise some concerns regarding the REWSs' ability to detect and track vessels within the Project Array Area and generate alarms in an efficient and timely manner. Therefore, the assessment was extended to include a study of the shadowing effects on the detection of vessels moving within the Project Array Area to establish the probability of the loss of detection due to turbine shadowing.

Modelling approach.

Turbine Shadowing

4.3.2.3 As outlined in Section 2.2, the initial modelling of turbine shadowing was based on optical shadowing. Optical shadowing assumes no diffraction effects, presenting a conservative scenario by neglecting improvements in shadow regions over extended distances. Depending on the size of the wind turbine and the radar height, these optical shadows may theoretically extend to the radar horizon. However, in practice, increasing the range between the target and the wind turbine reduces the attenuation of the target's returns due to diffraction effects and creeping waves. This characteristic of radar shadowing is illustrated in Figure 2.1.

4.3.2.4 Research indicates that a target located 1 km behind a wind turbine may experience a 6 dB reduction in returned power, while targets positioned significantly farther away typically, in terms of tracking vessels within the windfarm, the tracker software is encounter only a 2 dB reduction in radar echo strength (Butler and Johnson, 2003). These findings align well with a recent measurement campaign conducted by Ultra Electronics, which examined the effects of wind farms on REWS performance in the eastern Irish Sea (Greenwell, 2016). Similarly, studies by Danoon and Brown (2014) suggest that shadowing may have limited impact on REWS performance, owing to diffraction effects and the size of the vessel, which may exceed the shadow region produced by individual wind turbines. Consequently, subsequent modelling efforts have incorporated diffraction and creeping wave effects to better represent target detection within shadowed regions.

Vessel Dimension Model

4.3.2.5 Vessels exceeding one thousand gross tons (GT) are the primary safety concern for offshore platforms. These vessels vary significantly in size, with typical lengths ranging from 15 m to 60 m. In contrast, shadows cast by wind turbines are relatively narrow, typically spanning between 4 m and 20 m in width. This difference implies that a large

1,000 GT vessel may experience partial shadowing as it passes through these regions (illustrated in Figure 3.5).

4.3.2.6 Partial shadowing allows some radar energy to reflect back to the radar system, enabling potential detection by the REWS. While smaller vessels can generally be treated as point scatterers in modelling, larger vessels require more detailed assessment to account for the partial shadowing effects.

4.3.2.7 To address the concerns raised by Spirit Energy (Section 2.8), the vessel size and shape were modelled based on a representative 1,000 GT fishing vessel, as shown in Figure 4.29, which outlines its key dimensions. Including both the width and length of the vessel in the model allows for a more accurate evaluation of partial shadowing effects and the detectability of the vessel as it traverses narrow shadow regions. However, it is worth noting that the selected vessel dimensions are conservative, as 1,000 GT vessels can reach lengths of up to 50 m.



Figure 4.29: Illustration of the dimensions of a typical 1000GT vessel used for the shadowing analysis

Path modelling

4.3.2.8 The primary concern for the REWS operator is the potential allision risk posed by vessels navigating through the Project Array Area towards offshore platforms. Consequently, the assessment focused specifically on potential allision paths within the Project Array Area, prioritizing trajectories with direct collision vectors toward the Spirit Energy offshore platforms.

4.3.2.9 To accurately model these potential collision paths, the assessment considered trajectories radiating outward from each of the four evaluated platforms (namely, the South Morecambe CPC, South Morecambe DP 6, South Morecambe DP 8 and the North Morecambe platform). The paths were modelled using an angular increment of 0.01 degrees to ensure a comprehensive and representative analysis of possible vectors within the defined region. While it is recognised that additional paths (non-radial paths) could theoretically result in collision vectors with the platforms, these are expected to exhibit similar or reduced probabilities of signal loss due to the geometric configuration of the turbines and platforms.

4.3.2.10 In evaluating the impact of shadowing on allision risk, the study focused exclusively on paths that have a clear collision vector with the platforms. Paths that intersect with

wind turbines before reaching the platforms were excluded, as they do not pose a direct allision risk. This distinction is illustrated in Figure 4.30, where a valid path (depicted in green) successfully passes through shadowing regions towards South Morecambe DP6, while a disregarded path (depicted in red) intersects with a turbine before reaching the platform.

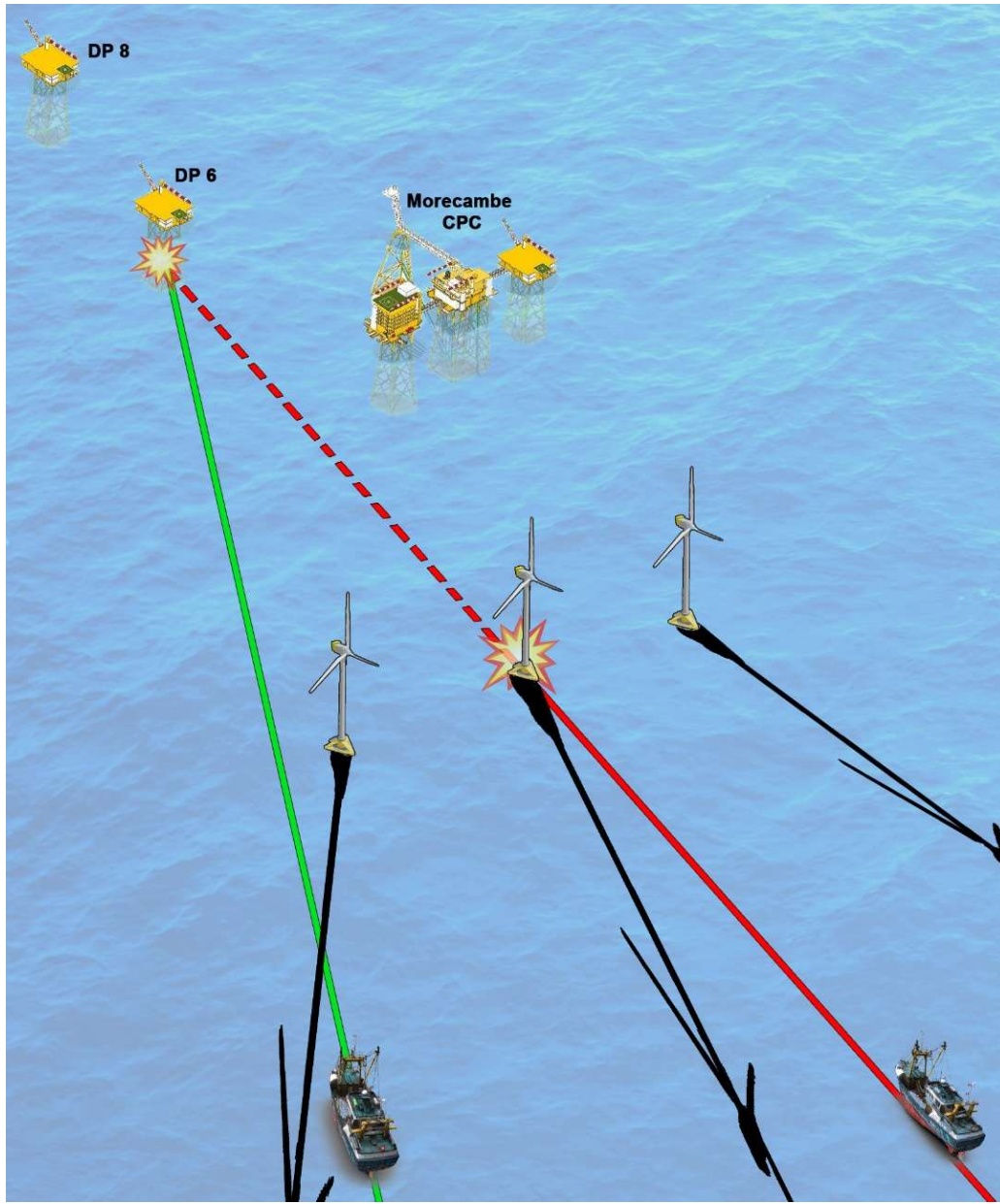


Figure 4.30: Paths that are considered within the shadowing analysis

4.3.2.11 To isolate the shadowing effects specifically associated with turbines from the Morecambe Generation Assets, the assessment was confined to the radar sector encompassing the Project Array Area. The assumption was made that radar coverage in other sectors would remain unaffected by turbine shadowing. Including these unaffected areas in the analysis could dilute the observed shadowing effects. By focusing solely on the Project Array Area sector, the study provides a more precise estimation of the probability of signal loss within this specific region, rather than across

the entire radar coverage area. This approach aims to provide a targeted and fair assessment of the potential risks posed by vessel paths within the Project Array Area.

REWS Tracking software considerations

4.3.2.12 When assessing the impact of shadowing on REWS performance, it is essential to recognise that the system is equipped with tracking software designed to compensate for most of the detection momentary signal losses of the vessels. Typically, the tracking software establishes a track for a vessel after successfully detecting it over a predefined number of radar rotations. Once the track is established, the software can maintain the track and predict the vessel's location during short-term losses using historical data that include the target's speed and trajectory.

4.3.2.13 However, if a target remains undetected over an extended number of radar rotations, the tracking software's confidence in the track decreases, potentially resulting in the target being removed from the track list. The exact number of radar rotations required to establish or discard a track is not publicly available. Therefore, the results of this assessment are presented across multiple radar rotation to account for varying levels of tracking resilience.

4.3.2.14 In the study, the raw data of the results for each analysed trajectory include the number of radar rotations during which a target is lost due to shadowing effects. These results are then expressed as probabilities, representing the likelihood of such events occurring across all considered paths within the assessed sector. This probabilistic approach provides insight into the frequency and distribution of shadow-induced tracking losses.

4.3.2.15 Additionally, the radar data within REWS are typically integrated with AIS data. AIS data is significantly less susceptible to interruptions caused by turbine shadowing, as it relies on independent transmission signals rather than radar reflections. While explicit confirmation is unavailable, it is assumed that Spirit Energy may incorporate AIS data within their REWS system.

4.3.2.16 By accounting for both radar tracking dynamics and the potential integration of AIS data with the REWS will provide an alternative source of vessel information and location which can complement the data when temporary radar losses are experienced. Therefore, the impact of the Morecambe Generation Assets (if available) the resultant tracking capability would significantly improve in comparison to the consideration of the radar data in isolation on nearby REWS installation is.

Modelling Results

4.3.2.17 The shadowing study evaluates each of Spirit Energy's platforms by comparing the target vessel's location to the regions of shadow produced by nearby wind turbines. Under the assumption of optical shadowing, if a target is fully positioned within a turbine's shadow, no reflections are detected at the REWS. As a result, the target becomes momentarily undetectable during that radar rotation, effectively causing a temporary loss from the tracking system.

4.3.2.18 In the modelling process, the target continues to move along its predefined trajectory at a speed of 12 knots, with its position continuously reassessed relative to the turbine shadow regions. The model tracks and records the number of consecutive radar rotations during which the target remains undetectable, compiling these occurrences into raw data for further analysis. An example of these results is presented in Figure 4.31, which illustrates the temporary loss of a vessel over eight consecutive radar

rotations as it travels towards the North Morecambe platform. Although these losses are observed when the vessel is approximately 6 km away from the shadow-casting turbine, the target is still categorised as lost under the optical shadowing assumption.

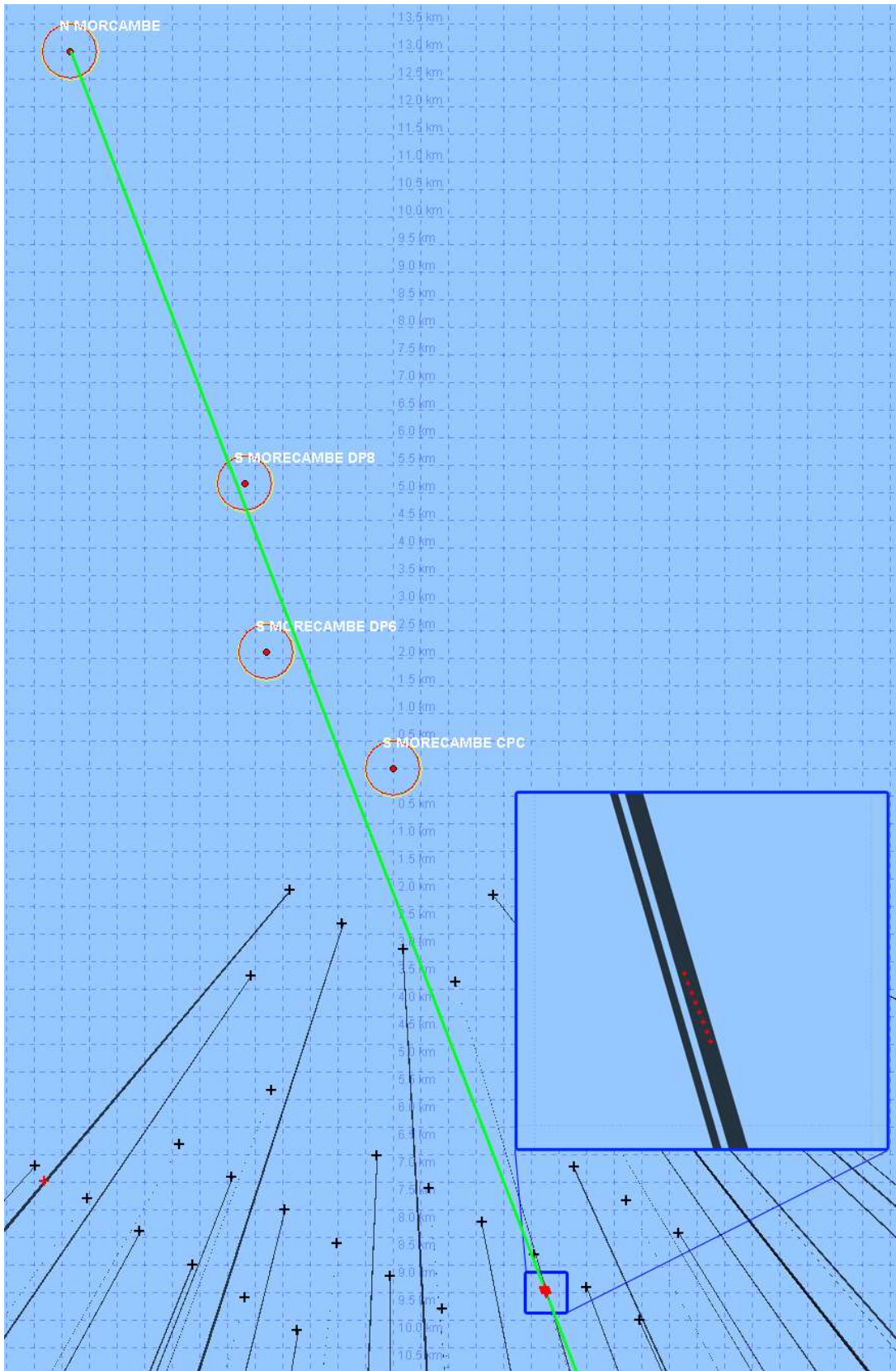


Figure 4.31: Results showing loss of detection of a vessel over 9 radar rotations due to turbine shadowing

4.3.2.19 When the data from all potential trajectories within the sector are aggregated, the results are expressed as probabilities of tracking loss events across multiple radar rotations. These probabilities are shown in Figure 4.32, which represents tracking losses under the assumption of optical shadowing, where signal attenuation does not diminish with increased distance from the shadow-casting turbine.

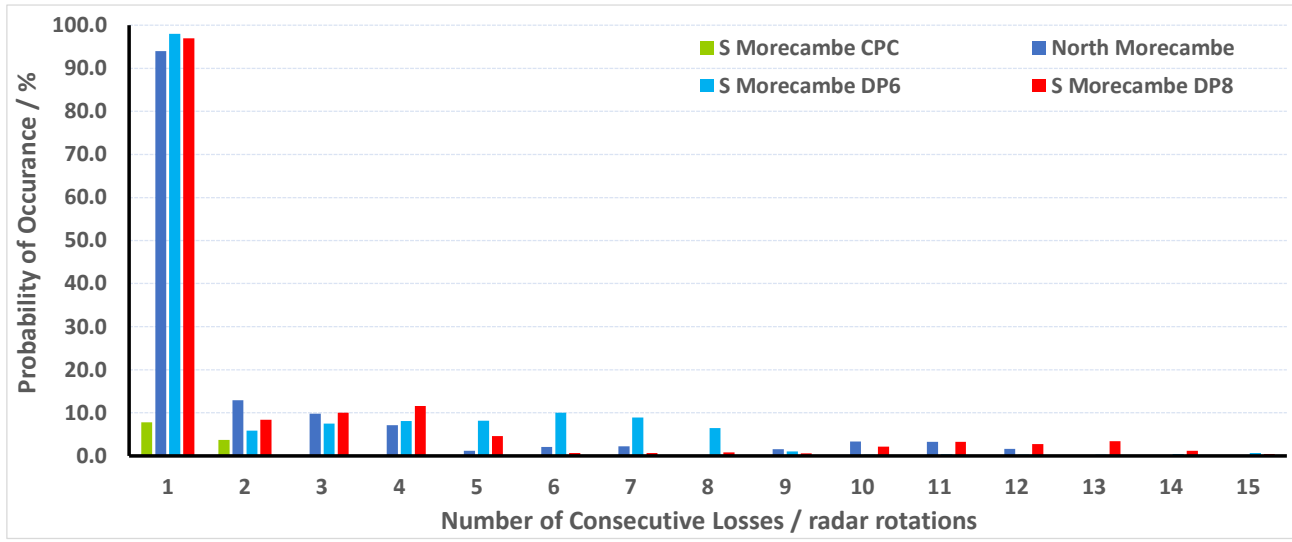


Figure 4.32: Probability of losing a vessel in optical-shadowing over multiple radar rotations

4.3.2.20 The results the probability of occurrence of consecutive radar tracking losses across four assessed platforms: South Morecambe CPC, South Morecambe DP6, South Morecambe DP8, and North Morecambe. The highest probability of detection losses occurs during a single-radar rotation across all platforms. South Morecambe DP6, South Morecambe DP8, and North Morecambe have single-rotation loss probabilities approaching 100%, indicating that momentary signal losses due to shadowing are the most frequent across these sectors -as expected to be relatively low and manageable. This observation aligns with the understanding that short-term interruptions are common in shadowed regions but are often mitigated by the REWS tracking software through predictive algorithms based on the vessel's historical trajectory and speed data.

4.3.2.21 However, it is noted that as the number of consecutive radar rotations without the need for mitigation measures-detection increases, the probability of occurrence declines sharply. For two to three consecutive losses, the probability drops below 12%, and beyond five radar rotations, occurrences are notably rare across all assessed platforms. This trend suggests that extended radar signal losses are infrequent and likely occur under very specific conditions.

4.3.2.22 It can also be noted that the South Morecambe CPC consistently demonstrates the lowest probability of losses across all radar rotation counts. This is due to the geometric positioning relative to the wind turbine shadows. I.e, if a vessel on a collision

trajectory falls with a shadow region, it is more likely to collide with the shadow-casting wind turbine prior to colliding with the South Morecambe CPC.

4.3.2.23 Losses extending beyond ten consecutive radar rotations are minimal across all platforms. However, it is noted that while the tracking software is capable of compensating for short-term losses, prolonged interruptions may eventually erode tracking confidence, potentially resulting in the loss of the target from the radar track list.

4.3.2.24 As mentioned previously, assuming optical shadowing is expected to produce conservative estimates -especially at extended ranges between the target and the shadow-casting turbine. Analysis of the range between the assessed target locations and the shadow-casting turbines show that all cases occur at ranges that are more than 2 km away from the shadow-casting turbines. This is shown in Figure 4.33 that indicates that the vast majority of occurrences are more than 5 km away from the turbines.

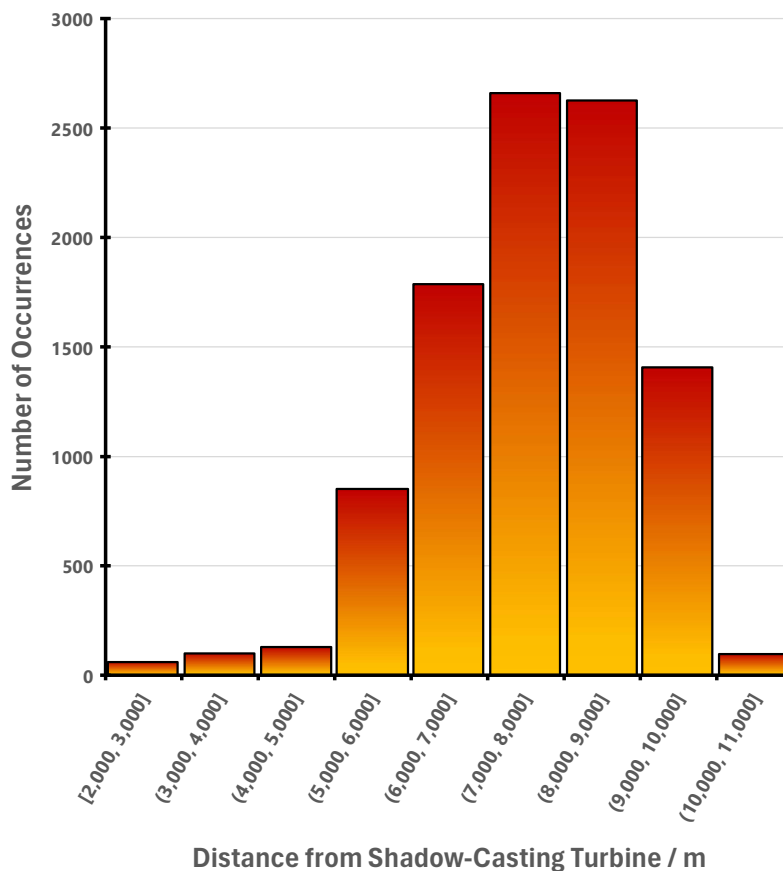


Figure 4.33: Frequency distribution of the distances between targets and the shadow casting turbines

4.3.2.25 Therefore, for completeness, additional modelling efforts were included to estimate the effects of diffraction and creeping waves, which will result in reduced shadowing intensity over longer distances from the shadow-casting turbines. The models used adapted geometrical theory of diffraction (GTD) and uniform theory of diffraction (UTD) approximation to estimate the shadowing intensity behind the turbine tower. Figure 4.34 shows the attenuation that the target echo would experience by being within the shadow regions at different ranges from the turbine tower. Additionally, Figure 4.35

show the estimated return levels from the target vs range and the local threshold levels.

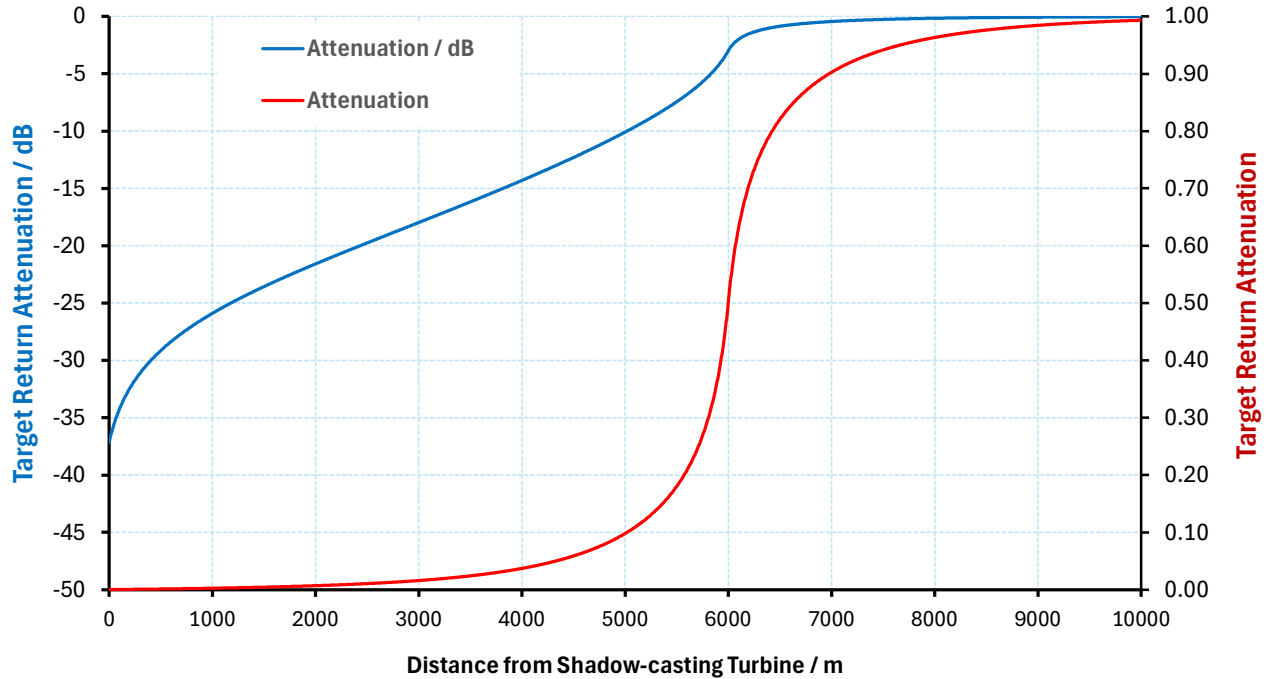


Figure 4.34: Target returns attenuation levels vs range from the shadow-casting tower

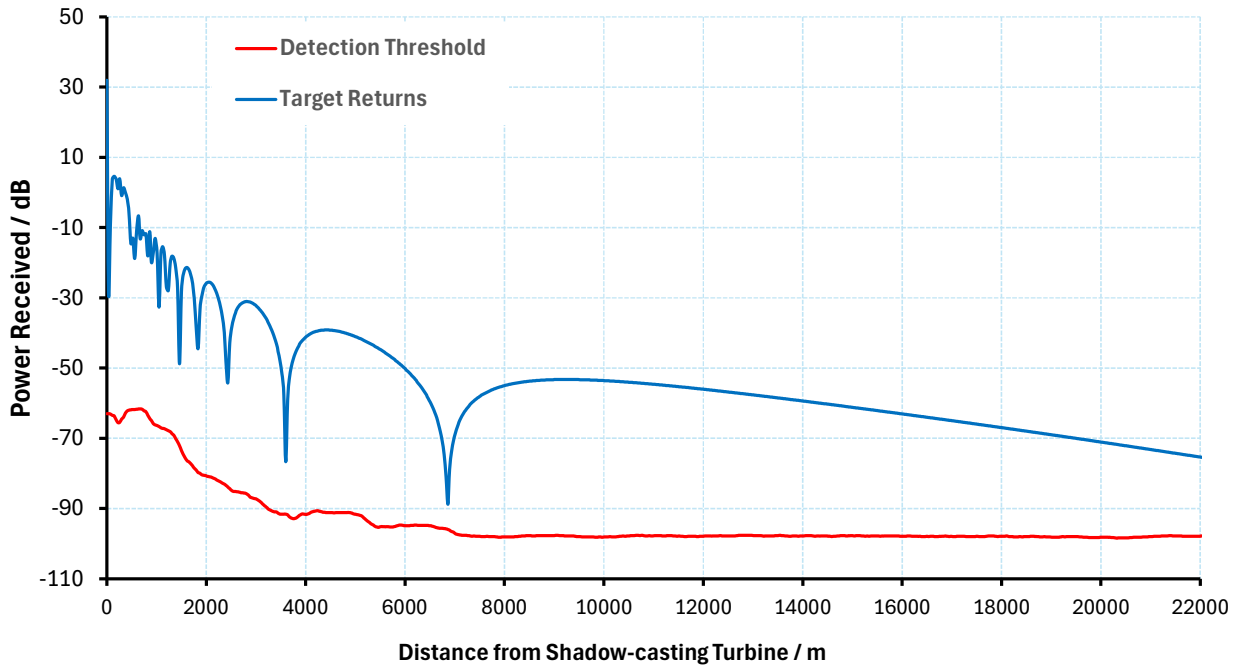


Figure 4.35: Power received from target and detection threshold vs range

4.3.2.26 The comparison of Figure 4.34 and Figure 4.35 show that, in most cases, the target received power is more than 20 dB above the detection threshold. Therefore, the effect of shadowing is not expected to push the returns of targets below the detection

threshold (as indicated in Figure 4.32, the minimum distance between the target and the shadow-casting tower was more than 2 km, which would result in maximum attenuation of 22 dB)

4.3.2.27 Figure 4.36 presents the results of the same loss probability analysis while incorporating the effects of diffraction and creeping waves within the shadow regions. It can be noted that these physical phenomena can largely mitigate the attenuation effects, allowing some radar energy to bend around the turbine structure or propagate along its surface, reducing the severity of the shadowing impact over greater distances and enabling targets to be detected.

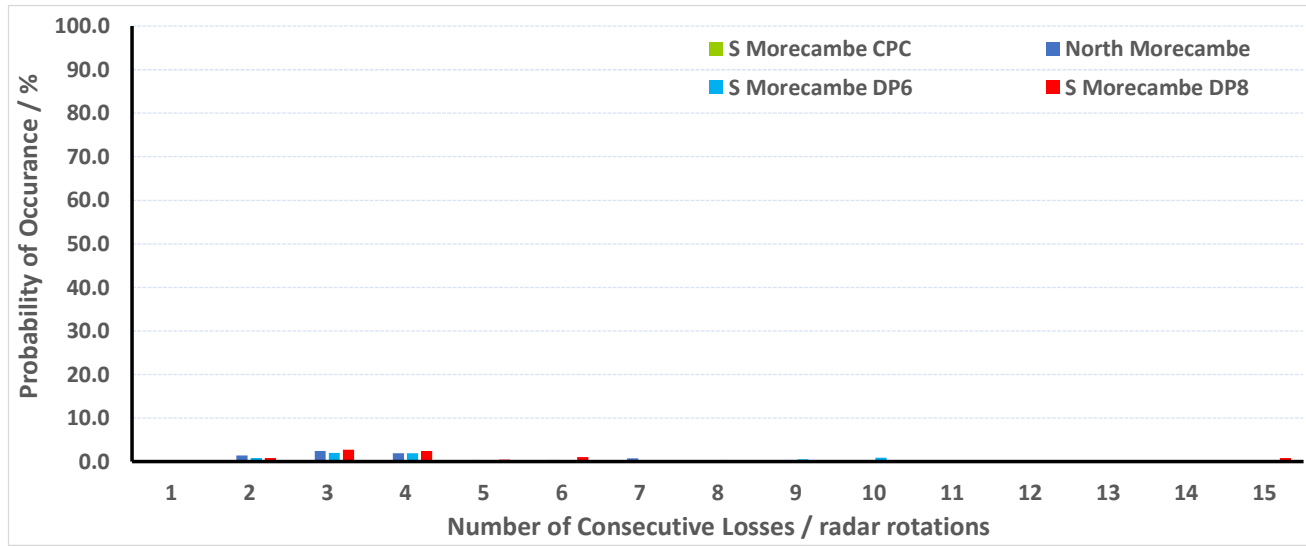


Figure 4.36: Probability of losing a vessel over multiple radar rotations when considering diffraction and creeping wave effects

4.3.2.28 The comparison between the results shown in Figure 4.32 and Figure 4.36 highlights the importance of considering both optical and diffraction-based models in evaluating radar tracking losses. While optical shadowing provides a conservative estimate, the inclusion of diffraction and creeping effects offers a more representative understanding of the actual operational performance of the REWS under shadowing conditions. The results indicate that the shadowing may introduce some losses of detection, however this is expected to be largely compensated for by the tracking software. Furthermore, if AIS data integration is confirmed within the REWS system, it would provide an additional layer of resilience, as AIS transmissions are less susceptible to shadowing effects from wind turbines.

4.3.1.2

4.4 Cumulative assessment

4.4.1.1 The Morecambe Generation Assets REWS assessment area covers a number of existing windfarms (Barrow, Burbo Bank, Burbo Bank Extension, Gwynt y Môr, North Hoyle, Walney 1, Walney 2, Walney Extension 3, Walney Extension 4 and Ormonde) along with windfarms that are at various stages in their planning and consent process (Awel y Môr, Mona Offshore Wind Project and Morgan Generation Assets). The windfarms that are within the study area are shown in [Figure 4.37](#) [Figure 4.29](#).

MORECAMBE OFFSHORE WINDFARM GENERATION ASSETS

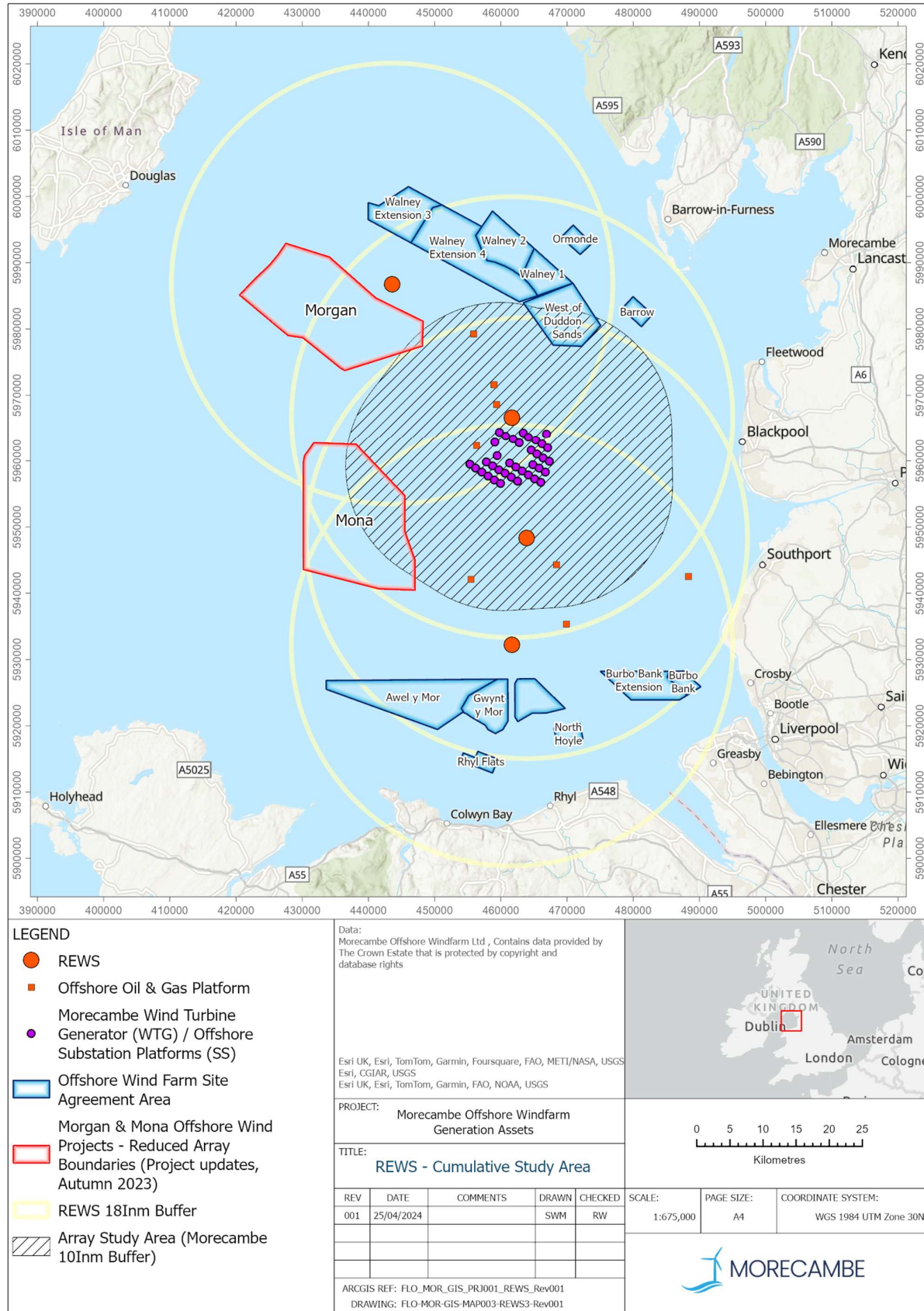


Figure 4.3729: REWS study area for the cumulative assessment.

4.4.1.2 At the time of conducting the REWS assessment, the locations and layout of the turbines the Awel y Môr Offshore Windfarm were unavailable to the Applicant. Additionally, it was noted that Awel y Môr is sufficiently far from the REWS installations and the Morecambe Generation Assets and it is therefore not expected to add to the impact on the REWS. Therefore, its potential impact in the cumulative assessment was not modelled for this report.

4.4.1.3 However, including the potential impact of the Mona Offshore Wind Project and The Morgan Generation Assets is considered more applicable due to their and proximity to the Morecambe Generation Assets and the REWS installations in the region. Hence, this report presents the modelling results of the combined impact on the REWS from Morecambe Generation Assets in combination with Mona Offshore Wind Project and Morgan Generation Assets.

4.4.2 Cumulative REWS assessment of Morecambe Generation Assets with Mona Offshore Wind Project and Morgan Offshore Wind Project: Generation Assets

4.4.2.1 The locations and layouts of turbines within the Mona Offshore Wind Project and the Morgan Generation Assets were not available at the time of the study. Therefore, an indicative layout for both windfarms was produced based on publicly available data, including project update newsletters issued by each project in Autumn 2023 to notify stakeholders that the array boundaries for each project had been reduced since their respective PEIR assessments and that the maximum number of turbines for each project had also been reduced. The number of turbines, minimum turbine separation, and the indicative sizes of the turbines were used to produce an indicative uniform grid layout. Both Morgan and Mona were each assumed to have a maximum of 96 turbines and 4 offshore substation platforms. The sizes of the turbines were assumed to have a maximum rotor diameter of 320m. It is recognised that that the turbine geometry and layout for these projects would change in the future and the assumed location of the turbines may not be representative of the final layouts. However, it is deemed to be acceptable for the purposes of this study in order to establish an estimate of the detection losses due to turbine echoes and shadowing. Hence both Mona Offshore Wind Project and the Morgan Generation Assets were included in the cumulative assessment.

4.4.2.2 The next step in the REWS assessment is to model the impact of the Morecambe Generation Assets, Mona Offshore Wind Project, Morgan Generation Assets cumulatively and the existing windfarms. This was done in a similar manner to the process shown in previous sections. The modelled layouts are shown in [Figure 4.38](#)~~Figure 4.30~~ while the REWS returns, expected threshold levels and the detection regions are illustrated in [Figure 4.39](#)~~Figure 4.31~~ to [Figure 4.50](#)~~Figure 4.42~~.



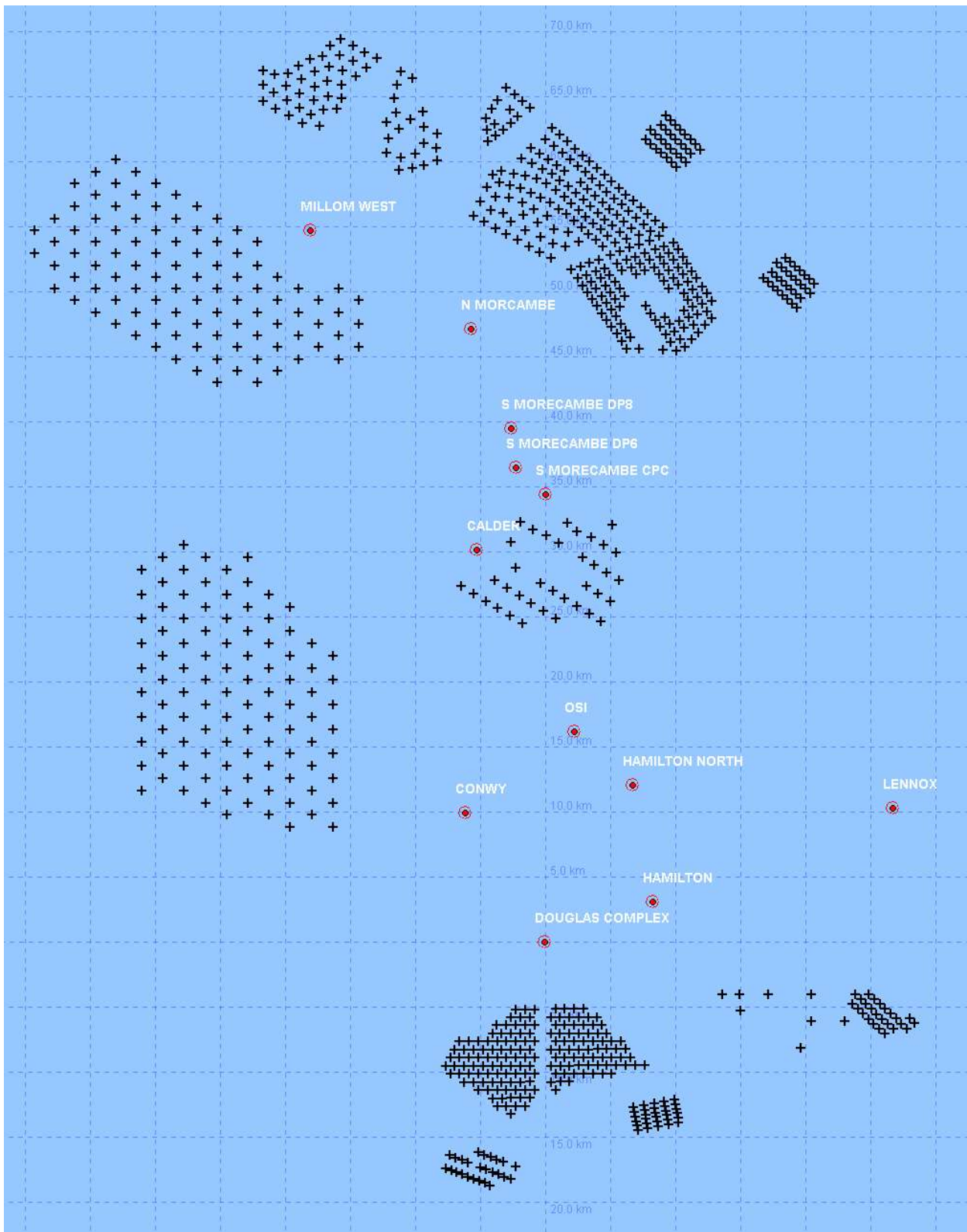
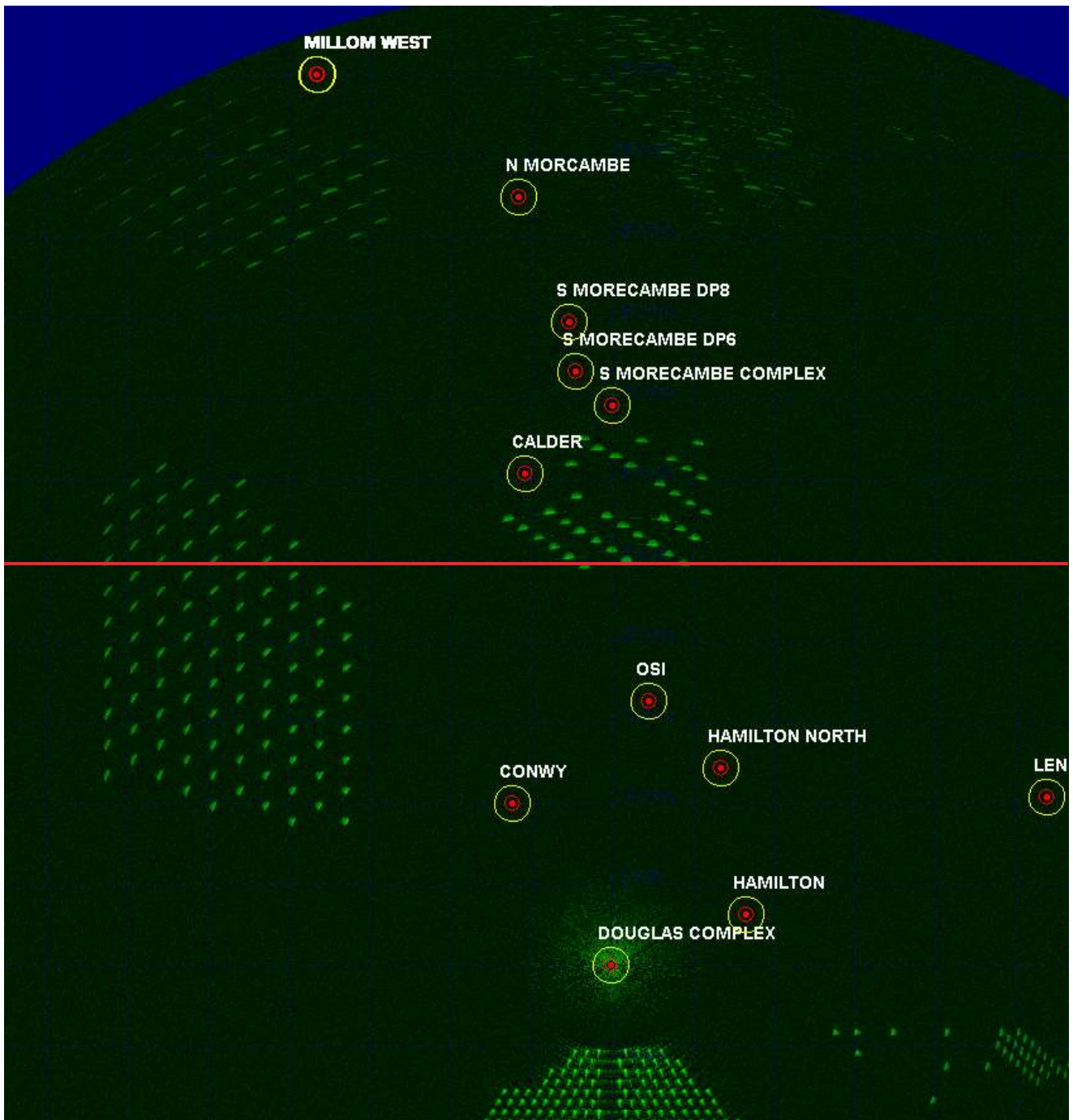


Figure 4.3830: Modelled cumulative layout of the Morecambe Generation Assets with Mona Offshore Wind Project and Morgan Generation Assets showing the indicative location of the wind turbines and the location of oil and gas platforms in the region.



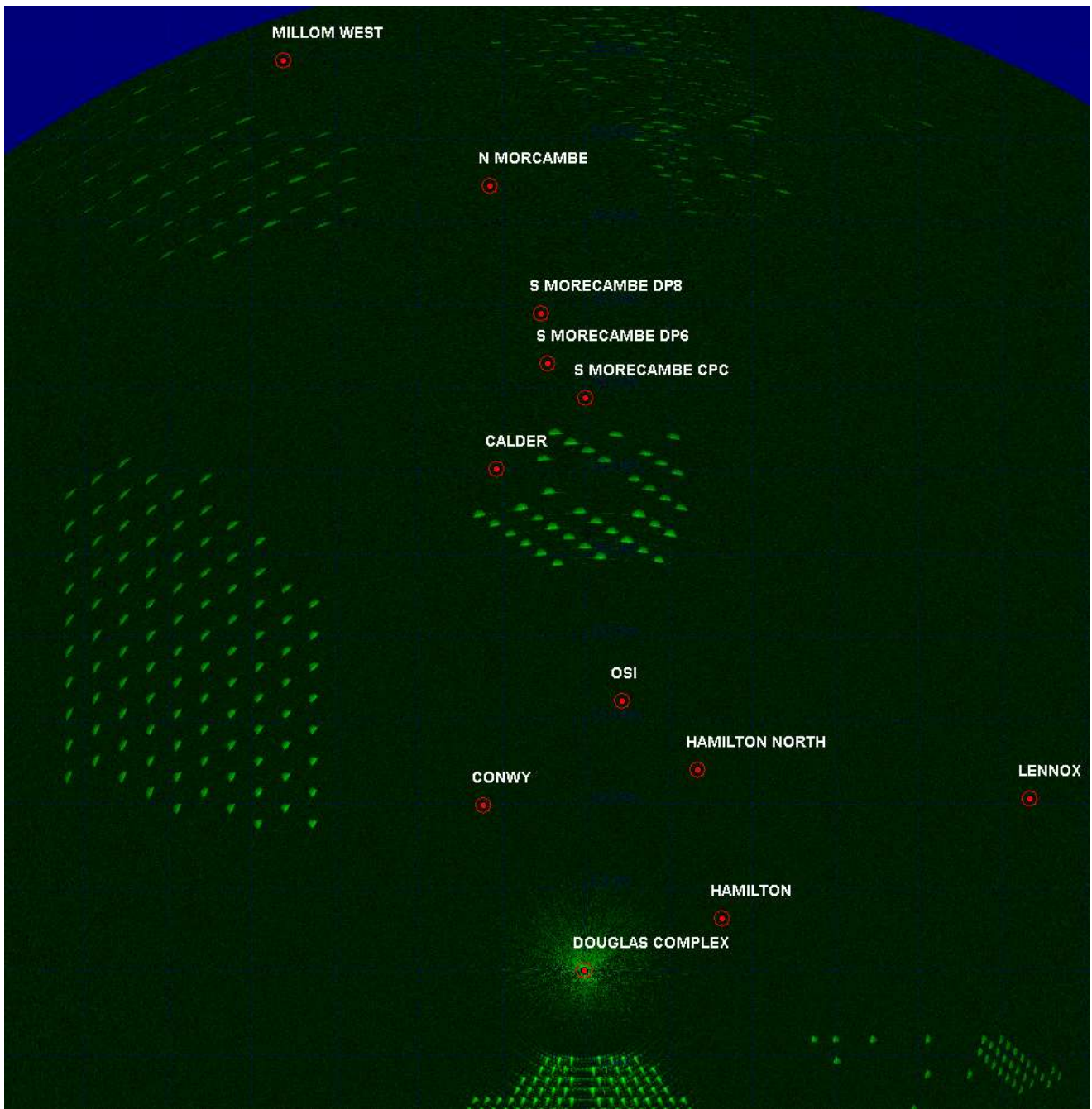
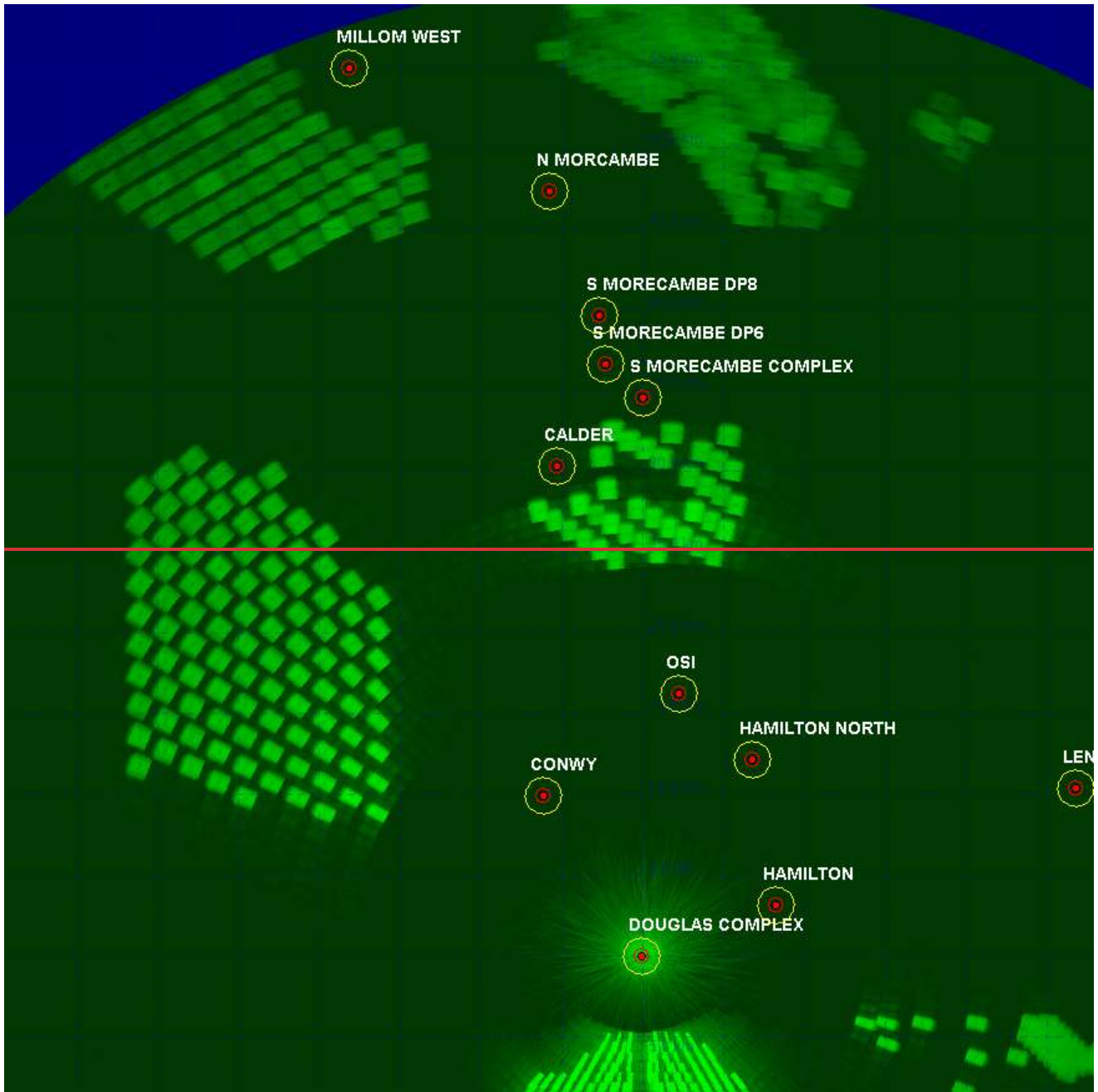


Figure 4.3931: ENI Energy's Douglas platform REWS clutter map showing returns from the wind turbines and sea clutter.



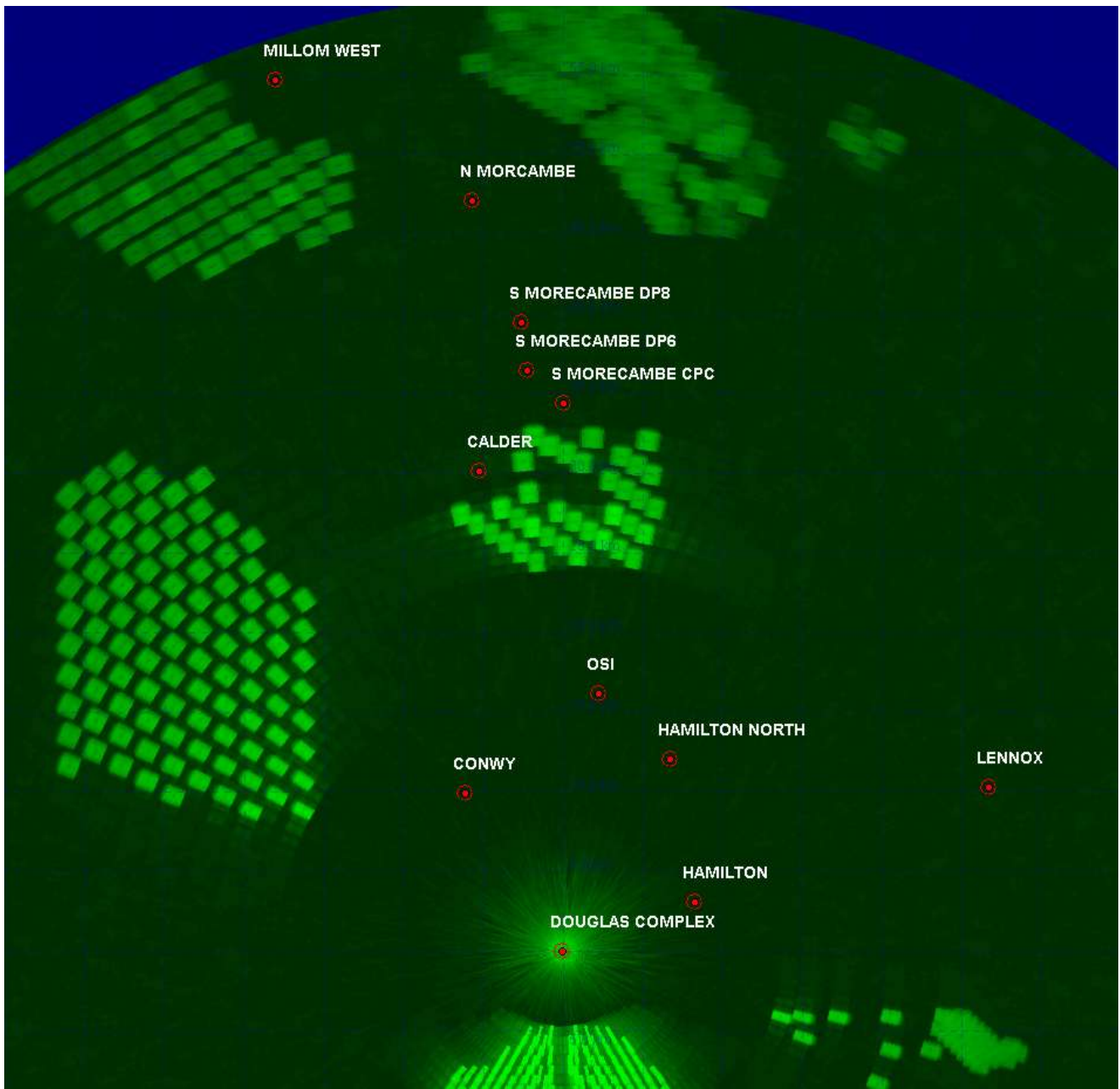
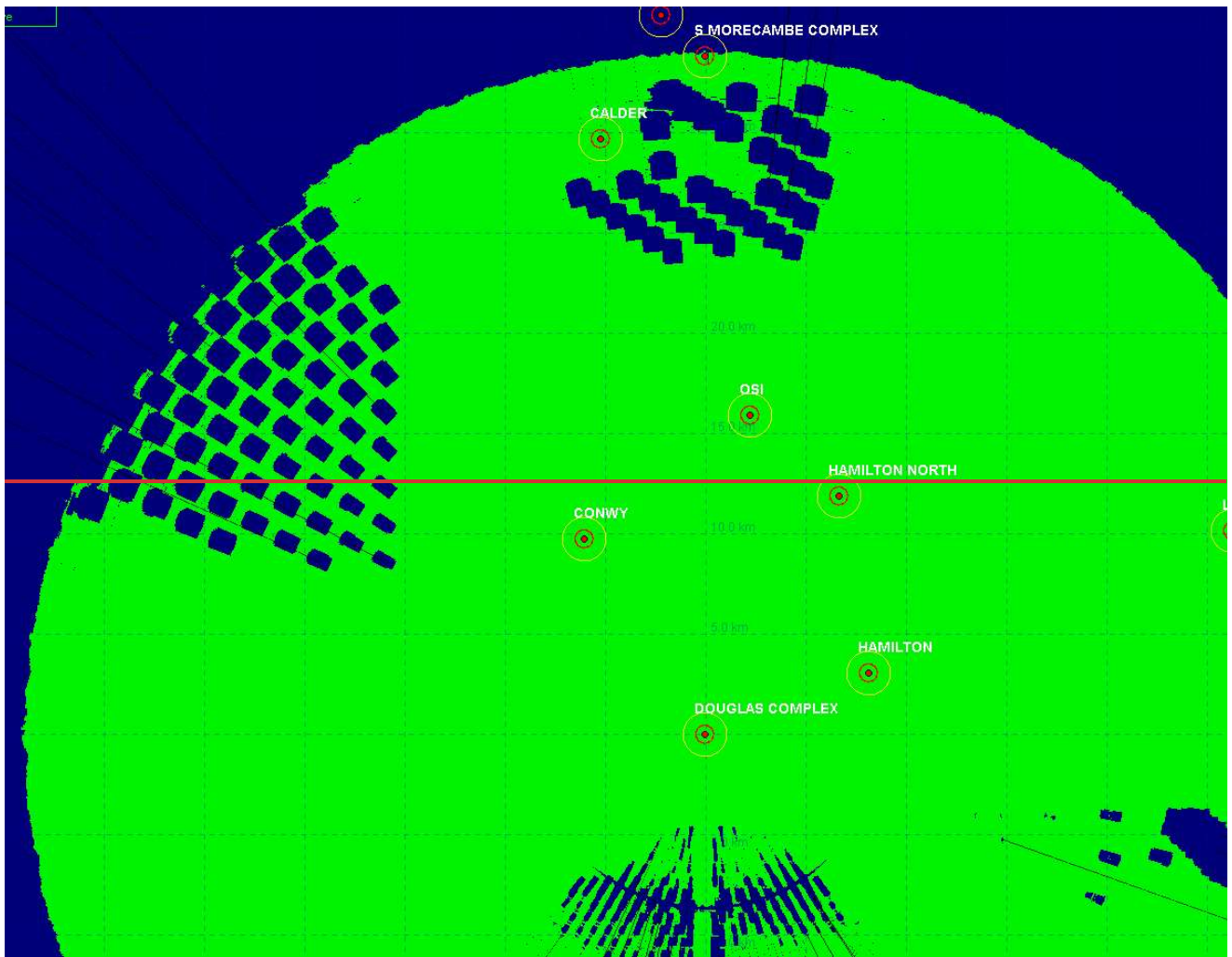


Figure 4.4032: ENI Energy's Douglas platform REWS detection threshold.



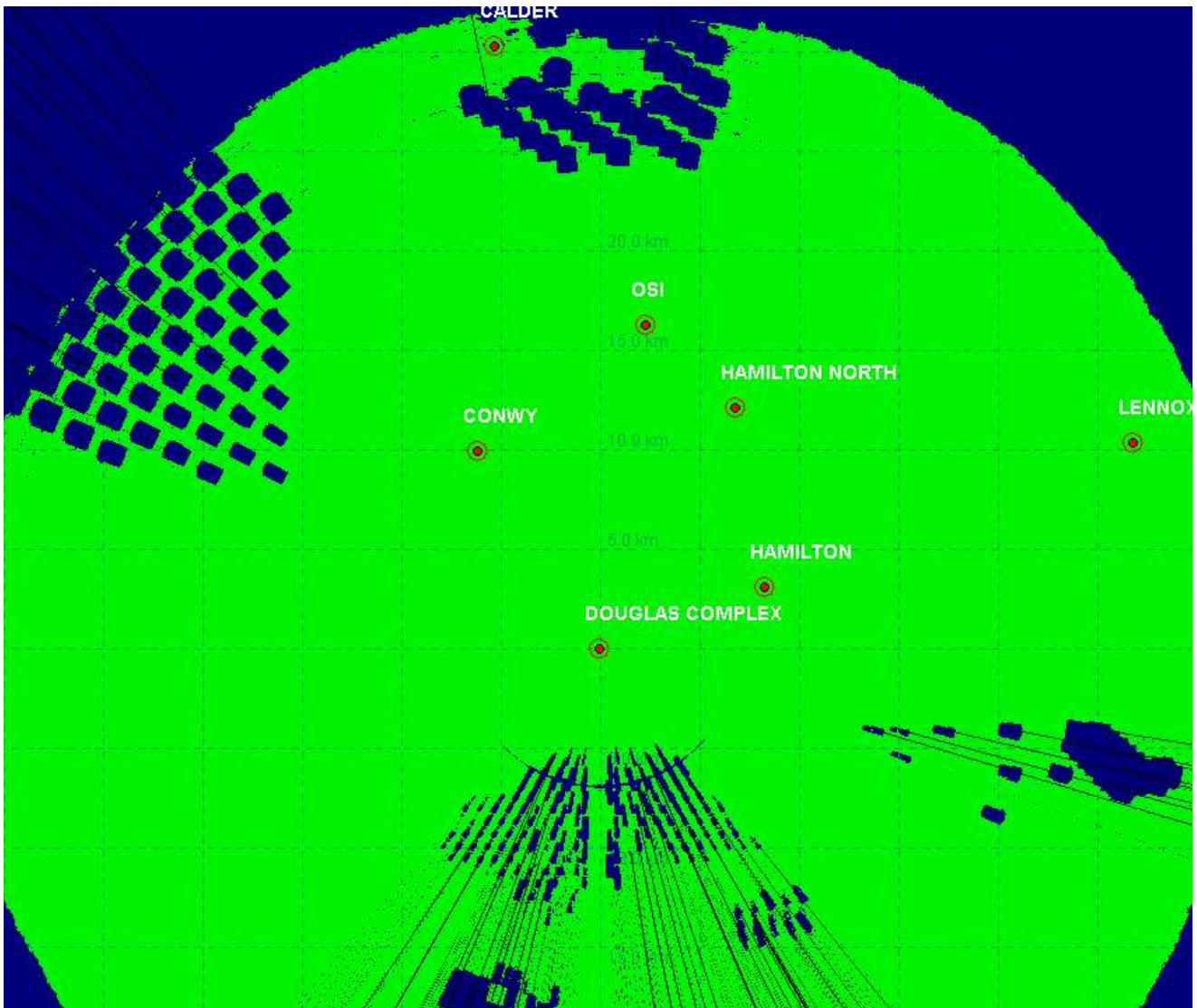
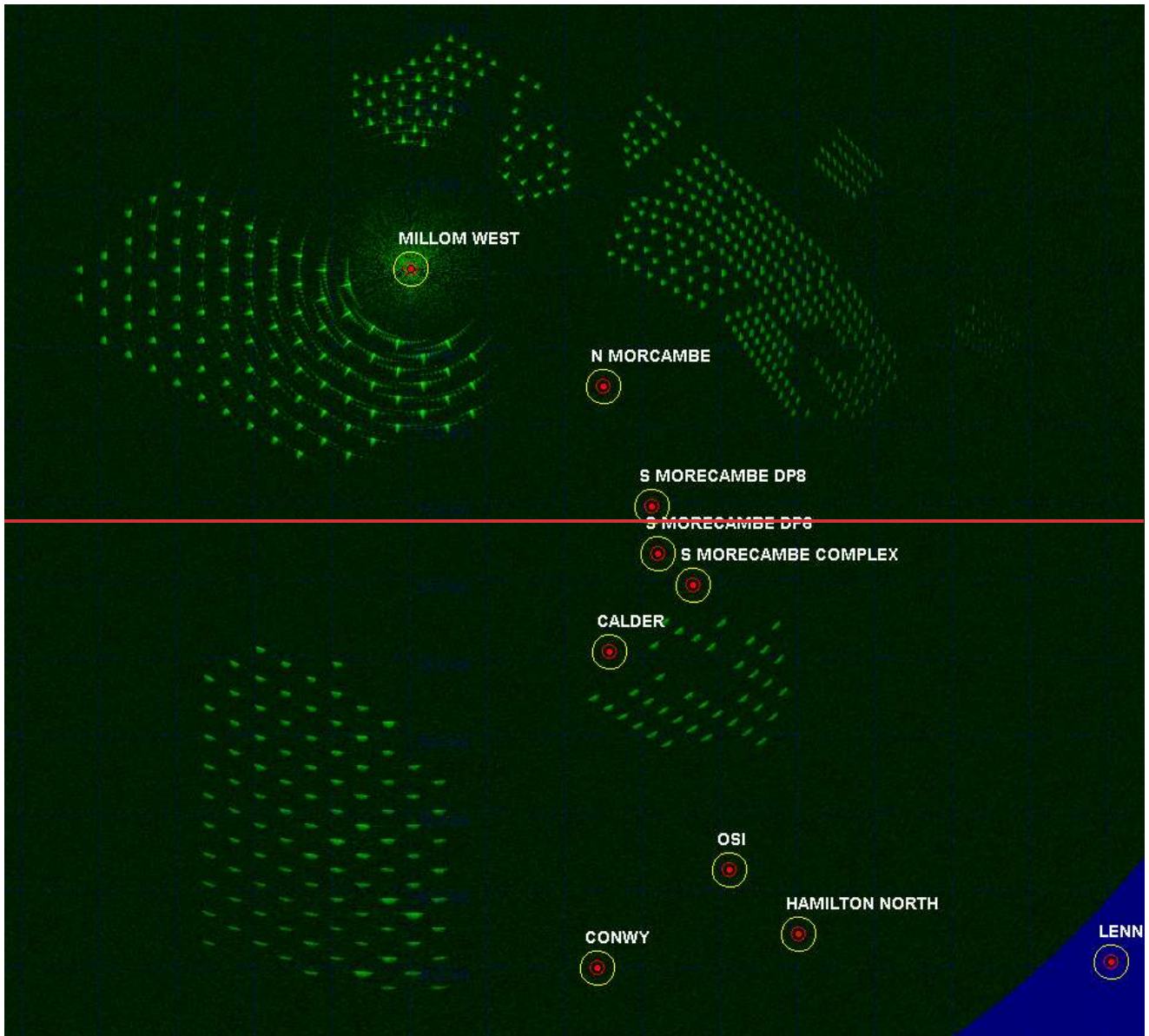


Figure 4.4133: ENI Energy's Douglas platform REWS detection plot showing loss regions for a ~~4000420~~ 4000420 m2 target.



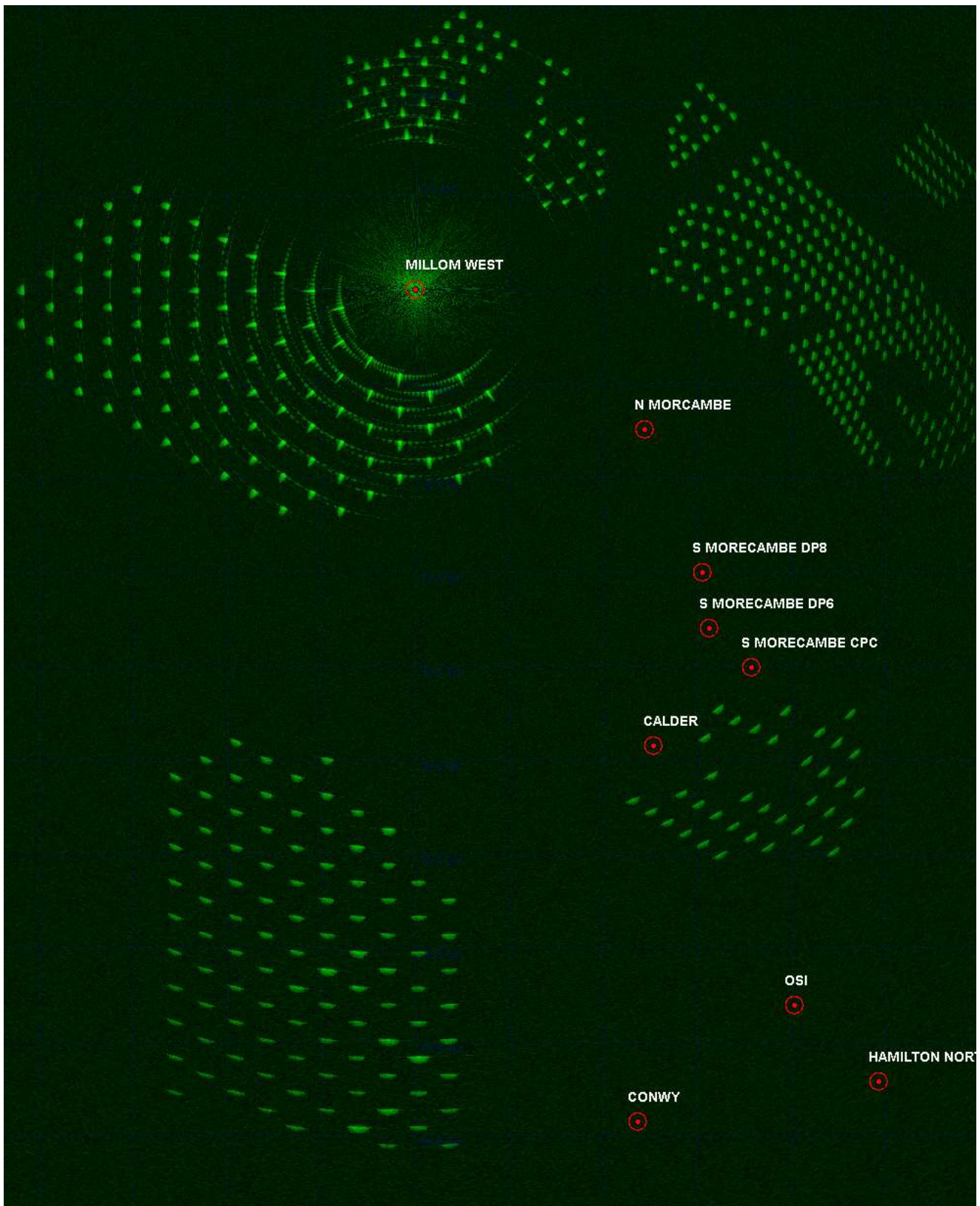
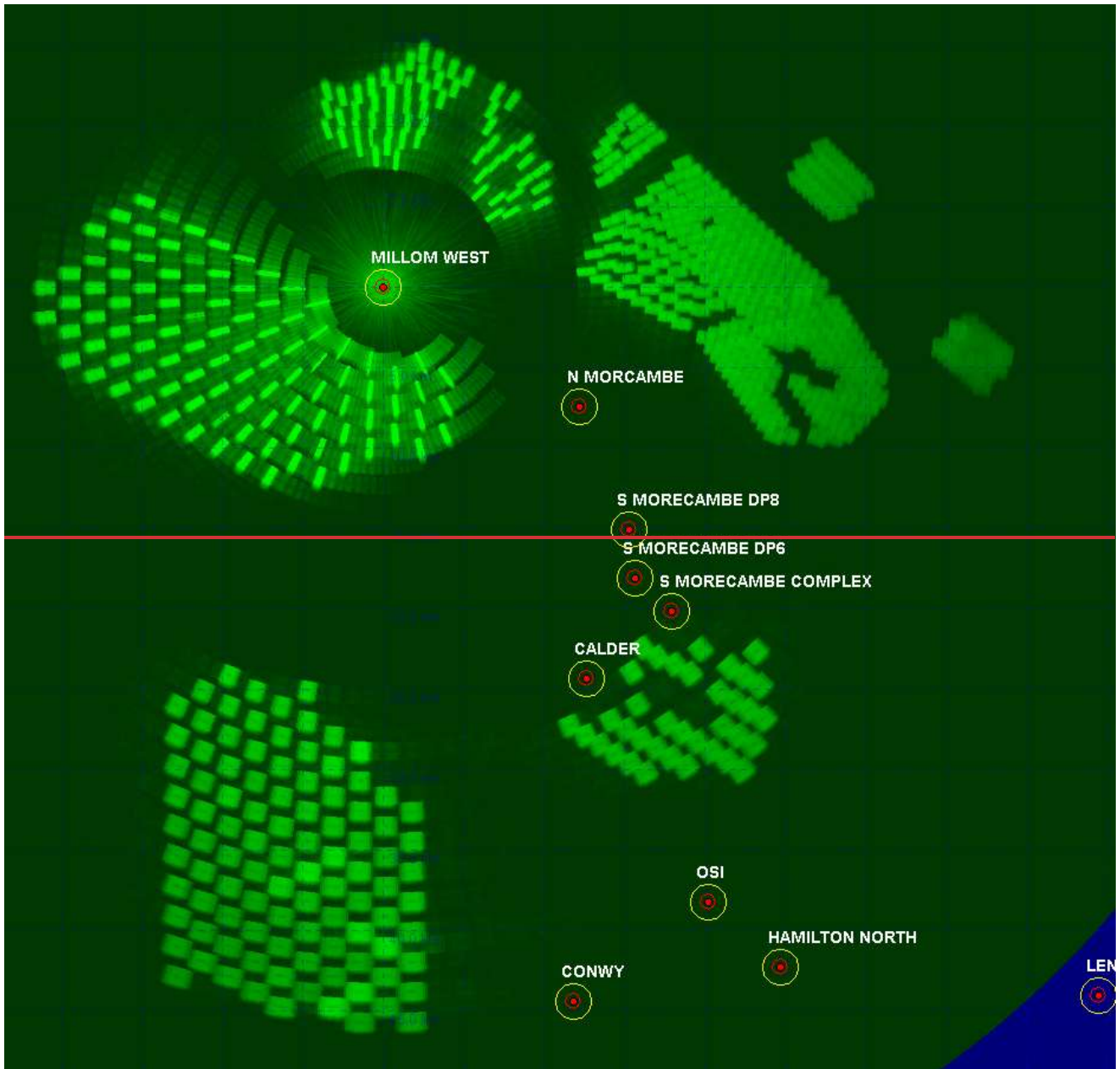


Figure 4.4234: Harbour Energy's Millom West platform REWS clutter map showing returns from the wind turbines and sea clutter.



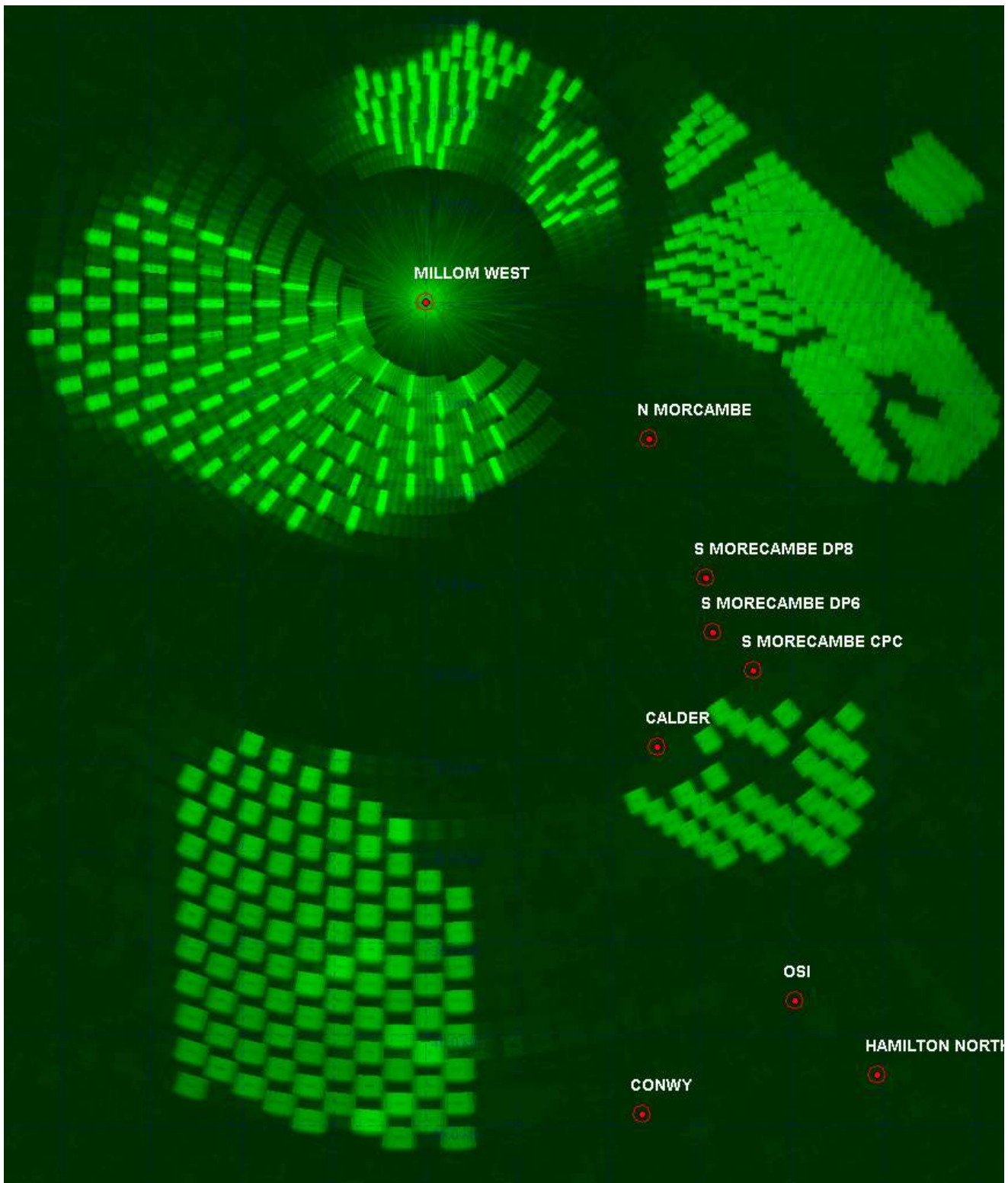
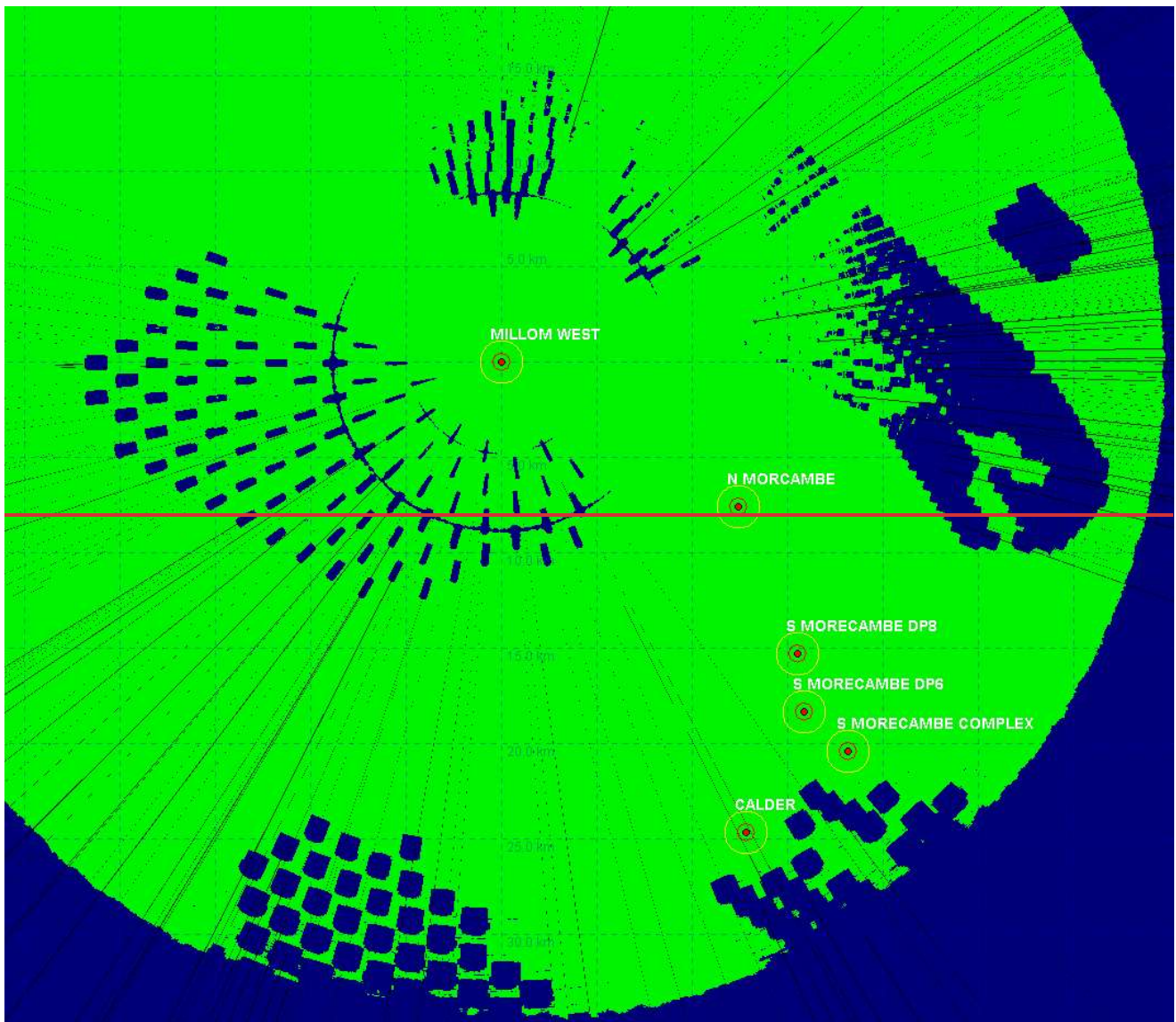


Figure 4.4335: Harbour Energy's Millom West platform REWS detection threshold.



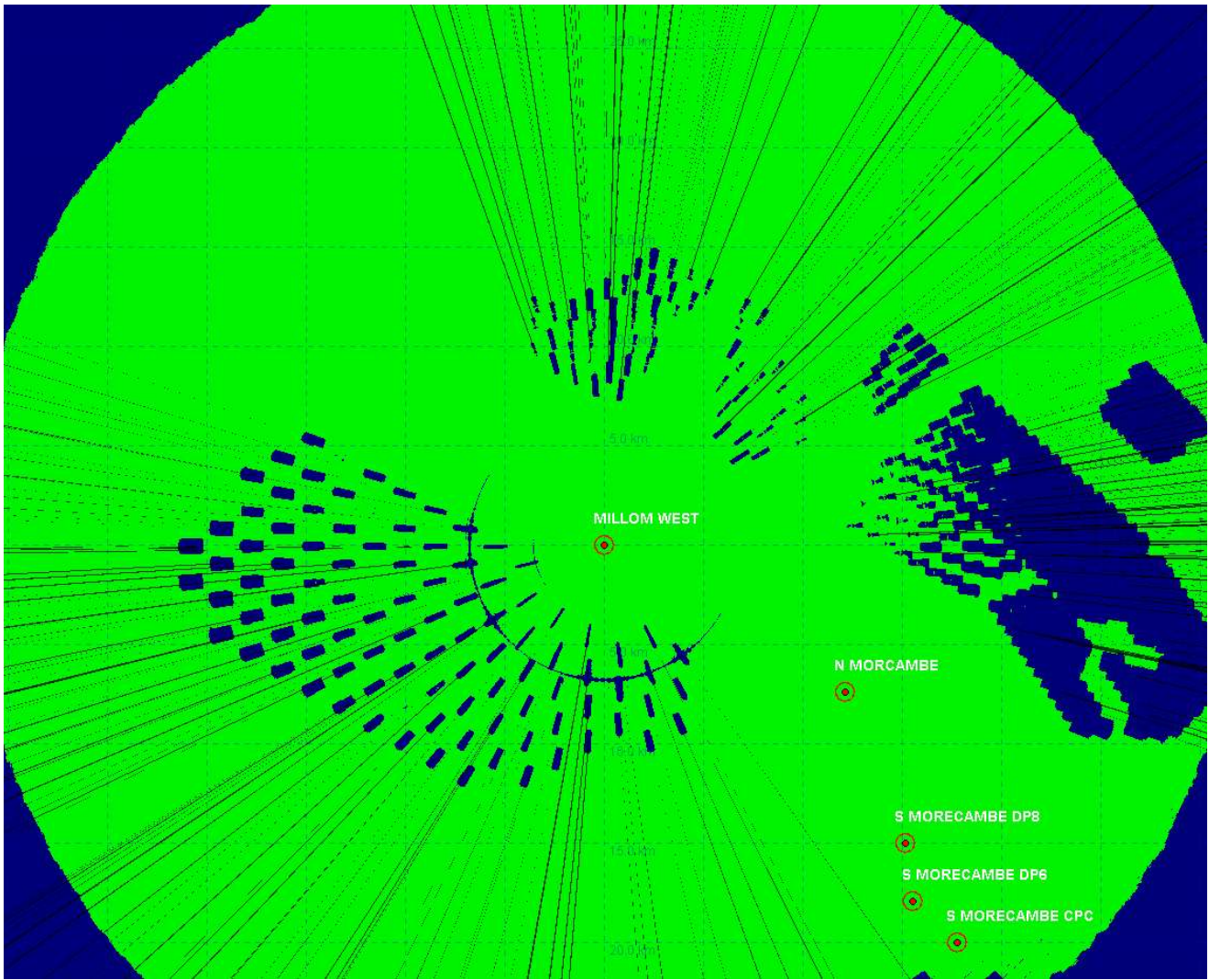


Figure 4.4436: Harbour Energy's Millom West platform REWS detection plot showing loss regions for a **1000420** m2 target.



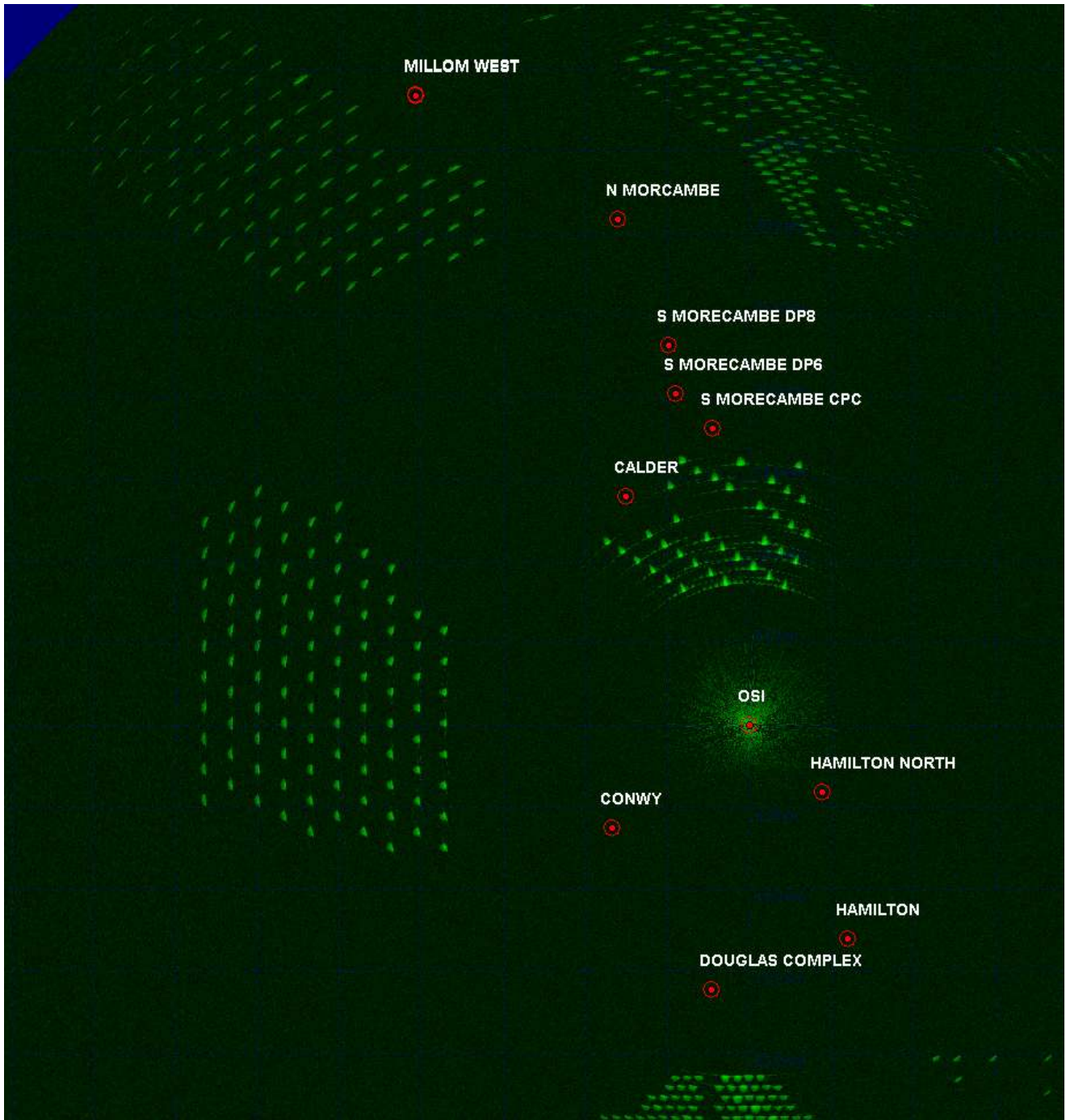
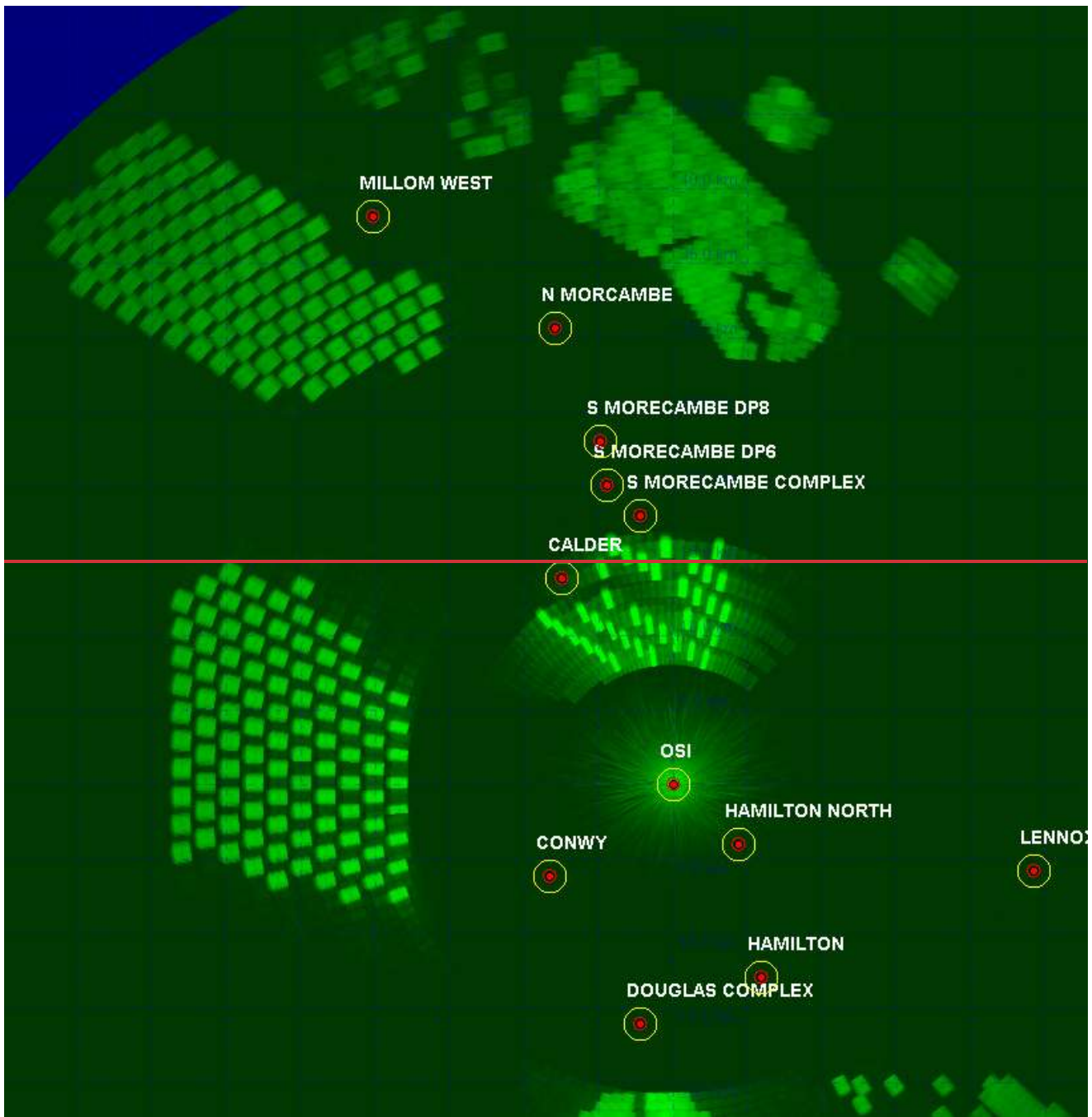


Figure 4.4537: ENI Energy's OSI REWS detection clutter map showing returns from the wind turbines and sea clutter.



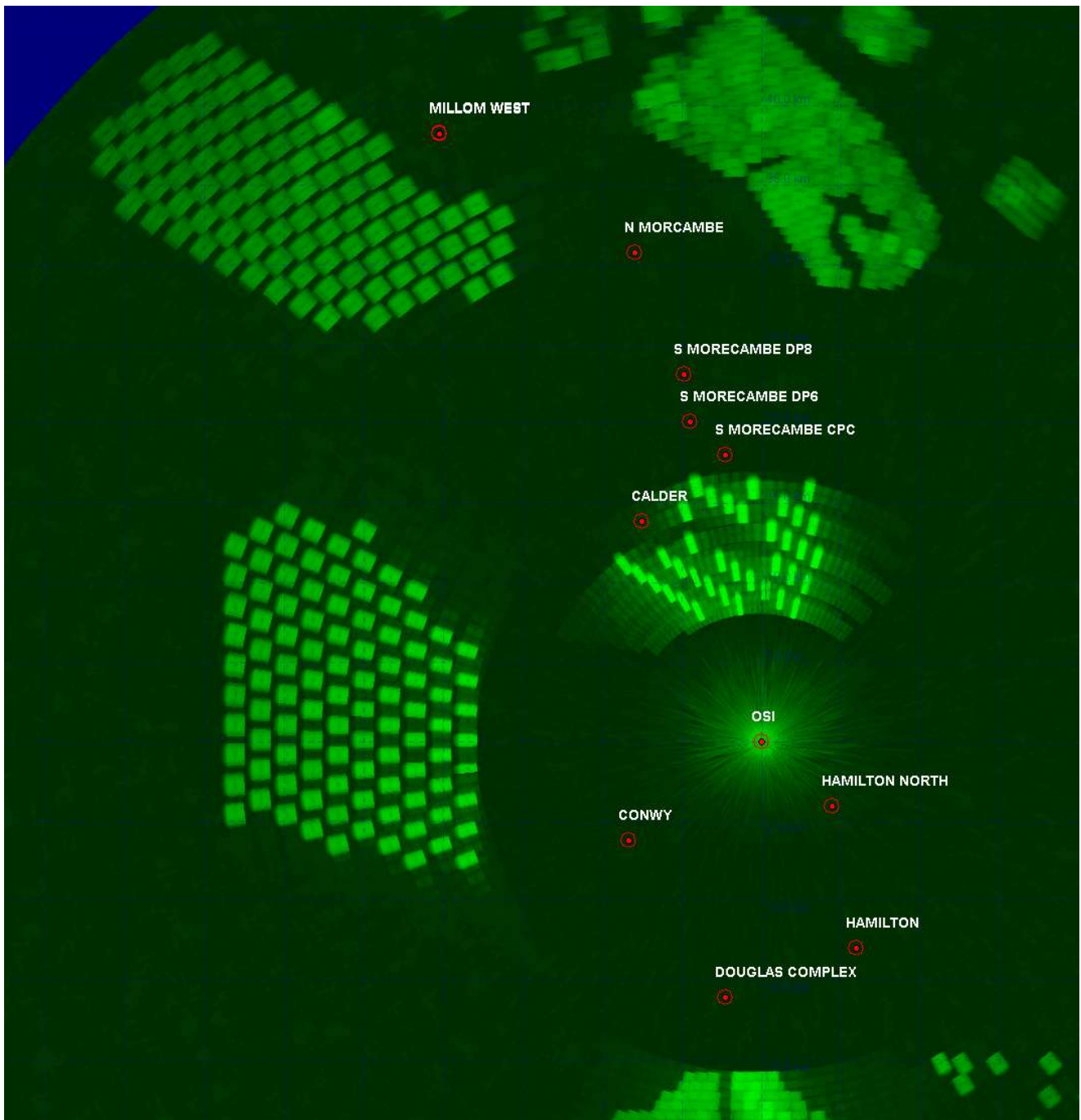
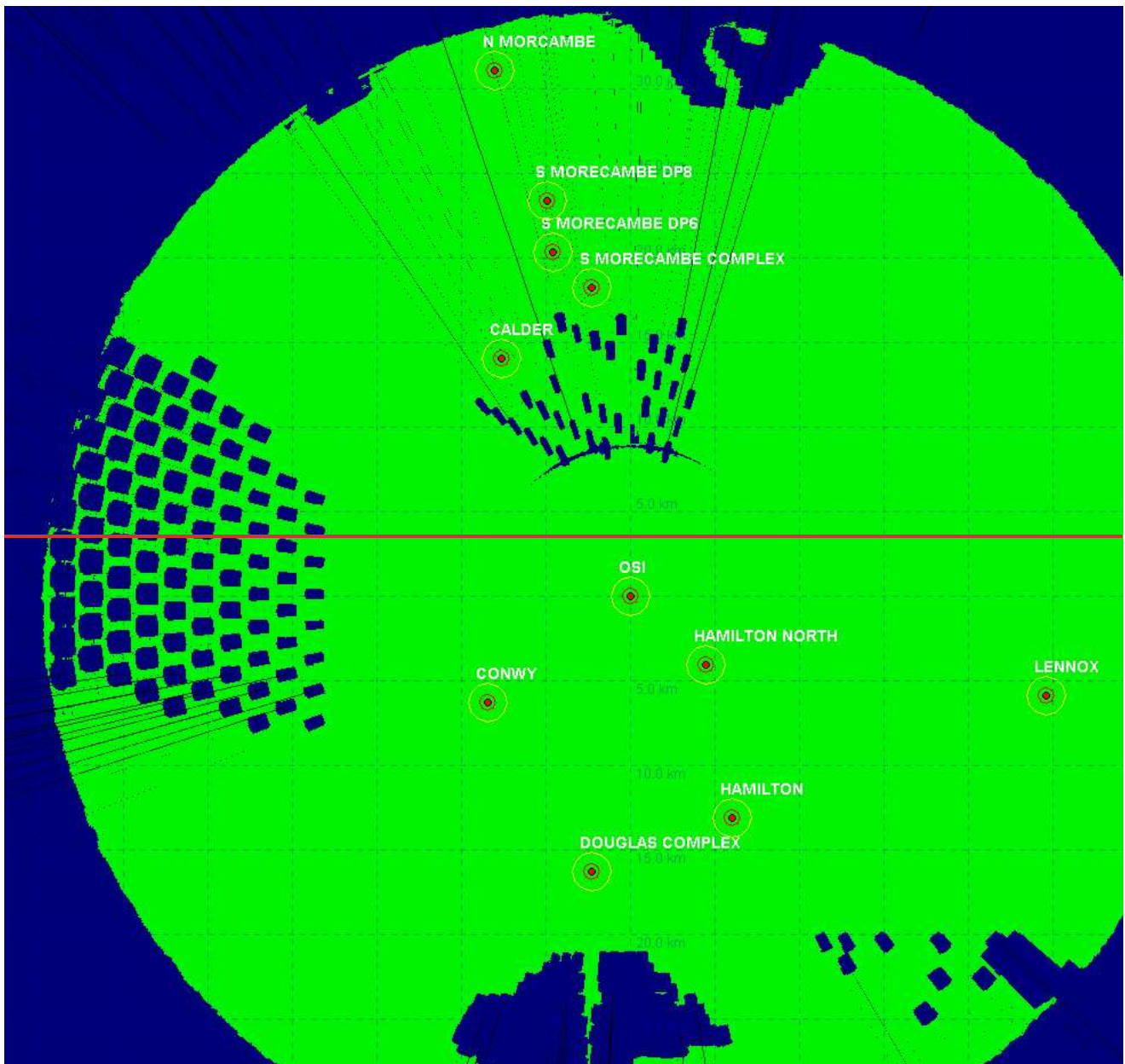


Figure 4.4638: ENI Energy's OSI REWS detection threshold.



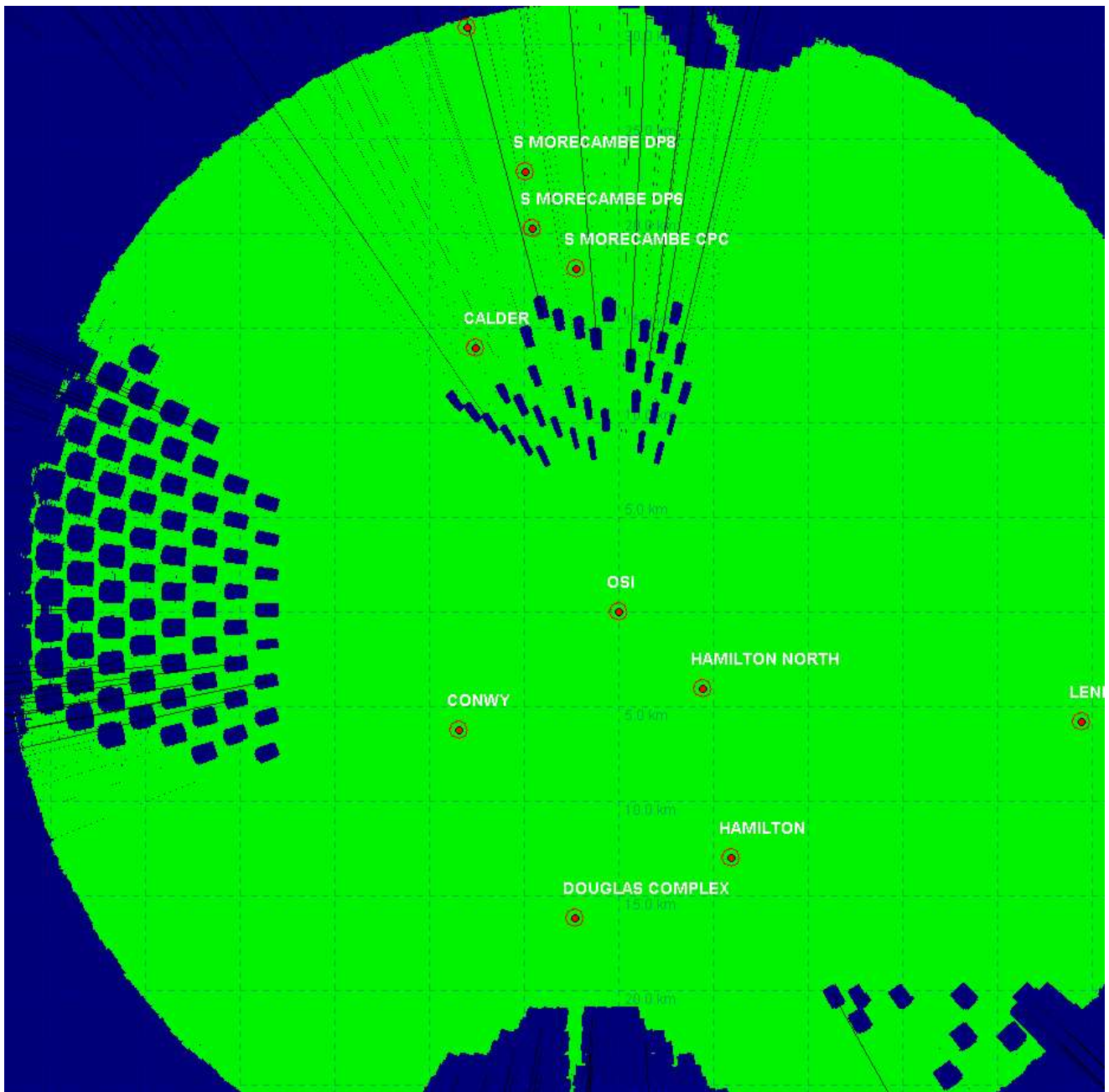
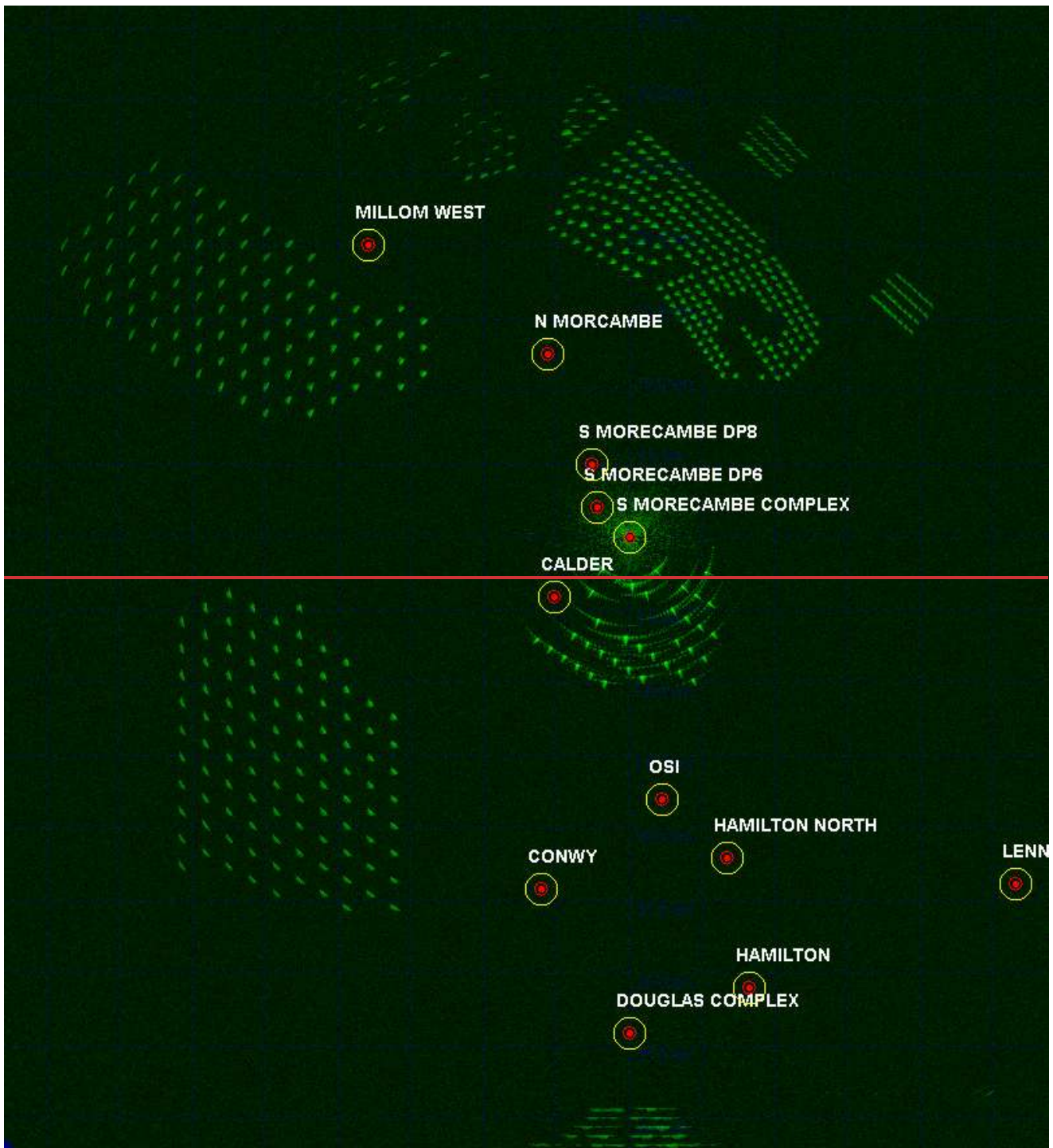


Figure 4.4739: ENI Energy's OSI REWS detection plot showing loss regions for a **1000420** m2 target.



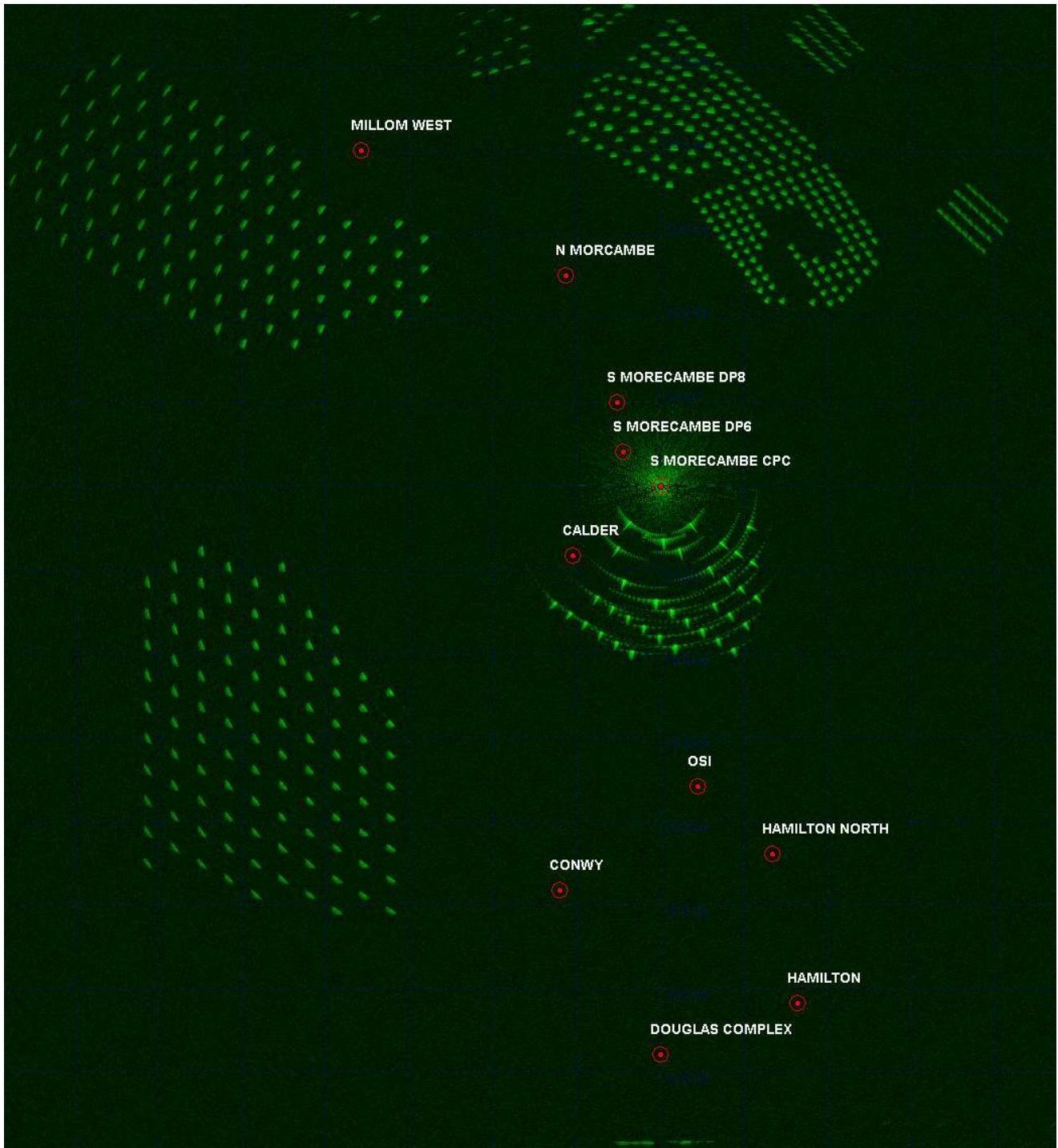
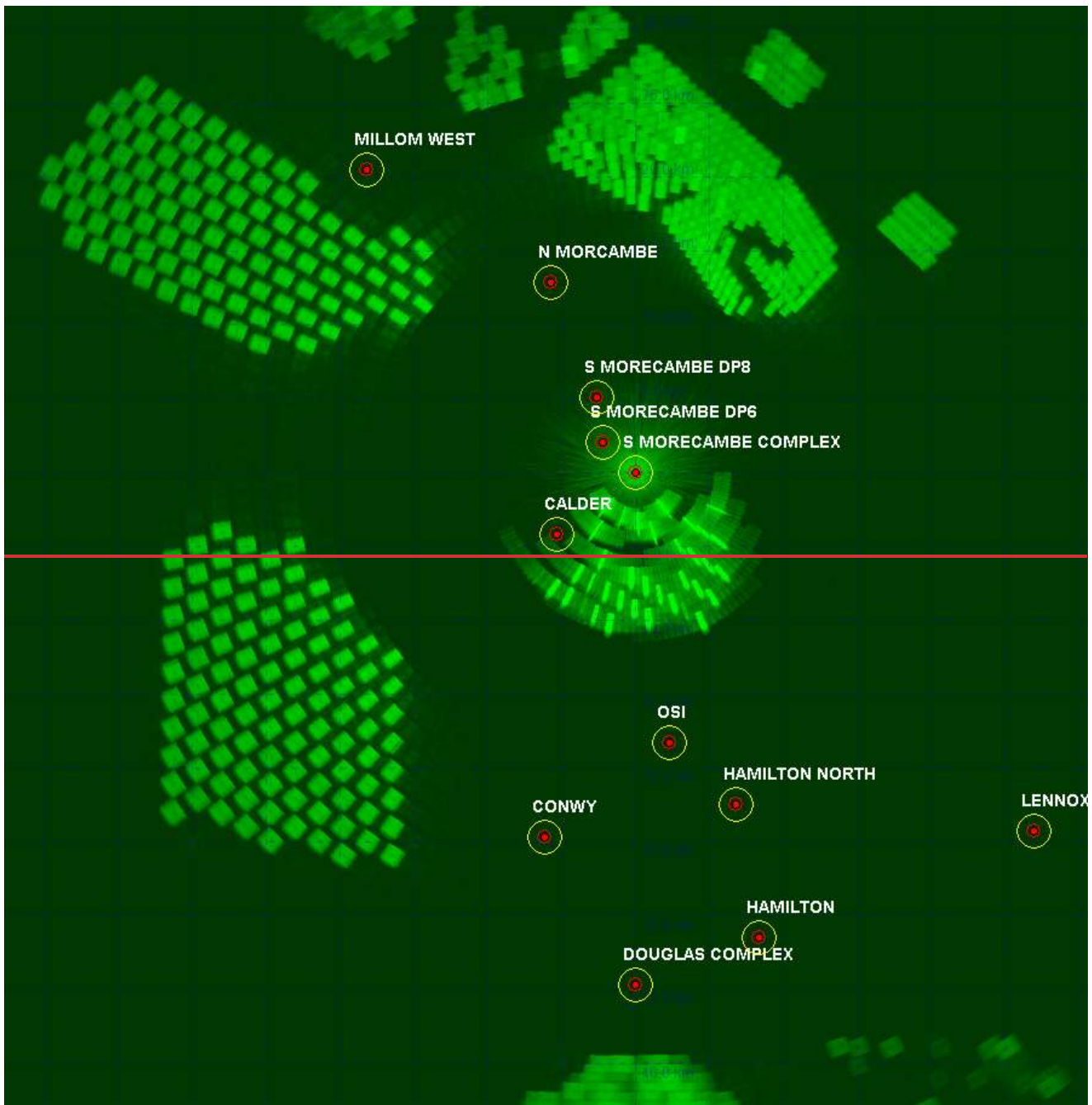


Figure 4.4840: Spirit Energy's South Morecambe AP1 platform REWS clutter map showing returns from the wind turbines and sea clutter.



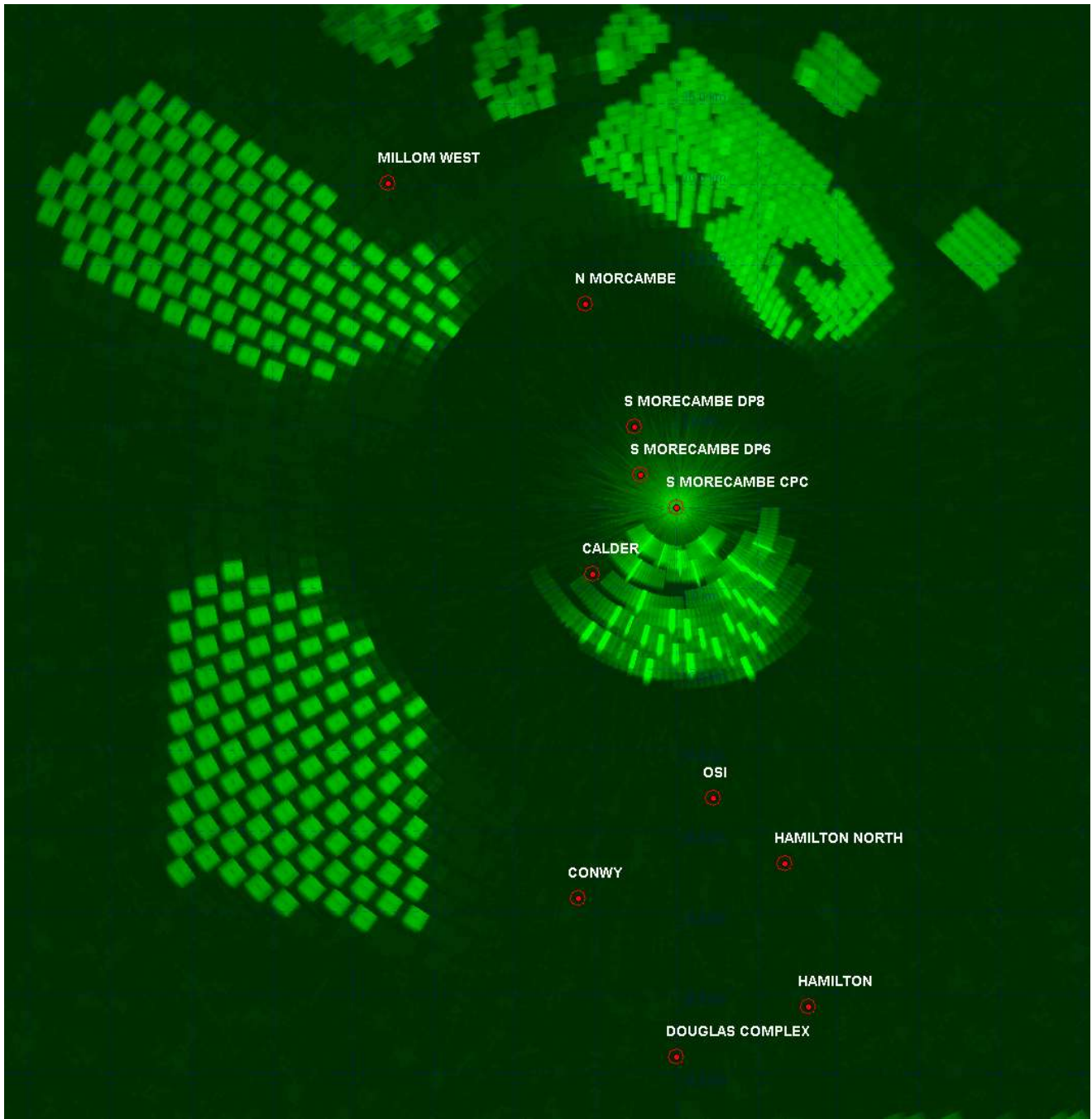
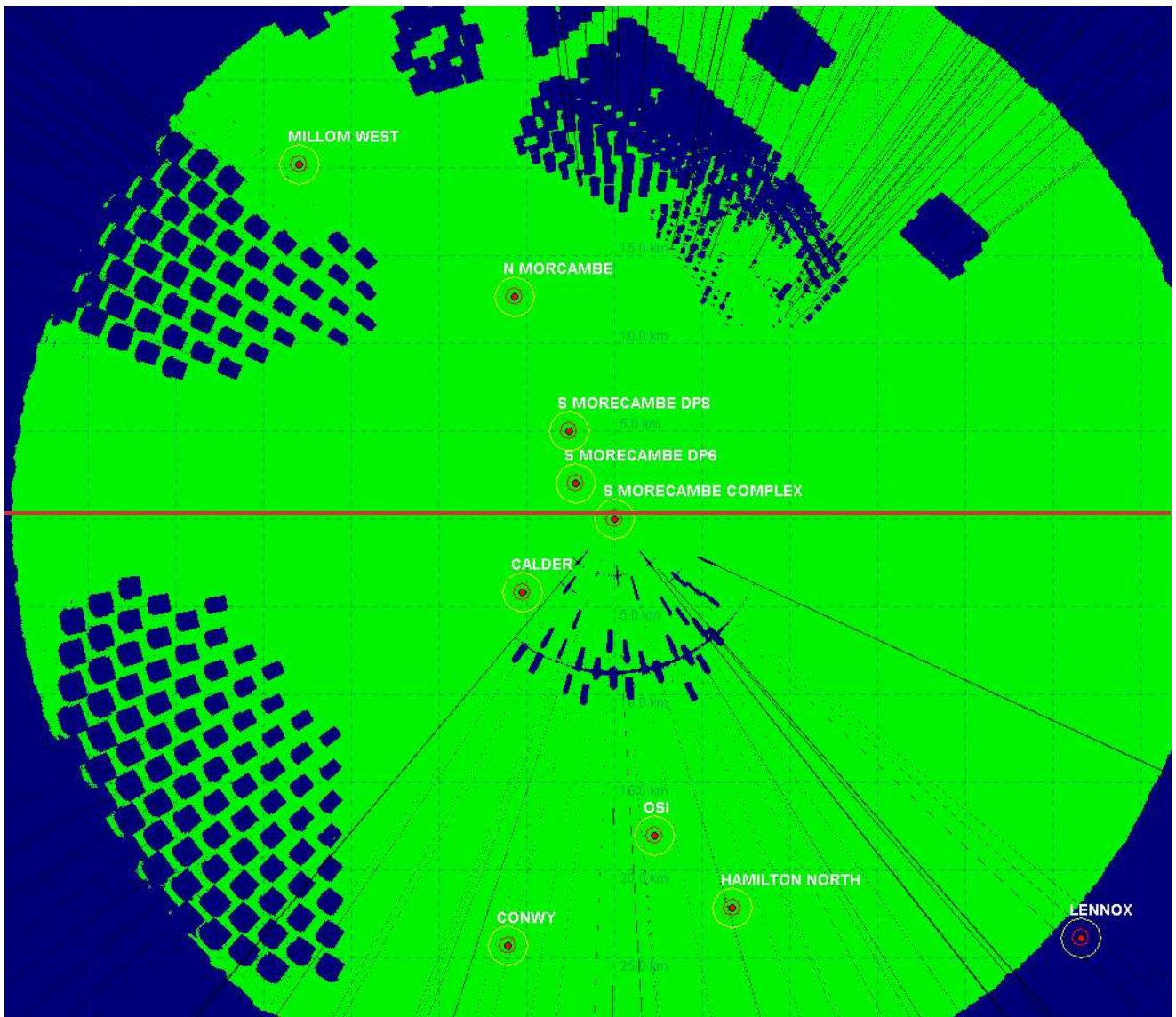


Figure 4.4941: Spirit Energy's South Morecambe AP1 platform REWS detection threshold.



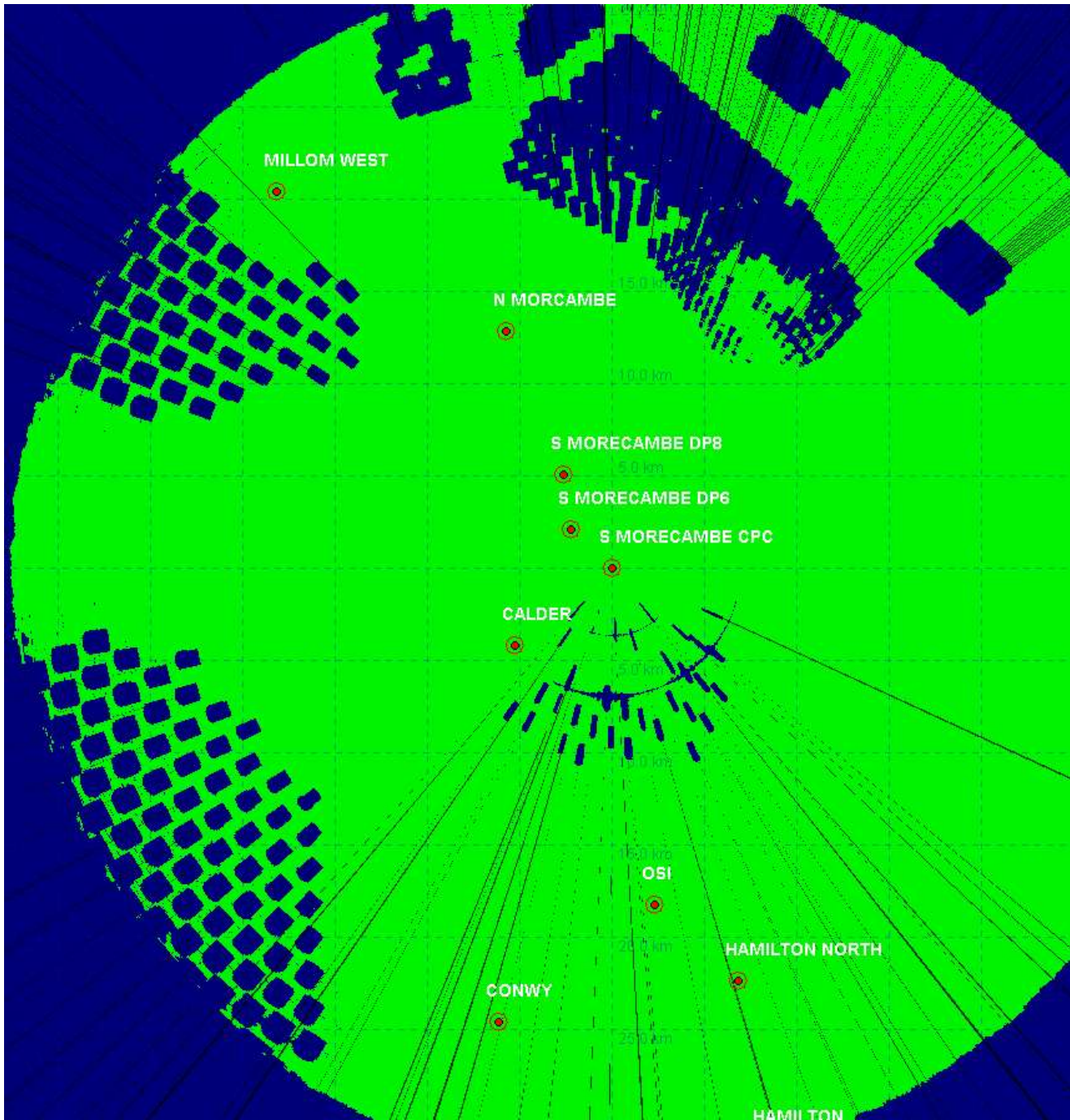


Figure 4.5042: Spirit Energy's South Morecambe AP1 platform REWS detection plot showing loss regions for a 1000420 m2 target.

4.4.3 Conclusions and comments on the cumulative REWS assessment of Morecambe Generation Assets with other proposed windfarms in the study area

4.4.3.1 As noted in Section 4.4.2, the impact of the Awel y Môr Windfarm could not be modelled within this study due to the lack of turbine size parameters and turbine layout for the windfarm. Additionally, the Awel y Môr Offshore Windfarm is considered to be

sufficiently far from the REWS installations and it is not expected to contribute to the cumulative effects or the conclusions of this study.

- 4.4.3.2 Although REWS installation on ENI's Douglas platform may detect turbines with the Awel y Môr Windfarm, in general Awel y Môr is not expected to create a notable cumulative impact with Morecambe Generation Assets alone or cumulatively with the Mona Offshore Wind Project and Morgan Generation Assets on REWS due to its location and distance from the REWS.
- 4.4.3.3 The modelling results set out in Section 4.4.2 of the cumulative assessment on the REWS installations on ENI Energy's Douglas platform, Harbour Energy's Millom West platform, ENI Energy's OSI and Spirit Energy's South Morecambe AP1 platform show that the raw, single scan detection performance is affected adversely within the windfarm regions. Due to the presence of the proposed Morecambe Generation Assets and other windfarms in the study area, there will be small gaps in the detection map due to the elevated thresholds and shadowing effects from the wind turbines.
- 4.4.3.4 However, as discussed previously, these effects will be largely mitigated by the advanced tracking techniques within the REWS. Additionally, the integration of the available AIS data with the REWS coverage will provide an alternative source of vessel information and location within the zones where the REWS may lose detection. Therefore, the models show that the impact of the cumulative effect of the Morecambe Generation Assets along with Mona Offshore Wind Project and the Morgan Generation Assets on detection performance of nearby REWS installations is expected to be relatively low and will be manageable without the need for further mitigation measures.

5 ASSESSMENT OF THE REROUTED TRAFFIC ON REWS ALARM RATES

5.1 Overview

- 5.1.1.1 The REWS uses the radar returns to monitor and track vessels within the detection region and alert the operator when a proximity violation or an allision threat is detected. The REWS uses a defined set of rules to identify a breach of the CPA and TCPA parameters. For the assessed platforms, the alarm parameters and conditions are as outlined in paragraph 3.5.1.1.
- 5.1.1.2 Within this technical report, the effect of the rerouting of traffic on the REWS alarm rates have been modelled based on the existing traffic in the region and the predicted alterations to the traffic around the Morecambe Generation Assets.
- 5.1.1.3 Due to the location of proposed windfarms and the predicted changes to the existing shipping traffic routes, this assessment considers the effect of rerouted shipping routes on the existing offshore platforms (i.e. Conwy, Douglas DA, Douglas DW, Hamilton, Hamilton North, Lennox, Calder, Millom West, North Morecambe DPPA, South Morecambe AP1, South Morecambe CPP1, South Morecambe DP1, South Morecambe DP6, South Morecambe DP8 and the OSI).

5.2 Routes and alarms modelling

- 5.2.1.1 A review of vessel movements in the region, and predicted shipping reroutes to account for the Morecambe Generation Assets is provided in Appendix 14.1 Navigation Risk Assessment of the Environmental Statement (Document Reference 5.2.14.1). This includes measured [radar and](#) AIS data for the base case and predicted data for future reroutes around the Morecambe Generation Assets. The routes and their statistical data (including each routes' mean and standard deviation) were imported into the REWS models. The statistical data enables the REWS models to estimate the width of the shipping route and the likelihood of vessels to deviate from the central (mean) route. Accounting for possible deviations from the central line of the route in a manner which is representative to the real movements of traffic in the region provides a good indication of the overall existing and future alarm rates.
- 5.2.1.2 The route statistical data is given as a set of discrete points along key locations on the route containing the mean and the 90th percentile width of the route. Once the discrete route data were imported, the models then used linear interpolation between data points to extract the standard deviation at intermediate points. The mean and standard deviation is then used to generate 1,000 paths along each route in both the forward and reverse directions (a total of 2,000 runs per route). This was done in order to generate a large set of data that can then be used for statistical analysis. This large number of runs was then used to estimate the probability of raising TCPA or CPA alarms for each route. The probability of raising an alarm was then multiplied by the number of vessels travelling on each route per year to establish the number of alarms expected per year for each platform.
- 5.2.1.3 For each of the platforms considered in the assessment (i.e. Conwy, Douglas DA, Douglas DW, Hamilton, Hamilton North, Lennox, Calder, Millom West, North Morecambe DPPA, South Morecambe AP1, South Morecambe CPP1, South Morecambe DP1, South Morecambe DP6, South Morecambe DP8 and the OSI), the assessment utilised the CPA/TCPA parameters described in paragraph 5.1.1.1 above. In order to better model the impact of moving vessels on TCPA alarms, marine traffic

data collected as part of the overarching Navigation Risk Assessment process was used to estimate a speed distribution representative of routed vessels in the area of most relevance to the REWS report. This provides a good approximation of the speeds of different sizes of vessels in the region. A TCPA/CPA alarm was assumed to be raised whenever a vessel breached the alarm rules.

5.2.1.4 Typically, an amber TCPA alarm is triggered when a vessel is heading along a vector that would bring it within 0.6 nm from a protected platform within a specified time range (35 minutes for manned installations and 25 minutes for NUIs). If the vessel continues along its path and is 25 minutes away from a manned installations or 15 minutes from an NUI, the alarm status would escalate to a red alarm. In scenarios whereby multiple platforms are present in the region a vessel may trigger multiple TCPA alarms for different platforms along the route of the vessel. If a vessel raises a TCPA alarm, the REWS operator or the ERRV crew would attempt to establish radio contact with the vessel to make them aware of the presence of platforms along the routes. If no radio contact is established the ERRV would be deployed to intercept the vessel and issue audio and/or visual warnings to get the attention of the crew on the offending vessel. Hence, it is assumed within this study that once an alarm triggered and addressed by the REWS operator or ERRV crew, no alarm escalation would occur and no further alarms are registered for other platforms along the route, as it is assumed that the vessel has already been communicated with and is known to be under command and aware of the platforms.

5.2.1.5 Finally, to avoid false alarms due to temporary vector breach of the TCPA while vessels are turning, the models were set to only issue a TCPA alarm if the vessel continues to breach the TCPA rules for more than 36 radar rotations (as noted in section 5.1 above).

5.3 Modelling the base case traffic (pre-development of the Morecambe Generation Assets)

5.3.1.1 In order to be able to estimate a change in alarm rates due to the rerouting of traffic around the proposed projects array areas, a base case scenario was considered. The base case scenario utilises the existing traffic data within the region, as provided by [radar and](#) AIS data, along with extrapolated data in the regions where no data was available.

5.3.1.2 This study assessed a region of 10 nm around the proposed project’s array area to provide a sufficient range to assess the TCPA alarms. The complete lists of commercial and ferry routes are shown in [Table 5.1](#)~~Table 5.4~~ and Table 5.2 respectively and are illustrated in [Figure 5.2](#)~~Figure 5.2~~ and [Figure 5.1](#)~~Figure 5.4~~. [Figure 5.3](#)~~Figure 5.3~~ illustrates the modelled routes output for 1,000 runs, showing the variation of route traffic around the mean line. Individual red lines/strands represent the modelled possibilities of vessels travelling along the modelled routes.

Table 5.1: Commercial shipping routes in the region and the number of vessels travelling on each route per day.

Route number	Average transits per year	Description (main ports, also may include alternative ports)
1	1563	Skerries TSS to Liverpool TSS (E)
2	428	W Isle of Man (IoM) to Liverpool TSS (E)

MORECAMBE OFFSHORE WINDFARM GENERATION ASSETS

Route number	Average transits per year	Description (main ports, also may include alternative ports)
3	1610	Liverpool TSS to Skerries TSS (W)
4	525	Liverpool TSS to Skerries TSS
5	17	Inshore Anglesey to Liverpool
6a	13	Off Skerries TSS to Barrow (E)
6b	10	Off Skerries TSS to Heysham (E)
7	4	Off Skerries TSS to Barrow (W)
8	7	Heysham to Off Skerries TSS (W)
9	36	Irish Sea to Liverpool SS (E)
10	13	Liverpool TSS to Inshore Anglesey (W)
11	45	Liverpool TSS to Central Irish Sea (W)
12	137	Liverpool TSS to Irish Sea via Skerries TSS (W)
13	533	Liverpool TSS to W IoM (W)
14	184	E IoM to Heysham
15a	10	Liverpool to E IoM - W
15b	54	Liverpool to E IoM - Central
15c	14	Liverpool to E IoM - E
16	6	Douglas to Heysham
18	153	Liverpool to W IoM
19	9	Douglas to Liverpool TSS (E)
20	60	Southern Irish Sea to Solway Firth
21	42	Off Skerries TSS to Solway Firth
22	8	Douglas to Liverpool TSS
23	66	Liverpool to E West of Duddon Sands
24	9	Liverpool to Off Skerries TSS (via NE Anglesey)
25	13	Colwyn Bay to W IoM
26	55	Liverpool TSS to Northern Ireland (W)
27	6	Douglas to Liverpool

Table 5.2: Ferry shipping routes in the region and the number of vessels travelling on each route per day.

Route number	Average transits per year	Description (main ports, also may include alternative ports)
F1	1451	Heysham to Douglas IoM
F2	593	Liverpool to Douglas IoM
F3	1099	Heysham to Carlingford Lough

MORECAMBE OFFSHORE WINDFARM GENERATION ASSETS

F4	606	Heysham to Dublin
F5	194	Liverpool to Belfast E (W of Morecambe)
F6	1098	Liverpool to Belfast W
F7	196	Liverpool to Belfast E
F8	1094	Heysham to East IoM
F9	226	Liverpool to Belfast W (TSS E)
F10	166	Liverpool to Belfast W (TSS W)
F11	294	Liverpool to Dublin 3
F12	1627	Liverpool to Dublin 2
F13	1331	Liverpool to Dublin 1

MORECAMBE OFFSHORE WINDFARM GENERATION ASSETS

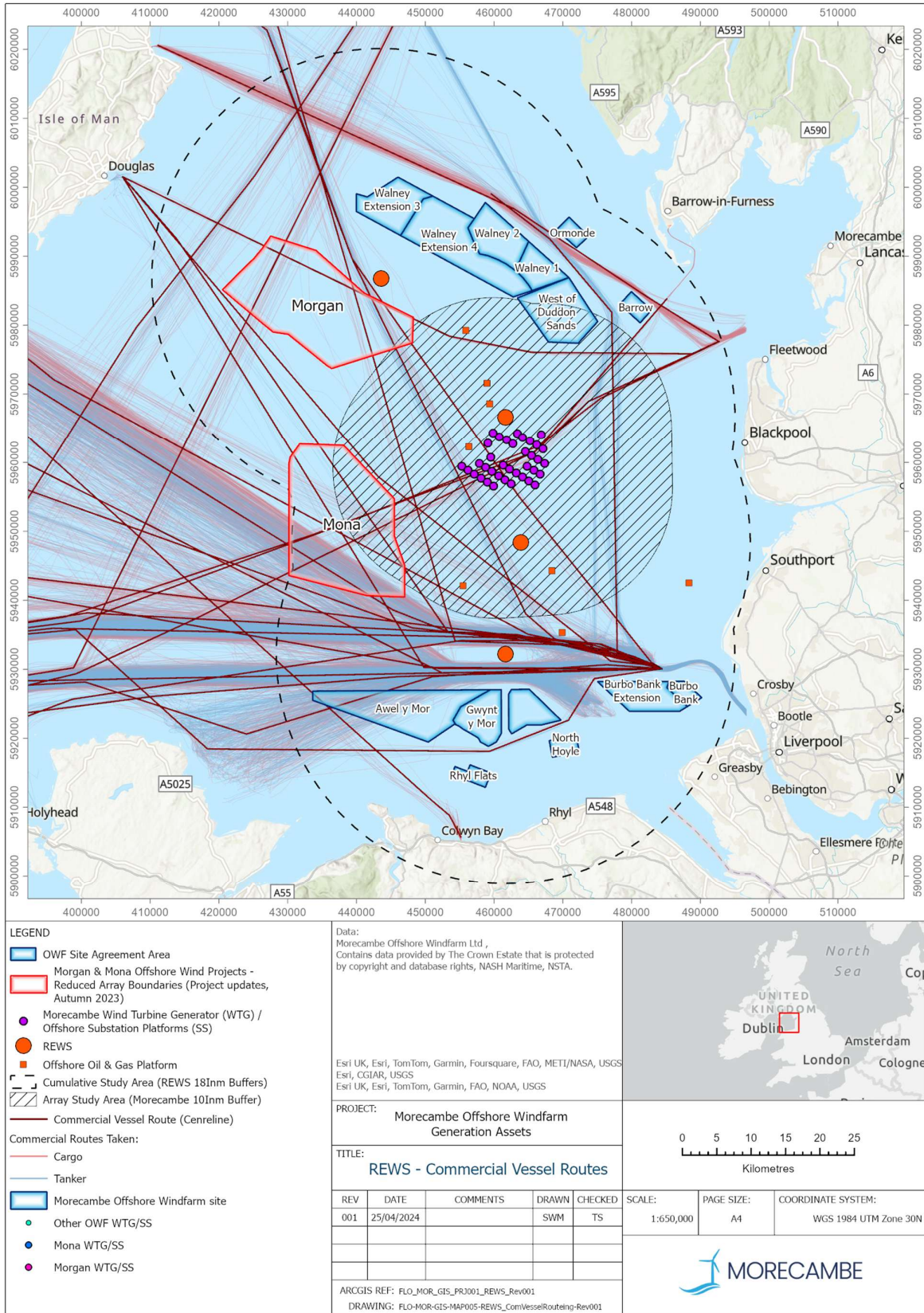


Figure 5.1: Existing commercial routes within and around the Morecambe Generation Assets Array Area.

MORECAMBE OFFSHORE WINDFARM GENERATION ASSETS

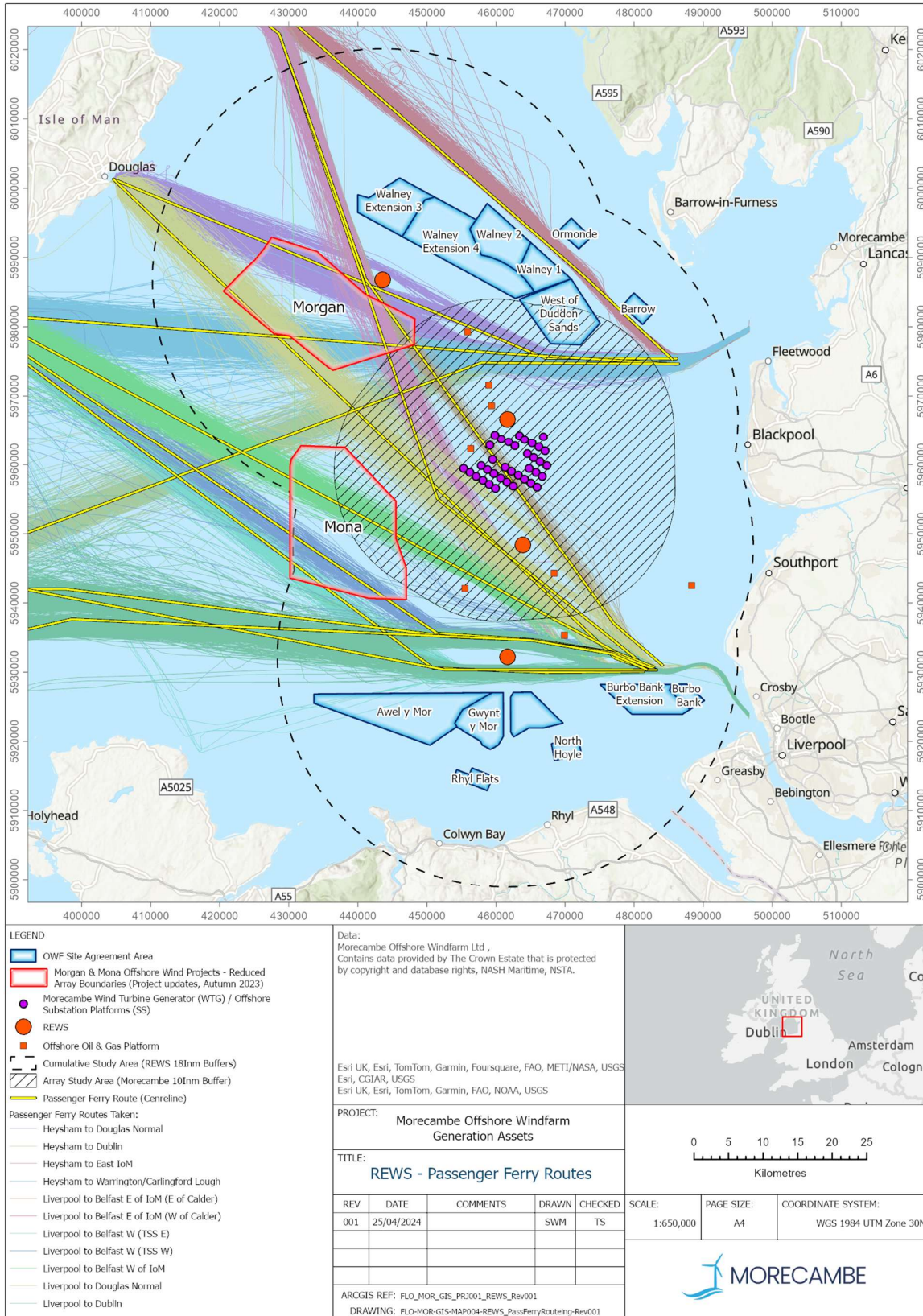
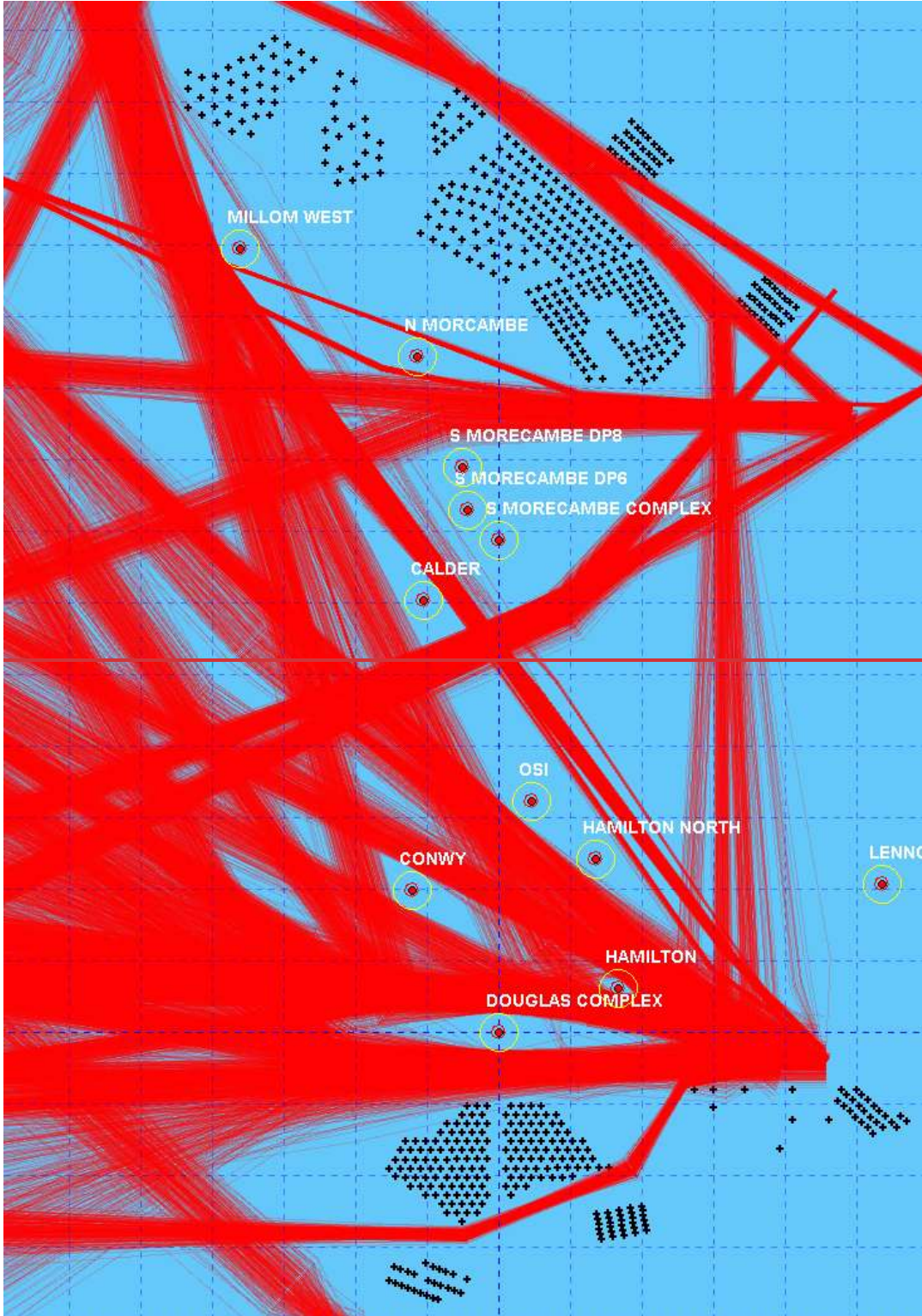


Figure 5.2: Existing ferry routes within and around the Morecambe Generation Assets Array Area.



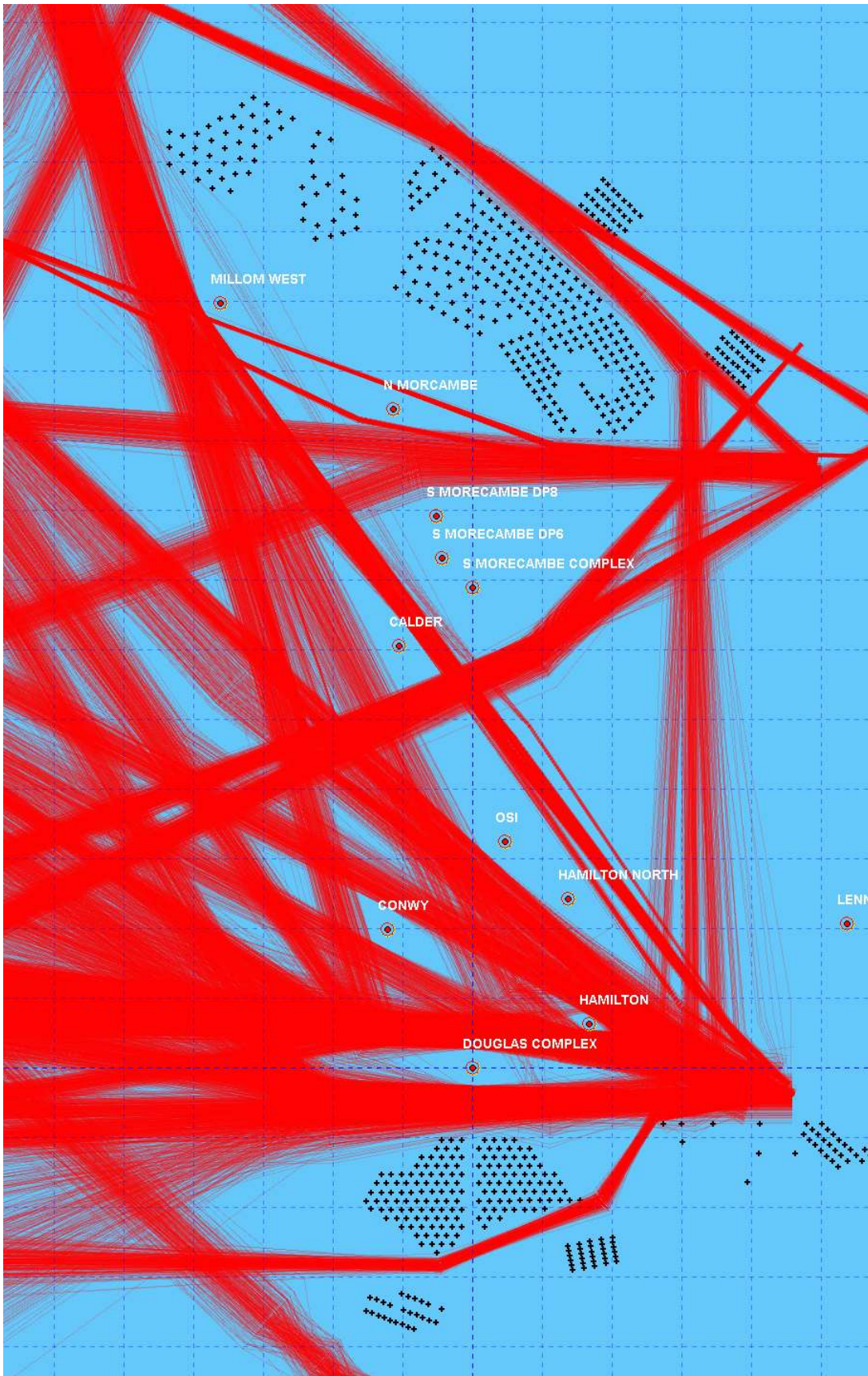
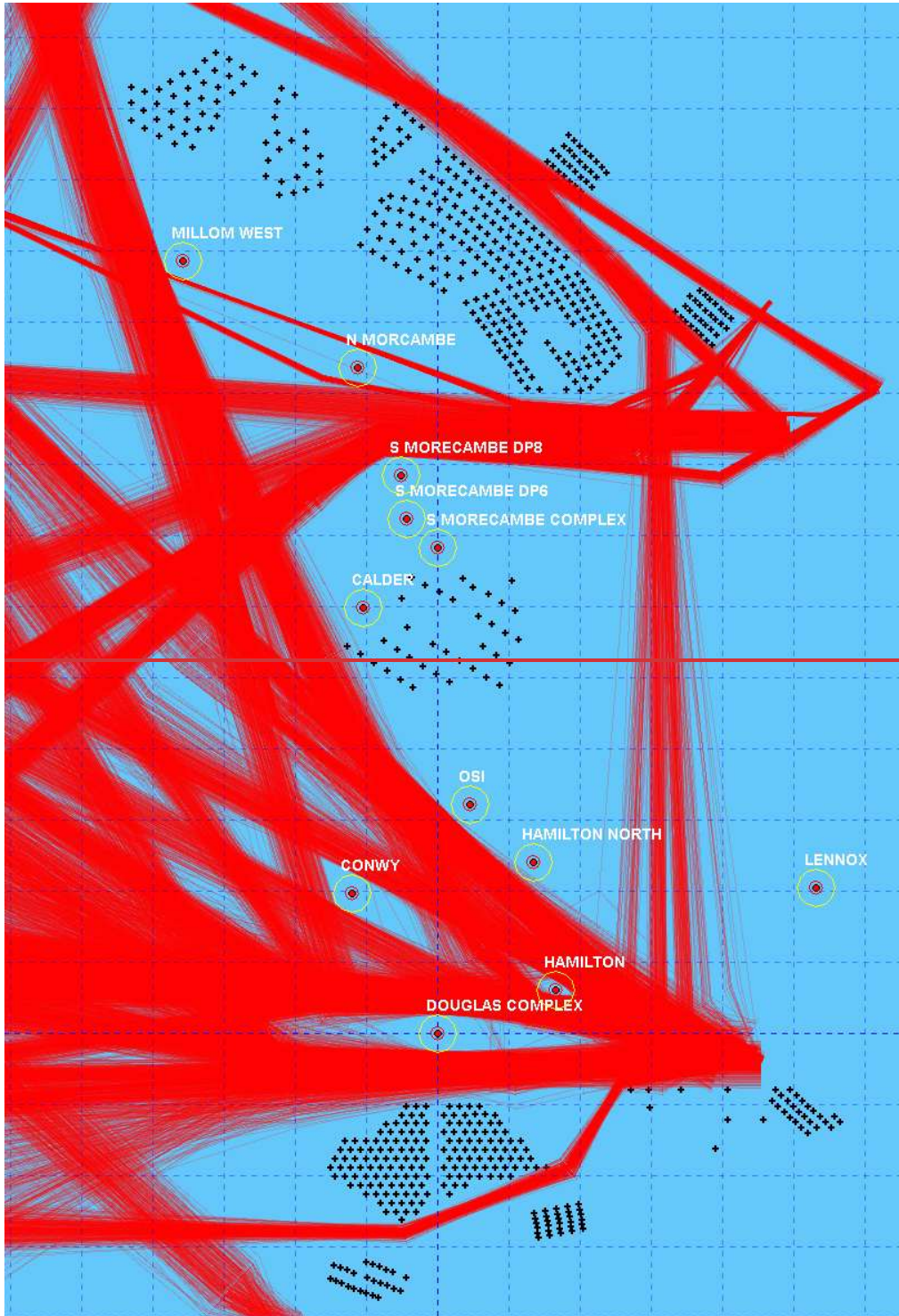


Figure 5.3: Modelled existing shipping routes (1,000 variations each route).

- 5.3.1.3 The models were used to simulate each route in both directions and identify each type of alarm on every platform. Using the statistical nature of the data, a probability of alarm is calculated for each platform by taking the number of alarms triggered over the 1,000 runs and presenting this as a platform percentage. This probability is then used in conjunction with the data in [Table 5.1](#) ~~Table 5.1~~ and Table 5.2 to estimate the number of alarms per year for each platform.
- 5.3.1.4 It is noted that in some cases within the base case scenario, some routes raised no alarms while other routes show some probability of alarms in the existing (base) case. This is due to the proximity and direction of the route as well as the statistical nature/width of the route.
- 5.3.1.5 Additionally, due to simplifying assumption when representing the existing routes in the form of a mean line with a set of 90th percentile widths, the resultant modelled routes did not follow the exact behaviour of the measured routes when vessels are travelling near offshore platforms. This was identified during the modelling process but due to the lack of data it was deemed acceptable at this stage for modelling use. Therefore, although the results presented are an estimate of the existing effect of traffic on the REWS alarms, it provides a good basis from which to compare predicted future cases.

5.4 Modelling the predicted shipping reroutes around the Morecambe Generation Assets in isolation and cumulatively with other windfarms in the study area

- 5.4.1.1 In a similar manner to the base-case scenario, the vessel traffic around the Morecambe Generation Assets (in isolation) was modelled based on the reroutes predicted and described in Appendix 14.1 Navigation Risk Assessment of the Environmental Statement (Document Reference 5.2.14.1). Both the mean line for each route, along with its standard deviation, were considered in the model. This data was then used to create 1,000 runs for each route in either direction (total of 2,000 runs) to provide sufficiently large set of results to undergo statistical analysis of the data and the modelled routes are shown in [Figure 5.4](#) ~~Figure 5.4~~. Once each route was modelled and the yearly alarm rates were obtained, the modelling results for the predicted traffic were compared against the base case.
- 5.4.1.2 Similarly, the rerouted traffic due to the cumulative presence of the Morecambe Generation Assets with Mona Offshore Wind Project and Morgan Generation Assets were modelled based on the predicted reroutes described in Appendix 14.2 Cumulative Regional Navigation Risk Assessment (CRNRA) of the Environmental Statement (Document Reference 5.2.14.2). The modelled routes are shown in [Figure 5.5](#) ~~Figure 5.5~~.



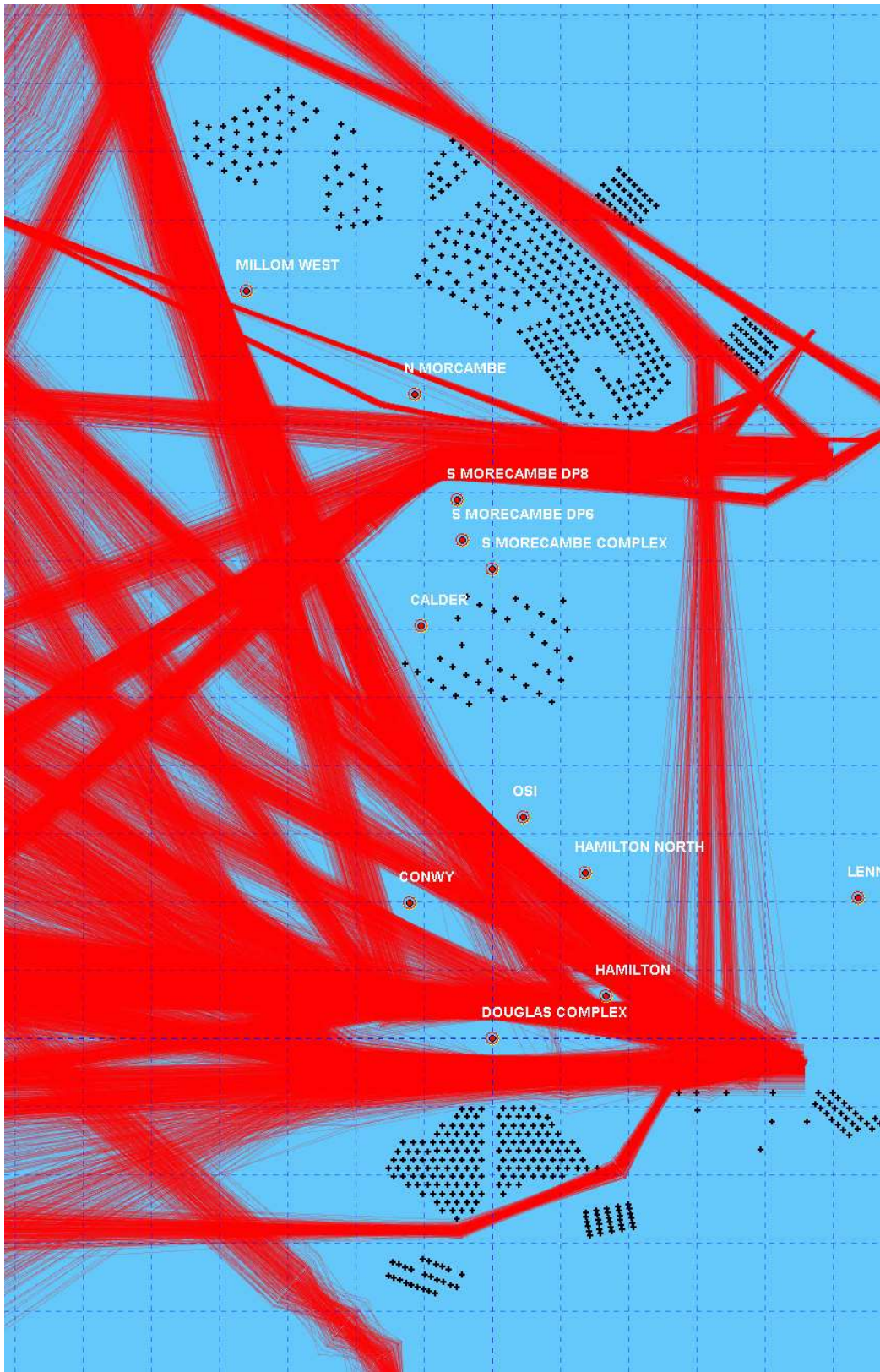
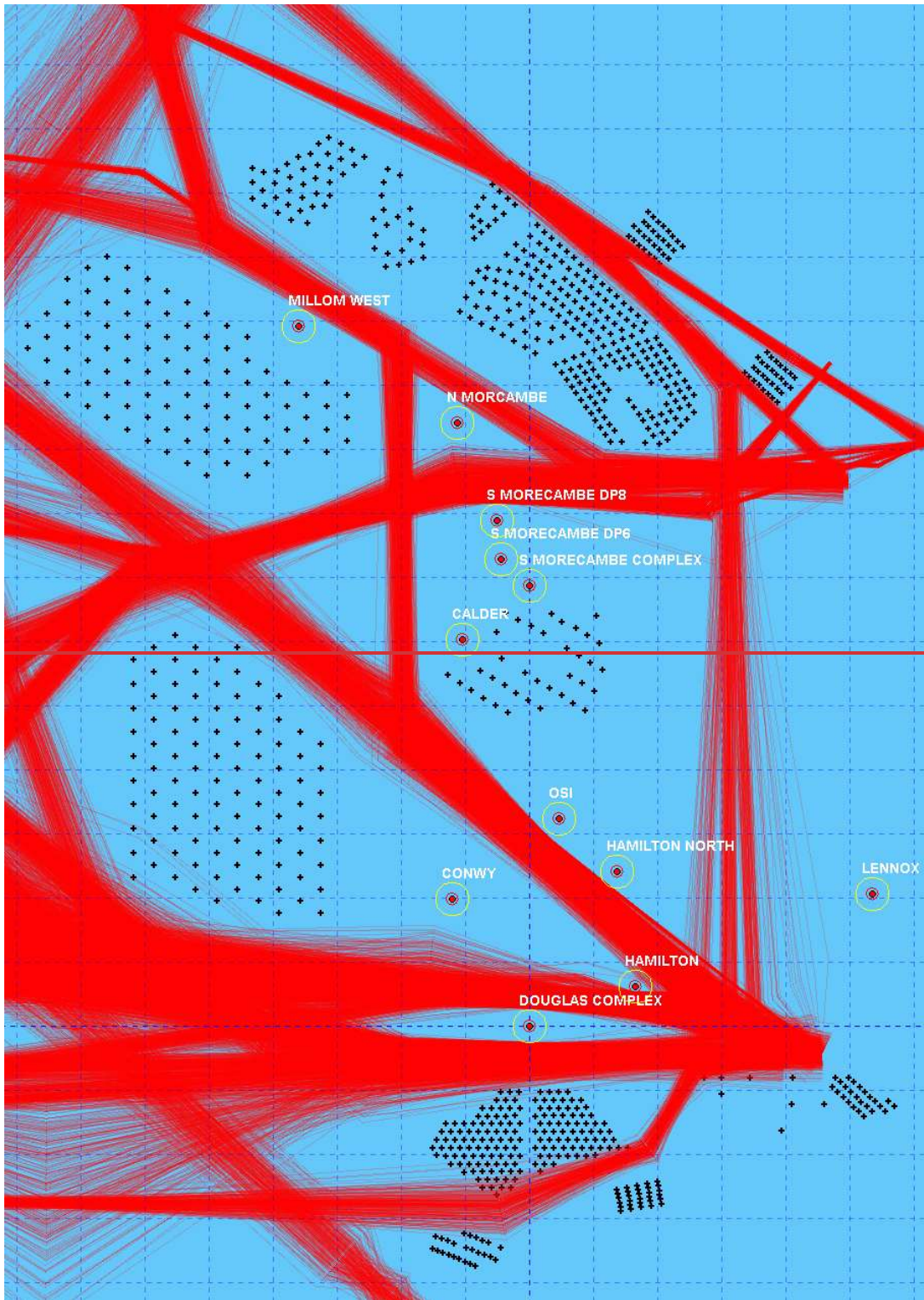


Figure 5.4: Modelled shipping routes post-construction of the Morecambe Generation Assets.



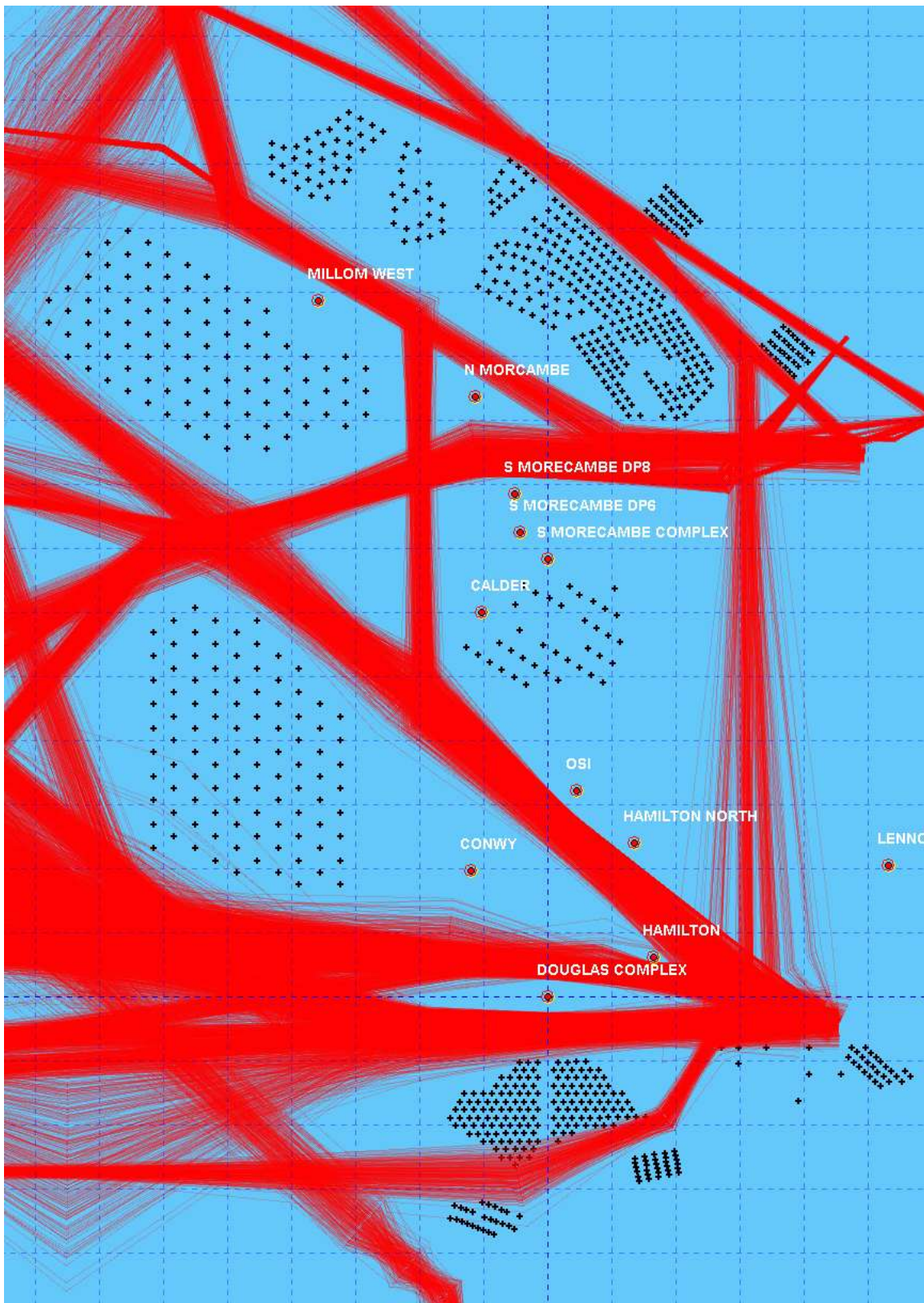


Figure 5.5: Modelled shipping routes post-construction of the Morecambe Generation Assets with Mona Offshore Wind Project and Morgan Generation Assets cumulatively.

5.5 Modelling results and comparison of the base case and the predicted shipping reroutes around the Morecambe Generation Assets in isolation and around Morecambe Generation Assets with Mona Offshore Wind Project and Morgan Generation Assets cumulatively

5.5.1.1 To understand the potential impact of proposed projects on the alarm rates, the modelled data from the existing base case was compared against the post construction modelling results. The comparison looks at the number of alarms each platform is expected to have in a one-year period. The data compares both Amber and Red TCPA alarms for the base case, Morecambe Generation Assets in isolation and Morecambe Generation Assets alongside Mona Offshore Wind Project and Morgan Generation Assets cumulatively. The annual alarm rates modelling results for each platform are shown in [Figure 5.6](#) ~~Figure 5.6~~ to [Figure 5.17](#) ~~Figure 5.17~~.

5.5.1.2 To simplify the comparison, [Table 5.3](#) ~~Table 5.3~~ shows the estimated difference in alarm rates between the base case and the two other considered scenarios (i.e. Morecambe Generation Assets in isolation and the cumulative case with Mona Offshore Wind Project and Morgan Generation Assets).

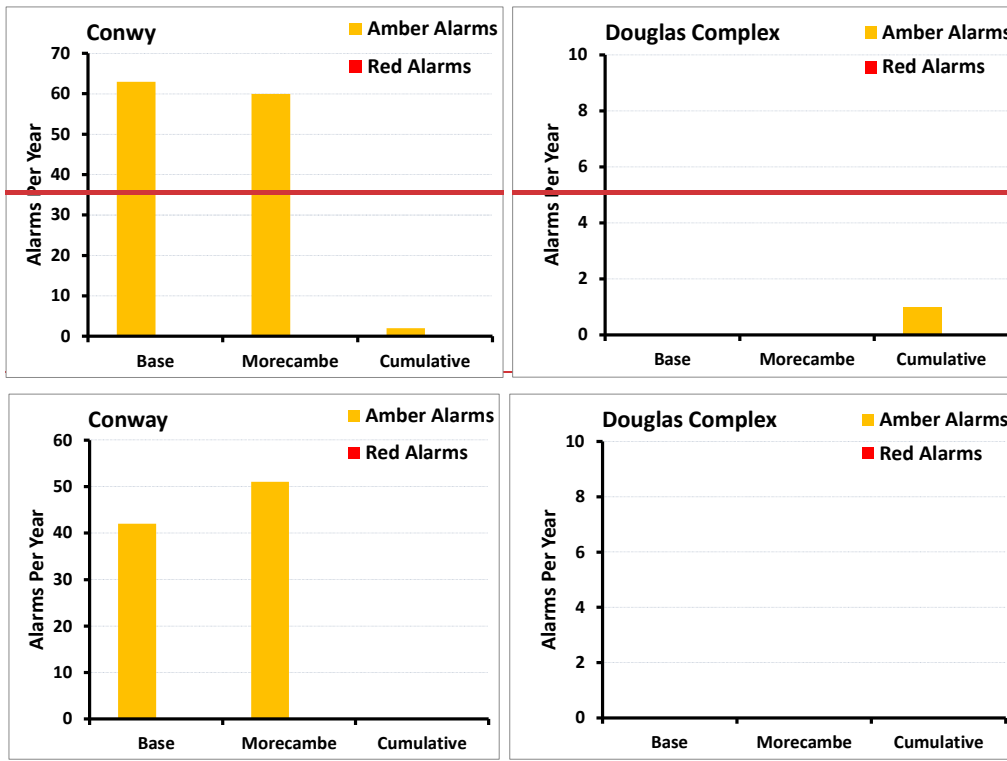


Figure 5.6: Modelled yearly alarm rates for the Conway platform. Figure 5.7: Modelled yearly alarm rates for the Douglas Complex.

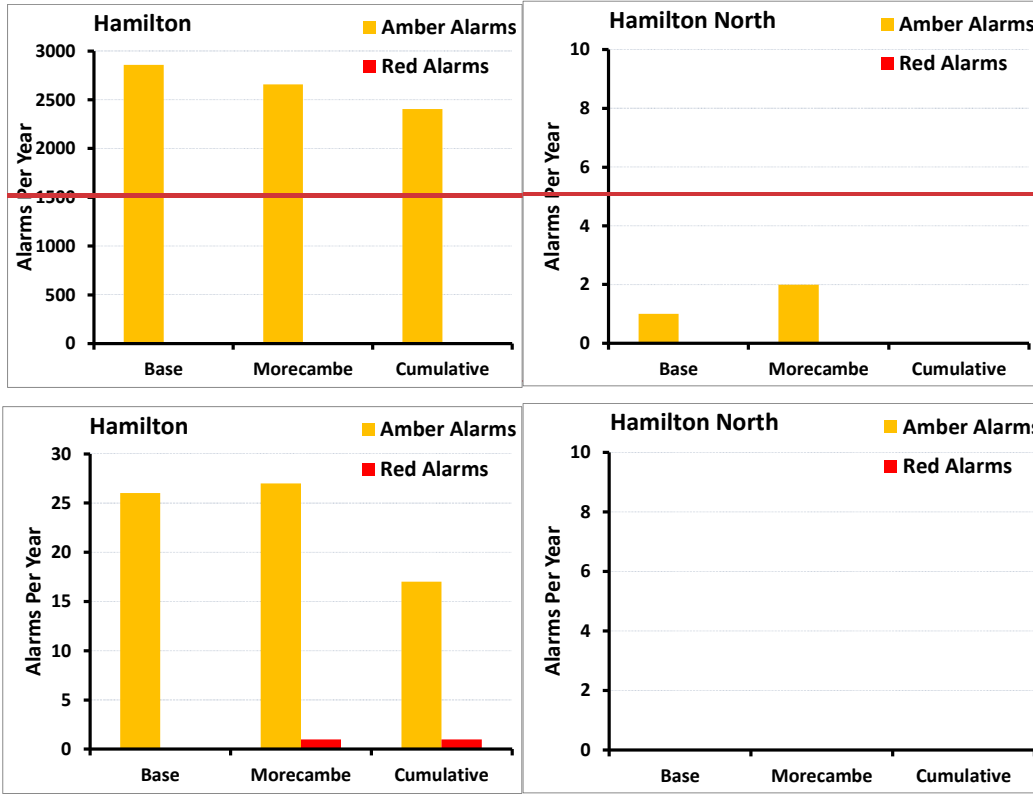


Figure 5.8: Modelled yearly alarm rates for the Hamilton platform.

Figure 5.9: Modelled yearly alarm rates for the Hamilton North platform.

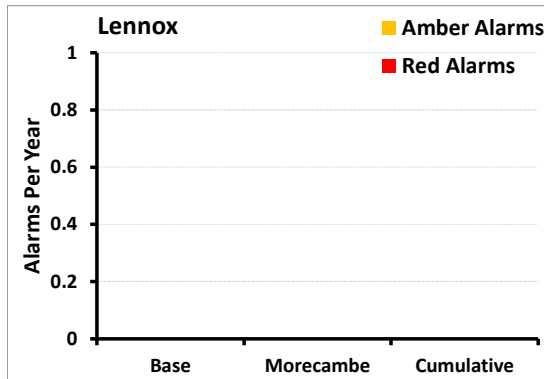


Figure 5.10: Modelled yearly alarm rates for the Lennox platform.

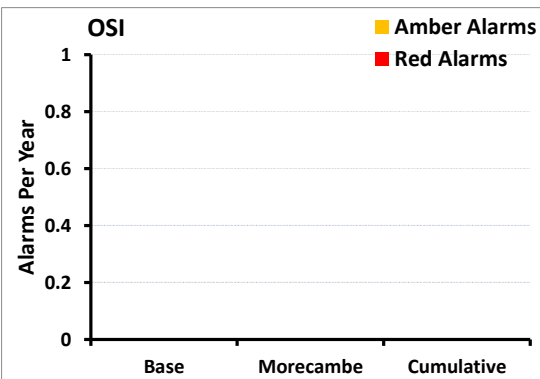


Figure 5.11: Modelled yearly alarm rates for the OSI.

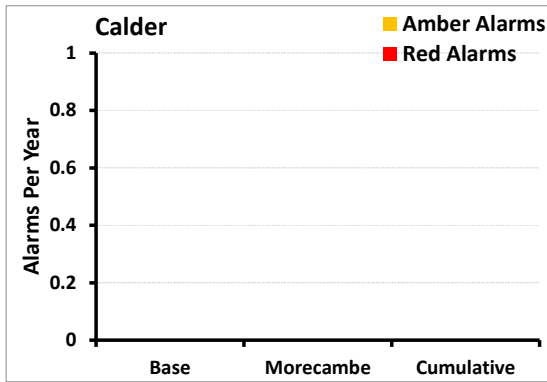


Figure 5.12: Modelled yearly alarm rates for the Calder platform.

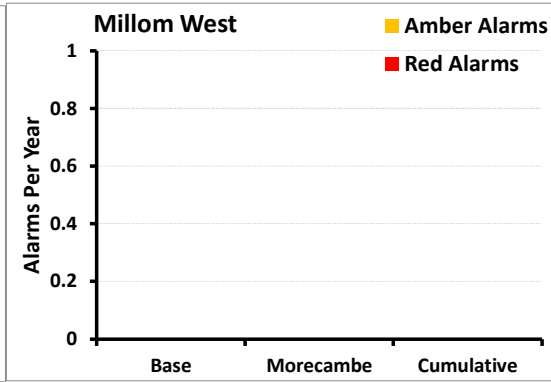


Figure 5.13: Modelled yearly alarm rates for the Millom West platform.

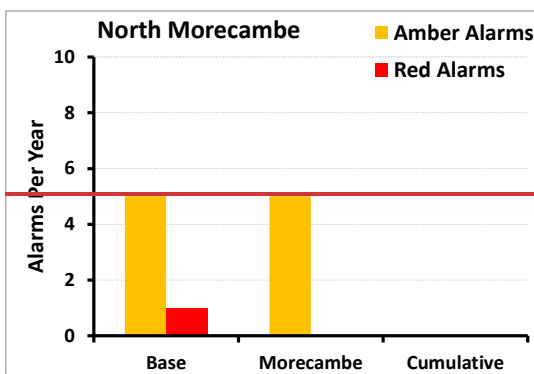


Figure 5.14: Modelled yearly alarm rates for the North Morecambe platform.

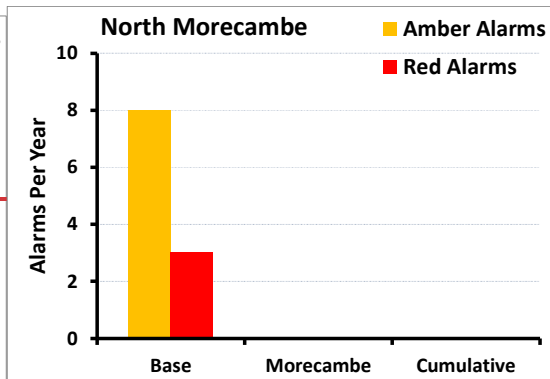
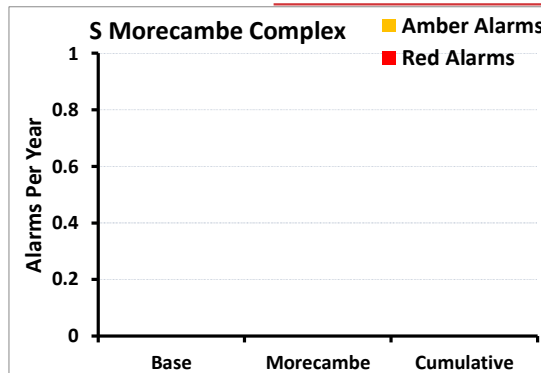


Figure 5.15: Modelled yearly alarm rates for the South Morecambe AP1 platform CPC.



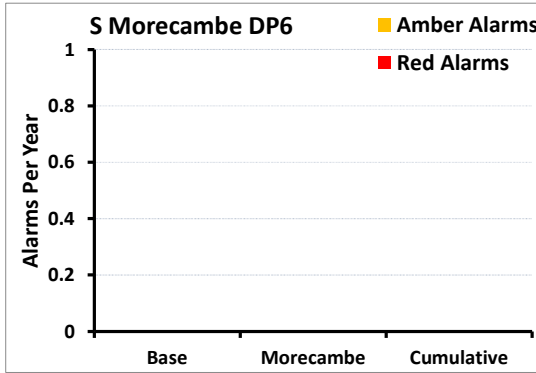


Figure 5.16: Modelled yearly alarm rates for the South Morecambe DP6 platform.

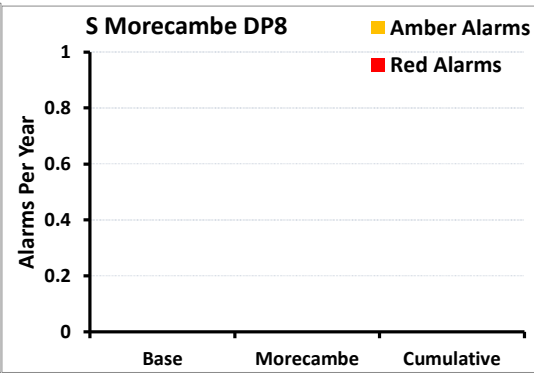


Figure 5.17: Modelled yearly alarm rates for the South Morecambe DP8 platform.

Table 5.3: The estimated change in yearly alarm rates against the base case (green = reduced alarms / no change, white = small alarm increase/decrease, orange = elevated alarm increase).

(*) The models use statistical data to generate a large number of paths along a given route (adhering to a Normal Distribution specified by the provided route data). The results are expected to vary slightly (by approximately ±1%) between each run due to the nature of the Normal Distribution of the generated paths.

Platform	Change* in yearly alarm rates considering Morecambe in isolation		Change* in yearly alarm rates considering the cumulative effect with Mona and Morgan	
	Orange	Red	Orange	Red
Conwy	-39	0	-6142	0
Douglas Complex	0	0	40	0
Hamilton	-2041	-1	-4549	01
Hamilton North	40	0	-40	0
Lennox	0	0	0	0
Osi	0	0	0	0
Calder	0	0	0	0
Millom West	0	0	0	0
N Morecambe	0-8	-13	-58	-13
S Morecambe Complex	0	0	0	0
S Morecambe Dp6	0	0	0	0
S Morecambe Dp8	0	0	0	0
Total Change	-2032	-2	-51759	-12

5.6 Remarks on the TCPA/CPA alarm modelling results

5.6.1.1 The existing base case sees regular traffic in the proposed Morecambe Array Area and surrounding region (Figure 5.3Figure 5.3). For this reason, Spirit Energy has deployed a REWS installation on South Morecambe AP1 to protect and manage their

offshore platforms in the regions. A large set of measured data of the vessels operating in the region is available to inform the base case scenario. The measured data was captured using AIS [data and radar](#) data of vessels travelling around the proposed projects array area. However, to assess the effects of the base case scenario on the REWS alarm rates, certain simplifying assumptions were made. These assumptions would allow the models to generate a large statistical dataset to calculate the average alarm rates per platform per year. Hence, the measured data were represented based on their statistical behaviour at a number of waypoints along the route. The routes were given as a set of discrete points along key locations on the route containing the mean and the 90th percentile width of the route. However, upon closer inspection of the measured data and the resultant modelled routes, it was noted that the measured data showed that the vessel operators actively avoid being too close to the offshore oil and gas installations. This can be observed by examining [Figure 5.2](#) and [Figure 5.1](#) around the vicinity of the Calder, Conwy, Hamilton platforms as well as the OSI. This active avoidance act by the vessels operators is not typically modelled within the assessment as it was not included within the statistical representation of the data. Active avoidance however was included in this study within the REWS models and was modelled based on selecting the best routes that conforms to the statistical nature of the data as well as keeping out of the exclusion zones around these platforms. This can be noted in [Figure 5.3](#) around the above-mentioned installations.

5.6.1.2 It is worth noting that this modelling procedure relies on statistical data rather than active avoidance and may cause the models to produce more alarm rates than what is experienced by the REWS operators in the existing base case. If the statistical representation of the measured data should include the active avoidance of the offshore installations, the models can be modified to include them in future assessments if needed.

5.6.1.3 It is also worth noting that the models generate a large number of vessel paths within each route by generating the way points in a random manner (based on the mean and standard deviation of each route). Therefore, the results of the statistical analysis may vary slightly depending on the normal distribution around the mean line of each route. Therefore, some of the small changes in the alarm rates observed (less than 1%) can be assumed to fall within the error margins of the predicted data and the statistical approach used within the models.

5.7 Conclusions of the TCPA/CPA alarm modelling

5.7.1.1 The modelling results_ for both the Morecambe Generation Assets in isolation and cumulatively with other windfarms indicate that the assessed platforms will not experience a change in yearly alarm rates.

When drawing conclusions from the results of the models there are two aspects that need to be considered; the number of alarms the REWS operator must deal with, and the system's ability to respond to potential risks of allision.

5.7.1.2 It is noted that the proposed Morecambe Generation Assets will have an impact on the rerouted traffic in the region and some vessels will travel closer to the platforms due to the location of the windfarms and the corridors formed between the proposed project and the existing windfarms. The findings of Appendix 14.1 Navigation Risk Assessment of the Environmental Statement (Document Reference 5.2.14.1) suggests that there will not be a notable increase in the risk of allision with the platforms. Therefore, the REWS is expected to continue to detect, track and issue alarms in a timely manner without an added risk of allision.

5.7.1.3 The REWS operators may need attend to the alarms more carefully during adverse weather conditions. However, it is anticipated that this measure would be implemented by operators under adverse weather conditions under their existing operational procedures. Therefore, the study concludes that there will be no impact on the REWS TCPA/CPA alarm rates from the Morecambe Offshore Generation Assets alone or cumulatively with Mona Offshore Windfarm Project and Morgan Offshore Generation Assets. Hence no mitigation measures will be needed.

6 MICROWAVE COMMUNICATION LINKS ASSESSMENT

6.1 Overview

6.1.1.1 Offshore oil and gas platforms often utilise microwave communications links to transmit operational data and communicate status and other critical information regarding the operation and maintenance of these platforms. The presence of large structures close to line-of-sight communication links may interfere with the performance of the link and may reduce the effectiveness and efficiency of communication protocol. Interference can also be caused by scattering from large structures that aren't in the way of the link. However, offshore windfarms may be located within the same regions of the oil and gas platforms.

6.1.1.2 This assessment considers the potential impact of the proposed Morecambe Generation Assets on the existing microwave communications links onboard the ENI Energy platforms and the Spirit Energy Platforms operating in the Irish Sea.

6.1.1.3 The following ENI Energy installations were identified to have microwave communication links:

- Douglas
- Conwy
- Hamilton
- Hamilton North
- Lennox
- The OSI.

6.1.1.4 The following Spirit Energy installations were identified to have microwave communication links:

- North Morecambe DPPA
- South Morecambe AP1
- Barrow North (onshore).

6.1.1.5 [Figure 6.1](#) shows the layout of the platforms and the considered links. It is worth noting that during the consultation process, only the platforms with the communication links were provided. The exact network of hops was not defined and hence not all possibilities were to be considered. The models were instead used to consider the closest turbine to the abovementioned platforms and assess the potential impact on any link operated by the platforms.

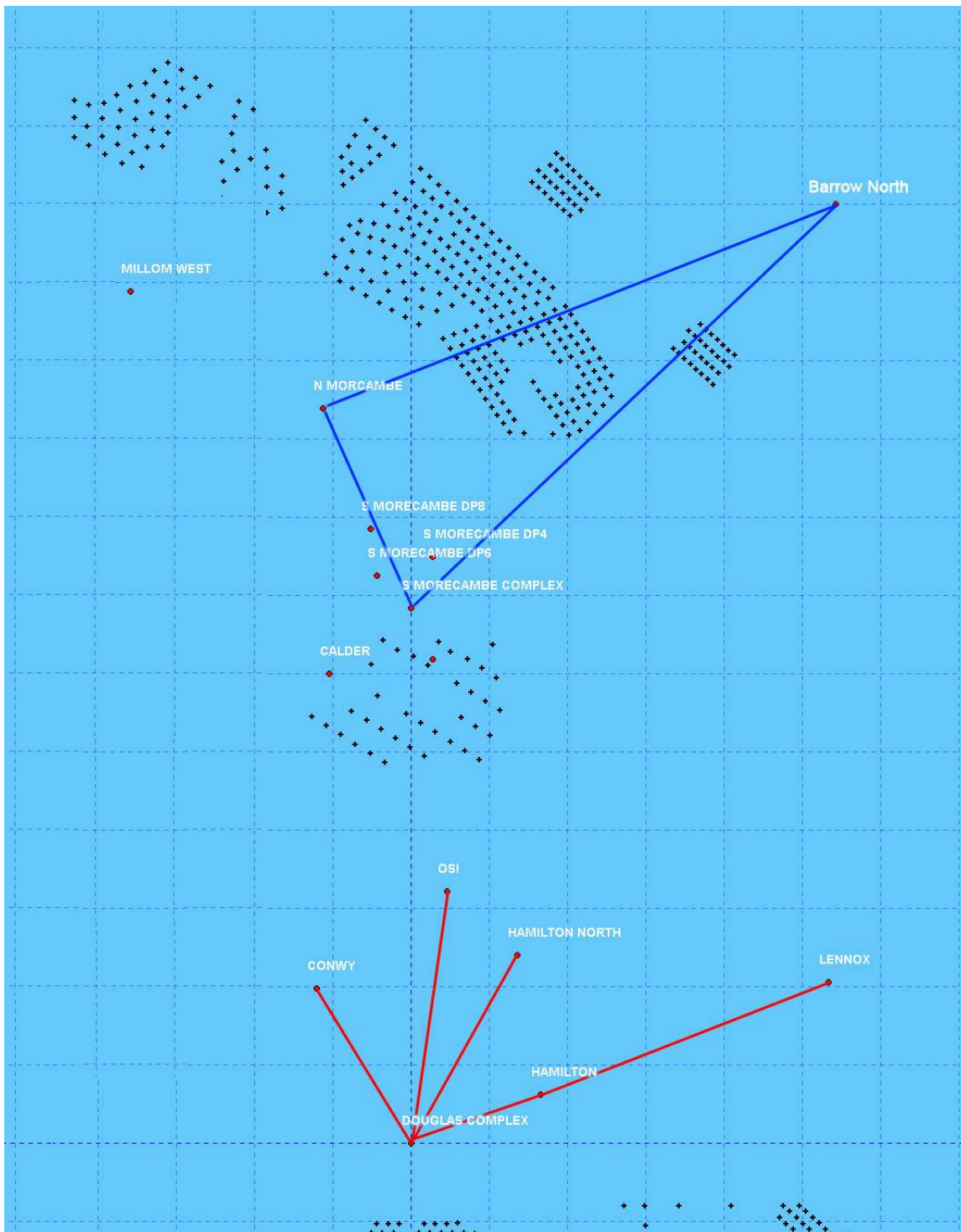


Figure 6.1: Layout of the modelled platforms and the communication links considered.

6.2 Modelling parameters

6.2.1.1 The interaction between wind turbines and communications links can be complex in nature and will depend on a number of parameters related to the communication link, the wind turbines and the local environment. In this assessment, the modelling process considered the specifications of the communication links and has also undertaken

detailed modelling of the wind turbine scattering to establish the exclusion zones recommended by Ofcom. These exclusion zones are to ensure that the integrity and efficiency of the communication links are maintained.

6.2.2 Communication link parameters

Hop length

6.2.2.1 The performance of communication link depends on a number of key parameters. Arguably, the most important is the hop length, which refers to the distance between the two communicating sites. The hop length is obtained by comparing the coordinates of the communicating platforms and deriving the line-of-site distance between the two antennas.

Gain and antenna radiation pattern

6.2.2.2 Antenna pattern was modelled in accordance with the ITU-R F.699-4 recommendation, which details a methodology to model the radiation pattern for line-of-sight microwave communications links. This approach is also used by Ofcom for their recommended procedure for modelling the impact of windfarms on communication links (Bacon, 2002).

6.2.2.3 The maximum gain of the antenna is calculated using the frequency and physical size of the antenna. These parameters are discussed below.

Antenna size and operational frequency

6.2.2.4 The size of the communications antenna and the operational frequency will determine the gain of the antenna. This in turn will impact the quality of the signal transmission and reception. Within this assessment the links are modelled to operate at 7.5GHz, which is the common frequency, which offshore oil and gas platforms use for their line-of-site communications.

6.2.2.5 The size of the antenna was not available at the time of modelling and therefore was assumed to be 1.2m. This size of antenna is commonly used within offshore communications links and is expected to increase the size of the exclusion zone around the sites. This would result in more pessimistic interference patterns and would then result in a more conservative approach to the siting analysis.

6.2.3 Wind turbine parameters

6.2.3.1 A summary of the MDS parameters for the communication link interface modelling is presented in [Table 3.1](#)~~Table 3.1~~. As discussed previously in the REWS assessment (section 3.2) the RCS models used the MDS geometry of the proposed turbines to model the bistatic scattering around the wind turbine at different angles and ranges. This is a critical step in the calculation of the exclusion zones, and it is often stated in other studies as an assumption that may limit the validity of these studies. The geometry of the bistatic RCS modelling is shown in [Figure 6.2](#)~~Figure 6.2~~ while the results of the bistatic RCS modelling of the wind turbine are shown in [Figure 6.3](#)~~Figure 6.3~~.

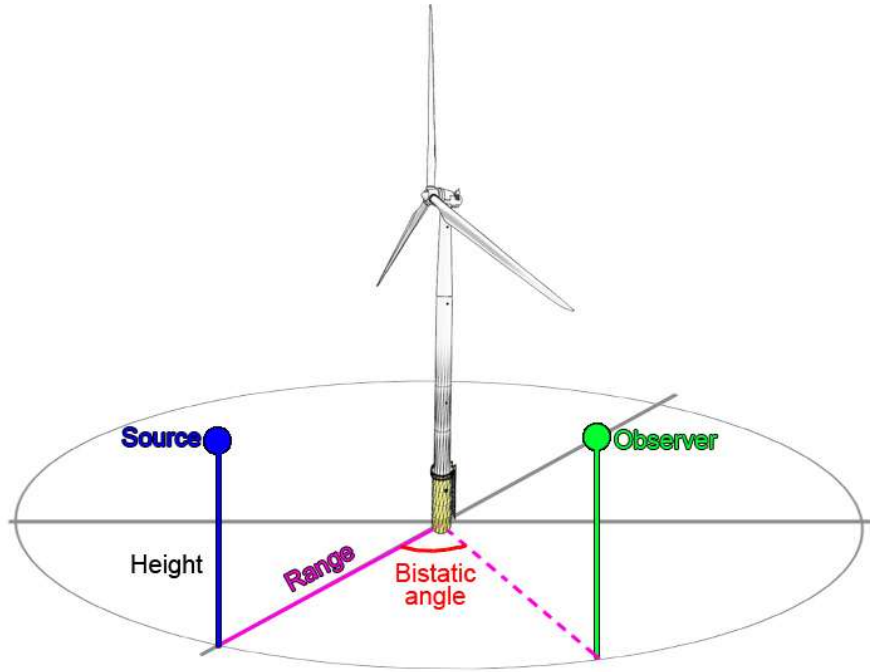


Figure 6.2: Geometry and parameters used in the wind turbine bistatic RCS modelling.

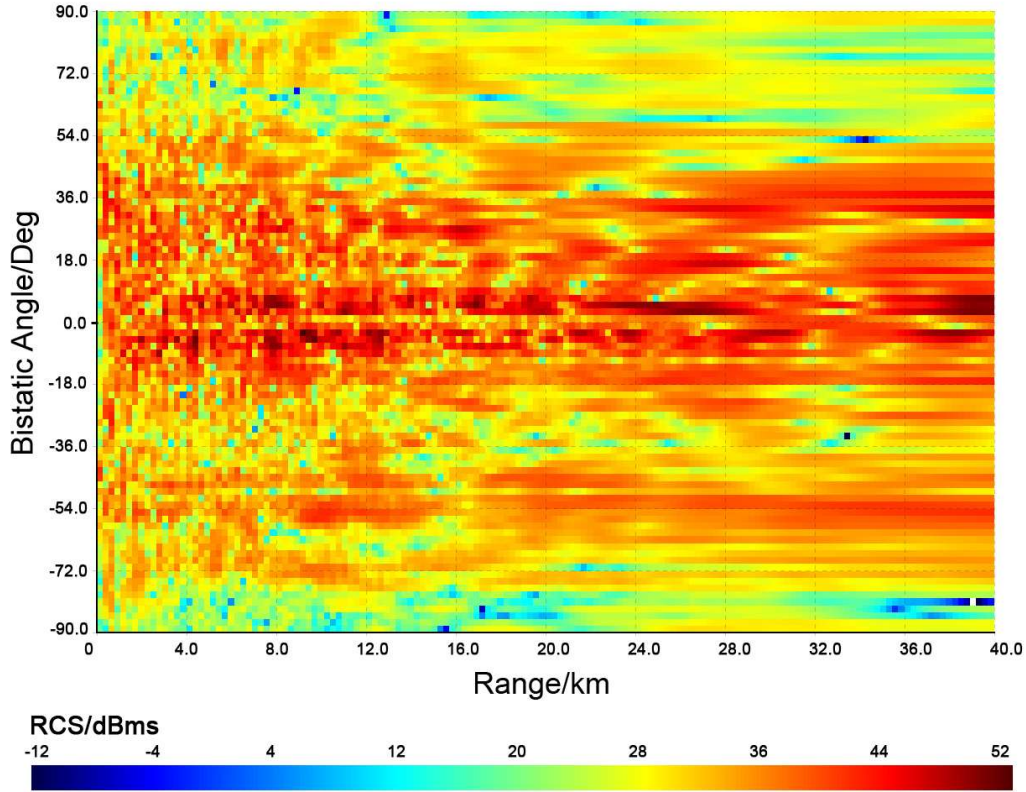


Figure 6.3: Bistatic RCS modelling results of the proposed MDS wind turbine.

6.2.4 Exclusion zones modelling

6.2.4.1 The modelling work presented within this assessment follows the recommended Ofcom methodology to calculate the safe distances between wind turbines and microwave communications links to avoid negative effects (Bacon, 2002).

6.2.4.2 It is noted that the impact of wind turbines might occur due to three phenomena. The interaction of the wind turbine with nearfield of the antenna radiation region, the diffraction of the communication signals around the wind turbines within the Fresnel zone and the reflection of the signal off nearby turbines.

6.2.4.3 This section will explain the modelling methodology of each interference mechanism and the required exclusion zone needed to avoid such interactions. This section uses the microwave communication link between Douglas and Hamilton as an example to illustrate the exclusion zones considered within this study. The results of other communication links in the region are summarised in [Table 6.1](#)~~Table 6.4~~ and [Table 6.2](#)~~Table 6.2~~.

6.2.5 Nearfield calculations

6.2.5.1 The nearfield is a region around the antenna whereby the radiation characteristics of the antenna is still forming. The presence of obstacles and/or reflecting objects within this region may interfere with the antennas' radiation pattern and can change the power transmission efficiency within the communication link. Therefore, wind turbines should be excluded from the near-field of any microwave antennas since it is not possible to accurately predict the effect they will have on the performance of the antenna.

6.2.5.2 The nearfield distance ends where the far-field region begin. The distance to the far-field region can be approximated by considering the dimensions of the antenna as well as the operational frequency. As mentioned previously in the antenna parameter modelling, it was assumed that all the communication links are operating at 7.5GHz and has an antenna diameter of 1.2m. This would result in a near-field exclusion zone with a radius of 72m around each antenna. This is illustrated as circular region around the sites as shown in [Figure 6.4](#)~~Figure 6.4~~ as the amber region. This is generally quite a small area and is unlikely to be a significant factor in the placement of wind turbines.

6.2.6 Diffraction region calculations

6.2.6.1 Diffraction of electromagnetic waves occur when an object is in the path of an advancing wavefront. Diffraction can detrimentally modify the wavefront if the object obstructs part of the waves path of travel. It should be noted that the object does not need to be a good reflector for this to happen. Diffraction effects can also occur when the obstructing object is totally absorbing. Avoidance of diffraction effects can be guaranteed by requiring obstructing structures to be outside a specified Fresnel zone of a radio link.

6.2.6.2 When considering the impact of wind turbines on communication links, it is recommended that turbines be excluded from an elliptical area equivalent to the area bounded by the 2nd Fresnel zone. The diffraction exclusion zone is as illustrated as the red ellipse in [Figure 6.4](#)~~Figure 6.4~~. The diffraction exclusion zone will have a maximum width at the midpoint between the two sites. To simplify the results of the study, this report will only present the maximum width of the diffraction exclusion zone for each of the considered links.

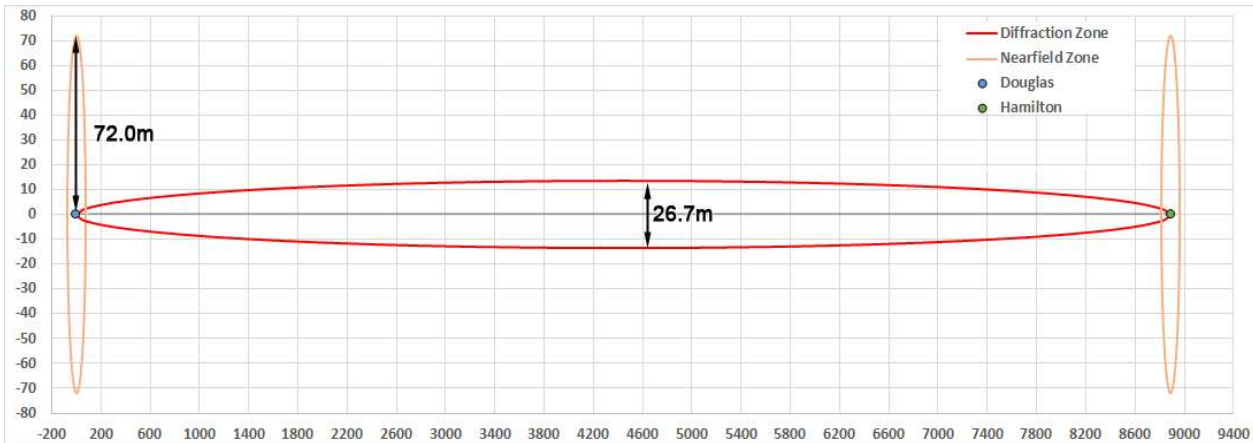


Figure 6.4: Illustration of the nearfield and diffraction exclusion zones.

6.2.7 Reflection region calculations

6.2.7.1 When electromagnetic waves illuminate an object some of the incident energy is re-radiated in various directions. Wind turbines will reflect a large portion of the incident wave in all directions. This is because at microwave frequencies, many surfaces are either curved or rough in comparison with the wavelength. The re-radiated energy may be somewhat concentrated in a specular direction, but a significant proportion often exists in other directions.

6.2.7.2 Therefore, if a microwave communications link transmitter illuminates a wind turbine and some of the scattered wave enters the receiver, the result is a multipath situation. Unless the level of the scattered signal is negligible compared to the direct signal, the combination of the signals and the time differences between their modulation may cause performance degradation.

6.2.7.3 This is calculated such that any scattered signal from the wind turbine outside the zone will arrive at the receiver with an amplitude sufficiently smaller than the direct signal such that its effect, even allowing for the delayed arrival, will be negligible. This calculation is based on the concept of carrier-to-interference ratio (C/I), usually expressed in dB. A fixed radio link is often designed to operate under different values of C/I.

6.2.7.4 The choice of C/I ratios will depend on the modulation and coding schemes of the link and the required performance. For the radio link to function with minimal degradation, a minimum value of C/I must be achieved and for the purposes of this study a target of C/I of 33dB was chosen -which is the figure quoted by Ofcom for design of a 28MHz/32QAM radio link. Note that this would provide sufficient protection for reflections from the wind turbines located close to the edge of the exclusion zone.

6.2.7.5 This study used the modelled bistatic RCS of the proposed MDS turbines shown in [Figure 6.3](#). The RCS value fluctuates significantly with respect to the range and bistatic angle. At ranges between 5km and 25km a conservative average of 44dBm² is considered to be suitable for the purposes of this study.

6.2.7.6 The modelling results of the C/I for the Douglas – Hamilton communication link is shown in [Figure 6.5](#). For the purpose of this assessment only values that are under 33 dB are considered to form the exclusion zone. [Figure 6.6](#) shows the exclusion zone with C/I ratio under the 33 dB limit.

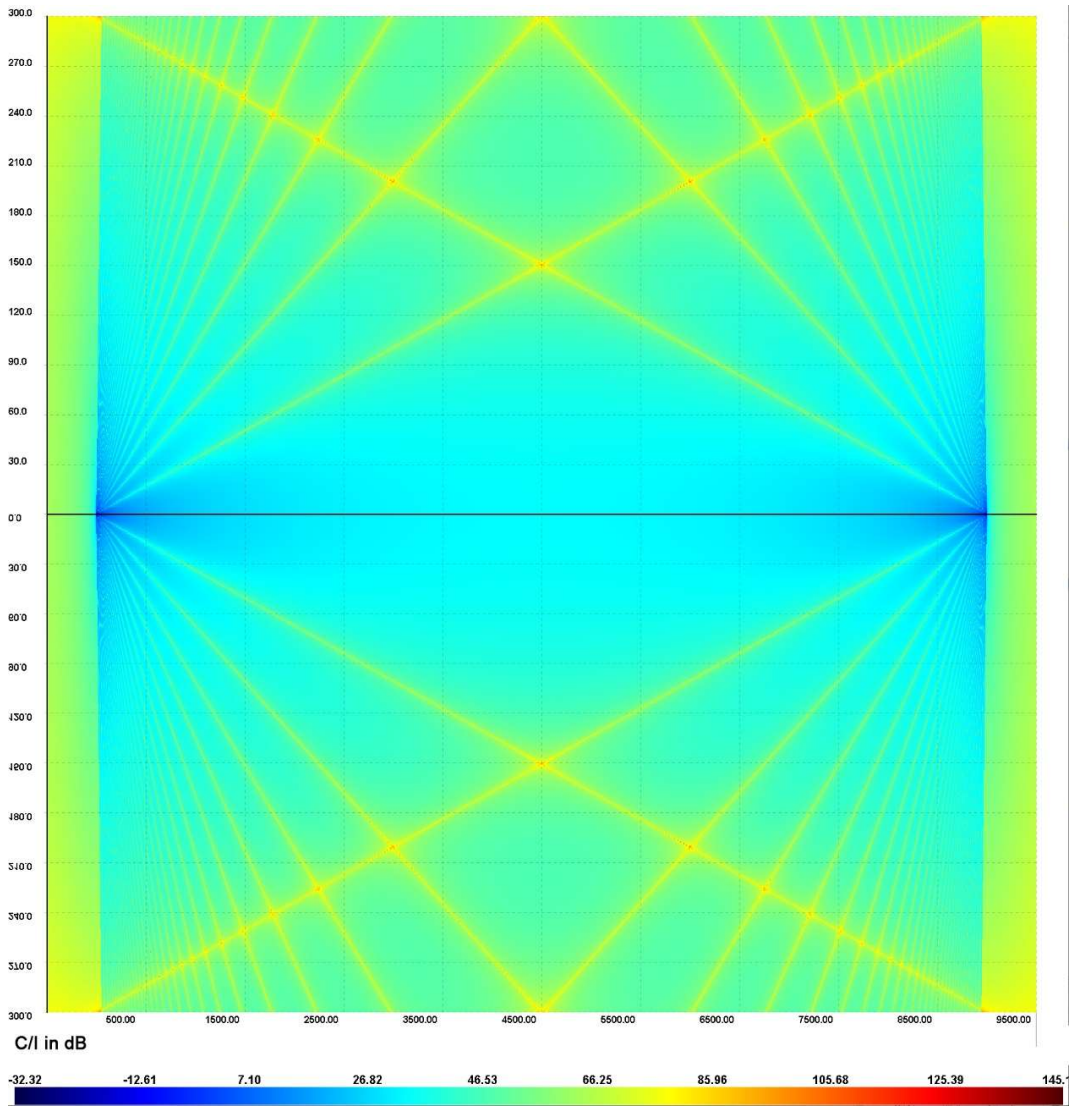


Figure 6.5: The signal to noise ratio around the Douglas – Hamilton link.

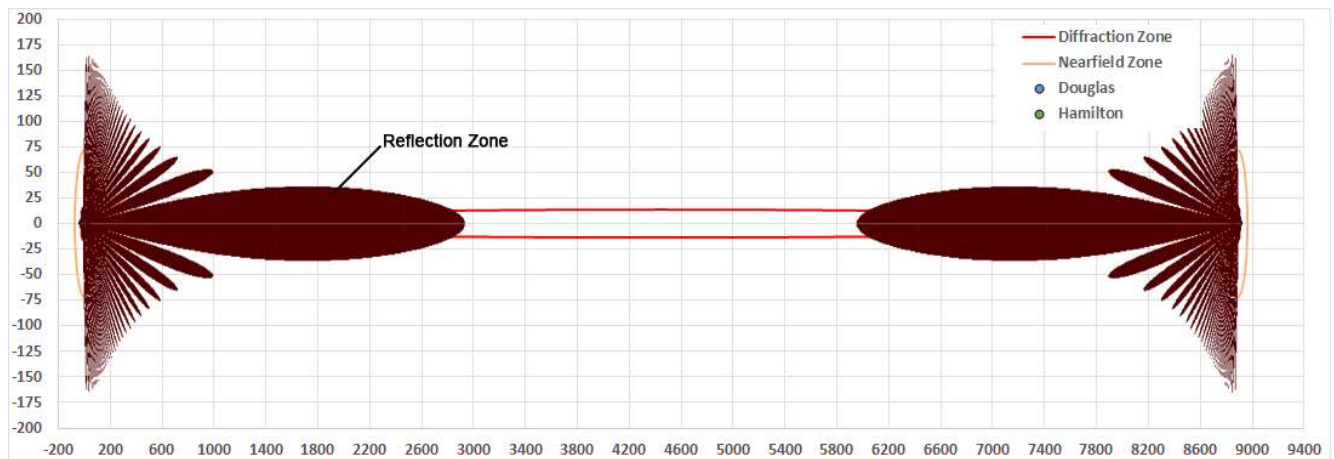


Figure 6.6: Illustration of the refraction exclusion zone resulting in C/I less than 33 dB.

6.2.7.7 It can be noted that the exclusion zone is closely related to the radiation pattern of the antenna. Therefore, to simplify the results further, only the maximum length and maximum width of the exclusion zones are considered. This is illustrated in [Figure 6.7](#) whereby the reflection is represented as a rectangle, while the refraction and nearfield regions are represented as ellipses.

6.2.7.8 It should be noted that the reflection interference is only significant within a few km of each end of the link – outside that area the exclusion zone is dominated by diffraction effects where the exclusion zone is defined by the 2nd Fresnel zone.

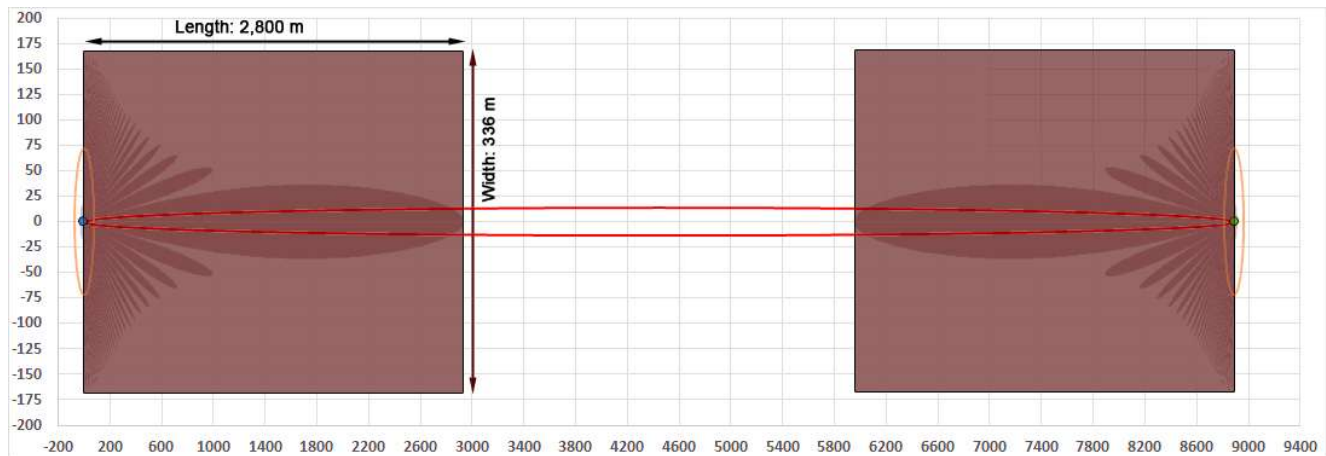


Figure 6.7: Simplified illustration of all exclusion zones around the Douglas – Hamilton link.

6.3 Exclusion zone modelling results

6.3.1.1 Using the methodology outlined above the exclusion zones for each link are summarised in [Table 1.6](#) [Table 6.1](#) for the Spirit Energy assets and in [Table 1.7](#) [Table 6.2](#) for the ENI Energy assets. Also, the distance between the nearest turbine and the communication link is included in the last column.

Table 6.1: Exclusion zones around the Spirit Energy microwave communication links.

Site one	Site two	Hop length (km)	Reflection zone length (km)	Reflection zone width (km)	Diffraction zone max width (m)	Nearest turbine (km)
Barrow North	North Morecambe DPPA	35.4	2.220	0.362	53.2	15.4
North Morecambe DPPA	South Morecambe AP1	14.0	2.475	0.359	33.4	2.8
South Morecambe AP1	Barrow North	37.4	2.152	0.390	54.7	2.8

Table 6.2: Exclusion zones around the ENI Energy microwave communication links.

Site one	Site two	Hop length (km)	Reflection zone length (km)	Reflection zone width (km)	Diffraction zone max width (m)	Nearest turbine (km)
Conwy	Douglas	11.6	2.560	0.342	30.5	15.1
Hamilton	Douglas	8.9	2.800	0.336	26.7	24.4
Hamilton North	Douglas	13.9	2.475	0.360	33.3	12.7
Lennox	Douglas	28.7	2.200	0.390	45.9	24.4
OSI	Douglas	16.3	2.390	0.370	36.2	8.6
Conwy	Lennox	32.8	2.695	0.400	51.3	15.1

6.4 Remarks on the microwave communication links modelling

6.4.1.1 The modelling results show that the Morecambe Generation Assets Array Area is located sufficiently far from the considered microwave communications links onboard ENI Energy and Spirit Energy platforms.

6.4.1.2 Based on the modelled parameters for the communications links and turbines, this study concludes that there will be no negative impact from Morecambe Generation Assets. Hence, no mitigation measures will be needed.

7 SUMMARY AND FINAL REMARKS

7.1 General REWS returns modelling summary

- 7.1.1.1 This assessment was undertaken for the MDS based on the available project parameters. The presence of wind turbines is expected to affect the REWS by introducing shadow regions and increasing the detection threshold around the wind turbines which may reduce the REWS' ability to detect and track targets within the affected area.
- 7.1.1.2 The RCS profile will depend on the size and the geometry of the wind turbines ultimately built within the Morecambe Generation Assets Array Area, along with other external factors such as blade bending and tower vibration.
- 7.1.1.3 An existing, generic 5MW wind turbine geometry was used and scaled up to provide a 3-dimensional representation of the MDS turbine geometry. Towers with monopile transition pieces were modelled, providing a worst-case scenario for the RCS that exceeds the MDS scenario for RCS.
- 7.1.1.4 Optical shadowing was used initially to approximate the shadowing effects produced by the wind turbine towers. This assumes no diffraction around the tower and hence extended shadow lengths. For the updated shadowing analysis, GTD and UTD were used to approximate the effects of diffraction and creeping waves. This was done to address the comments from Spirit Energy as indicated in Section 2.8. Details of the modelling parameters can be found in Section 3.8 and Section 4.3.2
- 7.1.1.5 The shadows from the towers are assumed to generate detection nulls for point targets. The modelling results show that the width of the nulls varies between 4 and 15m. For larger vessels over 1,000GT (which are the main concern for the oil and gas platforms), the dimensions of the vessel may exceed the width of the shadowing null. This can cause a portion of the radar signal to be reflected back to the radar. Depending on the levels of the reflected energy, it may be possible to detect the vessel while moving behind the wind turbines.
- 7.1.1.6 Some of the assumptions considered within the wind turbine RCS and shadow modelling are expected to overestimate the effects of wind turbines on REWS. Measurements show that the radar shadows from turbines diminish gradually with range due to the diffraction effects. Additionally, turbine materials, exact geometry, manufacturing tolerances, and external effects such as blade and tower bending due to wind loading are expected to effect and reduce the RCS of the wind turbines. This report considered the worst-case scenario using the MDS parameters for the Morecambe Generation Assets.
- 7.1.1.7 REWS often use proprietary thresholding algorithms which are dependent on the system configuration and the operating environment. CA CFAR is applied over the clutter map to provide a constant 10^{-5} probability of false alarm. The CA-CFAR within this study used two range cells on both sides of the cell under test as the guard region while the averaging considered six range cells on both sides of the guard region. In Azimuth the modelled CA-CFAR used one guard cell and two averaging cells on both sides in azimuth.
- 7.1.1.8 The test vessel parameters were chosen based on the information provided by the REWS operators and comply with the IALA VTS modelling standards.
- 7.1.1.9 In conclusion, the REWS returns modelling results of the Morecambe Generation Assets in isolation and the cumulative assessment of the Morecambe Generation Assets with Mona Offshore Wind Project and the Morgan Generation Assets on the

REWS installations (on ENI Energy's Douglas platform, Harbour Energy's Millom West platform, ENI Energy's OSI, Spirit Energy's South Morecambe AP1 platform) show that due to the presence of the turbines there would be small gaps in the detection map due to the elevated thresholds and shadowing effects from the wind turbines. However, these effects will be largely resolved by the built-in advanced tracking techniques within the REWS. Additionally, the integration of the available AIS data with the REWS coverage will provide an alternative source of vessel information and location within the zones where the REWS may lose detection.

- 7.1.1.10 Therefore, the models show that the impact of the Morecambe Generation Assets in isolation and the cumulative impact of the Morecambe Generation Assets with Mona Offshore Wind Project and Morgan Generation Assets on detection performance of nearby REWS installation is expected to be low and will be manageable without the need for further mitigation measures.

7.2 General TCPA/CPA modelling summary

- 7.2.1.1 The shipping routes and reroutes were modelled based on the available data provided by NASH Appendix 14.1 Navigation Risk Assessment of the Environmental Statement (Document Reference 5.2.14.1 and Appendix 14.2 Cumulative Regional Navigation Risk Assessment of the Environmental Statement (Document Reference 5.2.14.2)), which included measured radar and AIS data for the base case and predicted data for future reroutes around Morecambe Generation Assets in isolation and cumulatively with Mona Offshore Wind Project and Morgan Generation Assets. The data included route widths based on their 90th percentiles. This was then used to derive the mean central line and the standard deviation values along each assessed route and reroute.
- 7.2.1.2 The modelled routes and reroutes were chosen based on their general direction and proximity to the existing oil and gas platforms operating near the projects array areas. The routes were chosen for their proximity for CPA alarms assessment and for their general heading vectors for TCPA alarms assessment.
- 7.2.1.3 Once the proposed project is constructed, some routes may remain unchanged relative to the assessed platforms while others might result in closer or further proximity to the platforms. However, within this assessment, all the provided routes were modelled to establish the base case alarm rates which are present prior to the introduction of Morecambe Generation Assets and Morecambe Generation Assets cumulatively with Mona Offshore Wind Project and Morgan Generation Assets.
- 7.2.1.4 One thousand vessel paths were generated along each route in both the forward and reverse directions (a total of 2,000 runs per route). This was used to estimate the probability of raising a TCPA and/or CPA alarm for each route on each of the assessed platforms. The number of expected alarms per year was derived from the frequency of vessels travelling along each route.
- 7.2.1.5 The models were set to only issue a TCPA alarm if the vessel continues to breach the TCPA rules for more than 36 radar rotations. This was implemented to avoid false alarms due to temporary vector breach of the TCPA while vessels are turning.
- 7.2.1.6 The results show that there would be no increase in the number of CPA or TCPA alarms when assessing the Morecambe Generation Assets in isolation or cumulatively with Mona Offshore Wind Project and Morgan Generation Assets. Therefore, no mitigation measures will be needed.
- 7.2.1.7 It is also noted that the proposed project will have an impact on the rerouted traffic in the region and some vessels will travel closer to the platforms due to the location of

the windfarms and the corridors formed between the proposed project and the existing windfarms. This however is not expected to increase the risk of allision with the platform as concluded in Appendix 14.1 Navigation Risk Assessment of the Environmental Statement (Document Reference 5.2.14.1).

7.3 Assumptions and further considerations

- 7.3.1.1 The variation of returns in range cells due to rotation of the blades may cause the tracker to initiate false tracks. In order for the false track to raise a TCPA alarm the generated track needs to maintain its vector for a set number of radar rotations (typically 5 to 10). This is deemed to be very unlikely and has not been previously reported; however, the effect of this cannot be quantified due to not having access to the supplier's proprietary algorithms used within the system.
- 7.3.1.2 The study of the shadowing and masking depends on the indicative layout of the proposed projects array areas and was based on the indicative layout within the design envelope. Should the final turbine positions change significantly, the details of the shadowing and masking analysis may be affected and may need checking. Slight changes within tens of metres due to seabed conditions are not expected to change the shadowing effects significantly. It is also worth noting that if a reduction in the number of wind turbines is expected; this will reduce the effects on the REWS.
- 7.3.1.3 The introduction of wind turbines to the radar coverage area will increase the number of target detections. Depending on the tracker configuration, turbine detections may be included in the track-table. The track-table is transmitted to ERRV's via a low bandwidth UHF telemetry link. Using non-acquire zones and configuring the tracker to include only moving targets in the track-table may reduce the load on the UHF links. However, the effect of the track-table size and the UHF links are not considered within the scope of this study as it falls within the effects on wireless UHF communications rather than radar or microwave communication links.
- 7.3.1.4 The REWS uses a tracking algorithm to predict the vessels movement and compensate for momentary loss of detection. Such tracking algorithms are proprietary to the manufacturer. In general, such tracking may allow improved performance in the projects array areas vicinity to compensate for temporary losses due to raised threshold levels or shadowing effects. However, typically a track will be established within 5 to 10 rotations of the radar antenna (for antenna with 24 RPM, this is equivalent to 12.5 – 25 seconds).
- 7.3.1.5 Large (time varying) returns from turbines might cause the processed tracks from vessels to be seduced into the large turbine returns causing errors in tracking. This will be corrected after a number of radar rotations and the correct track will be resolved eventually. However, this is dependent on the tracking algorithm and post signal processing, which may be mitigated by using narrow non-acquire zones around each wind turbine.
- 7.3.1.6 Improvements to the CFAR performance might be achieved by using more sophisticated CFAR algorithms with different weighting on the averaging cells in order to improve the radar performance within the windfarm. Also, modification to the way that the CFAR calculations compute the threshold average over the windfarm might be modified to minimise the blind regions.

REFERENCES

- Bacon, D.F. (2022) A proposed method for establishing an exclusion zone around a terrestrial fixed radio link outside of which a wind turbine will cause negligible degradation of the radio link performance, Version 1.1, 28th October 2002.
- Baker, R. (2007) Investigation of Technical and Operational Effects on Marine Radar Close to Kentish Flats Offshore Wind Farm. MARICO 2007, BWEA Report.
- Butler, M.M. and Johnson, D.A. (2003) Feasibility of Mitigating the Effects of Wind farms on Primary Radar. AMS Ltd, ETSU W/14/00623/REP.
- Danoon, L. and Brown, A. K. (2014) Modelling the radar shadowing effects of the Burbo Bank Wind Farm Extension on the BHP Billiton Radar Early Warning System. The University of Manchester, 2014.
- Danoon, L. Al-Mashhadani, W. Greenwell, K. Revie, C. Brown, A. K. (2018) Reducing the effect of offshore wind farms on the REWS CFAR detection threshold. *22nd International Microwave and Radar Conference (MIKON)*, Poznan, Poland,
- Greenwell, K. (2016) Mitigation Strategies for the Effects of Offshore Wind farms on ULTRA Radar Early Warning Systems. Ultra ES, 2016.
- Jago, P. and Taylor, N. (2002) Wind Turbines and Aviation Interests - European Experience and Practice. ETSU W/14/00624/REP, DTI PUB URN No. 03/515, 2002.
- Love, S. (2014) Report on the Predicted Impact of the Burbo Bank Wind Farm Extension on the BHP Billiton Radar Early Warning System. Ultra ESS, 2014.
- Poupart, G.J. (2003) Wind Farms Impact on Radar Aviation Interests. BWEA Radar Aviation Interests Report. DTI report number W/14/00614/00/REP, September 2003.
- QinetiQ (2005) An assessment of the impact of the proposed Gwynt y Môr wind farm on marine radio navigation and communications systems.
- Terma (2021) Wind turbine RCS assessment from radar data recorded at Hornsea One, Document No. 1739964-RA, 2021.
- Wind Energy, Defence & Civil Aviation Interests Working Group (2002) Wind Energy and Aviation Interests – Interim Guidelines. ETSU W/14/00626/REP, October 2002.